GL01056

GEOTHERMAL RESERVOIR ASSESSMENT CASE STUDY, NORTHERN BASIN AND RANGE PROVINCE, NORTHERN DIXIE VALLEY, NEVADA

Conducted for:

U. S. Department of Energy
Contract number DE-AC08-79ET27006

Work Performed under Subcontract to:

Southland Royalty Company
Fort Worth, Texas

Conducted by:

Mackay Minerals Research Institute
University of Nevada, Reno, Nevada

Submitted:

January 31, 1980

Note: Sets of the color photographs contained in Chapter 4 of this report may be obtained by writing E.J. Bell, Mackay School of Mines, University of Nevada, Reno, Nevada 89557. Cost of reproduction ($10.00) should be remitted with a written request.

LIST OF AUTHORS

Chapter 1. INTRODUCTION

Elaine J. Bell, Michael E. Campana, Roger L. Jacobson, Lawrence T. Larson, and D. Burton Slemmons

Chapter 2. REGIONAL SETTING

Elaine J. Bell

Chapter 3. STRUCTURAL-TECTONIC ANALYSIS

Robert A. Whitney

Chapter 4. PETROLOGIC ALTERATION STUDIES

Thomas R. Bard

WATER CHEMISTRY

Russell W. Juncal and Thomas R. Bard

Chapter 5. HYDROLOGY AND HYDROGEOCHEMISTRY

Burkhard W. Bohm, Roger L. Jacobson, Michael E. Campana, and Neil L. Ingraham

Chapter 6. SHALLOW TEMPERATURE SURVEY

Michael E. Campana, Roger L. Jacobson, and Neil L. Ingraham

Chapter 7. MODELS OF THE DIXIE VALLEY GEOTHERMAL SYSTEM

Elaine J. Bell, D. Burton Slemmons, Robert A. Whitney, Thomas R. Bard, Roger L. Jacobson, Michael E. Campana, Russell W. Juncal, Lawrence T. Larson, Burkhard W. Bohm, and Neil L. Ingraham

Chapter 8. EVALUATION OF THE INTEGRATED MODEL OF THE DIXIE VALLEY GEOTHERMAL SYSTEM

Elaine J. Bell, Michael E. Campana, Roger L. Jacobson, Lawrence T. Larson, D. Burton Slemmons, Thomas R. Bard, Burkhard W. Bohm, Neil L. Ingraham, Russell W. Juncal, and Robert A. Whitney

TABLE OF CONTENTS

Table of Contents (cont'd) Page

Table of Contents (cont'd)

Table of Contents (cont'd)

LIST OF FIGURES

List of Figures (cont'd)

List of Figures (cont'd)

List of Figures (cont'd)

LIST OF PLATES

LIST OF TABLES

Chapter 1. INTRODUCTION

By: Elaine J. Bell, Michael E. Campana, Roger L. Jacobson, Lawrence T. Larson, and D. Burton Slemmons

1.0 INTRODUCTION

1.1 Foreward

This report was prepared for the U. S. Department of Energy (DOE) in compliance with conditions of the statement of work as part of Contract number DE-AC08-79ET27006 for Geothermal Reservoir Assessment in the northern Basin and Range Province. Work was performed by the Mackay Minerals Research Institute (MMRI) under subcontract to Southland Royalty Company (SRC), Fort Worth, Texas.

The MMRI, with the Mackay School of Mines as lead agency, is charged with performing research in the general field of non-renewable resources. Optimal use of the staff and facilities of the University results from the various components of the University cooperating in interdisciplinary research. The Geothermal Reservoir Assessment of Dixie Valley by the MMRI involved both the Mackay School of Mines (MSM) and the Desert Research Institute (DRI). MSM and DRI personnel performed the investigations and prepared the following final technical report on the Dixie Valley Geothermal System. Table 1-1 lists specific individuals involved in the project, their respective affiliation, title, investigation areas, and level of effort. Primary responsibility for accomplishing the tasks listed in the statement of work resided with the Graduate Research Fellows under the technical supervision of the Principal Investigators. The specific personnel and their individual responsibilities in completing the various investigations are indicated in Chapters 3 through 6 of this report.

The overall reservoir assessment dealt with the northern Dixie Valley area, Nevada (Figure 1-1; Plate I). Specific investigations conducted within the study area included: 1) Structural-Tectonic Analysis; 2) Petrologic Alteration Studies; 3) Hydrology and Hydrogeochemistry; and 4) Shallow Temperature Survey. The results of these investigations are presented in the following technical report in a written format supplemented by appropriate graphic data and appended information.

1.2 Purpose

The purpose of the MMRI program was to develop an integrated model of the Dixie Valley area with respect to a geothermal system based upon both pre-existing data and data derived from the scope of

Table 1-1. MMRI Personnel

Name	Affiliation*	Title (Areas of Investigation)**	Level of Effort
Bard, Thomas R.	MSM	GRF (PA; STS)	8 man-months
Bell, Elaine J.	MSM	PI/Administrator (S-T; PA)	6 1/2 man-months
Bohm, Burkhard W.	DRI	GRF (HG)	7 man-months
Campana, Michael E.	DRI	PI (H; HG; STS)	1/2 man-month
Dowden, John E.	DRI	GRF (H; HG; STS)	1/4 man-month
Henne, Mark S.	DRI	GRF (H; HG; STS)	1/4 man-month
Ingraham, Neil L.	DRI	GRF (H; STS)	2 1/2 man-months
Jacobson, Roger L.	DRI	PI (HG; H; STS)	1/2 man-month
Johnson, Cady	DRI	GRF (STS)	2 1/2 man-months
Juncal, Russell W.	MSM	GRF (PA; STS)	6 man-months
Kearl, Peter M.	DRI	GRF (H; HG)	1/2 man-month
Larson, Lawrence T.	MSM	Project Administrator	1 man-month
McKay, Alan	DRI	Technician (H; HG)	1 man-month
Nosker, Sue C.	MSM	GRF (PA)	1 1/2 man-months
Slemmons, D. Burton	MSM	PI (PA; S-T)	1 man-month
Wheatcraft, Steven	DRI	Geologist (H; HG)	1/2 man-month
Whitney, Robert A.	MSM	GRF (S-T: STS)	8 man-months

*MSM -- Mackay School of Mines; DRI -- Desert Research Institute.

**GRF -- Graduate Research Fellow; PI -- Principal Investigator; PA - Petrologic Alteration Studies; STS -- Shallow Temperature Survey;S-T -- Structural-Tectonic Analysis; HG -- Hydrogeochemistry; H -- Hydrology.

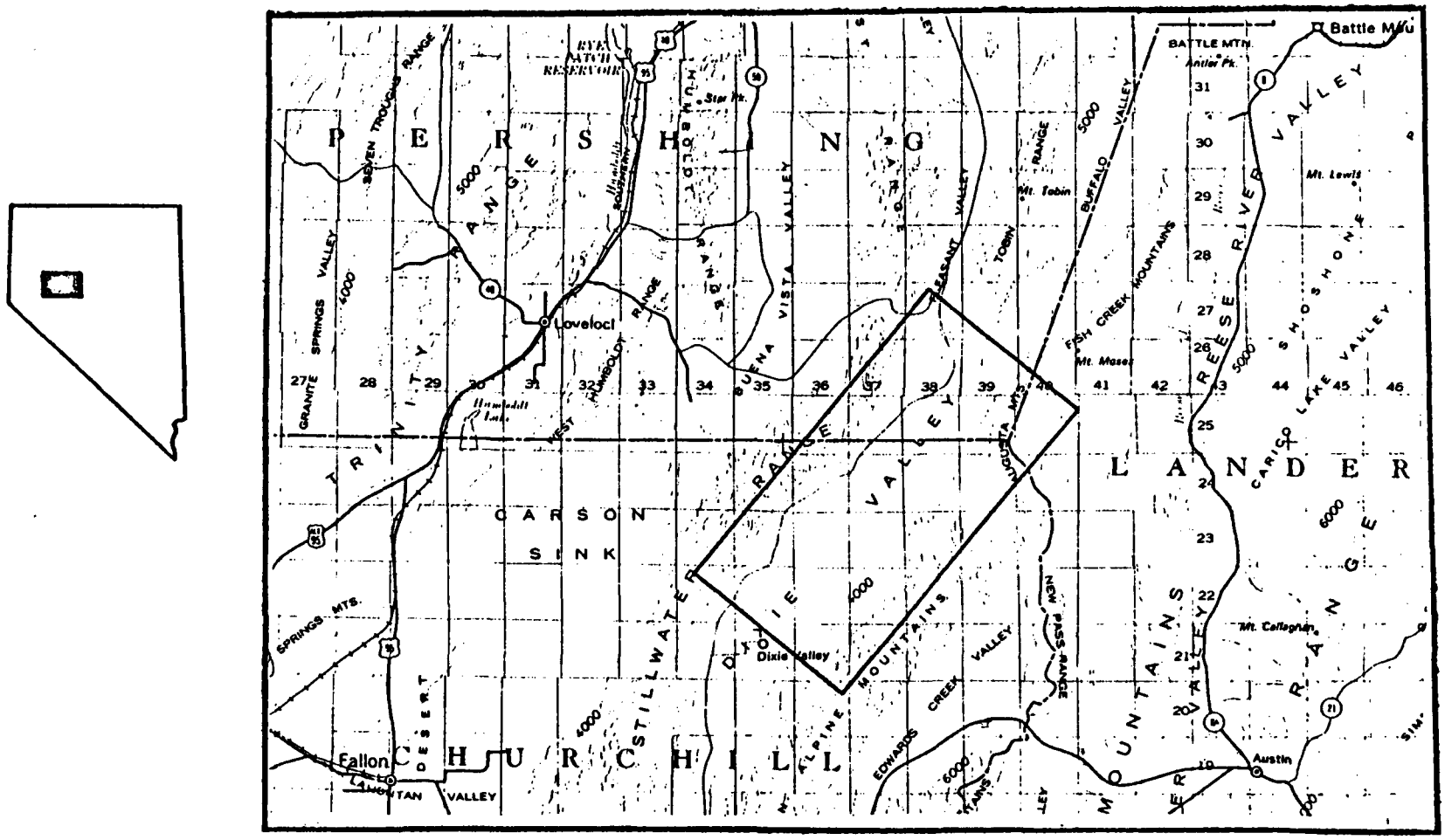

Figure 1-1. Index map of Dixie Valley study region. Shaded area of State shown enlarged. Specific study area outlined on enlarged map is shown in detail on Plate I.

work summarized below. This model will then serve the DOE as a case study of a Basin and Range geothermal system.

1.3 Scope

The scope of the study as outlined in Appendix A, Scope of Work, of both the Prime Contract and Subcontract (Contract number DE-AC08-79ET27006) included the following major tasks for each phase of investigation:

Structural-Tectonic Analysis

(1) Review and evaluate available fault and lineament maps and high-altitude photography.

(2) Conduct low-sun-angle and "snow lapse" photography studies.

(3) Conduct field structural mapping.

(4) Correlate and interpret data and develop a structural model.

Petrologic Alteration Studies

(1) Analyze subsurface samples from thermal gradient hole drilling and representative surface samples.

(2) Describe lithology and petrologic variation in drill holes.

(3) Conduct detailed mapping of the primary stratigraphic units of the valley fill.

(4) Review existing lithology and mineralogy data.

(5) Integrate the above petrologic studies with the structural-tectonic studies.

Hydrology-Hydrogeochemistry

(1) Review available hydrologic-hydrogeochemical data.

(2) Sample selected wells, springs, and fumaroles.

(3) Perform selected trace element and isotopic analyses.

(4) Collect temperature data from existing wells and springs.

(5) Determine recharge and groundwater flow rates and estimate reservoir geometry.

(6) Construct an aquifer flow model.

Shallow Temperature Survey

(1) Install and monitor a shallow depth temperature survey consisting of about 200 one-meter deep holes for a 6-month period.

(2) Statistically evaluate the cumulative and individual readings of the survey.

(3) Compare the near-surface hydrothermal discharge system with subsurface temperature gradient hole data.

(4) Evaluate the validity of the shallow temperature survey as a geothermal exploration technique.

Model the Dixie Valley Geothermal System

(1) Develop an integrated model of the Dixie Valley region with respect to a geothermal system based on pre-existing data and data derived from the above listed tasks.

(2) Evaluate the Dixie Valley Geothermal System model.

Note:

During the course of investigation, Task 3 of the Petrologic Alteration Studies was transferred to the tasks to be accomplished under the Structural-Tectonic Analysis. This modification of the outlined program was based on 1) an increasing awareness of the integral relationship of the valley-fill stratigraphic units and their geographic distribution to the structural-tectonic history of the valley and 2) the extreme lateral and vertical variations (facies changes) inferred for the subsurface based upon limited drill hole information. More extensive subsurface stratigraphic data are needed upon which to base any subsurface-surface petrologic correlations.

1.4 Study Approach and Methods

Because the MMRI program involved several phases of study, the specific approach and methods of each investigation are presented in the respective chapters of this report. Models were developed based on the specific data of each of the various phases of investigation. These 'single-phase' models were then integrated to derive the model of the Dixie Valley Geothermal System.

1.5 Report Organization

This final technical report is presented in chapter format with each chapter authored by the person(s) primarily responsible for data development and accomplishing the tasks as outlined in the statement of work. The regional setting is presented in Chapter 2 to provide a basic framework within which to evaluate the data presented in the following chapters. Chapters 3 through 6 are devoted to each phase of the MMRI program of investigation. Chapters 2 through 6 serve as the basis for the integrated model of the Dixie Valley Geothermal Sys-

tem in Chapter 7. Chapter 8 evaluates the model in terms of completeness, conflicts in the existing data, and recommendations for further study that would verify and refine the model. Where necessary, graphic display of data in the form of tables, charts, photographs, figures, or maps is included to supplement and enhance the text presentation.

Preparation of the final technical report involved the following process:

(1) Authorship of the respective chapters on the various phases of investigation.

(2) Collation of Chapters 1 through 6 to form the Draft Final Report (DFR).

(3) Review of DFR by all MMRI project personnel and by key SRC personnel.

(4) Integration of data and 'single-phase' models to derive a model for the Dixie Valley Geothermal System and to evaluate the model. Cooperative effort by all MMRI personnel and key SRC personnel.

(5) Preparation of DFR Chapters 7 and 8.

(6) Review of DFR Chapters 7 and 8 by all MMRI personnel and key SRC personnel.

(7) Preparation of Final Technical Report.

1.6 Acknowledgements

On behalf of the Graduate Research Fellows and ourselves, we express our sincere appreciation to the following representatives of Southland Royalty Company: Mr. Jere Denton, District Manager of Natural Resources, for initiating the joint venture between SRC and the MMRI, and for his continuing support, cooperation and guidance since the inception of this project; and Mr. Dennis S. McMurdie, Geothermal Geologist, for his probing questions and assistance during the course of our investigations. We also wish to acknowledge the stimulating discussions prompted by Mr. Richard L. Jodry, Energy Consultant to Southland Royalty Company.

We wish to acknowledge the participation of Mr. William D'Olier and Mr. Lou de Leon of Thermal Power Company in coordinating the deep exploratory drilling program in Dixie Valley with the MMRI investigations.

Dennis T. Trexler of the Nevada Bureau of Mines and Geology provided guidance and advice during the stages of proposal preparation

for this project and continued to be a source of administrative guidance throughout the course of the project; we especially thank him for his assistance. Purchasing agreements and bookkeeping were ably handled by Mrs. Betsy Peck, Ms. Sheryl Harding, Ms. Alta Sly, and Mrs. Louise Gibbs. Superb secretarial services provided by Mrs. Soni Cox, Mrs. Barbara Salmon, Mrs. Carol Hackney, Ms. Alta Sly, Mrs. Alma Smith and Ms. Mollie Stewart made the preparation of this report possible. Ms. Alice Kellames (MSM) is thanked not only for her patience but also for her capable assistance in handling personnel contracts and numerous unforeseen problems. Dale Schulke (DRI) was indispensable in dealing with the myriad of administrative, budget and other problems that arose during the course of the study. Contract expenditure records were maintained in a timely and efficient manner by Mr. James Murphy and Mr. Barry Myers of the UNR Controllers Office.

We wish to express our appreciation to the U. S. Department of Energy for their willingness to support the MMRI and its research in Dixie Valley. We would particularly like to thank Mr. Joe Fiore of the U. S. DOE for his cooperation and encouragement.

Special thanks are extended to Mr. and Mrs. Sheldon Lamb whose hospitality and cooperation were of inestimable value to the field effort of MMRI personnel in Dixie Valley.

We wish to extend our thanks to numerous other support personnel of the Mackay School of Mines and the Desert Research Institute who assisted our efforts toward completion of this project. Special thanks are due Ms. Patricia Harris and her staff at the DRI water analysis laboratories for providing excellent chemical analysis and related services, often under extremely difficult conditions. Jack Dowden, Cady Johnson, Robert Broadbent, W. Alan McKay, Rod Fricke, Mark Henne, David Bratberg, and Richard Goldfarb performed field work above and beyond the call of duty. Ron Sheen was invaluable in the portions of this project that involved computer analysis, and W. Alan McKay performed excellent drafting work.

And finally, we wish to thank Sun Oil Company for the grapes on the vine that aided us in understanding the complex nature of the Dixie Valley Geothermal System.

Chapter 2. REGIONAL SETTING

By: Elaine J. Bell

2.0 REGIONAL SETTING

2.1 Introduction

The geotectonic history of western Nevada, encompassing Dixie Valley, is unique and complex. Because the western Great Basin is a result of the dynamic interaction of the Pacific and North American Plates, the following discussion is focussed on the plate tectonic evolution of the California-Nevada region. While this interaction of lithospheric plates is not fully understood, the present state-of-the-art knowledge can be utilized for discerning a regional geotectonic framework for the Dixie Valley Geothermal System. This chapter is a summary; the reader is referred to Wilson (1971, 1976) for discussions of the basic concepts of plate tectonics, and to Atwater (1970) and Ernst (1979a) for more detailed evaluations of the Cenozoic plate interactions in western North America. Figure 2-1 illustrates selected key Cordilleran tectonic elements discussed in the following sections.

2.2 Geotectonic History

2.2.1 Precambrian

Three major divisions of the Precambrian are recognized in the Great Basin and adjoining regions: metasedimentary (schist and paragneiss) and plutonic rocks older than about 1400 million years (my); unmetamorphosed sedimentary rocks approximately comparable in age to the Belt Supergroup, 850 to 1250 my; and the unmetamorphosed uppermost Precambrian sedimentary rocks probably less than about 850 my old. The metasedimentary and plutonic rocks older than 1400 my are extensive in the surface and subsurface of Wyoming, Utah, Arizona and California east of the Wasatch Line. West of the Wasatch Line they are sparsely exposed in southeastern California, and in southern Idaho and northern Utah. Supposed older Precambrian rocks that crop out in southern Nevada (Ekren and others, 1971) may also be metamorphosed strata of latest Precambrian or Paleozoic age (Stewart and Poole, 1974). Unmetamorphosed to slightly metamorphosed pregeoclinal sedimentary rocks equivalent to the Belt Supergroup are recognized in northern Utah, southeastern California and in the Grand Canyon region of Arizona.

A distinctive diamictite unit (a rock composed of large clasts in a finer grained matrix) is considered to be of glacial origin (Critt-

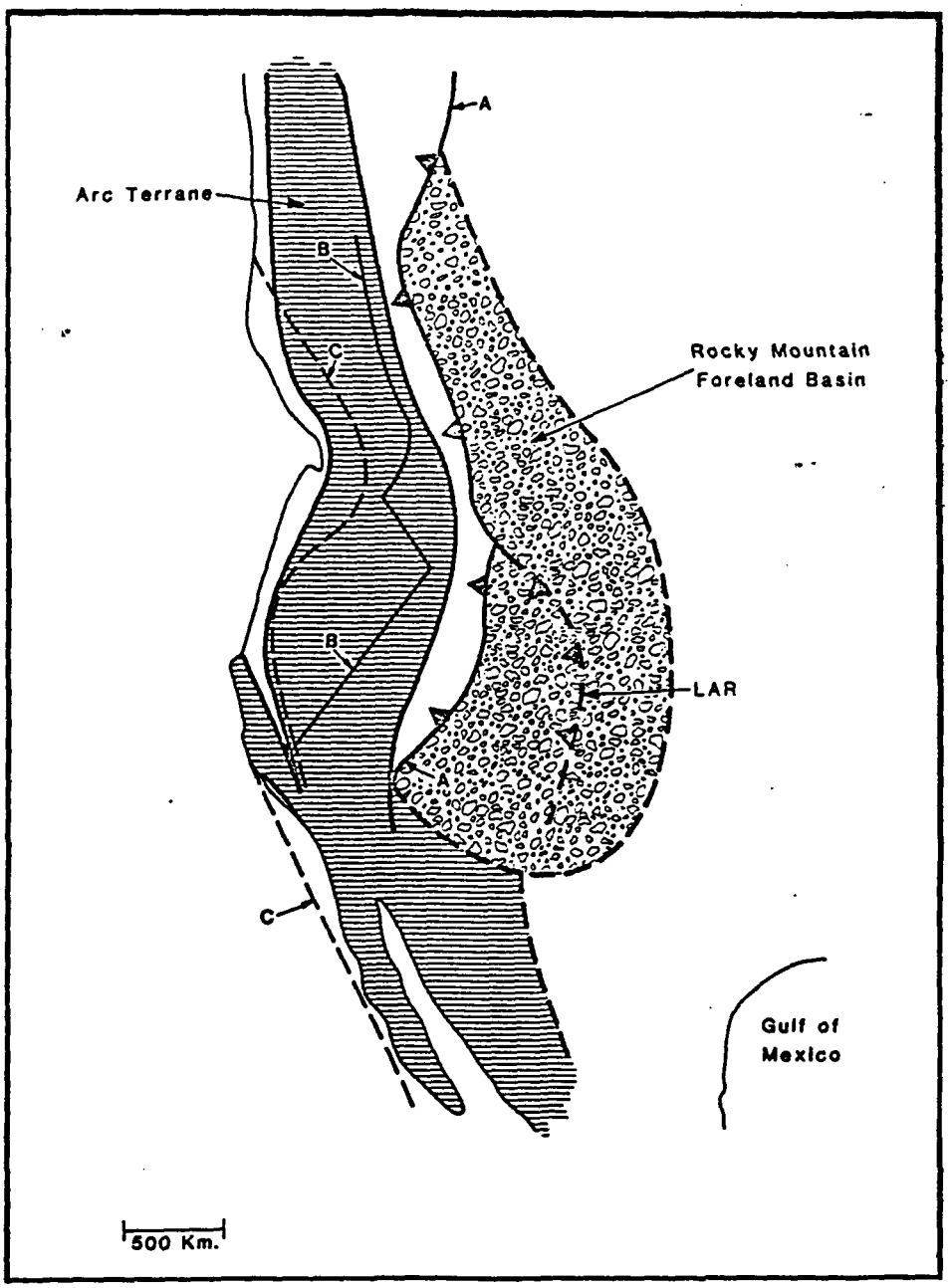

Figure 2-1. Diagrammatic sketch map of western North America showing selected key Cordilleran tectonic elements. Arc terrane is the main core belt of post-Triassic origen related to subduction of oceanic lithosphere beneath the continental margin. Line A denotes main backarc fold-thrust belt; Laramide front (LAR) is shown where it broke part of the foreland basin; line B is the edge of rifted Precambrian basement along the pre-Devonian continental margin; and Line C is edge of continental crust prior to initiation and evolution of the Cordilleran continental-margin arc-trench system. (from Dickinson, 1976)

enden and others, 1972; Stewart, 1972). A key component of this Windemere succession along the whole length of the Cordillera is a unit of tillites and glaciomarine turbidites. Part of a diamictite-volcanic sequence, this unit occurs at or near the base of the uppermost Precambrian rocks throughout westernmost North America from Alaska to California, with potassium-argon ages between 827 and 918 my on a greenstone member in northeastern Washington (Miller and others, 1973). This is the oldest unit that has a depositional pattern related to the Cordilleran geosyncline. A major change in the tectonic pattern of North America appears to have been initiated shortly before the deposition of the diamictite, and this change is inferred to mark the beginning of the geosyncline (Stewart, 1972).

The Cordilleran geosynclinal rocks described in this section range in age from latest Precambrian to late Devonian and consist of miogeoclinal carbonate and transitional assemblage rocks and of eugeoclinal siliceous assemblage rocks within the Great Basin. In general, these strata are well-sorted chemically mature sediments produced along an Atlantic-type continental margin (Figure 2-2a). At least half of the thickness of lower Paleozoic and uppermost Precambrian geosynclinal deposits are uppermost Precambrian and lower Cambrian quartzite and siltstone, and lesser carbonate rock and conglomerate. Because of the uncertainty in the Precambrian-Cambrian boundary (Stewart and Suczek, 1977), this terrigenous detrital sequence, which thickens westward, or northwestward from 300 m at about the Wasatch Line to locally as much as 7,500 m will be considered as a unit.

Three facies of the uppermost Precambrian and lower Cambrian rocks are generally recognized: (1) a quartzite and siltstone facies in the eastern Great Basin; (2) a siltstone, carbonate, and quartzite (transitional) facies in the central Great Basin; and (3) a siliceous and volcanic facies in the western Great Basin. The eastern and transitional facies comprise the terrigenous detrital sequence.

The eastern facies (Merriam and Anderson, 1942) or Millard belt (Kay, 1951) is miogeoclinal and consists mostly of thick cliff-forming fine- to medium-grained quartzite units ranging in composition from arkose to orthoquartzite (Stewart, 1970) separated by units of siltstone. Conglomerate, limestone and dolomite units are also present in thin layers (less than 30 m thick). Mafic volcanic flows and

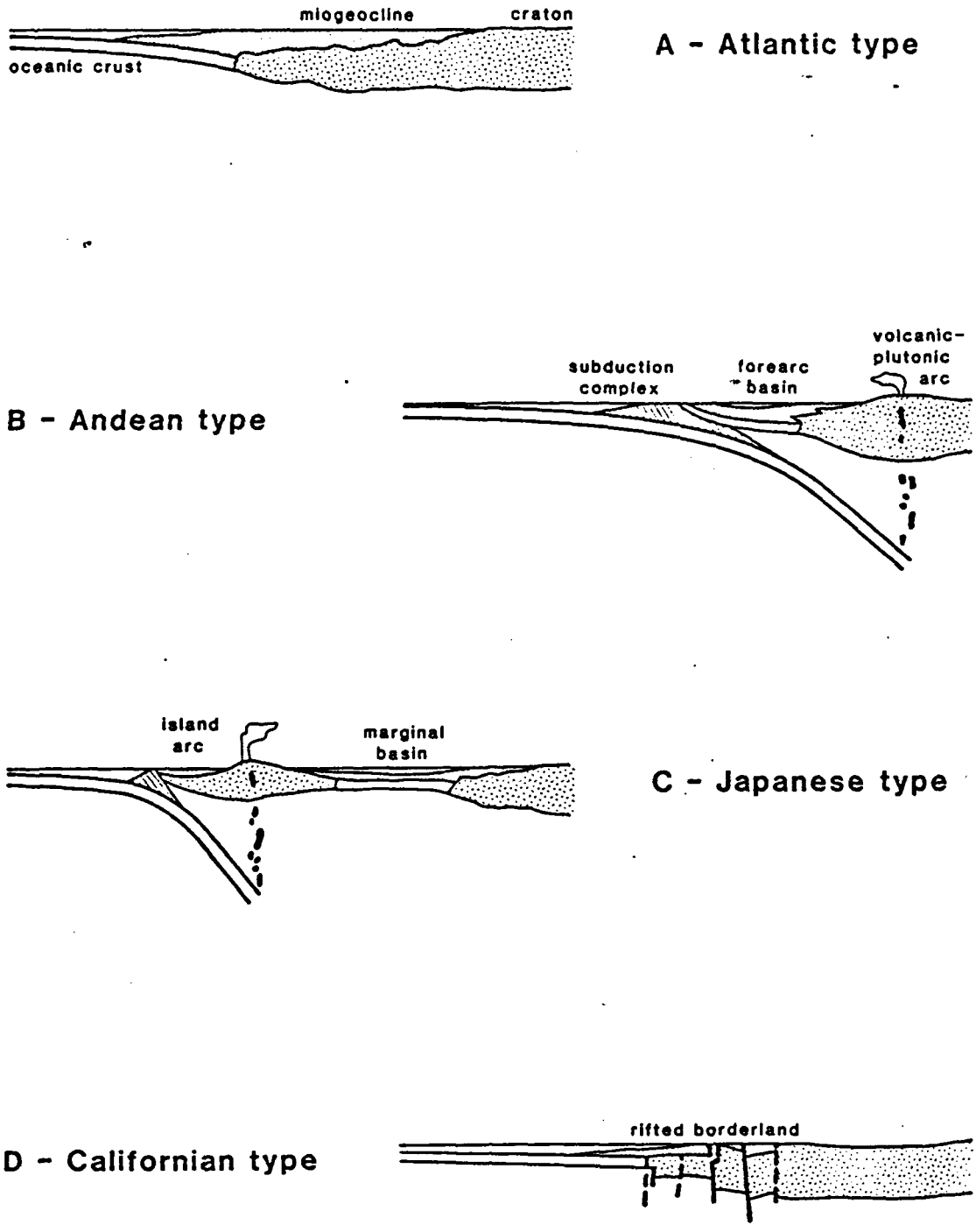

Figure 2-2. Diagrammatic sketch of the four major types of continental margins showing crustal topologies: (A) Atlantic type, divergent margin; (B) Andean type, convergent margin; (C) Japanese type, convergent margin; and (D) Californian type, transform margin. (from Ernst, 1979; after Dickinson, 1976)

breccias occur in this facies in the eastern Great Basin (Stewart, 1972, 1974). One mafic volcanic breccia in Utah is radiometrically dated as 570 my old (Crittenden and Wallace, 1973). The transitional siltstone, carbonate, and quartzite facies in central Nevada and southeastern California is thick and fossil-rich. It contains large amounts of siltstone (or phyllitic siltstone), thin to thick units of limestone and dolomite, and fine- to very fine-grained quartzite (Nelson, 1962; Stewart, 1970; Albers and Stewart, 1972). Fossils, including trilobites, archeocyathids, pelecypods, Hyolithes, Salterella, Skolithus, and algae indicate a Cambrian age from 650 (?) to 540 my (Palmer, 1971; Stewart, 1970; Nelson, 1976). The terrigenous detrital sequence is dominantly of shallow-water origin as indicated by an abundance of algae and archeocyathids and by the local occurrence of mudcracks, raindrop imprints, and runzel marks (Barnes and Klein, 1975; Klein, 1975) that indicate local exposure. Herringbone cross stratification, reactivation surfaces, superimposition of current ripples on larger current ripples, flaser and lenticular bedding, and other sedimentary structures as well as trace fossils indicate that sediments deposited by tidal currents occur in some units (Stewart, 1970; Barnes and Klein, 1975; Klein, 1975).

The siliceous and volcanic facies in the western Great Basin is identified in one locality near Battle Mountain and is represented by the Scott Canyon Formation (Roberts, 1964). It is allochthonous, known only in fault contact with both overlying and underlying units, and probably was transported eastward at least 80 km by the end of the Devonian-early Mississippian Antler Orogeny. It is composed of several thousand meters of chert, argillite and greenstones and minor amounts of sandstone, quartzite, and limestone (Roberts, 1964; Theodore and Roberts, 1971). The greenstone includes flows, which are in part massive and in part pillow lavas, and pyroclastic rocks ranging from fine tuffs to coarse breccias. Originally, these flows were probably mafic andesites or basalts, with subsequent alteration typical of volcanic rocks that have been extruded in a submarine environment (Roberts, 1964). The limestone occurs in lenses and contains algae, sponges, archeocyathids, and trilobites considered to be early or middle Cambrian in age. However, radiolaria in chert have been ten-

tatively assigned a Devonian age by Brian Holdsworth (Stewart and Suczek, 1977) suggesting that the Scott Canyon may consist of structurally interleaved rocks of at least two ages, a structural relation commonly mapped in other eugeosynclinal terranes in Nevada (Stanley and others, 1977). The exact age relations of the various parts of the Formation are not presently known. The Scott Canyon Formation may be a relatively deep-water oceanic deposit (Stewart and Poole, 1974). However, fossil material such as algae and archeocyathids is indicative of shallow-water origin. This anomaly may be explained as occurring in slump deposits or in structurally interleaved shallow-water layers in a predominantly deep-water deposit. Alternatively, the shallow-water deposits could have been on the flanks of oceanic volcanoes.

The type and distribution of Precambrian and lower Cambrian sediments are related to the tectonic setting of western North America during that time period. Two continental terrace wedge accumulations, the Belt-Purcell Supergroup and the Windemere Group and conformable Paleozoic strata (the Cordilleran miogeosyncline) may require two periods of continental rifting: one between 1400 to 1450 my ago and 1600 to 1700 my ago (Gabrielse, 1972) and the second approximately 850 my ago (Stewart, 1972, 1976). Whether initial Precambrian rifting was pre-Belt or pre-Windemere, by the beginning of Cambrian time the continental margin along western North America was reshaped and was the site of initial Cordilleran miogeoclinal deposition. Stewart and Suczek (1977) incorporate the concept that the Windemere deposits may have accumulated locally in rift-valley basins that formed prior to the main stage of rifting. The time of these events is poorly known, but rift valleys may have formed from 800 to 900 my ago and the main rifting event not until perhaps 650 my ago. In this setting, the terrigenous detrital sequence is related to erosion of the initial bulge or uplifted area created by thermal expansion during continental rifting (Figure 2-3). Rocks older than the rifting episode(s) would have been removed by rifting; the various detached fragments separated by suture belts may lie within the composite modern continent of Eurasia (including Alaska) (Dickinson, 1979).

The cessation of deposition of terrigenous detritus in the miogeocline by the end of early Cambrian time is related to the destruction of the bulge by thermal contraction due to cooling and by erosion.

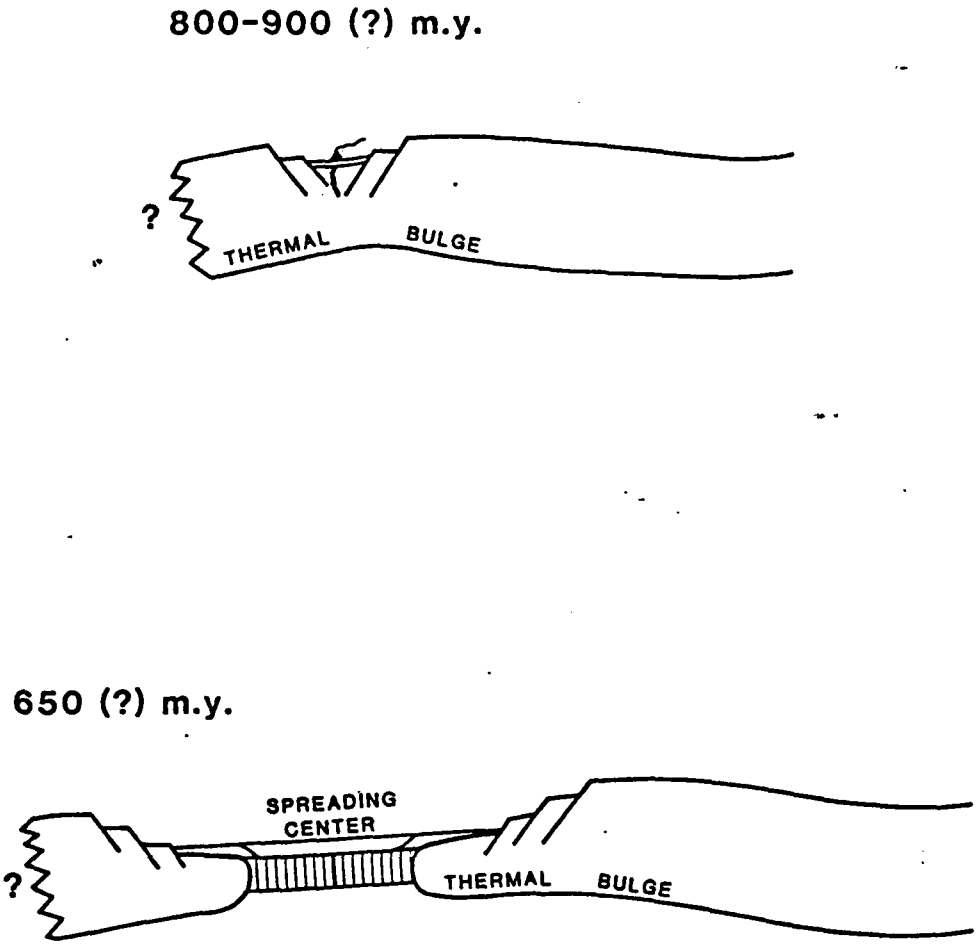

Figure 2-3. Diagrammatic sketch of late Precambrian and Cambrian development of western North America. Note the thermal bulge associated with the rift. (from Stewart and Suczek, 1977)

The ocean then transgressed eastward into cratonic areas. As a consequence, coarse detrital material was trapped in coastal areas on the craton and the miogeoclinal shelf was an area of carbonate deposition relatively free of detrital material. Figure 2-4 depicts the distal margin of the Precambrian basement (Dickinson, 1979). The location of the rifted continental margin transecting the Great Basin suggests that Precambrian age deposits are not present in western Nevada, and in particular, in Dixie Valley. The Scott Canyon Formation, as discussed above, may represent post-rifting Cambrian and younger Paleozoic deposits rather than a Precambrian eugeosynclinal sequence.

2.2.2 Paleozoic

2.2.2.1 Cambrian - Devonian (Antler Orogeny)

During the Cambrian, seas continued to transgress the continent and by late Cambrian they extended 600 to 1000 km east of the margin of the miogeocline, and much of the western United States was a shallow sea. Based upon unit thicknesses and sedimentary facies distributions, the ancient Pacific continental margin of North America extended from southern-most Idaho southward into southeastern California (Figure 2-5) prior to the end of the late Devonian-early Mississippian Antler orogeny (Burchfiel and Davis, 1972; Stewart and Poole, 1974; Stewart and Suczek, 1977). The onlapping sediments thicken from about 1 km on the southeast to almost 10 km on the north and northwest.

Development of the miogeocline culminated in the formation of a major oceanic basin by sea-floor spreading by Ordovician time. In late Ordovician or Silurian, westward subduction of this oceanic basin formed a volcanic arc -- the Klamath-Sierra arc. The continental margin had a Japanese-type configuration (Figure 2-2c), with a complicated offshore pattern of marginal seas and intra-oceanic island arcs (Figure 2-5) (Burchfiel and Davis, 1972; Monger and others, 1972; Silberling, 1973; Churkin, 1974). As subduction continued and the arc migrated eastward toward the continent, a lower Paleozoic accretionary wedge was formed.

During the middle to late Devonian, arc volcanism stepped eastward onto the accretionary wedge. The Antler orogeny marked the culmination of arc-continent collision as the leading edge of the accre-

The ocean then transgressed eastward into cratonic areas. As a consequence, coarse detrital material was trapped in coastal areas on the craton and the miogeoclinal shelf was an area of carbonate deposition relatively free of detrital material. Figure 2-4 depicts the distal margin of the Precambrian basement (Dickinson, 1979). The location of the rifted continental margin transecting the Great Basin suggests that Precambrian age deposits are not present in western Nevada, and in particular, in Dixie Valley. The Scott Canyon Formation, as discussed above, may represent post-rifting Cambrian and younger Paleozoic deposits rather than a Precambrian eugeosynclinal sequence.

2.2.2 Paleozoic

2.2.2.1 Cambrian - Devonian (Antler Orogeny)

During the Cambrian, seas continued to transgress the continent and by late Cambrian they extended 600 to 1000 km east of the margin of the miogeocline, and much of the western United States was a shallow sea. Based upon unit thicknesses and sedimentary facies distributions, the ancient Pacific continental margin of North America extended from southern-most Idaho southward into southeastern California (Figure 2-5) prior to the end of the late Devonian-early Mississippian Antler orogeny (Burchfiel and Davis, 1972; Stewart and Poole, 1974; Stewart and Suczek, 1977). The onlapping sediments thicken from about 1 km on the southeast to almost 10 km on the north and northwest.

Development of the miogeocline culminated in the formation of a major oceanic basin by sea-floor spreading by Ordovician time. In late Ordovician or Silurian, westward subduction of this oceanic basin formed a volcanic arc -- the Klamath-Sierra arc. The continental margin had a Japanese-type configuration (Figure 2-2c), with a complicated offshore pattern of marginal seas and intra-oceanic island arcs (Figure 2-5) (Burchfiel and Davis, 1972; Monger and others, 1972; Silberling, 1973; Churkin, 1974). As subduction continued and the arc migrated eastward toward the continent, a lower Paleozoic accretionary wedge was formed.

During the middle to late Devonian, arc volcanism stepped eastward onto the accretionary wedge. The Antler orogeny marked the culmination of arc-continent collision as the leading edge of the accre-

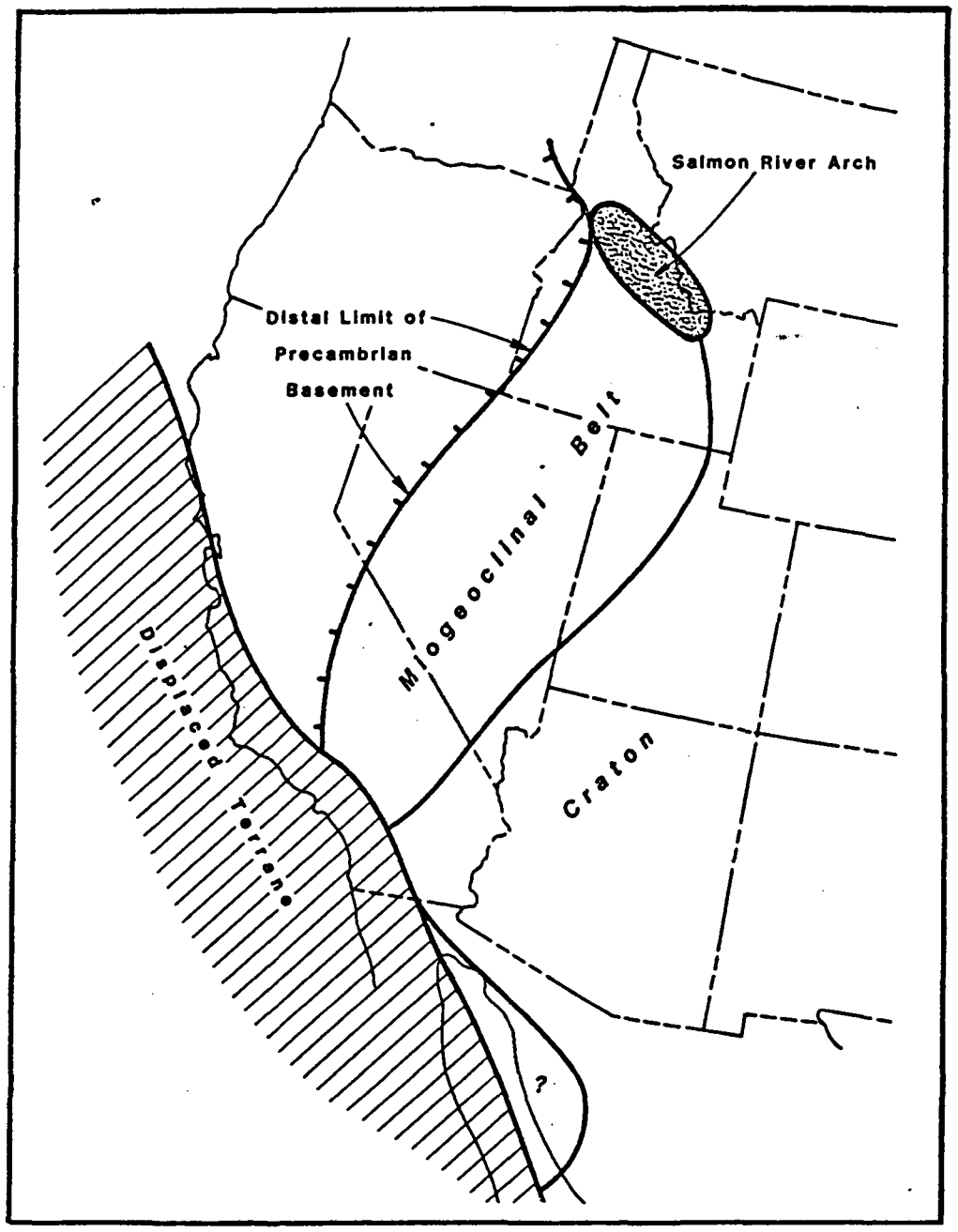

Figure 2-4. Diagrammatic sketch of early Paleozoic Cordilleran rifted continental margin. Note the location of the distal limit of Precambrian basement. (from Dickinson, 1979)

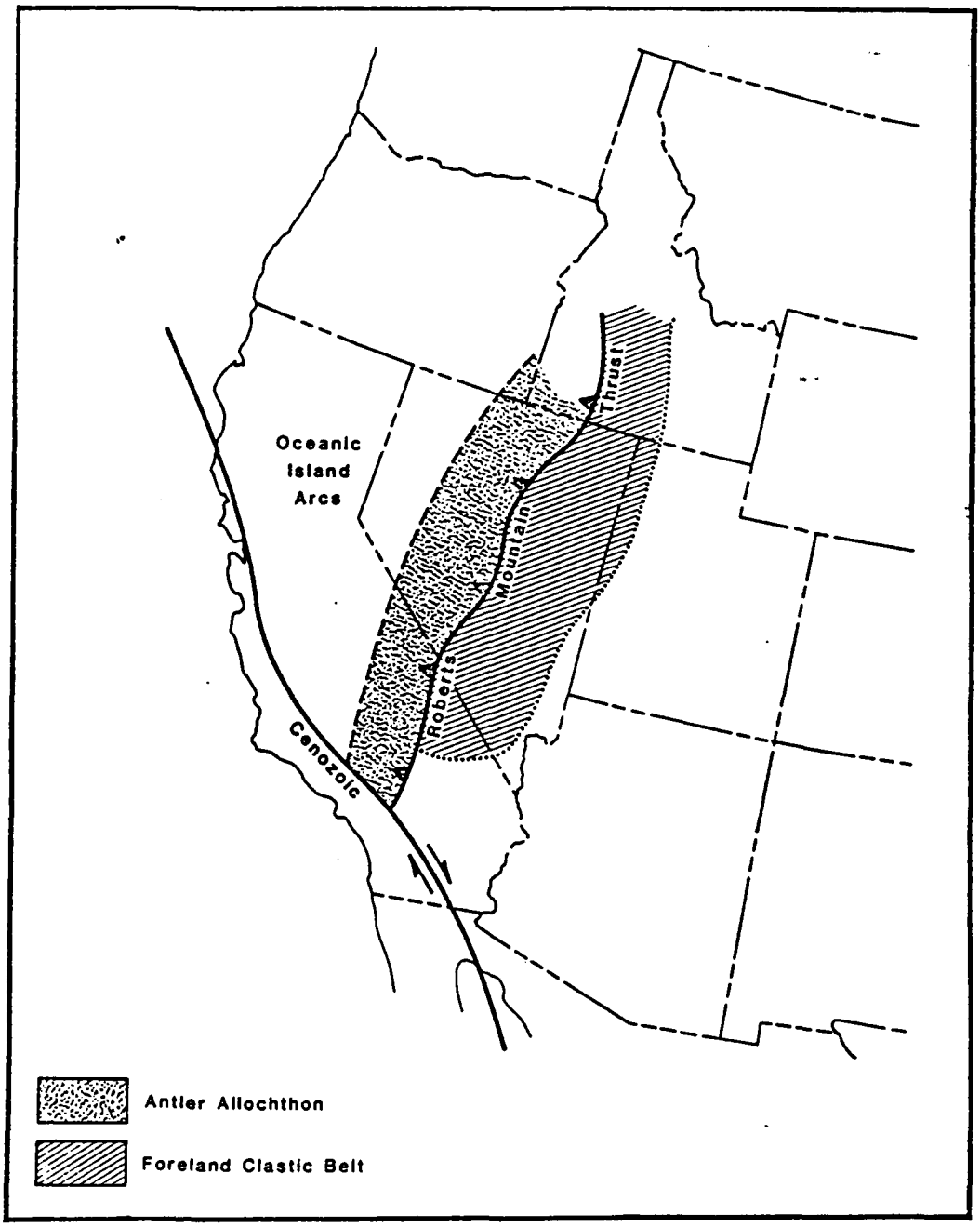

Figure 2-5. Generalized plate tectonic setting of California and Nevada during the Antler Orogeny. (from Ernst, 1979)

tionary wedge was thrust over the continent along the Roberts Mountains Thrust (the Harmony and Valmy-Vinini Formations in Nevada), bringing volcanogenic argillites of a subduction complex over an autochthonous miogeoclinal sequence (Stewart and Poole, 1974).

The upper Cambrian Harmony Formation originated as a sequence of turbidity flows in an extensive subsea fan complex on ocean floor west of the Cordilleran miogeocline (Suczek, 1977a,b). The sediments are believed to have been derived from the Salmon River arch, 400 km north (Stewart and Suczek, 1977). Underlain by upper Cambrian Paradise Valley Chert, both units were deposited as a fan complex on an abyssal plain floored by pelagic siliceous sediments.

The Valmy (Roberts, 1964; Gilluly, 1967; Gilluly and Gates, 1965) consists of conspicuous ledge-forming, poorly sorted quartzite and chert, with significant amounts of shale and greenstone. Numerous thrust fault slicing may account for the lack of lithologic continuity (Gilluly, 1967; Gilluly and Gates, 1965). Both the Valmy and the Vinini, a similar less quartzitic, more shaley unit to the east, include Ordovician and appreciable Devonian strata (Stanley and others, 1977; Jones and others, 1978). Schweikert and Snyder (1979) believe that the Valmy and Vinini should be regarded not as formations, but rather as tectonostratigraphic units that contain various lithologies that could range in age from Eocambrian to Devonian. Late Cambrian to Devonian deposition in the ocean basin produced pelagic and hemiterrigenous sediments, while carbonate and shale predominated in the miogeocline.

In order to close the extensive Eocambrian to Devonian ocean basin, the arc must have had reversed polarity (Figure 2-6) and faced southeastward, with the Roberts Mountains assemblage as part of an immense accretionary prism developed on the eastward side of the arc prior to collision (Dickinson, 1977, 1979; Schweikert and Snyder, 1979). Thus the stacking order of thrust sheets within the Roberts Mountains assemblage is related to the incorporation of successive packets of strata within the accretionary wedge during pre-collision subduction; higher structural units were accreted earlier and thus carried farther eastward than lower structural units. In the Shoshone, Galena and Sonoma Ranges, upper Cambrian Harmony generally occupied the highest post-Antler structural position, thrust over the Valmy-Vinini, which in turn was

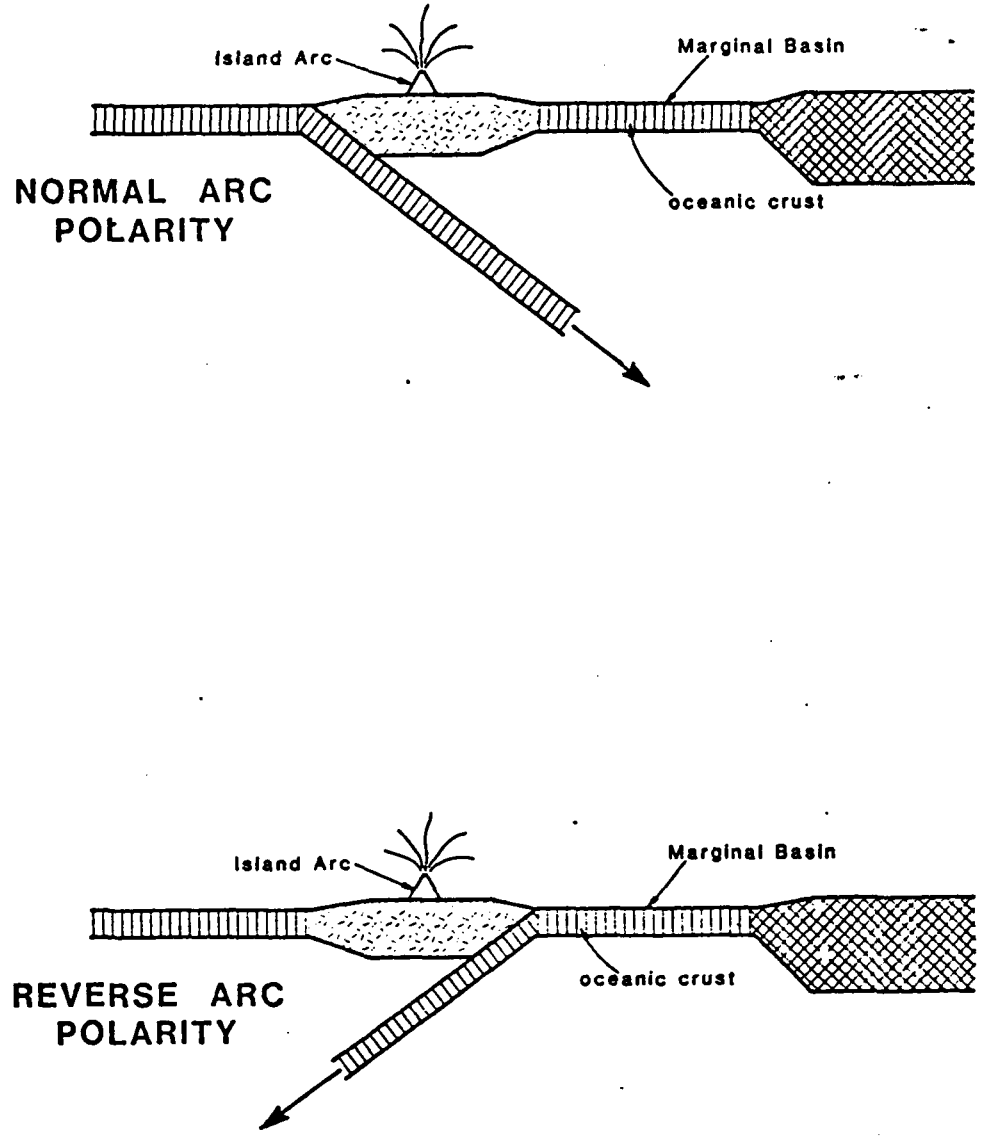

Figure 2-6. Diagrammatic sketch of normal arc polarity and reverse arc polarity relative to origin of oceanic marginal basins. (from Dickinson, 1977)

thrust over generally younger formations (Devonian Slaven Chert, Silurian Elder Sandstone) (Gilluly and Gates, 1965; Roberts, 1964; Silberling, 1975).

The location of pre-Ordovician oceanic crust remains a question. Since the Valmy-Vinini were probably deposited closer to the craton than the Harmony (i.e., farther from the rift), they presumably accumulated on older oceanic crust. The greenstone and quartzite within the Valmy-Vinini could be Cambrian or even Eocambrian in age, as they have not yet been dated (Schweikert and Snyder, 1979).

An island arc was active during Ordovician-Silurian time in order for westward subduction to occur. This arc and a related subduction sequence may be represented by the Alexander terrane. Paleomagnetic data of M. Jones and others (1977) very strongly supports the suggestion of D. L. Jones (1977) and Schweikert (1976, 1978) that the Alexander terrane in southeast Alaska, which contains abundant arc-like volcanic rocks of Ordovician, Silurian and Devonian ages (Churkin and Eberlein, 1977) was at or near the latitude of northern California during Ordovician and Silurian time.

Figure 2-7 depicts the early Paleozoic tectonic history for west-central North America. Subduction began beneath the Klamath-Sierra arc in late Ordovician or Silurian time (Figure 2-7A), with the incorporation of the Trinity ultramafic sheet into a nascent accretionary prism. During this interval, pelagic and hemiterrigenous sediment (in part the Valmy-Vinini) blanketed the ocean basin between the miogeocline and the arc. As subduction continued, the Harmony fan and the Valmy-Vinini were tectonically shuffled (thrust?) into a very large accretionary wedge (Figure 2-7B). This wedge formed the basement for arc volcanism which had stepped eastward by mid-Devonian. The Antler Orogeny marked the culmination of arc-continent collision. During the Antler Orogeny, the marginal basin closed, and the island arc was accreted to the continent, producing the Antler orogenic belt and foreland basin (Poole, 1974). Dickinson (1977) suggests westward consumption of the marginal basin, whereas Burchfiel and Davis (1975) explain a process of eastward plate descent involving uncoupling and overthrusting (obduction) of the island arc superstructure. The edge of the continent was partially subducted, causing the leading edge of the accretionary wedge to over-ride along the Roberts Mountains Thrust. Siliceous vol-

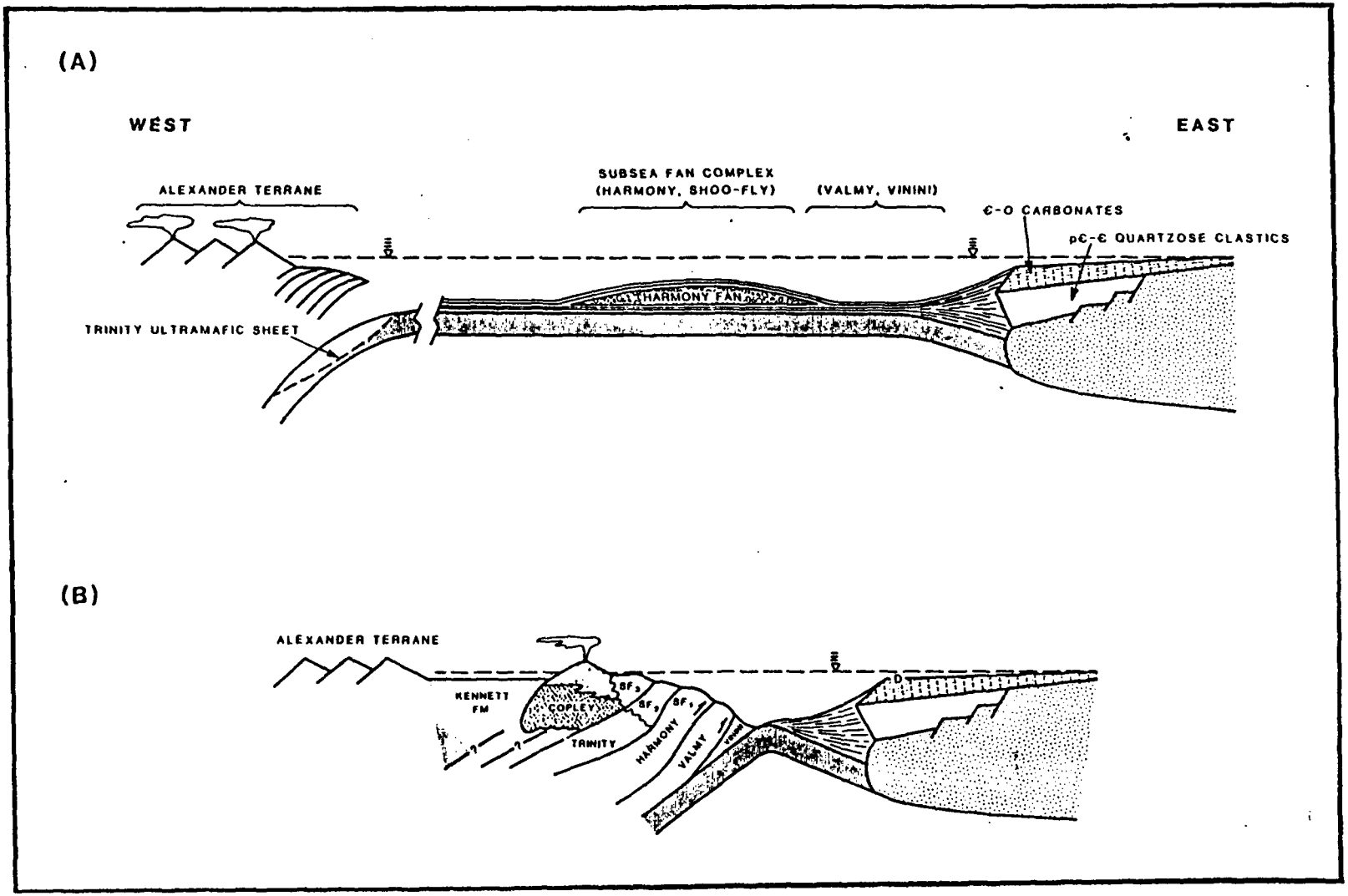

Figure 2-7. Schematic cross-section of early Paleozoic plate tectonics in late Ordovician.-Silurian time (A) and in Devonian time (B). (from Schweikert and Snyder, 1979)

canism (Sierra Buttes Formation) occurred during this event. The Roberts Mountains Thrust was not a geologically instantaneous cataclysmic event, but the result of a slow, passive, accretionary process. The last 80 km of forward growth may have taken much of the Devonian and part of the Mississippian. In one locality, forward growth stopped at about the end of the Devonian (Smith and Ketner, 1968), but farther north, it continued in early Mississippian time (Ketner, 1970).

2.2.2.2 Mississippian - Pennsylvanian

Closely following the Antler Orogeny, the arc polarity reversed to a westward facing direction (Figure 2-6), and "normal" island arc andesitic subduction initiated back-arc spreading creating a marginal basin. Unlike the present-day Japanese-type arcs (Figure 2-2c) which face the subducting oceanic plate, these island arcs faced the North American Plate reflecting westward underflow of the marginal basin. Sediments of the Havallah sequence accumulated in the eastern portion of the basin and a thick volcaniclastic wedge (the base of the Calaveras Complex; Schweikert, 1979) formed on the arc-side. The Havallah sequence was deposited on structural remnants of the Roberts Mountains assemblage and on new oceanic crust formed between the rifted blocks. With continued back-arc spreading and marginal basin growth, olistostromes of chert and argillite, with rare lenses of greenstone and shallow-water limestone, were shed (from the Peale Formation?) into the deeper parts of the basin. Portions of the arc during Mississippian and Pennsylvanian time were apparently characterized by volcanic quiescence as the cherts of the Peale formation were deposited (Schweikert and Snyder, 1979). Early Permian faunas, one typical of the arc and one typical of the miogeocline (Stewart and others, 1977) occur in limestone olistoliths in the Havallah, suggesting that portions of the marginal basin, particularly in the north, were relatively narrow (Schweikert and Snyder, 1979). The marginal basin was thus composed of some rifted remnants of the Roberts Mountains assemblage of lower Paleozoic age in addition to upper Paleozoic oceanic crust, pelagic and clastic sediments.

By early Pennsylvanian time deposition of thick sequences of sand, gravel and mud that had filled the Antler foreland trough had nearly ceased (Roberts and others, 1958; Poole, 1974). In northern Nevada,

siliceous detritus continued to form local deposits until middle Pennsylvanian. On a regional scale, however, the early and middle Pennsylvanian are characterized by cherty limestone essentially free of detrital sediment. This limestone can be identified by various local names, but probably formed a nearly continuous sheet of uniform lithology over a very extensive area. Near the end of Pennsylvanian time, then, the western Basin and Range area was one of a tranquil sea broken by small, sparse insular remnants of the Antler Orogenic highland belt.

2.2.2.3 Permian

Facies and isopachous trends for miogeoclinal and cratonal rocks of late Precambrian and Paleozoic age can be projected southwestward across the California-Nevada border. However, the few small exposures of Paleozoic or probable Paleozoic rocks present in the western Mojave and southern Sierra Nevada regions are not counterparts of the units projected toward their locations from the northeast. A number of explanations have been offered to explain the distribution of these "out-of-place" Paleozoic units. Poole (1974), Poole and Sandberg (1977) and Poole and others (1977) attribute the irregular trend and distribution of the Antler orogenic belt (Roberts Mountains assemblage) between southern California and western Nevada to dextral oroclinal bending of Mesozoic and Cenozoic age. Dickinson (1979) concludes that the irregular trend of the Antler orogenic belt between the two regions may be a consequence of an initially irregular pattern of rifts and transform faults that outlined the western margin of the continent in late Precambrian time.

Three differing--but not totally inconsistent and exclusive--interpretations are provided by Dickinson (1977), Ketner (1977) and Burchfiel and Davis (1979) for the Permian in western North America that relate to the distribution of both structural trends and stratigraphic sequences.

Dickinson (1977) has proposed an episode of Carboniferous rifting as an explanation for the termination of the Antler foreland basin. He states that evolution of the foreland basin was anomalous in that the phase of flysch deposition was not succeeded by a phase of molasse deposition, but instead by shelf conditions. The presence of turbidites in the Death Valley region, the presence of Permo-Penn-

sylvanian oceanic assemblages in the Golconda allochthon, and mid-Carboniferous terrestrial and marine strata unconformably overlying the Roberts Mountain allochthon are given among the supporting data for this episode of rifting.

Ketner (1977) identifies the Humboldt Orogeny as a regional tectonic uplift beginning in late middle Pennsylvanian and persisting through Permian time that produced a north-trending belt of highlands (Figure 2-8). The Humboldt highland belt was a range of islands and shoals that extended northward from southern California through Nevada and Idaho and probably into western Canada. The distribution of orogenic sediments indicates that the belt was at least a thousand kilometers in length; the volume of orogenic sediments suggests the belt was comparable to a large mountain range, such as the present-day Sierra Nevada. Sediments shed eastward from this belt were deposited in a shallow epicontinental sea (Phosphoria sea) and are mingled with limestone, dolomite, evaporites, spicule chert, and phosphorite; those shed westward were deposited in deeper water as debris flows and turbidites, and mingled with coarse volcanic sediments, tuffs, lava flows, and radiolarian cherts. The volcanic sediments, tuffs, and lavas emanated from an island-arc that lay parallel to, and a short distance west of, the tectonic belt. Along the southern Nevada-California border, where Paleozoic facies boundaries and the Antler belt trended northeast, the Humboldt highland tectonic belt trends northwest, transecting the entire width of the Cordilleran sedimentation belt (Figure 2-8). Through central Nevada, the axis of this belt parallels the distal margin of the Precambrian North American continent, and succeeding Paleozoic trends.

Burchfiel and Davis (1979), however, propose that the distribution of outcrops of Precambrian through Paleozoic rock assemblages (including Roberts Mountain and overlying upper Paleozoic clastic wedge sediments) in southern California is a result of southward displacement along a major fault sliver or slivers. Attendant faulting is considered to represent the left-slip truncation (Davis and others, 1978) of a part of the North American continental margin during Permo-Triassic time (Hamilton, 1969; Burchfiel and Davis, 1972, 1975). The sinuous trend of this continental block and its marginal faults (Figure 2-9) is the product of later Mesozoic and Cenozoic deformations and rota-

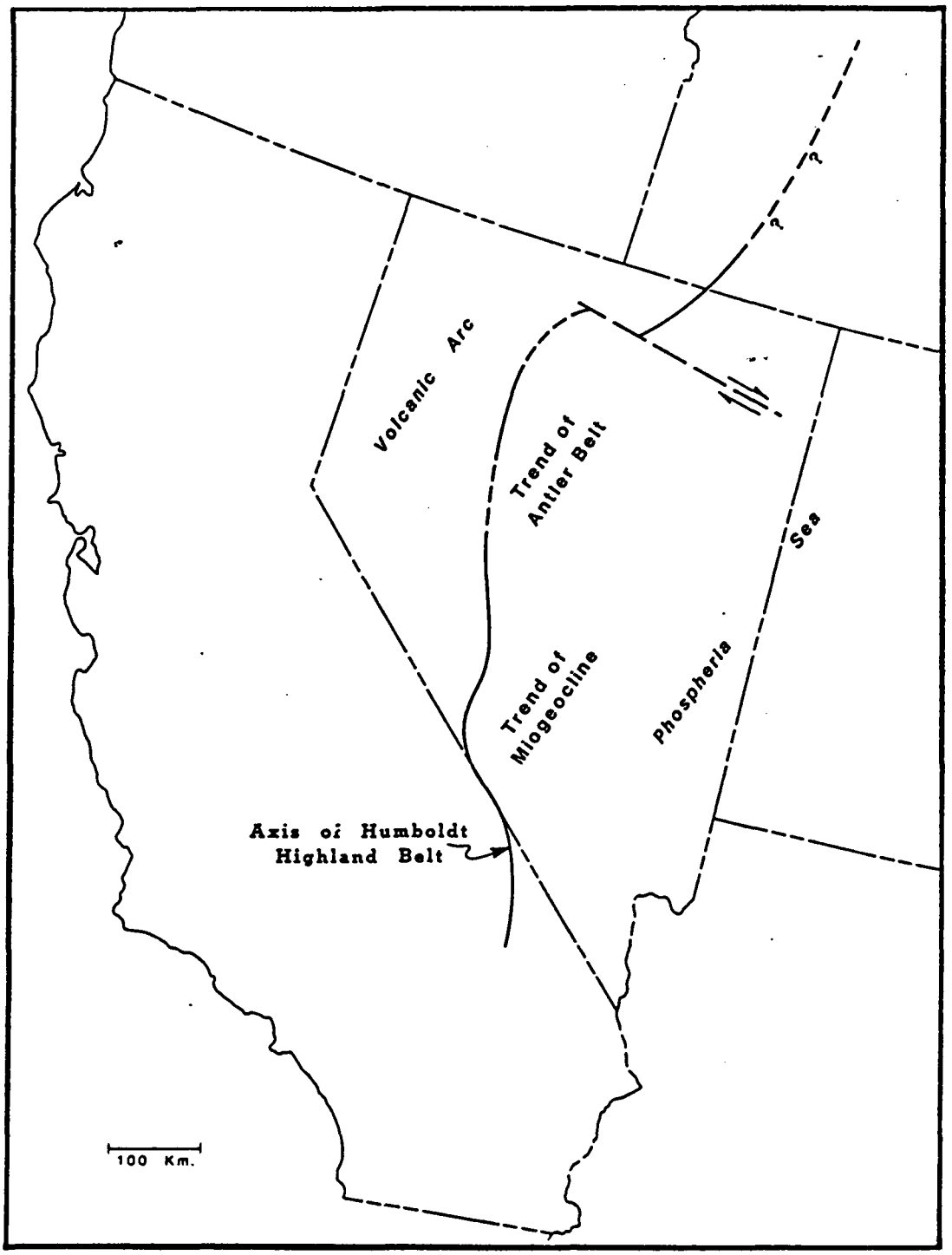

Figure 2-8. Diagrammatic sketch of Nevada showing position of the axis of the Humboldt highland belt in relation to the trend of the Antler Belt, the trend of the Cordilleran miogeocline, and the location of the Phosphoria sea. (from Ketner, 1977)

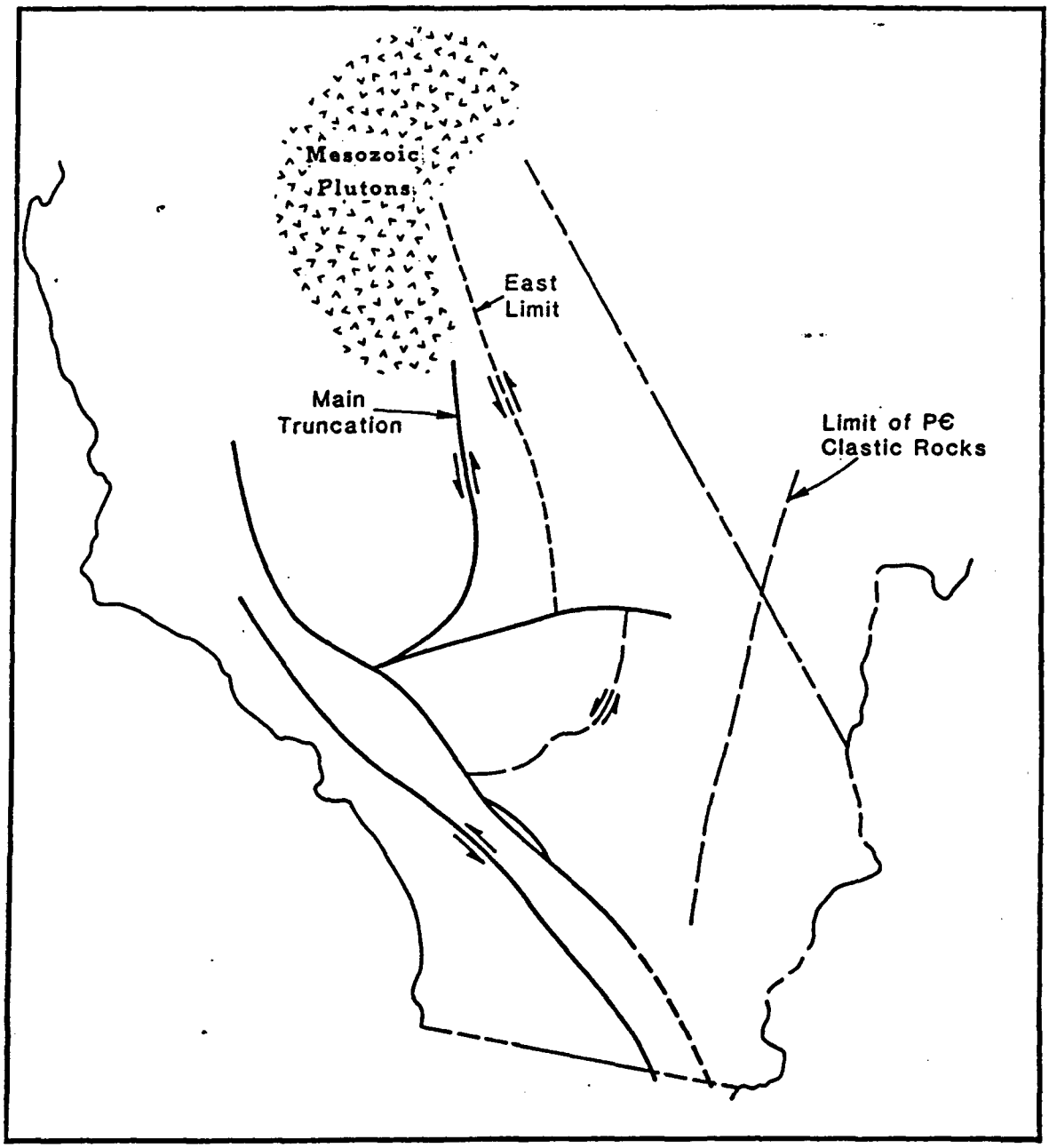

Figure 2-9. Diagrammatic sketch of southern California and Nevada showing location of the Permo-Triassic left-lateral truncation faults. Sinuous character of the faults is due to Cenozoic offsets. (from Burchfiel and Davis, 1979)

tions, with the northern extension of this zone obscured by younger Mesozoic plutonism. This truncation event must have occurred prior to the development of a Mesozoic marginal arc complex that cross-cuts Paleozoic geosynclinal and structural trends and must also pre-date the first phase of Mesozoic (Triassic) plutonic intrusion related to eastward subduction along a modified continental margin approximately 220 my ago (Evernden and Kistler, 1970; Silver, 1971). Lithologic and stratigraphic relationships, extensively discussed by Burchfiel and Davis (1972), in combination with the development of the Mesozoic arc and its associated volcanism thus place the time of continental truncation as middle to late Permian.

2.2.3 Mesozoic

2.2.3.1 Triassic (Sonoma Orogeny)

During the late Permian, the polarity of the island arc reversed again, and the arc began to subduct its own marginal basin. The Calaveras-Shoo Fly fault in California marks a deep-seated fault along which the island arc and its Paleozoic basement over-rode the marginal basin rocks of the Calaveras Complex during the initial phase of the Sonoma Orogeny. Eventually, the entire Calaveras-Havallah assemblage with numerous internal imbrications was obducted onto the continent as the Golconda allochthon. The Golconda thrust fault marks the maximum eastward extent of overthrusting of oceanic assemblages during the arc-continent collision of the Sonoma Orogeny (Figure 2-10).

In northwestern Nevada, the Sonoma orogen was sutured to the continent during mid-Triassic time (Silberling, 1973, 1975; Dickinson, 1977), being thrust across eroded remnants of the Antler allochton (Roberts Mountains assemblage). However, no prominent foreland basin formed to the east of the Sonoma orogen. Instead, local rapidly subsiding basins along the trend of the suture belt received thick clastic accumulations, such as the Auld Lang Syne Group (Burke and Silberling, 1973), in upper Triassic and lower Jurassic time.

In the western Great Basin (north-central Nevada), the rocks in the upper plate of the Golconda thrust are referred to as the Pumpernickel and Havallah Formations (Ferguson and others, 1951; Muller and others, 1951; Roberts, 1951). As originally defined at the type section in the Tobin Range (Muller and others, 1951), the Pumpernickel Formation is an assemblage of primarily greenstone, bedded chert, and argillite; and the Havallah is the overlying, presumably younger, assemblage of primarily bedded chert, quartzite, limestone, and argillite, locally with conglomerate. Stewart and others (1977), however, suggest that lithologic, stratigraphic, structural and faunal evidence indicate that the Pumpernickel and Havallah are not lithostratigraphic units but are instead tectonic successions of upper Paleozoic rocks.

In general, the Calaveras complex exhibits a greater degree of deformation and is more strongly metamorphosed than the Havallah. Similarly, the Leach Formation (Ferguson and others, 1951) in the East Range, west of the Tobin Range, consists of structurally interleaved Valmy and Havallah (Whitebread, 1978; Stewart and Carlson, 1976) and

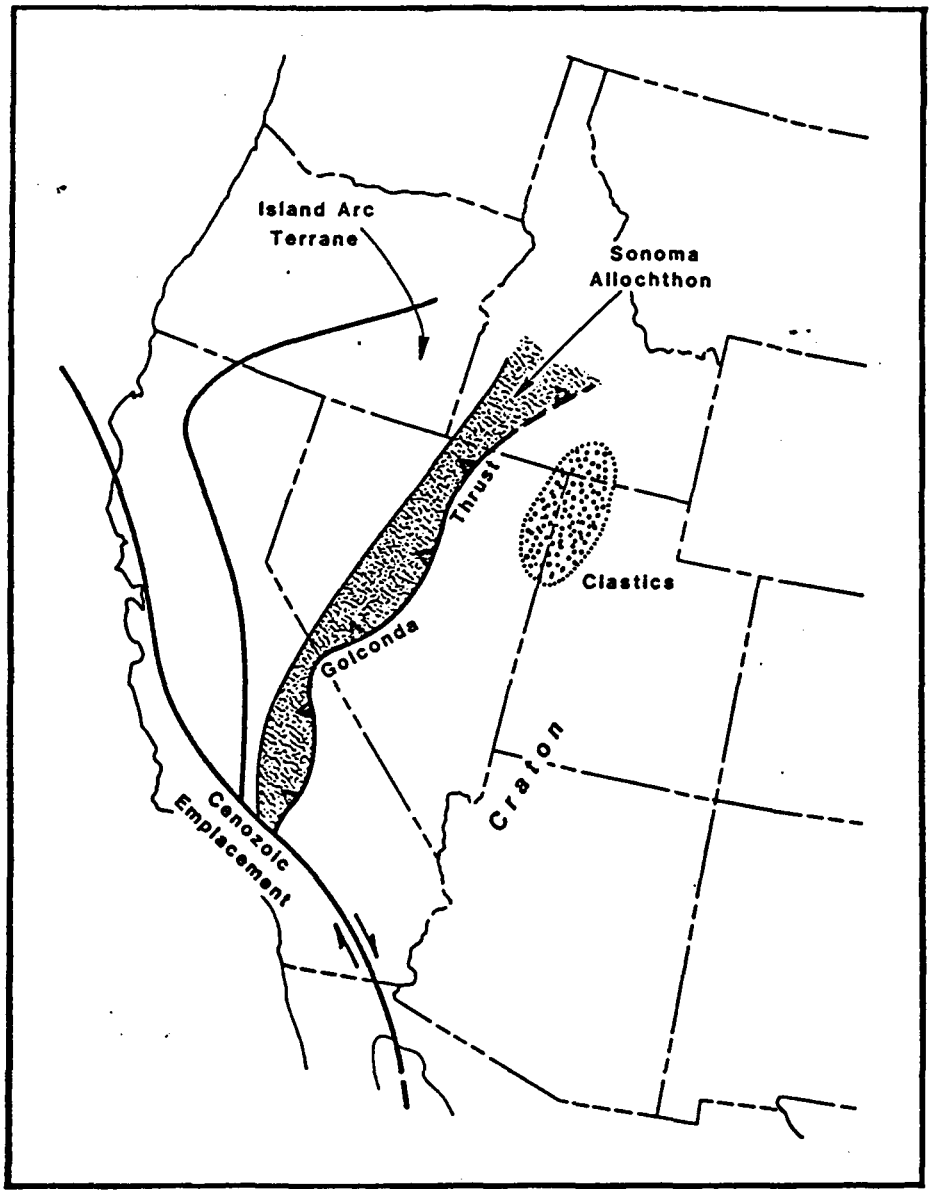

Figure 2-10. Generalized plate tectonic setting of California and Nevada during the Sonoma Orogeny. (from Ernst, 1979)

contains evidence of at least three episodes of deformation within the Sonoma Orogeny (Schweikert and Snyder, 1979). This distribution suggests that the grade of metamorphism and the degree of ductile deformation increased westward within the Golconda allochton toward the volcanic arc.

Melting within the siliceous sediments of the Havallah sequence may have produced the silicic pyroclastic rocks of the Koipato sequence, analogous to the Sierra Buttes Formation of the Antler Orogeny (Schweikert and Snyder, 1979; Dickinson, 1977). Burchfiel and Davis (1972, 1975) and Silberling (1973, 1975), however, interpret the Koipato as the earliest vestige of a continental margin magmatic arc established on the continental edge by polarity reversals following arc accretion during the Sonoma Orogeny.

The episode of continental accretion during the Sonoma Orogeny abruptly shifted the continental margin several hundred kilometers from central Nevada to the western or outer side of the former Klamath-Sierra arc terrane (Burchfiel and Davis, 1979b).

By late Triassic time, an Andean-type (Figure 2-2b) continental margin had developed. The western margin of the North American continent northward from the southern Sierras had become the site of oblique (?) plate convergence and transcurrent motion (transpression; Saleeby, 1979), eastward subduction of Pacific Ocean lithosphere, and widespread arc magmatism (Hamilton, 1969; Monger and others, 1972; Burchfiel and Davis, 1979b). This continental-margin arc-trench system (Dickinson, 1977) would persist into the early Tertiary and included the following tectonic elements from west to east: 1) subduction complex composed of imbricated wedges and melange belts of dislocated ophiolitic slices and disrupted oceanic sediments with overprints of blueschist metamorphism; 2) forearc basin of arc-derived clastics in simple stratigraphic and structural order; 3) magmatic arc composed at high structural levels of generally andesitic volcanics and volcaniclastics, with overprints of greenschist metamorphism, and at depth of granitic plutons, with higher grade thermal aureoles; 4) infrastructural belt of deep-seated dynamothermal metamorphism with the potential for associated anatectic plutons; 5) backarc fold-thrust belt of uplifted imbricate thrust sheets with decollement; and 6) retroarc foreland basin with exogeosynclinal

clastic wedges shed from orogenic highlands in the fold-thrust belt along its orogenic flank.

2.2.3.2 Jurassic - Cretaceous (Nevada and Sevier Orogenies)

Until middle Jurassic, the Cordilleran magmatic arc was an offshore island arc (Stanley and others, 1971; Monger and others, 1972) near the edge of the continental block with shelf seas behind it (Figure 2-11). The main shoreline met the arc near the southern limit of the present Great Basin. Local thrusts (Burchfiel and Davis, 1972, 1975) amd small plutons (Silberman and McKee, 1971; Armstrong and Suppe, 1973) in the Great Basin record the inception of a backarc fold-thrust belt, and possibly the initiation of an infra-structure belt. These structures propagated northward with time.

The subduction zone is well located only in California in the Sierra Nevada foothills (Schweikert and Cowan, 1975). The site of the subduction zone was stepped westward from the Sierra Nevada foothills (Figure 2-11) to a position in the Coast Ranges. Local evolution (westward migration) of the continental margin resulted from the tectonic accretion of island-arc structures to the continental-margin subduction complex following consumption of the intervening oceanic lithosphere (Schweikert and Cowan, 1975). By late Jurassic time, the magmatic arc in California had also stepped westward, with the shift of the subduction zone, to occupy the Sierra Nevada foothills.

During the Nevadan Orogeny in the western Great Basin, plutonic and volcanic activity generally parallels pre-Triassic trends. The eastern limit of Jurassic volcanic rocks (Burchfiel and Davis, 1972) roughly corresponds with the 118^{o} line of longitude in western Nevada. Small, local thrusts also developed within Paleozoic rocks and early Mesozoic back-arc sedimentary and volcanic rocks. Hamilton (1969) and Dickinson (1969, 1970) related the plutonic rocks of this pulse of activity (160 to 210 my ago; Lanphere and Reed, 1973) to the underflow of the oceanic plate along the Pacific margin.

The partly contemporaneous middle Jurassic to Cretaceous Sevier Orogeny (Figure 2-12) is characterized by an eastward migrating zone of back-arc fold-thrusting principally in the eastern Great Basin affecting Cordilleran miogeoclinal Paleozoic rocks. A pulse of plutonic activity (132 to 158 my ago; Lanphere and Reed, 1973) corres-

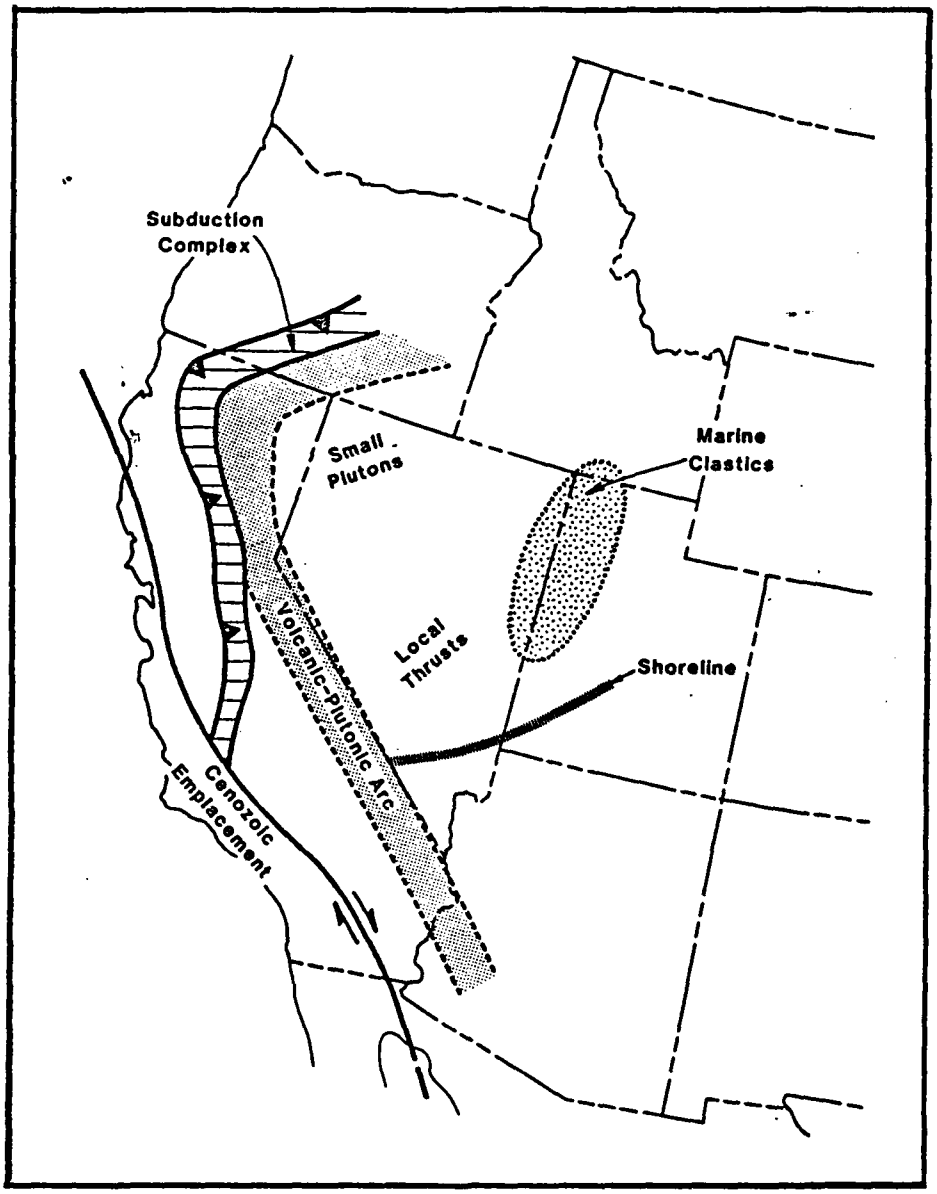

Figure 2-11. Generalized plate tectonic setting of California and Nevada during the Nevadan Orogeny. (after Dickinson, 1976; Ernst, 1979)

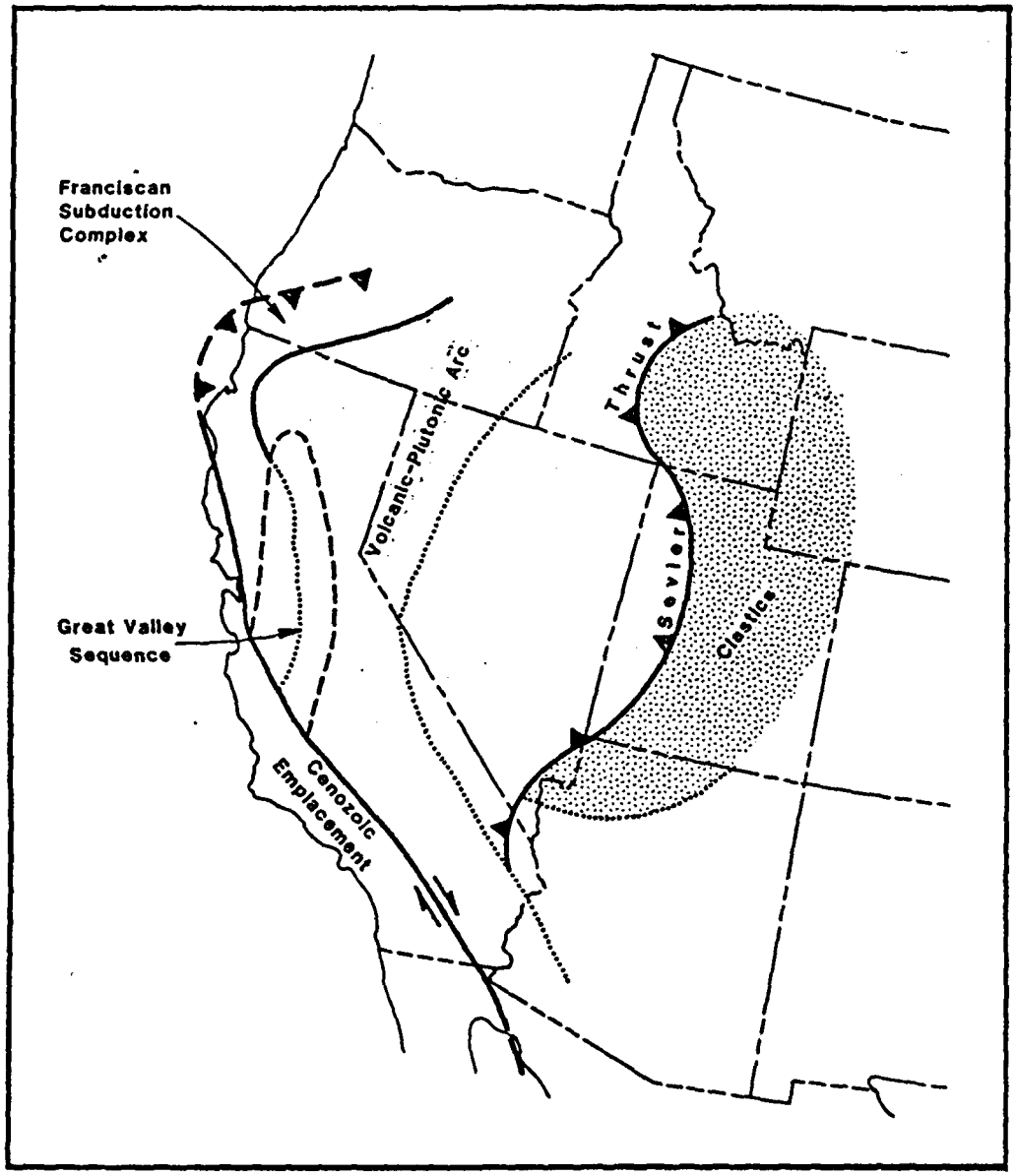

Figure 2-12. Generalized plate tectonic setting of California and Nevada during the Sevier Orogeny. (from Ernst, 1979)

ponds with the Sevier Orogeny. In general, this plutonism occurred farther eastward and northward of earlier Mesozoic intrusions.

By mid-Cretaceous time the magmatic arc had begun a retrograde migration (Dickinson, 1973) that continued throughout the Cretaceous and into the Tertiary. This trend is related to flattening of the Benioff Zone and entrainment of subducted slabs of Pacific lithosphere beneath the North American plate (Coney, 1973). Concurrent with retrograde movement of the arc, the subduction zone underwent prograde migration with accretionary growth of the Franciscan subduction complex. Thus, the arc-trench gap was progressively widened (Dickinson, 1973, 1977).

During the late Cretaceous both the retroarc foreland basin and forearc basin (Great Valley) achieved maximum extent. The arc-trench gap continued to increase. Locallized plutonic activity continued in Nevada, with five major intrusive episodes for the entire late Triassic to late Cretaceous time interval recognized in the Sierra Nevada (Kistler and others, 1971). Episodes of regional metamorphism can generally be correlated with the Mesozoic orogenic intervals.

2.2.4 Cenozoic

2.2.4.1 Tertiary

2.2.4.1.1 Paleogene (Paleocene - Eocene - Oligocene)

The Laramide (Cordilleran) Orogeny in the eastern Cordillera included thrusting and folding along the same trend as the earlier Sevier Orogeny as well as an eastern belt of basement uplifts (Figure 2-13). Laramide deformation involved regional crustal buckling of the interior foreland to produce fault-bounded and basement-cored uplifts in the eastern Cordillera (Robinson, 1972; McDonald, 1972). During this same Paleocene time interval, a prominent hiatus in arc magmatism covered the Great Basin, while subduction continued along the coast (Lipman and others, 1972). Dickinson and Snyder (1978) attribute these conditions to an episode of shallow subduction beneath the Cordillera. Cross (1973) and Suppe (1970) however, suggest the lack of magmatic activity is the result of temporary cessation of subduction and plate consumption along the segment of the continental margin affected by development of the proto-San Andreas transform fault.

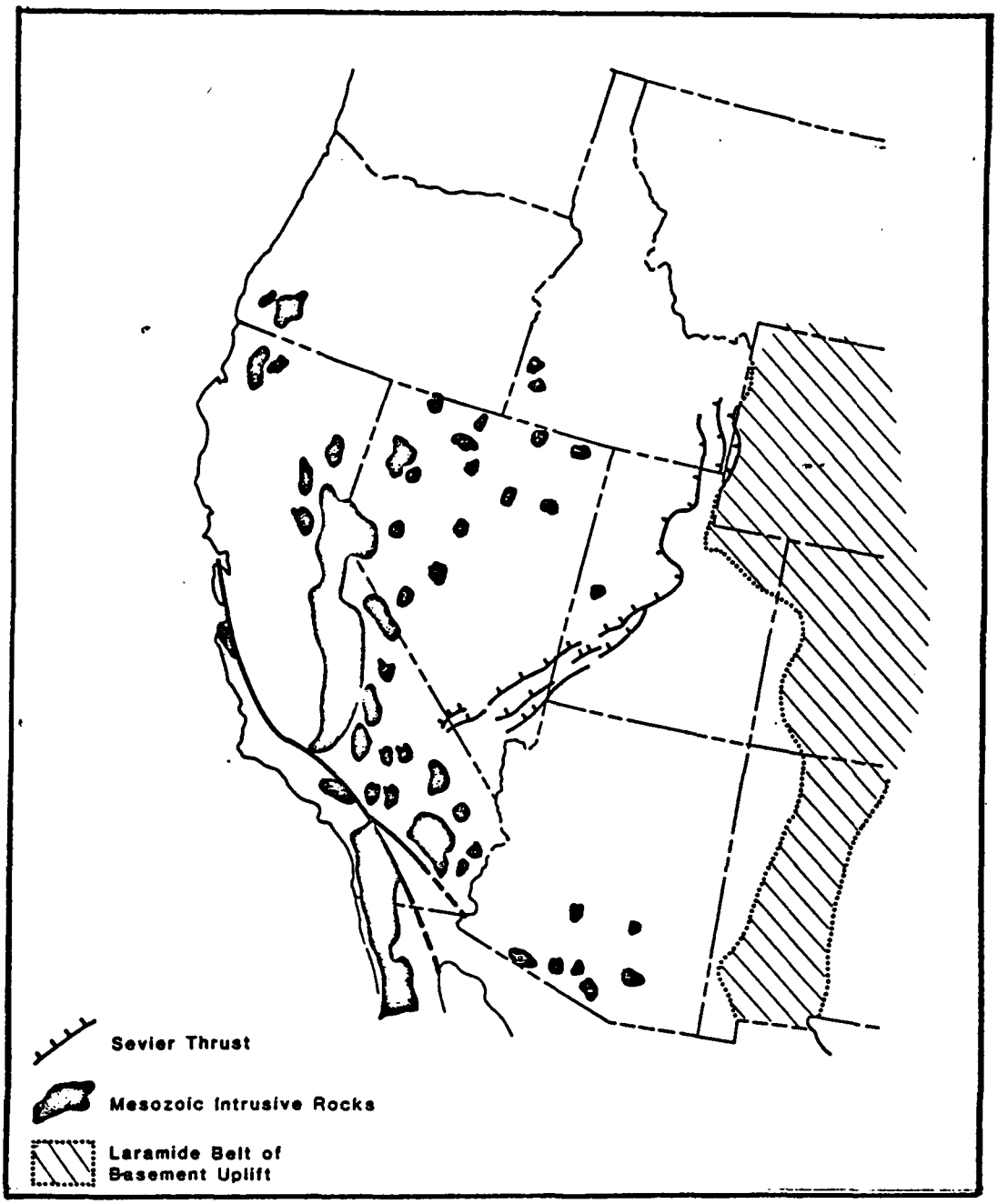

Figure 2-13. Generalized diagram of Mesozoic deformation belts in the western United States. (from Stewart, 1978)

Such a transform would prevent subduction of lithosphere beneath the continent to generate arc magmatism.

Armstrong (1974a) suggests that Laramide deformation reflects crustal contraction in a region where the lithosphere lacked sufficient ductility for the development of a backarc fold-thrust belt. Arc magmatism was dormant across the region between the Laramide uplifts and the proto-San Andreas. Burchfiel and Davis (1975) suggest that regional location of Laramide deformation reflects an eastward migration of the edge of the zone of lithosphere ductile enough to allow for crustal contraction. This is supported by the areal extent of arc magmatism when it resumed in the Oligocene extending to the Laramide uplifts in Colorado. These relationships must also be related to the subsurface geometry of subducted lithospheric slabs (Lipman and others, 1971) and the geometry of absolute plate motions (Coney, 1972, 1973). Coney (1971) has suggested a change in the direction of motion of the North American Plate corresponding with the change in pattern of igneous activity during the Laramide Orogeny.

Laramide deformation inland ended by about the end of the Eocene (Coney, 1971, 1972, 1973, 1976). The Laramide Orogeny was bracketed by major changes in global patterns of sea-floor spreading and motions of plates (Coney, 1976). This regionally extensive and profoundly compressional period of deformation may coincide with high convergence rates between the North American and Farallon plate to the west (Coney, 1978).

Contemporaneous with Laramide deformation in the Rocky Mountain, Colorado Plateau and eastern Great Basin region was an episode of tectonism in the Pacific trough--the Coast Range Orogeny. Deformation in the Coast Range belt was characterized by underthrusting along the continental margin and local intrusive activity (Dickinson, 1969, 1970, 1979; Page, 1970, 1979; Dewey and Bird, 1970). Both the Laramide and Coast Range belts developed in troughs that flanked the Mesozoic Nevadan and Sevier orogens and that were characterized by accumulations of thousands of feet of sediments derived from the orogens and local volcanic rocks of late Mesozoic age.

During the Paleocene and Eocene, the ancestral Cordillera extended unbroken from Mexico northward through western Nevada and into Canada.

The western Great Basin region (in central and eastern Nevada) received sediments from the Cordillera on the west and the Laramide uplifted region on the east in central Utah. Calc-alkaline volcanic activity was widespread in the Pacific Northwest and by the end of Eocene time had migrated through Idaho and perhaps into the northeastern corner of Nevada. Generally the Great Basin region was a low upland of subdued topography, westward external drainage, and extensive erosion. The earlier formed deformational structures and their accompanying terrains had been severely reduced to a surface probably no higher than a few hundred meters above sea level (Nelson, 1979).

The Oligocene was a time of progressive southwestward migration of volcanic activity across the Great Basin (Armstrong, 1975; Mckee and Silberman, 1975). By the end of the period volcanic activity had shifted from a diffuse belt in Utah and central Oregon to a northwest-trending belt in western Nevada. These volcanoes erupted calc-alkaline lavas and ash; the larger ash-flow eruptions resulted in the formation of collapse calderas in the Great Basin. The low topographic relief in the region offered little restriction to the ash-flow eruptions which spread over enormous areas as thin blankets of welded tuff (Figure 2-14).

The ancestral Cordillera, although now disrupted by ongoing rotation of the Klamath Mountains and Coast Range further north, became volcanically active in southeastern and east-central California and in northwestern Nevada (Nilsen and McKee, 1979). This relationship, in addition to the extensive regional volcanism in the western states, suggests that subduction must have been occurring along the entire western margin prior to collision with the Pacific Plate, which instituted a regime of right-slip transform faulting beginning about 29 my ago (Atwater, 1970; Atwater and Molnar, 1973).

The pattern of migrating calc-alkaline volcanism across the inland western United States during the Paleogene reflects, in part, the active subduction of the Farallon oceanic plate during this time. The lack of volcanic activity in the west-central part of the region during Paleocene and Eocene time (Lipman and others, 1972; Snyder and others, 1976) may be a result of strike-slip motion along a postulated proto-San Andreas fault in central and southern California (Cross,

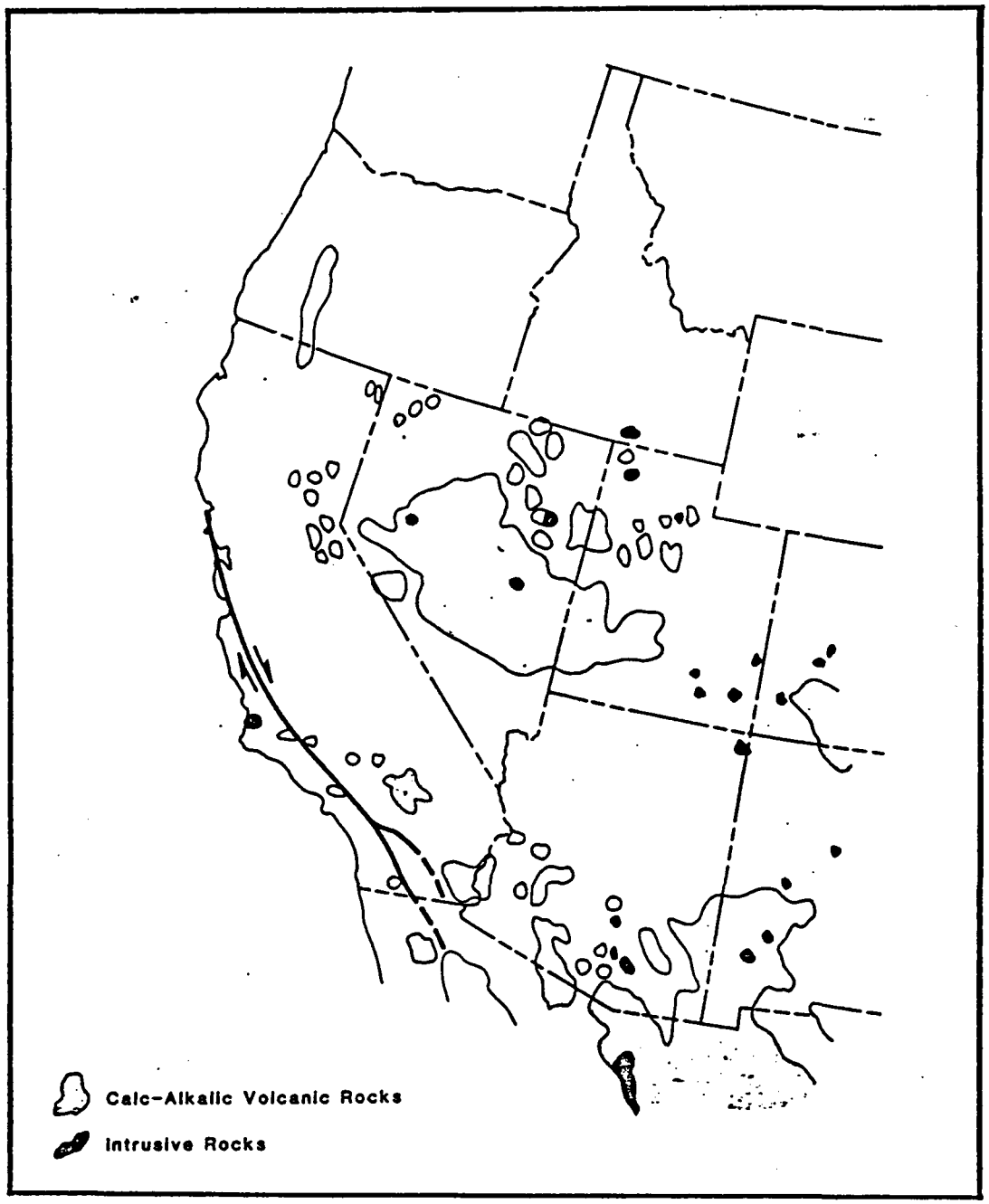

Figure 2-14. Generalized diagram of Oligocene volcanic rocks in the western United States. (from Stewart, 1978)

1973; Suppe, 1970; Nilsen, 1978); changing dips of the subducting Farallon plate (Coney and Reynolds, 1977; Keith, 1978; Burke and McKee, 1979); oblique subduction, rifting in southern California related to deposition, deformation, and eastward thrusting of the schists (Haxel and Dillon, 1978), or a combination of these factors (Nilsen and McKee, 1979).

Prior to 29 my ago, the Farallon Plate, separated from the Pacific Plate to the west by the East Pacific Rise spreading center, was being consumed at the subduction zone along western North America. The intersection of the spreading ridge with the subduction zone about 29 my ago changed the plate geometry and a transform fault system developed, marking the end of subduction along the southern California continental margin (Atwater and Molnar, 1973). As the transform boundary propagated northward, subduction was progressively terminated (Christiansen and Lipman, 1972; Lipman and others, 1972). The subducted plate continued to yield calc-alkalic volcanic rocks in the Basin and Range province, but by 18 my ago (early Miocene) this system was dead (Nilsen and McKee, 1979; Stewart, 1978). Coincident with the change in plate geometry, was the development of a new stress field that would control late Cenozoic tectonism and magmatic evolution in western North America, particularly the Great Basin.

2.2.4.1.2 Neogene (Miocene - Pliocene)

During early Miocene time the Sierra Nevada was an andesitic volcanic arc in which arc volcanism was progressively truncated from south to north as the continental margin transform fault system migrated northward. To the east, the Great Basin was dominated by intermediate volcanism. Rhyolitic volcanics and interbedded non-marine deposits were emplaced on an old erosion surface of low to moderate relief. This activity was not accompanied by any marked increase in tectonism with the exception of caldera collapse resulting from volcanic activity (McKee, 1971).

By mid-Miocene time, the remnant arc and subduction zone was about 2200 km in length and was bracketed by transform systems to the north and south (Christiansen and McKee, 1978). A subduction zone remains at the continental slope only along the continental edge segment adjacent to the Cascade arc (Silver, 1972). This configuration of relative plate

motions and interactions produced a stress field from the increasing Pacific-North American interaction that replaced the declining stress field from Farallon-North American plate interaction. Under these conditions, the regions of North America that had been heated and deformed during Oligocene arc magmatism behaved as ductile material and partial coupling developed. This forced extension across an axis essentially parallel to the continental margin arc about 300 to 400 km inland (Figure 2-15); extension roughly perpendicular to this axis opened a rift that was continuous northward from central Nevada (Christiansen and McKee, 1978). Stress relief at the base of the lithosphere along this rift produced basaltic magma generation in the upper mantle. In Nevada slight partial melting at considerable depth of a tectonically thickened Paleozoic sequence produced alkali-rich basalts. This change from intermediate-composition calc-alkaline to alkali-calcic suite to a bimodal basalt-rhyolite suite is correlated with the initiation of an episode of extensional faulting in the western United States by Christiansen and Lipman (1972), Lipman and others (1972), McKee and others (1970) and Armstrong and others (1969). Further north the plateau flood basalts (Figure 2-16) were produced by partial melting of Mesozoic oceanic crustal rocks.

During the next few million years, tectonic extension and uplift continued across the entire Great Basin region. Regional melting at the base of the lithosphere decreased lithospheric rigidity with subsequent deformation occurring at considerable depth by thinning of the crust and flowage of the mantle. Basaltic magma accumulation in the crust further increased regional heat flow, caused regional uplift and reduced rigidity. This resulted in progressive restriction of brittle deformation to upper-crustal levels away from the axial zone. Thus, faulting (seismicity) and basaltic volcanism have been progressively concentrated toward the Great Basin margins (Wasatch Line and Sierra front), and the axial zone may be hotter at depth than the margins (Christiansen and McKee, 1978).

The volcanic transition in most areas of the Great Basin was about 17 my ago (McKee and others, 1970; McKee, 1971). Christiansen and Lipman (1972), Proffett (1972), and Best and Hamblin (1978) have suggested a general northward migration of the time of inception of Basin and

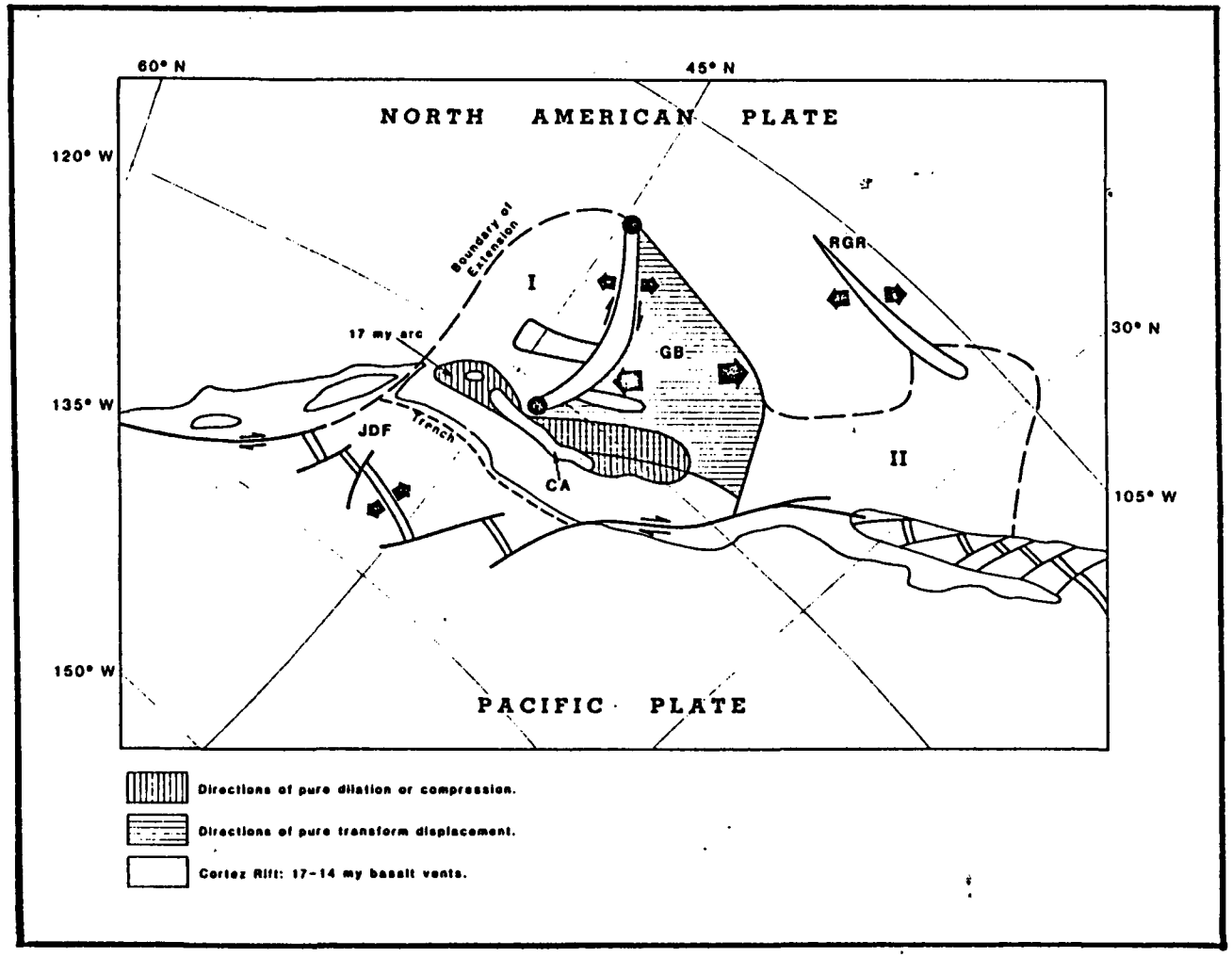

Figure 2-15. Generalized map of western United States showing late Cenozoic tectonic features and upper Cenozoic volcanic rocks in relation to Pacific-North American Plate interaction. Oblique Mercator projection of Atwater (1970); arrows indicate displacement vectors; volcanic centers shown as solid regions. CA - Active Cascade arc; GB - Great Basin, region of oblique extension; JDF - Juan de Fuca Plate, remnant of Farallon Plate; I - region of nearly inactive minor extension; II - region of nearly inactive major extension. (from Christiansen and McKee, 1978)

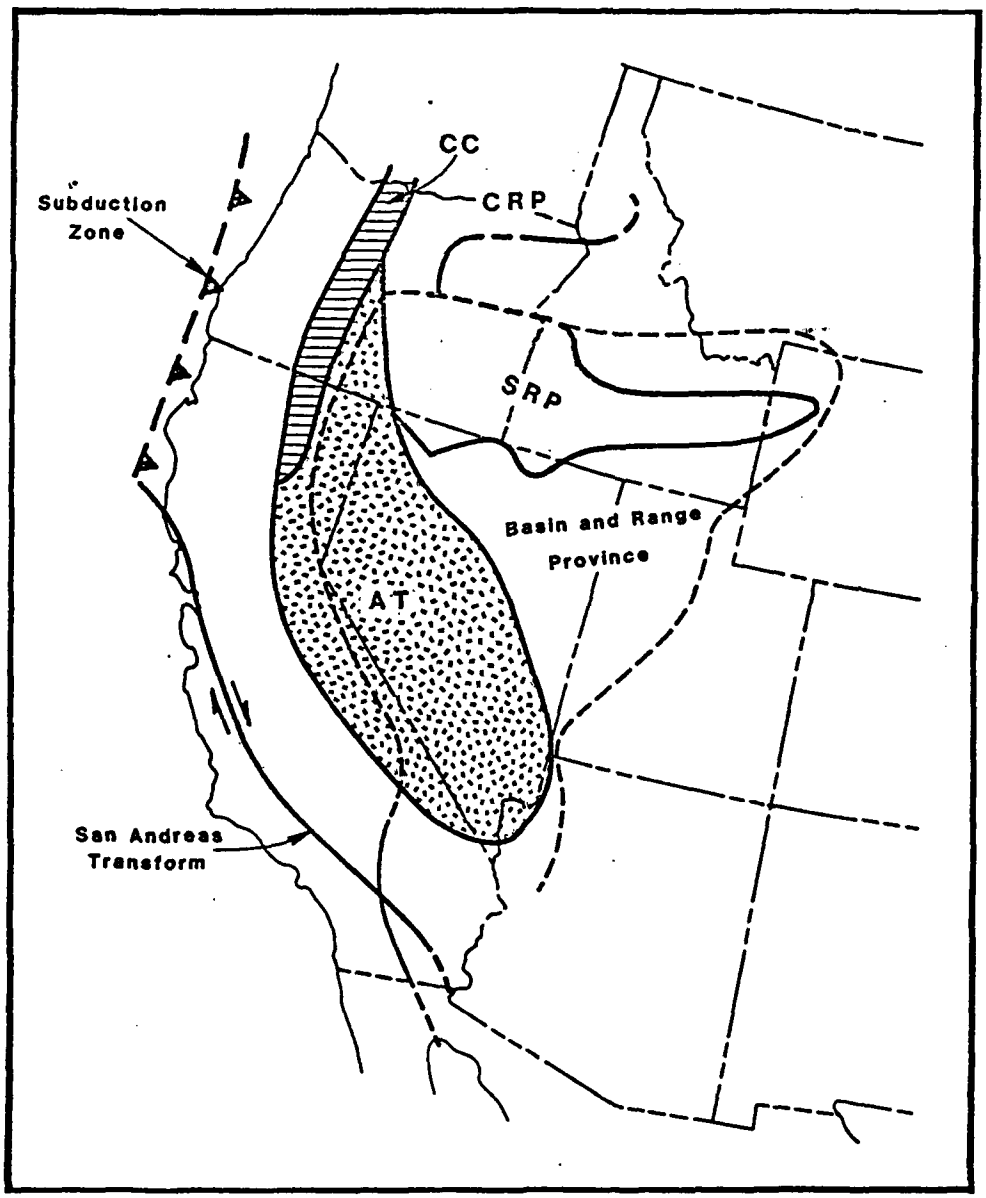

Figure 2-16. Generalized plate tectonic setting of the western United States, including the Great Basin, showing the Cordilleran arc-trench system in middle Miocene to Recent time. CC - Cascade Chain; CRP - Columbia River Plateau of mainly mid-Miocene flood basalts; SRP - Snake River Plain of mainly late Miocene and younger basalts. (from Dickinson, 1976)

Range faulting, with large sedimentary basins well defined by about 11 to 13 my ago (Axelrod, 1957; Robinson and others, 1968; Gilbert and Reynolds, 1973). Regional development of north-trending normal-fault bounded basins representative of present-day topography probably did not begin until mid-Pliocene time and continued into late Pliocene time (Stewart, 1978). During this time interval, approximately one km of uplift occurred in the Great Basin region and is documented by mid-Cenozoic floras (Proffett, 1972; Suppe and others, 1975).

Pliocene regional uplift, extension and graben formation in the Great Basin was coincident with an episode of uplift and westward migration of the Sierra Nevada. Tilting of the range was progressive with about one-third of the present tilt developed between 9.5 and 18 my ago and the latter two-thirds taking place in the last 9.5 my (Noble and Slemmons, 1975). Based on floral data, the Sierra Nevada was a broad ridge with elevations of about 3000 feet during late Miocene and early Pliocene time (Axelrod, 1962). By late Pliocene time the range stood at approximately its present elevation (Christensen, 1965).

The grabens produced by normal extensional faulting within the Great Basin became sites of interior drainage in which were deposited clastic wedges of fluvial, alluvial and lacustrine origin. The pattern of Basin and Range extension and non-marine sedimentation persisted through the Pliocene and into Pleistocene time. As the depositional basins filled, the drainage systems began to coalesce and exterior drainage developed.

2.2.4.2 Quaternary (Pleistocene - Recent)

The Pacific-North American plate interactions that developed during the Neogene have continued to produce regional extensional tectonics in the Great Basin-Sierra Nevada region through Quaternary time. The horsts and grabens within the Basin and Range Province have been enhanced by continued movements on normal tensional faults. Major historical earthquakes within the Province attest to the current activity along these zones (Ryall and others, 1966).

Depositional sequences indicate that the exterior drainage systems of late Pliocene-early Pleistocene time were replaced by interior basin drainage following the Pleistocene glacial cycles and coeval pluvial lakes, such as Lake Lahontan in western Nevada.

Quaternary basaltic activity has been concentrated near the margins of the Basin and Range Province (Best and Brimhall, 1974), with basalt erupted from vents along normal faults in only a few areas. Present volcanic arc activity in the western United States in the Sierra Nevada is limited to areas north of about 40 degrees latitude (Snyder and others, 1976).

The distribution and orientation of late Cenozoic extensional fault patterns in western North America clearly follow pre-existing patterns. Some similarity in the distribution of late Cenozoic extensional faulting and the position of the Paleozoic and latest Precambrian Cordilleran miogeosyncline can be noted, particularly the eastern margin of the Basin and Range with the Wasatch Line. A close correlation can be seen in the patterns of Mesozoic and earliest Cenozoic tectonic deformation, early and middle Cenozoic igneous activity, and late Cenozoic extensional faulting (review Figures 2-4 through 2-16).

2.3 Basin and Range Province Characteristics

The geotectonic history of western North America has resulted in the development of the Basin and Range Province that can be characterized by the parameters presented below.

2.3.1 Crustal Thickness

Seismic refraction data indicate a relatively thin crust, with average values ranging from 25 to 35 km (Pakiser, 1963; Pakiser and Zeitz, 1965; Prodehl, 1970). The region is characterized by a 25 km thick crust in the east and an 18 km thick crust on the west side (Dixie Valley region) of the Great Basin, with a 30 km thick central zone (Smith, 1978).

2.3.2 Upper Mantle Velocity

Low upper mantle (P_n) velocity values ranging from 7.7 km/sec to 7.9 km/sec (Herrin and Taggert, 1962; Pakiser, 1963; Koizumi and others, 1973) suggest a lithospheric plate of NE strike and SE dip within the upper mantle; such plates have been identified in areas of active subduction (Isacks and Molnar, 1971). However, the presence of tensional rather than compressive stresses normal to the zone and a maximum 15 km focal depth of earthquakes with no deeper seismic activity suggest that

the zone is inactive and that the present NW-SE extension may be at least partly due to a release of compressive stress behind a NE trending paleo-subduction zone (Koizumi and others, 1973). Termination of active subduction in the zone may have coincided with initiation of Basin and Range spreading approximately 17 my ago (Stewart, 1971).

2.3.3 Heat Flow

High average heat flow values of greater than 2.0 have been recorded for the Basin and Range (Lee and Uyeda, 1965; Roy and others, 1972; Morgan, 1974; Thompson and Burke, 1974) compared to normal continental values of about 1.5 HFU. Sass and others (1971) indicate consistently high values--mostly above 3 HFU--within the Battle Mountain High, which is located at the northern end of the Ventura-Winnemucca zone of historic seismicity and active faulting (Ryall and others, 1966). Blackwell (1978) indicates that transitions between thermal provinces are narrow (generally less than 20 km); therefore the sources directly responsible for the surface-measured variations in heat flow must be in the crust. Thermal boundaries also usually appear in areas of contemporary seismicity. The origin of the high heat flow of the Battle Mountain High is attributed by Sass and others (1971) to transient effects of a fairly recent crustal intrusion.

2.3.4 Fault Patterns

The pattern of fault rupture within the Basin and Range is generally described as high-angle normal faults trending north to northeast. However, Wright (1976) has shown that faulting within the Province is primarily related to the orientation of the structures with respect to the regional WNW tensional stress direction. Northwest trending faults have primarily right-lateral offsets similar to the San Andreas (e.g., Walker Lane) and NE trending faults have left-lateral offsets similar to that of the Garlock system of California (e.g., Carson Lineament). Extensional relationships generate horst and graben structures defined by predominantly normal-slip faults that parallel the N-S to N-NNE trends (e.g., Dixie Valley). Zones of extension are systematically spaced about 24 to 32 km apart. Considerable warping and tilting of the blocks accompany the faulting, particularly near the ends of elongate basins. The resultant fault pattern tends to be rhomboid or orthogonal and is

apparent on regional (e.g., Sierra Nevada front), local (e.g., Sand Springs Range, Churchill County, Nevada), and site-specific (e.g., Dixie Valley) scales (Trexler and others, 1978). The 15 km maximum focal depth common to the region suggests a lower limit to which the faults are propagated by brittle failure.

2.3.5 Strain Rates and Orientations

Focal-mechanism solutions compiled by Scholz and others (1971), Suppe and others (1975), and Smith and Lindh (1978) are compatible with conjugate faulting on N-S normal-slip and NE-SW and NW-SE strike-slip faults in response to regional strain directions. Strain measurements (Priestley, 1974; Ryall and Priestley, 1975) suggest regional and temporal changes in rate and direction of strain with alternation in compression and extension on the NW-SE principal axis. The orientation of the strain axes is in agreement with the earthquake focal mechanisms of the region. Extension across individual grabens averages about 2.4 km and total extension across the Basin and Range is estimated at 50 to 100 km (Hamilton and Myers, 1966; Stewart, 1971 ; Thompson and Burke, 1974), with extension rates on the order of 0.5 to 1.5 cm per year across the Province (Stewart, 1971; Thompson and Burke, 1974; Slemmons and others, 1979). The region appears to be a topographically up-domed area, averaging 1-2 km abcve sea level, with an area in the west-central Great Basin elevated the greatest amount, about 2.2 km (Suppe and others, 1975).

2.3.6 Petrologic Relationships

Prior to Basin and Range faulting, lower and middle Cenozoic volcanic rocks were largely intermediate composition becoming more alkalic toward the continental interior (Lipman and others, 1972). A major change to basaltic volcanism, including bimodal mafic-silicic associations, took place during late Cenozoic time at about the inception of Basin and Range faulting (Christiansen and Lipman, 1972). The transition began in the southeastern part of the region and moved northwestward. Prior to Basin and Range faulting, the upper mantle to a depth of about 100 km contained about 75 percent peridotite and pyroxenite and 25 percent eclogite (McGetchin and Silver, 1972). Eclogite is capable of converting into gabbro with a volume expansion of about 10 percent in response to a

rise in temperature or a decrease in pressure. The expansion of eclogite in only 60 km of mantle could produce an uplift of 1.5 km. The former eclogite may now be represented by gabbro dispersed in the mantle low velocity zone, or by crustal additions of basic metaigneous rock, or by basaltic volcanics.

2.3.7 Magnetic and Electrical Anomalies

Zietz (1969) showed that magnetic anomalies are subdued in amplitude and that long-wavelength anomalies are absent. This fact suggests that the lower crust and mantle may be above the Curie temperature (578° for magnetite). Porath and Gough (1971) measured geomagnetic fluctuations to determine variations in mantle electrical conductivity. The anomalies are well represented by variations in depth to a half-space conductivity 0.2 ohm-m^{-1}. The top of this conductor is inferred to correspond approximately with the 1500° isotherm. Depths to the surface of the conductor are about 190 km. These data generally support a hot upper mantle in the Basin and Range Province as compared to the surrounding regions. The predominant magnetic highs in western Nevada generally correspond with north trending belts of Miocene intrusives, including the mid-Miocene Cortez Rift of Mabey and others (1978).

2.4 References

Albers, J.P., and Stewart, J.H., 1972, Geology and mineral deposits of Esmeralda County, Nevada: Nevada Bur. Mines and Geol. Bull. 78, 80 p.

Armstrong, R.L., 1974a, Magmatism, orogenic timing and orogenic diachronism in the Cordillera from Mexico to Canada: Nature, v. 274, p. 348-351.

Armstrong, R.L., 1975, Cenozoic igneous history of the Cordillera north of 42° N (abs): Geol. Soc. America Abstr. with Programs, v. 7, no. 7, p. 981.

Armstrong, R.L., and Suppe, J., 1973, Potassium-argon geochronometry of Mesozoic igneous rocks in Nevada, Utah, and southern California: Geol. Soc. America Bull., v. 84, p. 1375-1392.

Armstrong, R.L., Ekren, E.B., McKee, E.H., and Noble, D.C., 1969, Space-time relations of Cenozoic silicic volcanism in the Great Basin of the western United States: Am. Jour. Sci., v. 267, p. 478-490.

Atwater, Tanya, 1970, Implications of plate tectonics for the Cenozoic tectonic evolution of western North America: Geol. Soc. America Bull., v. 81, no. 12, p. 3513-3535.

Atwater, Tanya, and Molnar, P., 1973, Relative motion of the Pacific and North American plates deduced from sea-floor spreading in the Atlantic, Indian, and South Pacific oceans: in Kovach, R.L., and Nur, A., eds., Proceedings, Conf. on Tectonic Problems of the San Andreas Fault System: Stanford Univ. Pubs. Geol. Sci., v. 13, p. 136-148.

Axelrod, D.I., 1957, Late Tertiary floras and the Sierra Nevadan uplift (California-Nevada): Geol. Soc. America Bull., v. 68, p. 19-45.

Axelrod, D.I., 1962, Post-Pliocene uplift of the Sierra Nevada, California: Geol. Soc. America Bull., v. 73, p. 183-198.

Barnes, J.J., and Klein, G. de V., 1975, Tidal deposits in the Zabriskie Quartzite, eastern California and western Nevada, in Ginsburg, R.N., ed., Tidal deposits: New York, Springer-Verlag, p. 163-169.

Best, M.G., and Brimhall, W.H., 1974, Late Cenozoic alkalic basaltic magmas in the western Colorado Plateaus and the Basin and Range transition zone, U.S.A., and their bearing on mantle dynamics: Geol. Soc. America Bull., v. 85, p. 1677-1690.

Best, M.G., and Hamblin, W.K., 1978, Origin of the northern Basin and Range province--Implications from the geology of its eastern boundary, in Smith, R.B., and Eaton, G.P., eds., Cenozoic tectonics and regional geophysics of the western Cordillera: Geol. Soc. America Mem. 152, p. 313-340.

Blackwell, D.D., 1978, Heat flow and energy loss in the western United States, in Smith, R.B., and Eaton, G.P., eds., Cenozoic tectonics and regional geophysics of the western Cordillera: Geol. Soc. America Mem.152, p. 175-208.

Burchfiel, B.C., and Davis, G.A., 1972, Structural framework and evolution of the southern part of the Cordilleran orogen, western United States: Am. Jour. Sci., v. 272, p. 97-118.

Burchfiel, B.C., and Davis, G.A., 1975, Nature and controls of Cordilleran orogenesis, western United States: Extensions of an earlier synthesis: Am. Jour. Sci., v. 275-A, p. 363-396.

Burchfiel, B.C., and Davis. G.A., 1979a, Triassic and Jurassic tectonic evolution of the Klamath Mountains-Sierra Nevada geologic terrane, in Ernst, W.G., ed., The geotectonic development of California: W.W. Rubey Volume no. 1, ch. 3, (in press).

Burchfiel, B.C., and Davis, G.A., 1979b, Mojave Desert and environs, in Ernst, W.G., ed., The geotectonic development of California: W.W. Rubey Volume no. 1, ch. 9, (in press).

Burke, D.B., and McKee, E.H., 1979, Mid-Cenozoic volcano-tectonic troughs in central Nevada: Geol. Soc. America Bull. (in press).

Burke, D.B., and Silberling, N.J., 1973, The Auld Lang Syne Group of late Triassic and Jurassic (?) age, north-central Nevada: U.S. Geol. Survey Bull. 1394-E, 14 p.

Christensen, M.N., 1965, Late Cenozoic deformation in the central Coast Ranges of California: Geol. Soc. America Bull., v. 76, p. 1105-1124.

Christiansen, R.L., and Lipman, P.W., 1972, Cenozoic volcanism and plate-tectonic evolution of the western United States, II. Late Cenozoic: Roy. Soc. London, Phil. Trans., v. 271, p. 249-284.

Christiansen, R.L., and McKee, E.H., 1978, Late Cenozoic volcanic and tectonic evolution of the Great Basin and Columbia Intermontane regions, in Smith, R.B., and Eaton, G.P., eds. Cenozoic tectonics and regional geophysics of the western Cordillera: Geol. Soc. America Mem. 152, p. 283-312.

Churkin, M. Jr., 1974, Deep-sea drilling for landlubber geologists--the southwest Pacific, an accordian plate tectonics analog for the Cordilleran geosyncline: Geology, v. 2, p. 339-342.

Churkin, Michael, Jr., and Eberlein, G.D., 1977, Ancient borderland terranes of the North American Cordillera: Correlations and microplate tectonics: Geol. Soc. America Bull., v. 88, p. 769-786.

Coney, P.J., 1971, Cordilleran tectonic transitions and motion of the North American plate: Nature, v. 233, p. 462-465.

Coney, P.J., 1972, Cordilleran tectonics and North America plate motion: Am. Jour. Sci., v. 272, p. 603-628.

Coney, P.J., 1973, Non-collision tectogenesis in western North America, in Tarling, D.H., and Runcorn, S.H., eds., Implications of continental drift to the Earth Sciences: Academic Press, New York, p. 713-727.

Coney, P.J., 1976, Plate tectonics and the Laramide Orogeny: New Mexico Geol. Soc. Special Pub. no. 6, p. 5-10.

Coney, P.J., 1978, Mesozoic-Cenozoic Cordilleran plate tectonics, in Smith, R.B., and Eaton, G.P., eds., Cenozoic tectonics and the regional geophysics of the western Cordillera: Geol. Soc. America Mem. 152, p. 33-50.

Coney, P.J., and Reynolds, S.J., 1977, Cordilleran Benioff zones: Nature, v. 270, p. 403-406.

Crittenden, M.D., Jr., and Wallace, C.A., 1973, Possible equivalents of the Belt Supergroup in Utah, in Belt symposium (Idaho U., Moscow) 1973, v. 1: Idaho Bur. Mines and Geol., p. 116-138.

Crittenden, M.D., Jr., Stewart, J.H., and Wallace, C.A., 1972, Regional correlation of upper Precambrian strata in western North America: Internat. Geol. Cong., 24th, Montreal, Sec. 1, p. 334-341.

Cross, T.A., 1973, Implications of igneous activity for the early Cenozoic tectonic evolution of western United States: Geol. Soc. America Abstr. with Programs, v. 5, p. 587.

Cross, T.A., and Pilger, R.A., 1974, Space/time distribution of late Cenozoic igneous activity in the western United States: Geol. Soc. America Abstr. with Programs, v. 6, p. 702.

Davis, G.A., Monger, J.W.H., and Burchfiel, B.C., 1978, Mesozoic construction of the Cordilleran "collage", central British Columbia to central California, in Howell, D.G., ed., Mesozoic paleogeography of the western United States, Pacific Coast Paleogeography Symp. no. 2, p. 1-32.

Dewey, J.F., and Bird, J.M., 1970, Mountain belts and the new global tectonics: Jour. Geophys. Res., v. 75, p. 2625-2647.

Dickinson, W.R., 1969, Evolution of calc-alkaline rocks in the geosynclinal system of California and Oregon, in Proceedings of the Andesite Conf., Oregon: Oregon Dept. Geol. and Mineral Industries Bull. 65, p. 151.

Dickinson, W.R., 1970. Relations of andesites, granites and derivitive sandstones to arc-trench tectonics: Rev. Geophys. Space Phys. 8, p. 813-860.

Dickinson, W.R., 1973, Widths of modern arc-trench gaps proportional to past duration of igneous activity in associated magmatic arcs: J. Geophys. Res., v. 78, p. 3376-3389.

Dickinson, W.R., 1976, Sedimentary basins developed during evolution of Mesozoic-Cenozoic arch-trench system in western North America: Canadian Jour. Earth Sci., v. 13, p. 1268-1287.

Dickinson, W.R., 1977, Paleozoic plate tectonics and the evolution of the Cordilleran continental margin, in Stewart, J.H., Stevens, C.H., and Fritsche, A.E., eds., Paleozoic paleogeography of the western United States: Pacific section, Soc. Econ. Paleontol. and Mineral.,Pacific Coast Paleogeography Symposium 1, p. 137-156.

Dickinson, W.R., 1979, Cenozoic plate tectonic setting of the Cordilleran region in the United States, in Armentrout, J.M., Cole, M. R., and TerBest, H., Jr., eds., Cenozoic paleogeography of the western United States: Soc. Econ. Paleontol. and Mineral., Pacific Section, Pacific Coast Paleogeography Symposium 3, p. 1-13.

Dickinson, W.R., 1979, Plate tectonics and the continental margin of California, in Ernst, W.G., ed., The geotectonic development of California: W.W. Rubey Volume no. 1, ch. 1, (in press).

Dickinson, W.R., and Snyder, W.S., 1978, Plate tectonics of the Laramide Orogeny: Geol. Soc. America Mem. 151, 370 p.

Ernst, W.G., ed., 1979a, The geotectonic development of California: W. W. Rubey Volume no. 1, (in press).

Ernst, W.G., 1979b, An interpretive account--California and plate tectonics: California Geol., v. 32, no. 9, p. 187-196.

Evernden, J.F., and Kistler, R.W., 1970, Chronology of emplacement of Mesozoic batholithic complexes in California and western Nevada: U.S. Geol. Survey Prof. Paper 623, p. 1-42.

Ferguson, H.G., Muller, S.W., and Roberts, R.J., 1951, Geology of the Winnemucca quadrangle, Nevada: U.S. Geol. Survey Geol. Quad. Map GQ-11.

Gabrielse, Hubert, 1972, Younger Precambrian of the Canadian Cordillera: Am. Jour. Sci., v. 272, p. 521-536.

Gilbert, C.M., and Reynolds, M.W., 1973, Character and chronology of basin development, western margin of the Basin and Range province: Geol. Soc. America Bull., v. 84, p. 2489-2509.

Gilluly, James, 1967, Geologic map of the Winnemucca quadrangle, Pershing and Humboldt Counties, Nevada: U.S. Geol. Survey Quad. Map GQ-656, scale 1:62,500.

Gilluly, James and Gates, Olcott, 1965, Tectonic and igneous geology of the northern Shoshone Range, Nevada: U.S. Geol. Survey Prof. Paper 465, 153 p.

Hamilton, W., 1969, Mesozoic California and the underflow of Pacific mantle: Geol. Soc. America Bull., v. 80, p. 2409-2430.

Hamilton, W., and Myers, W.B., 1966, Cenozoic tectonics of the western United States: Rev. Geophys., v. 4, p. 509-549.

Haxel, Gordon, and Dillon, John, 1978, The Pelona-Orocopia Schist and Vincent-Chocolate Mountain thrust system, southern California, in Howell, D.G., and McDougall, K.A., eds., Mesozoic paleogeography of the western United States: Soc. Econ. Paleontol. and Mineral., Pacific Section, Pacific Coast Paleogeography Symposium 2, p. 453-469.

Herrin, E., and Taggart, J., 1962, Regional variations in P_n velocity and their effect on the location of epicenters: Seis. Soc. America Bull. 52, p. 1037-1046.

Isacks, B.L., and Molnar, P., 1971, Distribution of stresses in the descending lithosphere from a global survey of focal-mechanism solutions of mantle earthquakes: Rev. Geophys., v. 9, p. 102-174.

Jones, D.L., Silberling, N.J., and Hillhouse, J.W., 1977, Wrangellia--A displaced terrace in northwestern North America: Canadian Jour. Earth Sci., v. 14, no. 11, p. 2565-2577.

Jones, D.L., Silberling, N.J., and Hillhouse, J.W., 1978, Microplate tectonics of Alaska--Significance for the Mesozoic history of the Pacific Coast of North America, in Howell, D.G., and McDougall, K.A., eds., Mesozoic Paleogeography of western United States: Pacific Section, Soc. Econ. Paleontol. and Mineral., Pacific Coast Paleogeography Symposium 2, p. 71-74.

Jones, M., Van der Voo, R., Churkin, M., Jr., and Eberlein, G.D., 1977, Paleozoic Paleomagnetic results from the Alexander terrane of southeastern Alaska (abstract): Trans. Am. Geophys. Union, v. 58, p. 743-744.

Kay, Marshall, 1951, North American geosynclines: Geol. Soc. America Mem. 148, 143 p.

Keith, S.B., 1978, Paleosubduction geometries inferred from Cretaceous and Tertiary magmatic patterns in southwestern North America: Geology, v. 6, no. 9, p. 516-521.

Ketner, K.B., 1970, Geology and mineral potential of the Adobe Range, Elko Hills, and adjacent areas, Elko County, Nevada: U.S. Geol. Survey Prof. Paper 700-B, p. 105-108.

Ketner, K.B., 1977, Late Paleozoic orogeny and sedimentation, southern California, Nevada, Idaho, and Montana, in Stewart, J.H., Stevens, C.H., and Fritsche, A.E., eds., Paleozoic paleogeography of the western United States: Soc. Econ. Paleontol. and Mineral., Pacific Section, Pacific Coast Paleogeography Symposium 1, p. 363-370.

Kistler, R.W., Evernden, J.F., and Shaw, H.R., 1971, Sierra Nevada plutonic cycle: Part I, Origin of composite granitic batholiths: Geol. Soc. America Bull., v. 82, p. 853-868.

Klein, G. de V., 1975, Paleotidal range sequences middle member, Wood Canyon Formation (late Precambrian), eastern California and Nevada, in Ginsburg, R.N., ed., Tidal deposits: New York, Springer-Verlag, p. 171-177.

Koizumi, C.J., Ryall, Alan, and Priestley, K.F., 1973, Evidence for a high-velocity lithospheric plate under northern Nevada: Seis. Soc. America Bull. 63, no. 6, p. 2135-2144.

Lanphere, M.A., and Reed, B.L., 1973, Timing of Mesozoic and Cenozoic plutonic events in Circum-Pacific North America: Geol. Soc. America Bull., v. 84, p. 3773-3782.

Lee, W.H.K., and Uyeda, S., 1965, Review of heat flow data, in Lee, W.H.K., ed., Terrestrial heat flow: Am. Geophys. Union Mono. Ser. no. 8, p. 87-190.

Lipman, P.W., Prostka, H.J., and Christiansen, R.L., 1971, Evolving subduction zones in the western United States as interpreted from igneous rocks: Science, v. 174, p. 821-823.

Lipman, P.W., Prostka, H.J., and Christiansen, R.L., 1972, Cenozoic volcanism and plate tectonic evolution of the western United States: I, Early and middle Cenozoic: Royal Soc. London Philos. Trans., v. 271, p. 217-248.

Mabey, D.R., Zietz, I., Eaton, G.P., and Kleinkopf, M.D., 1978, Regional magnetic patterns in part of the Cordillera in the western United States, in Smith, R.B., and Eaton, G.P., eds., Cenozoic tectonics and regional geophysics of the western Cordillera: Geol. Soc. America Mem. 152, p. 93-106.

McDonald, R.E., 1972, Eocene and Paleocene rocks of the southern and central basins, in Geologic atlas of the Rocky Mountain region: Rocky Mountain Assoc. Geol., p. 243-256.

McGetchin, T.R., and Silver, L.T., 1972, A crustal-upper mantle model for the Colorado Plateau based on observations of crystalline rock fragments in the Moses Rock dike: Jour. Geophys. Res., v. 77, p. 7022-7037.

McKee, E.H., 1971, Tertiary igneous chronology of the Great Basin in western United States--Implications for tectonic models: Geol. Soc. America Bull., v. 82, p. 3497-3502.

McKee, E.H., and Silberman, M.L., 1975, Cenozoic igneous history of the southern Cordillera south of 42° N (abs): Geol. Soc. America Abstr. with Programs, v. 7, no. 7, p. 196-197.

McKee, E.H., Noble, D.C., and Silberman, M.L., 1970, Middle Miocene hiatus in volcanic activity in the Great Basin area of the western United States: Earth and Planetary Sci, Letters, v. 8, p. 93-96.

Merriam, C.W., and Anderson, C.A., 1942, Reconnaissance survey of the Roberts Mountains, Nevada: Geol. Soc. America Bull., v. 53, p. 1675-1727.

Miller, F.K., McKee, D.H., and Yates. R.G., 1973, Age and correlation of the Windemere Group in northeastern Washington: Geol. Soc. America Bull., v. 84, p. 3723-3730.

Monger, J.W.H., Southes, J.G., and Gabrielse, H., 1972, Evolution of the Canadian Cordillera--A plate-tectonic model: Am. Jour. Sci., v. 272, p. 577-602.

Morgan, W.J., 1974, Heat flow and vertical movements of the crust, in Petroleum and Global Tectonics: Princeton Univ. Press.

Muller, S.W., Ferguson, H.W., and Roberts, R.J., 1951, Geology of the Mount Tobin quadrangle, Nevada: U.S. Geol. Survey Geol. Quad. Map GQ-7.

Nelson, C.A., 1962, Lower Cambrian-Precambrian succession, White-Inyo Mountains, California: Geol. Soc. America Bull., v. 73, p. 139-144.

Nelson, C.A., 1976, Late Precambrian-Early Cambrian stratigraphic and faunal succession of eastern California and the Precambrian-Cambrian boundary, in Moore, J.N., and Fritsche, A.E., eds., Depositional Environments of Lower Paleozoic Rocks in the White-Inyo Mountains, Inyo County, California: Pacific Section, Soc. Econ. Paleontol. and Mineral., Pacific Coast Paleogeography Field Guide 1, p. 31-42.

Nelson, C.A., 1979, Basin and Range province, in Ernst, W.G., ed., The geotectonic development of California: W.W. Rubey Volume no. 1, ch. 8, (in press).

Nilsen, T.H., 1978, Late Cretaceous geology of California and the problem of the proto-San Andreas fault, in Howell, D.G., and McDougall, K.A., eds., Mesozoic paleogeography of the western United States: Soc. Econ. Paleontol. and Mineral., Pacific Section, Pacific Coast Paleogeography Symposium 2, p. 559-573.

Nilsen, T.H., and McKee, E.H., 1979, Paleogene paleogeography of the western United States, in Armentrout, J.M., Cole, M.R., and TerBest, H., Jr., eds., Cenozoic paleogeography of the western United States: Soc. Econ. Paleontol. and Mineral., Pacific Section, Pacific Coast Paleogeography Symposium 3, p. 257-276.

Noble, D.C., and Slemmons, D.B., 1975, Timing of Miocene faulting and intermediate volcanism in the central Sierra Nevada and adjacent Great Basin: California Geologist, v. 28, p. 105.

Page, B.M., 1970, Sur-Nacimento fault zone of California: Continental margin tectonics: Geol. Soc. America Bull., v. 81, no. 3, p. 667-690.

Page, B.M., 1979, The southern Coast Ranges, in Ernst, W.G., ed., The geotectonic development of California: W.W. Rubey Volume no. 1, ch. 14, (in press).

Pakiser, L.C., 1963, Structure of the crust and upper mantle in the western United States: Jour. Geophys. Res., v. 68, p. 5747-5756.

Pakiser, L.C., and Zietz, I., 1965, Transcontinental crustal and upper mantle structure: Rev. Geophys., v. 3, p. 505-520.

Palmer, A.R., 1971, The Cambrian of the Great Basin and adjoining areas, western United States, in Holland, C.H., ed., Lower Paleozoic Rocks of the World: v. 1, Cambrian of the New World: Wiley-Interscience, New York, p. 1-78.

Poole, F.G., 1974, Flysch deposits of Antler foreland basin, western United States: Soc. Econ. Paleontol. Mineral., Spec. Pub. 22, p. 58-82.

Poole, F.G., and Sandberg, C.A., 1977, Mississippian paleogeography and tectonics of the western United States, in Stewart, J.H., Stevens, C.H., and Fritsche, A.E., eds., Paleozoic paleogeography of the western United States: Pacific Section, Soc. Econ. Paleontol. and Mineral., Pacific Coast Paleogeography Symposium 1, p. 67-86.

Poole, F.G., Sandberg, C.A., and Boucot, A.J., 1977, Silurian and Devonian paleogeography of the western United States, in Stewart, J. H., Stevens, C.H., and Fritsche, A.E., eds., Paleozoic Paleogeography of the western United States: Pacific Section, Soc. Econ. Paleontol. and Mineral., Pacific Coast Paleogeography Symposium 1, p. 39-65.

Porath, H., and Gough, D.I., 1971, Mantle conductive structures in the western United States from magnetometer array studies: Geophys. Jour. Roy. Astron. Soc., v. 22, p. 261-275.

Priestly, K.F., 1974, Crustal strain measurements in Nevada: Seis. Soc. America Bull. 64, p. 1319-1328.

Prodehl, C., 1970, Crustal structure of the western United States from seismic-refraction measurements in comparison with central European results: Z. Geophys., v. 36, p. 477-500.

Proffett, J.M., Jr., 1977, Cenozoic geology of the Yerington District, Nevada, and implications for the nature and origin of Basin and Range faulting: Geol. Soc. America Bull., v. 88, p. 247-266.

Roberts, R.J., 1951, Geology of the Antler Peak quadrangle, Nevada: U.S. Geol. Survey Geol. Quad. Map GQ-10.

Roberts, R.J., 1964, Stratigraphy and structure of the Antler Peak quadrangle, Humboldt and Lander Counties, Nevada: U.S. Geol. Survey Prof. Paper 459A. 93 p.

Roberts, R.J., 1972, Evolution of the Cordilleran fold belt: Geol. Soc. America Bull., v. 83, p. 1989-2002.

Roberts, R.J., Hotz, P.E., Gilluly, J., and Ferguson, H.G., 1958, Paleozoic rocks of north-central Nevada: Am. Assoc. Petroleum Geol. Bull., v. 42, p. 2813-2857.

Robinson, P., 1972, Tertiary history, in Geologic atlas of the Rocky Mountain region, Rocky Mountain Assoc., p. 233-242.

Robinson, P.T., McKee, E.H., and Moiola, R.J., 1968, Cenozoic volcanism and sedimentation, Silver Peak region, western Nevada and adjacent California, in Coats, R.R., Hay, R.L., and Anderson, C. A., eds., Studies in volcanology--A memoir in honor of Howel Williams: Geol. Soc. America Mem. 116, p. 577-611.

Rogers, J.J.W., Burchfiel, B.C., Abbot, E.W., Anepohl, J.K., Ewing, A. H., Koehnken, P.J., Novitsky-Evans, J.M., and Talukdars, S.C., 1974, Paleozoic and lower Mesozoic volcanism and continental growth in the western United States: Geol. Soc. America Bull., v. 85, no. 12, p. 1913-1924.

Roy, R.F., Blackwell, D.D., and Decker, E.R., 1972, Continental heat flow, in The nature of the solid earth, E. Robertson, ed., McGraw (667 p.), p. 506-543.

Ryall, A., and Priestley, K., 1975, Seismicity, secular strain, and maximum magnitude in the Excelsior Mountains area, western Nevada and eastern California: Geol. Soc. America Bull. 86, p. 1585-1592.

Ryall, Alan, Slemmons, D.B., and Gedney, L.D., 1966, Seismicity, tectonism and surface faulting in the western United States during historic time: Seis. Soc. America Bull. 56, no. 5, p. 1105-1135.

Saleeby, J.B., 1979, Kaweah serpentinite melange, southwest Sierra Nevada foothills, California: Geol. Soc. America Bull., v. 90, p. 29-46.

Sass, J.H., Lachenbruch, A.H., Monroe, R.J., Greene, G.W., and Moses, T.J., Jr., 1971, Heat flow in the western United States: Jour. Geophys. Res., v. 76, p. 6376-6413.

Scholz, D.H., Barazangi, M., and Sbar, M.L., 1971, Late Cenozoic evolution of the Great Basin, western United States, as an ensialic interarc basin: Geol. Soc. America Bull., 82, p. 2979-2990.

Schweikert, R.A., 1976, Early Mesozoic rifting and fragmentation of the Cordilleran orogen in the western U.S.A.: Nature, v. 260, p. 586-591.

Schweikert, R.A., 1978, Triassic and Jurassic paleogeography of the Sierra Nevada and adjacent regions, California and western Nevada, in Howell, D.G., and McDougall, K.A., eds., Mesozoic Paleogeography of the western United States: Pacific Section, Soc. Econ. Paleontol. and Mineral., Pacific Coast Paleogeography Symposium 2, p. 361-384.

Schweikert, R.A, 1979, Structural sequence of the Calaveras Complex between the Stanislaus and Tuolumne Rivers (abstract): Geol. Soc. America Abstracts with Programs, v. 11, p. 127.

Schweikert, R.A., and Cowan, D.S., 1975, Early Mesozoic tectonic evolution of the western Sierra Nevada, California: Geol. Soc. America Bull., v. 86, p. 1329-1336.

Schweikert, R.A., and Snyder, W.S., 1979, Paleozoic plate tectonics of the Sierra Nevada and Adjacent regions, in Ernst, W.G., ed., The geotectonic development of California: W.W. Rubey Volume no. 1, ch. 5, (in press).

Schweikert, R.A., Saleeby, J.B., Tobisch, O.T., and Wright, W.H., III, 1977, Paleotectonic and paleogeographic significance of the Calaveras Complex, western Sierra Nevada, California, in Stewart, J.H., Stevens, C.H., and Fritsche, A.E., eds., Paleozoic Paleogeography of the western United States: Pacific Section, Soc. Econ. Paleontol. and Mineral., Pacific Coast Paleogeography Symposium 1, p. 381-394.

Silberling, N.J., 1973, Geologic events during Permian-Triassic time along the Pacific margin of the United States, in Logan, A., and Hills, L.V., eds., The Permian and Triassic systems and their mutual boundary: Alberta Soc. Pet. Geol., Mem. 2, p. 345-362.

Silberling, N.J., 1975, Age relationships of the Golconda thrust fault, Sonoma Range, north-central Nevada: Geol; Soc. America Spec. Paper 163, 28 p.

Silberman, M.L., and McKee, E.H., 1971, Periods of plutonism in north-central Nevada: Econ. Geol., v. 66, p. 17-20.

Silver, L.T., 1971, Problems of crystalline rocks of the Transverse Ranges (abstract): Geol. Soc. America Abstracts with Programs, v. 3, p. 193-194.

Silver, E.A., 1972, Pleistocene tectonic accretion of the continental slope off Washington: Marine Geol. 13, p. 239-249.

Slemmons, D.B., VanWormer, D., Bell, E.J., and Silberman, M.L., 1979, Recent crustal movements in the Sierra Nevada-Walker Lane region of California-Nevada, Part I, Rate and style of deformation: Tectonophys., v. 52, p. 561-570.

Smith, J.F., Jr., and Ketner, K.B., 1975, Stratigraphy of Paleozoic rocks in the Carlin-Pinon Range area, Nevada: U.S. Geol. Survey Prof. Paper 867-A, 87 p.

Smith, R.B., 1978, Seismicity, crustal structure, and intraplate tectonics of the interior of the western Cordillera, in Smith, R. B., and Easton, G.P., Cenozoic tectonics and regional geophysics of the western Cordillera: Geol. Soc. America Mem. 152, p. 111-144.

Smith, R.B., and Lindh, A.G., 1978, Fault-plane solutions of the western United States--A compilation, in Smith, R.B., and Easton, G.P., Cenozoic tectonics and regional geophysics of the western Cordillera: Geol. Soc. America Mem. 152, p. 107-110.

Snyder, W.S., Dickinson, W.R., and Silberman, M.L., 1976, Tectonic implications of space-time patterns of Cenozoic magmatism in the western United States, Earth Planet Sci. Letters.

Stanley, K.O., Chamberlain, C.K., and Stewart, J.H., 1977, Depositional setting of some eugeosynclinal Ordovician rocks and structurally interleaved Devonian rocks in the Cordilleran mobile belt, Nevada, in Stewart, J.H., Stevens, C.H., and Fritsche, A.E., eds., Paleozoic Paleogeography of the western United States: Pacific Section, Soc. Econ. Paleontol. and Mineral., Pacific Coast Paleogeography Symposium 1, p. 259-274.

Stewart, J.H., 1970, Upper Precambrian and Lower Cambrian strata in the southern Great Basin, California and Nevada: U.S. Geol. Survey Prof. Paper 620, 206 p.

Stewart, J.H., 1971, Basin and Range structure: A system of horst and grabens produced by deep-seated extension: Geol. Soc. America Bull. 82, p. 1019-1044.

Stewart, J.H., 1972, Initial deposits in the Cordilleran geosyncline: Evidence of a late Precambrian (850 my) continental separation: Geol. Soc. America Bull., v. 83, p. 1345-1360.

Stewart, J.H., 1974, Correlation of uppermost Precambrian and lower Cambrian strata from south to east central Nevada: U.S. Geol. Survey Jour. Res., v. 2, no. 5, p. 609-618.

Stewart, J.H., 1976, Late Precambrian evolution of North America: Plate tectonic implication: Geology, v. 4, p. 11-15.

Stewart, J.H., 1978, Basin-range structure in western North America--a review, in Smith, R.B., and Eaton, G.P. , eds., Cenozoic tectonics and regional geophysics of the western Cordillera: Geol. Soc. America Mem. 152, p. 1-32.

Stewart, J.H., and Carlson, J.E., 1976, Geologic map of north-central Nevada: Nevada Bureau of Mines and Geology Map 50.

Stewart, J.H., and Poole, F.G., 1974, Lower Paleozoic and uppermost Precambrian Cordilleran miogeocline, Great Basin, western United States, in Dickinson, W.R., ed., Tectonics and Sedimentation: Soc. Econ. Paleontol. and Mineral. Special Pub. 22, p. 28-57.

Stewart, J.H., and Poole, F.G., 1975, Extension of the Cordilleran miogeosynclinal belt to the San Andreas fault, southern California: Geol. Soc. America Bull., v. 86, p. 205-212.

Stewart, J.H., and Suczek, C.A., 1977, Cambrian and latest Precambrian paleogeography and tectonics in the western United States, in Stewart, J.H., Stevens, C.H., and Fritsche, A.E., eds., Paleozoic Paleogeography of the western United States: Pacific Section, Soc. Econ. Paleontol. and Mineral., Pacific Coast Paleogeography Symposium 1, p. 1-18.

Stewart, J.H., MacMillan, J.R., Nichols, K.M., and Stevens, C.H., 1977, Deep-water upper Paleozoic rocks in north-central Nevada--a study of the type area of the Havallah Formation, in Stewart, J.H., Stevens, C.H., and Fritsche, A.E., eds., Paleozoic Paleogeography of the western United States: Pacific Section, Soc. Econ. Paleontol. and Mineral., Pacific Coast Paleogeography Symposium 1, p. 337-348.

Suczek, C.A., 1977a, Sedimentology and petrology of the Cambrian Harmony Formation of north-central Nevada (abstract): Geol. Soc. America Abstracts with Programs, v. 9, p. 510.

Suczek, C.A., 1977b, Tectonic relations of the Harmony Formation, northern Nevada: Unpublished Ph.D. dissertation, Stanford University, Stanford, California, 96 p.

Suppe, J., 1970, Offset of late Mesozoic basement terrains by the San Andreas fault system: Geol. Soc. America Bull., v. 81, p. 3253-3258.

Suppe, John, Powell, Christine, and Berry, Robert, 1975, Regional topography, seismicity, Quaternary volcanism, and the present-day tectonics of the western United States: Am. Jour. Sci., v. 275A, p. 397-436.

Theodore, T.G., and Roberts, R.J., 1971, Geochemistry and geology of deep drill holes at Iron Canyon, Lander County, Nevada: U.S. Geol. Survey Bull. 1318, 32 p.

Thompson, G.A., and Burke, D.B., 1974, Regional geophysics of the Basin and Range Province: Ann. Rev. Earth and Planetary Sci., v. 2, p. 213-238.

Trexler, D.T., Bell, E.J., and Roquemore, G.R., 1978, Evaluation of lineament analysis as an exploration technique for geothermal energy western and central Nevada: Rept. for U.S. Dept. of Energy, NVO-0671-2, 78 p.

Whitebread, D.H., 1978, Preliminary geologic map of the Dun Glen quadrangle, Pershing County, Nevada: U.S. Geol. Survey Open-File Report 78-407.

Wilson, J.T., 1971, Continents adrift - Readings from Scientific American: W.H. Freeman and Co., 172 p.

Wilson, J.T., 1976, Continents adrift and continents aground - Readings from Scientific American: W.H. Freeman and Co., 230 p.

Wright, L., 1976, Late Cenozoic fault patterns and stress fields in the Great Basin and westward displacement of the Sierra Nevada block: Geology, v. 4, p. 489-494.

Zietz, I., 1969, Aeromagnetic investigations of the earth's crust in the United States, in The Earth's Crust and Upper Mantle, P.J. Hard, ed., Am. Geophys. Union Mono. 13 (735 p.), p. 404-415.

Chapter 3. STRUCTURAL-TECTONIC ANALYSIS

By: Robert A. Whitney

3.0 STRUCTURAL-TECTONIC ANALYSIS

3.1 Introduction

3.1.1 Purpose and Scope

This study was undertaken to develop a geologic model for the Dixie Valley geothermal system with respect to structural and tectonic features. The study was conducted in two stages: Stage I included evaluation of available geophysical and geologic data, including fault and lineament maps and various imagery formats, such as Landsat, SKYLAB, NASA underflights, AMS photography and other conventional and low-sun-angle (LSA) photography. A bibliography search was initiated during Stage I. Stage II consisted of conducting a LSA photographic program of the study area, interpreting the resultant photography, and field checking the photogeologic data. Field work also included a preliminary fault scarp morphology study and compilation of a generalized surficial geologic map of the study area.

3.1.2 Methods and Analytical Techniques

3.1.2.1 Literature Search

The literature search was conducted primarily at the library of the University of Nevada-Reno; results of a limited computer search conducted by the Lawrence Livermore Laboratory, University of California-Berkeley, were incorporated into the reference bibliography. Additional pertinent geologic and geophysical data were provided by Southland Royalty Company. The literature search was initiated during Stage I of the investigation and continued throughout the program to incorporate pertinent new articles.

3.1.2.1 Low-Sun-Angle Photography

Six low-altitude aerial missions were flown under low-sun conditions from March to August, 1979, to generate LSA photographic coverage of the study area. A turbo-charged Cessna 207, designed for in-cabin mounting of the aerial camera and viewfinder, was chartered for each mission. The camera used for this program was a K17 military camera with 9x9 format and 6-inch focal length high speed lens actuated by a mechanical switch. The camera was manually leveled and timing of photo intervals was accomplished with an auto-reset stopwatch.

Navigation for the photography was by in-flight guidance from

1:62,500 scale topographic maps of the study area. Photos were flown along flight lines subparallel to the regional structure of N31E - S31W. Flight altitude approximated 6000 feet above mean terrain to yield photography with an approximate 1:12,000 scale. Flight lines were spaced at 1 5/16 miles to yield 20 percent side lap with photo intervals timed to yield 60 percent forelap for adequate stereoscopic images.

Kodak Tri-X (#2403) high speed black and white aerographic film was used for four missions, and Kodak Double-X (#2405) black and white aerographic films was used for two missions. The film was commercially processed and printed by America Aerial Surveys of Sacramento, California. A total of 1,324 images of good to excellent quality were obtained for the study region; an index of these images is incorporated on Plate II.

Flight times to obtain optimum results from LSA photography are defined by Slemmons (1969) as the two-hour intervals beginning one-half hour after sunrise and ending one-half hour before sunset. These optimum time intervals were used for the LSA program in Dixie Valley.

Seasonal variations in sun azimuth indicated an early spring program for optimum LSA imagery with respect to the regional trends in Dixie Valley (Slemmons, 1969; Glass and Slemmons, 1978; Slemmons, pers. commun., 1979). Approximately 90 percent of the imagery was obtained in early March under optimal conditions, with follow-up flights conducted in June and August.

Slemmons (1969) and Glass and Slemmons (1978) summarize the advantage of using highlighting techniques versus shadowing techniques for structural enhancement. The latter was used where possible in the program to detect very subtle structural features.

Interpretation of all stereoscopic images (LSA, NASA and AMS imagery) was accomplished with a Wild ST-4 stereoscope. Structural and tectonic photographic interpretations were delineated on mylar overlays on alternate images and then transferred to preliminary 7½-minute topographic quadrangle sheets (1:24,000 scale) with the aid of a Bausch and Lomb Zoom Stereo Transfer Scope. These map sheets were reduced by Photo-Mechanical Transfer (PMT) and assembled into a composite map (Plate II). Field verification of structural interpretations was conducted during the summer and fall of 1979.

3.1.2.3 Snow-lapse Photography

Snow-lapse photography planned for the winter months of late 1978 and 1979 was not accomplished. Major regional snowstorms occurred on December 19 and 20, 1978, and on February 22 and 23, 1979. Aerial reconnaissance flights immediately following the two storms (December 20, 1978, and February 23, 1979) verified the lack of adequate snow cover in Dixie Valley to accomplish a snow-lapse study.

The frontispiece, a Landsat composite color image of west-central Nevada, shows the regional extent of the storm of December 19 and 20, 1978. Dixie Valley, in the center portion of the image, is anomalously devoid of snow cover. This situation which recurred throughout the winter months, may be the result of local climatic influences, or a valley-wide 'hot spot' effect reflecting the underlying geothermal system.

3.1.2.4 Surficial Geology

Generalized surficial geology of northern Dixie Valley was delineated by interpretation of black and white 1:62,500 scale AMS photographs, with refinements based upon the 1:12,000 scale LSA photography. Because the various surficial geologic units correspond with specific geomorphic surfaces that also indicate genetic origin of the units, the surficial geology is presented as a generalized geomorphic surfaces map (Plate III). Surface and near-surface samples of the various units were collected for grain-size analysis; the results are presented in Appendix A.

3.1.2.5 Fault Scarp Morphology

Fault scarp morphology studies were conducted within the study area on scarps delineated on LSA photography. The method of Wallace (1977) was used to profile scarps by laying a stadia rod directly on the scarp and measuring its inclination. Scarps of moderate to high relief were chosen for profiling; graphic presentations of these profiles are presented in Appendix B.

3.1.3 Previous Work

Numerous authors have conducted studies within the Dixie Valley region. However, only those papers in the various critical disciplines that contributed most to the present study are listed here. Active faulting in Dixie Valley and nearby areas was studied by Larson (1957),

Slemmons (1957a,b), Burke (1967), and Ryall and Malone (1971). Regional studies were conducted by Stewart (1971), Thompson and Burke (1974), Wright (1976), and Speed (1976). Geologic maps of the Dixie Valley region were prepared by Page (1965), Willden and Speed (1974), and Johnson (1977). Geophysical data of Smith (1967, 1968), Meister (1967), Thompson and others (1967), Thompson and Burke (1974), Exploration Data Consultants (1976), Senturion Sciences (1977, 1978), and Keplinger and Associates, Inc. (1978) were integrated into this report.

3.1.4 Acknowledgements

Numerous discussions with Dennis McMurdie, Jere Denton, and Dick Jodry of Southland Royalty Company and Larry Larson, Burt Slemmons, and Elaine Bell of Mackay School of Mines contributed to the development of ideas and helped to focus the investigations of the structural-tectonic and geologic character of Dixie Valley as expressed in this chapter. Capable field assistance was provided by Tom Bard, Russell Juncal, Anne Zelenski, Anna Evashko, Cady Johnson, Neil Ingraham and Rod Fricke of the University of Nevada-Reno. Grain-size analyses of selected surficial deposit samples conducted by Anne Zelinski were gratefully incorporated into this report. Appreciation is extended to the many photogeology students at UNR who assisted on the photographic missions; and to Frank Elliott and Pat Miller, pilots for Aviation Services Inc., for always putting the plane on course and making it home on "empty". Technical and editorial review by MMRI and SRC personnel, in particular Dennis McMurdie, Burt Slemmons, Larry Larson and Elaine Bell, significantly improved this chapter.

3.2 ANALYTICAL RESULTS

3.2.1 Geomorphic Setting and Surficial Geology

A generalized geomorphic map of the study area is presented on Plate III. The area is bounded by the Stillwater Range to the northwest, the Clan Alpine and Augusta Mountains to the southeast, Jersey and Pleasant Valleys to the northeast, the southernmost extent of the Humboldt Salt Marsh to the southeast.

Five distinct geomorphic surfaces were delineated by photogeologic interpretation (Plate III): (1) active alluvial fan surfaces, (2) inactive or highly dissected alluvial fan surfaces, (3) surfaces developed

by lacustrine processes, (4) composite or undifferentiated surfaces produced by aeolian, alluvial, and lacustrine processes, and (5) the surface of the presently active playa. These surfaces represent distinct geologic and geomorphic environments (including paleo-environments) and can be correlated with distinct surficial geologic units that are assumed to be present at depth but with lateral and vertical facies changes.

The active alluvial fans are eroded bedrock material derived from nearby mountain ranges and consist of clay-, silt-, sand-, and cobble- to boulder-size material of the varying lithologies present in the mountain ranges. Appendix A contains grain-size distribution curves for representative samples of the active fans and other surficial deposits. In general, coarser and heavier material would be preferentially deposited near the apex of a fan with finer and lighter materials being carried further down the apron (Ritter, 1979; Hooke, 1967, 1968).

The older alluvial fan deposits are similar to those of the active fans, but the older surfaces are primarily undergoing degradation. These surfaces are highly dissected and surface cobbles are coated with desert varnish.

The landforms produced by lacustrine deposition include deltas, strand lines, and longshore bars. The strand lines are conspicuous sandy deposits presently being subjected to subaerial erosion. The delta deposits and longshore bars are relatively stable and consist of well sorted cobbles, pebbles and silt with little or no primary clay or sand. The cobbles form large patches of desert pavement and are coated with desert varnish. Carbonate cobbles on the surface exhibit flutes from aeolian processes. Locally longshore bars have dammed pre-lacustrine drainages resulting in the ponding of fine-grained (clay- and silt-size) alluvium on the upslope side. Many of these dams have been breached by more recent fluvial activity.

The composite geomorphic surfaces include valley fill deposits derived from three distinct genetic processes. These undifferentiated deposits are predominantly silt with major amounts of clay and minor amounts of sand and gravel. This composition suggests two presently active processes with a third inactive. Active aeolian and alluvial processes are depositing predominantly finer particles. The scattered sand grains are possibly aeolian with the finer silt and clay being the outwash from active alluvial fans. The occasional cobbles are assumed

to be the result of flash flooding which has carried larger material beyond the active alluvial fan surfaces. Much of the silt is a result of inactive lacustrine processes and thus, may be Lahontan in age.

The active playa deposits are composed of fine sand, silt and clay-sized particles and salt crystals (predominantly sodium chloride). The center of the presently active playa is marshy with active deposition of sodium chloride. The water level fluctuates and, with the extreme low relief of the playa, the surface extent of the marsh varies greatly. Surrounding the marsh is a zone composed of clay and silt with salt crystals emplaced by littoral action as the water level fluctuates. Three sides of the high water area are bounded by conspicuous "beach berms" which may result from the capture of aeolian material by salt cementation as salt water is carried to these areas by capillary action from the marsh and evaporated. Locally sparse vegetation is present near the perimeter of the active playa with conspicuous mounds of aeolian material, mostly silt, built up around isolated bushes. Some areas of the playa are sparsely populated by salt grasses.

3.2.2 Structural-Tectonic Features

The structural-tectonic features map (Plate II) is a composite of features delineated by photogeologic interpretation of previously available imagery and the LSA imagery generated by this study. Fault zones, generalized as a single line, are shown on Plate IV. Interpretation of features critical to the structural analysis have been verified in the field. The structural-tectonic features delineated by surface expression correspond with subsurface structures delineated by gravity, aeromagnetic, and other geophysical surveys (Meister, 1967; Smith, 1968; Stewart, 1971; Senturion Sciences, 1977, 1978; Koenig and others, 1976; Keplinger and Associates, 1978) (Figure 3-1).

3.2.2.1 Old Stillwater Fault

This range-front fault zone bounds the Stillwater Range to the southeast and trends N36E from the southern edge of the study area near Dixie Meadows into Pleasant Valley on the northern edge of the study area. The zone is marked at the surface by very fresh appearing scarps in alluvium and bedrock, alignment of fumaroles, vegetation and tonal contrasts, back-facing grabens, breccia slumps, and slumps. Geomorphic

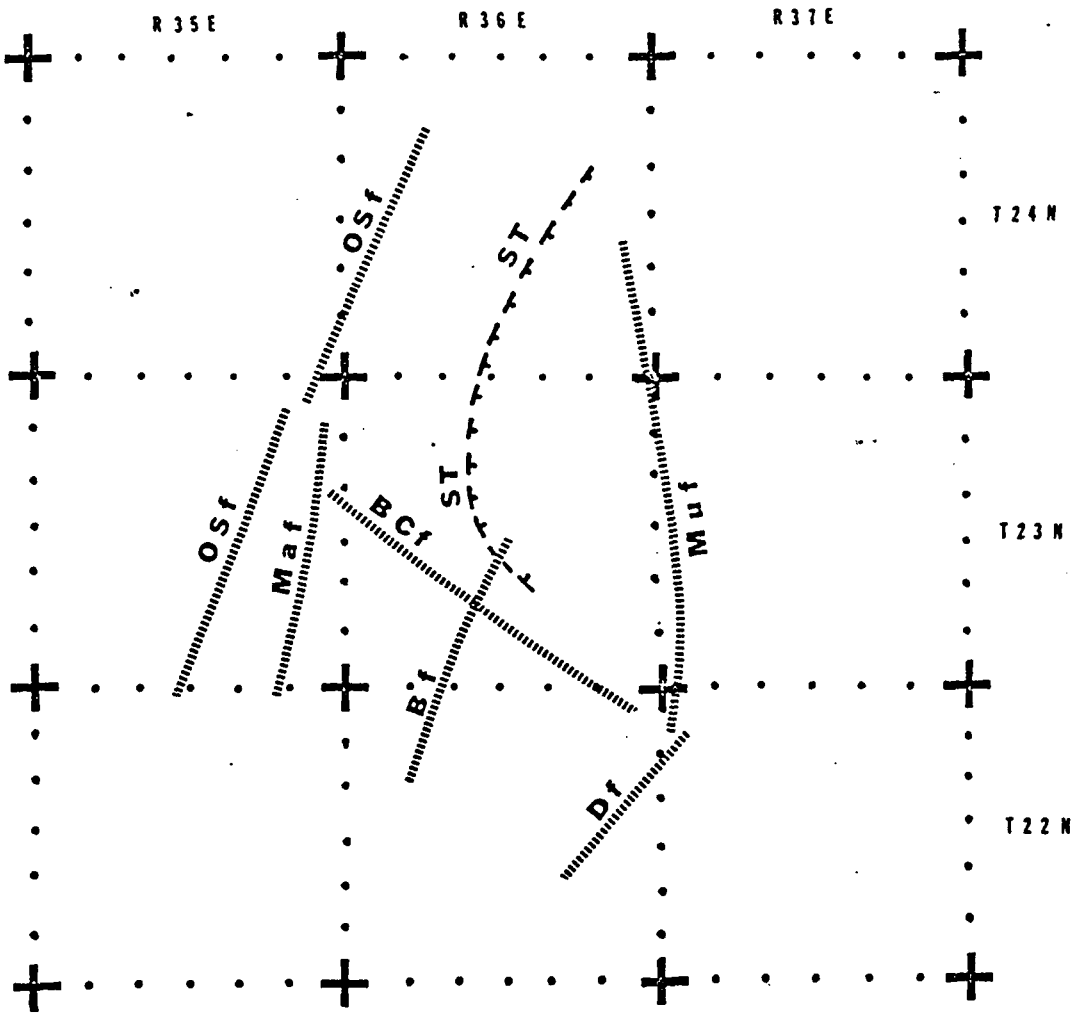

Figure 3-1. Diagrammatic sketch of major structural elements defined by aeromagnetic data interpretation by Senturion Sciences (1977, 1978). Bf - Buckbrush fault; Df - Dyer fault; Maf - Marsh fault; Muf - Mud fault; OSf - Old Stillwater fault; ST - Stillwater Thrust fault (?); BCf - Bernice Creek fault.

features indicate this zone is very active and include 'V' shaped valleys and steep faceted spurs with little or no dissection (Glass and Slemmons, 1978) and fault scarps in alluvium with a very high slope angle or even free face (Wallace, 1979). Slemmons (1966) indicates the southern portion of this zone ruptured in the 1954 Dixie Valley earthquake as far north as the Boyer Ranch. Mrs. Sheldon Lamb of the Boyer Ranch (verbal commun., 1979) reports that features near the Boyer Ranch were liquefaction phenomena and the actual fault surface rupture extended only as far north as Dixie Meadows.

Field measurements of a southeast dip of 50 to 60 degrees for this zone are consistent with the literature (Slemmons, 1957a; Larson, 1957; Page, 1965; Burke, 1967; Meister, 1967; Ryall and Malone, 1971; Stewart, 1971). Site-specific evidence for the southeast dip includes: (1) measurable fault planes on bedrock surfaces, (2) surficial geomorphic expression of normal faulting including back-facing grabens, and (3) fault plane solutions for a N55W tensional (Sigma 1) direction in northern Dixie Valley (Ryall and Malone, 1971). First order Riedel shears (Tchalenko, 1970) indicate the fault zone has a minor right-slip component. Regional studies also indicate extension of the study area in a general N55W direction (Thompson and Burke, 1973; Wright, 1976). This data is incompatible with the interpretation of aeromagnetic data by Senturion Sciences (1977, 1978) indicating a N55W dip for this zone.

The maximum elevation of the Stillwater Range to the northwest of the fault zone is greater than 7200 feet and alluvial fill in the valley to the southeast of the fault zone is nearly 2000 feet below the present valley elevation indicating greater than 6000 feet total vertical displacement along this zone.

3.2.2.2 Marsh Fault

The Marsh fault extends from the southern edge of the study area along a N30E trend to intersection with the Old Stillwater fault in Section 36, T24N, R35E. The surface expression, although somewhat subdued along the northwest edge of the Humboldt Salt Marsh, is marked by stream and vegetation alignments, subtle scarps and grabens. Scarps preserved in Sections 6 and 7, T23N, R35E, and Sections 10 and 16, T22N, R35E, indicate normal faulting with the southeast block downdropped. This is compatible with aeromagnetic interpretations (Senturion Sciences, 1977,

1978).

3.2.2.3 Buckbrush Fault

The Buckbrush fault is a semi-arcuate fault concave to the southwest trending N30E from the southern edge of the study to the Bernice fault when it splays into two branches. Both splays intersect the Old Stillwater fault: the western splay in Section 4, T24N, R36E, and the eastern splay near the Senator fumeroles in Sections 28 and 29, T25N, R37E. Surface expression is marked by scarps, spring and vegetation alignments, and vegetation and tonal contrasts. The northwest block is downdropped in the southern portion of the zone but relative movement is not discernible in the northern portion.

3.2.2.4 Mud Fault

The Mud fault trends N36E from the Dixie Settlement area to Section 4, T23N, R35E, then follows a N15E trend to Sou Hills. Surface expression of the southern portion indicates the northwest block is downdropped. Near Sou Hills several interpretations are possible: (1) the fault joins the frontal fault system on the east side of Pleasant Valley (Pleasant Valley fault), (2) the fault joins the Old Stillwater fault system and continues along the west side of Pleasant Valley, or (3) the fault is related to the frontal fault system on the east side of the Tobin Range (Tobin fault).

A southeast splay of this fault, mapped by Secturion Sciences (1977, 1978) as the Mud fault, shows surface expression as moderate scarps near the mouth of Deep Canyon and trends N25E to intersection with the main zone is Section 30, T23N, R37E. However, this splay could be related to the Shoshone fault with the Mud fault being a separate and distinct structure. In either interpretation, the block northwest of this splay is downdropped.

3.2.2.5 Dyer Fault

The Dyer fault transects the study area along a N36E trend from the mouth of Meadow Spring Canyon on the south and is the frontal fault of the Clan Alpine and Augusta Mountains. The northwest block is downdropped along this zone. A splay of this fault appears to arc across Dixie Valley just north of Hole-in-the-Wall and join the frontal fault

system on the west side of the Tobin Range in Pleasant Valley (Pleasant Valley fault).

The Clan Alpine Mountains reach a height in excess of 8,800 feet, with alluvial fill of unknown thickness below the 3600 feet mean elevation valley floor, which indicates greater than 5000 feet total vertical displacement along this zone.

3.2.2.6 Bernice Fault

The Bernice fault is a main crosscutting feature in northern Dixie Valley. Surface expression of vegetation and tonal contrasts and stream and spring alignments indicate the zone extends along an arcuate trace northwest from Bob Canyon toward the Dixie site in the Stillwater Range. A splay of this zone may arc to the north and join the Marsh fault near Section 17, T23N, R36E. Surficial geomorphic deposits indicate the southwest block is downdropped as the lowest area of the valley floor; the salt marsh is immediately southwest of the fault trace. However bedrock geology near the Dixie Site indicates the northeast block may be downdropped, as does aeromagnetic data (Senturion Sciences, 1977, 1978) Surface expression is subtle and relative movement on the zone is not discernible from surface evidence.

3.2.2.7 Stillwater Thrust

Senturion Sciences (1977, 1978) postulated a thrust fault in the center of the study area based on interpretation of aeromagnetic data. No surface expression of a thrust fault was discerned by photogeologic interpretation.

3.2.2.8 Mississippi Fault

Another fault zone (Mississippi fault) extends across Dixie Valley along a S40E trend from the mouth of Mississippi Canyon, crosscutting the valley. Surface expression includes low scarps, vegetation and tonal contrasts, and stream alignments. These features are subtle but indicate the southwest block is downdropped. Surficial geomorphic deposits indicate the opposite may be true as the Humboldt Salt Marsh lies immediately northeast of this zone.

3.2.2.9 Dixie Meadows Fault

A major fault zone (Dixie Meadows fault) trends N36E from the southern edge of the study area across Dixie Meadows, sub-parallel to and between the Old Stillwater and Marsh faults. This Dixie Meadows fault corresponds to the valley branch splay of the Stillwater Range frontal fault of Trexler and others (1978). The zone continues in an arcuate path concave to the northwest and merges with the Old Stillwater fault in Sections 35 and 36, T24N, R35E. The fault zone apparently re-emerges from the Old Stillwater fault zone just northeast of this area and again forms an arcuate zone which intersects the frontal fault system in Section 14, T24N, R36E. The southwest block is downdropped as evidenced by numerous slumps, asymmetric grabens, and southeast facing scarps. Spring and vegetation alignments are also present. Liquefaction phenomena, including slumps and sand boils, are present along the portions of this fault that lie near highly saturated playa deposits. Slemmons (1957a) has mapped surface rupture on this zone during the 1954 Dixie Valley - Fairview Peak earthquake in Dixie Meadows.

3.2.2.10 Shoshone Fault

A fault (the Shoshone fault) northwest of and sub-parallel to the Dyer fault trends N30E with maximum surface expression near the mouth of Shoshone Creek. In addition to vegetation contrasts, surface expression is marked by scarps which indicate the block to the northwest is downdropped. Hyder Hot Springs may be associated with this structure.

3.2.2.11 Pleasant Valley Fault

The Pleasant Valley fault is the frontal fault system on the west side of the Tobin Range. The fault zone is wide but activity in 1915 created a very sharp southwest facing scarp from surface rupture near the bedrock-alluvium contact (Slemmons, 1966). This zone crosses the Sou Hills to the southwest and apparently ends in the northern portion of Dixie Valley.

3.2.2.12 Tobin Fault

The frontal fault zone on the east side of the Tobin Range (Tobin fault) extends southwest into the study area and apparently dies out in

the north end of Dixie Valley. A splay of this fault may cross to the southeast of Sou Hills and merge with the Old Stillwater fault. Scarps along this zone indicate the southeast block is downdropped. Sou and Seven Devils Hot Springs may be associated with this structure.

3.2.2.13 White Rock Canyon Fault

A fault (White Rock Canyon fault) traces diagonally north-south across the Stillwater Range, following White Rock Canyon in the study area. This fault may join the Old Stillwater fault immediately southwest of the mouth of White Rock Canyon and trend south, splaying from the Old Stillwater fault in Section 23 of T23N, R35E. Surface expression for this zone includes vegetation and tonal contrasts and lineations in Dixie Valley, displaced bedrock in White Rock Canyon and, regionally, the apparent left-lateral displacement of the Humboldt gabbroic complex (Humboldt lopolith of Speed, 1976) (Figure 3-2).

The displacement shown on the Humboldt complex contrasts with that proposed by Smith (1968). From aeromagnetic data Smith (1968) interpreted about 1 mile of right lateral displacement of the eastern portion of the complex on what corresponds to the Buckbrush fault in this report. A review of this data indicates a noticeable anomaly which Smith interpreted as the southern edge of the complex beneath alluvium in Dixie Valley. This anomaly may instead correspond to a downdropped southwest block on the Mississippi fault. Another anomaly crossing the valley about 11 miles to the northeast may represent the southern boundary of the Humboldt complex in Dixie Valley (Figures 3-3 and 3-4). This interpretation is consistent with outcrops of the gabbroic complex in the Clan Alpine Mountains and Stillwater Range. Figures 3-5 and 3-6 depict the aeromagnetic data of Smith (1968) re-interpreted to include the left-lateral White Rock Canyon fault.

3.2.3 Fault Scarp Morphology

A preliminary fault scarp morphology study was initiated along the Old Stillwater and Tobin faults, primarily to discern number of movements and amount of displacement on scarps in alluvium near White Rock Canyon and Sou Hot Springs. The methods of Wallace (1977) were used. Scarp profiles for these traverses are presented in Appendix B.

Profiles 1 through 5 are on the Old Stillwater fault near White

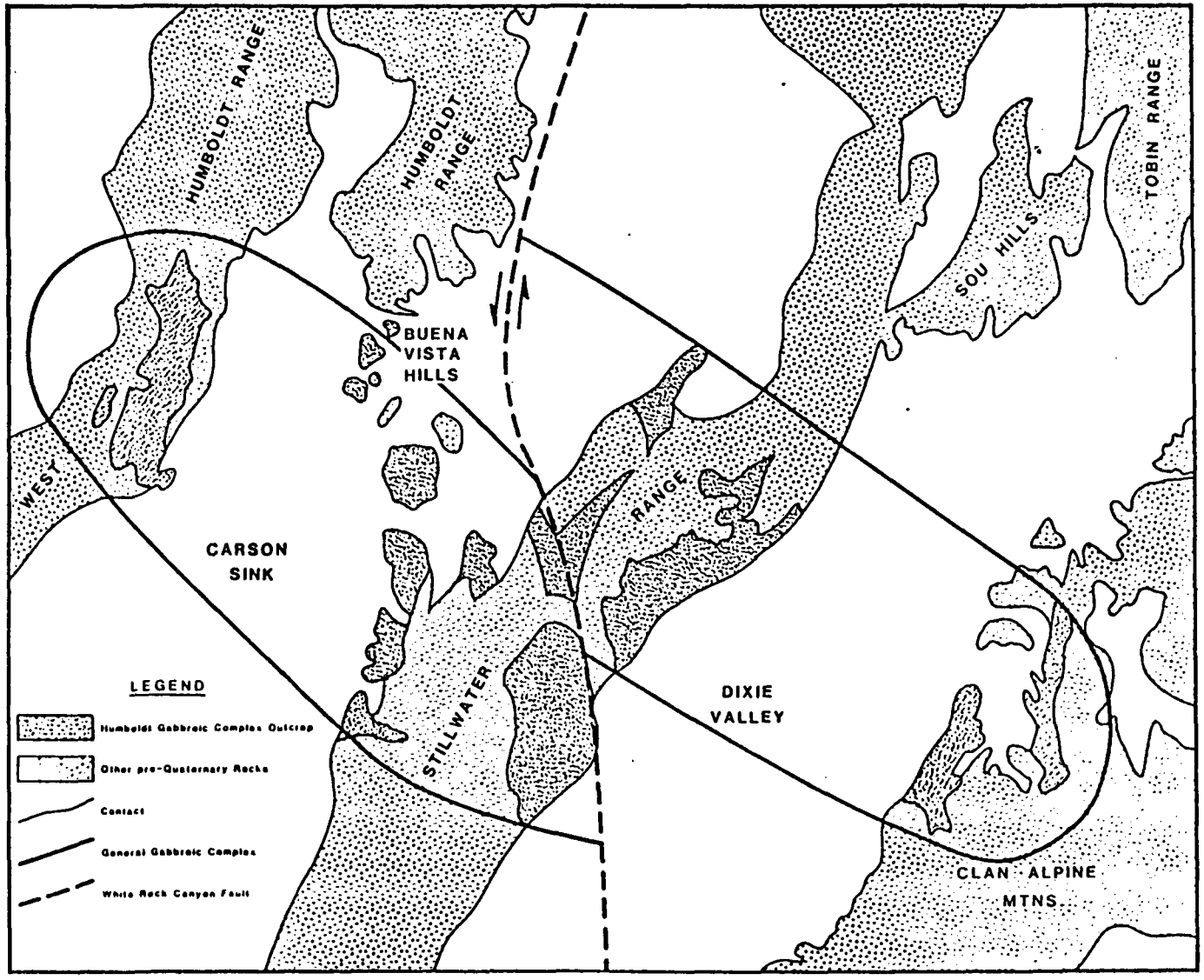

Figure 3-2. Generalized geologic map showing extent of Humboldt gabbroic complex (Humboldt Lopolith of Speed, 1976)

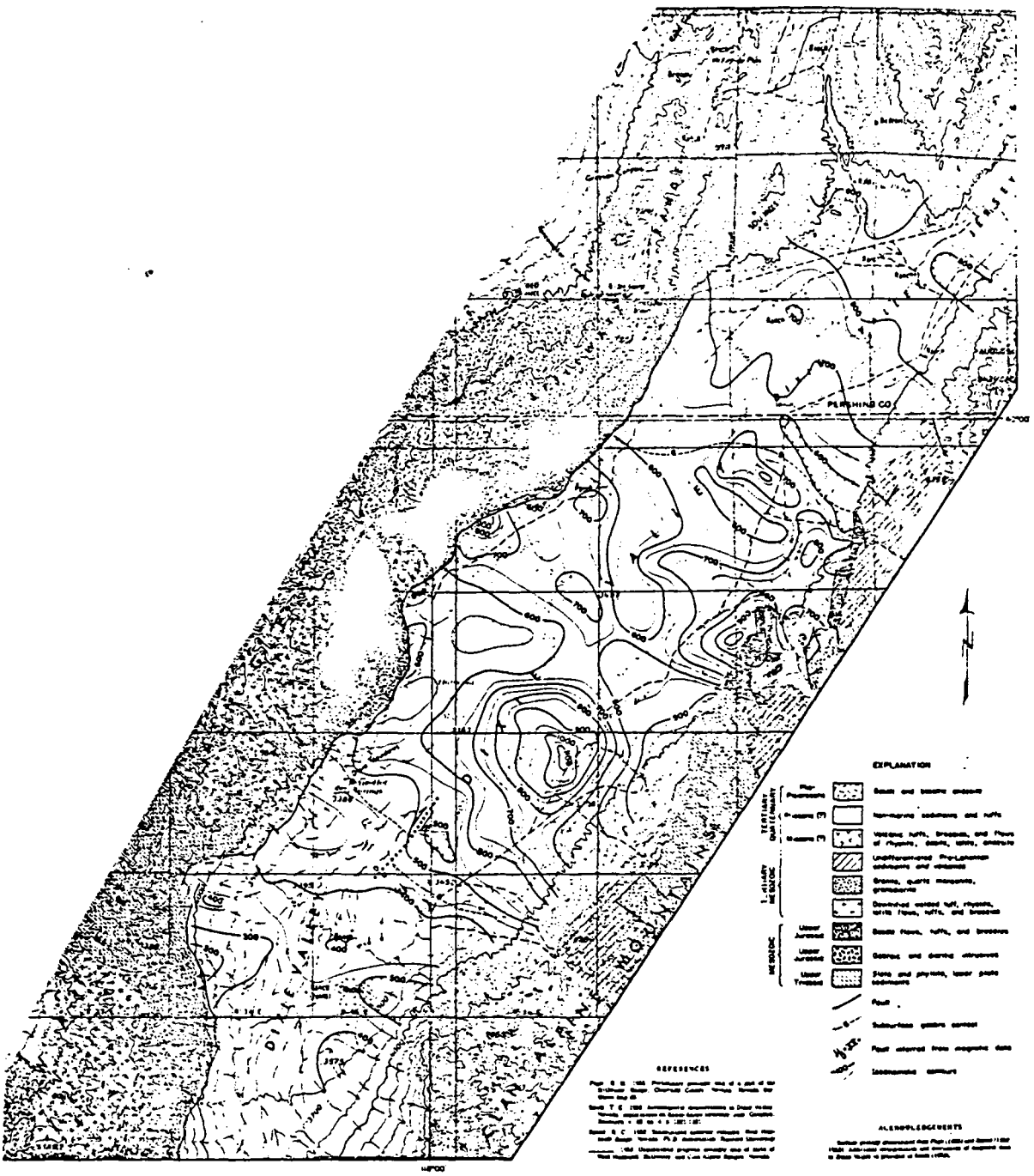

Figure 3-3. Aeromagnetic map of Dixie Valley. Approximately one to two miles of right-lateral offset is interpreted across the southern boundary of the gabbro by Smith (1971).

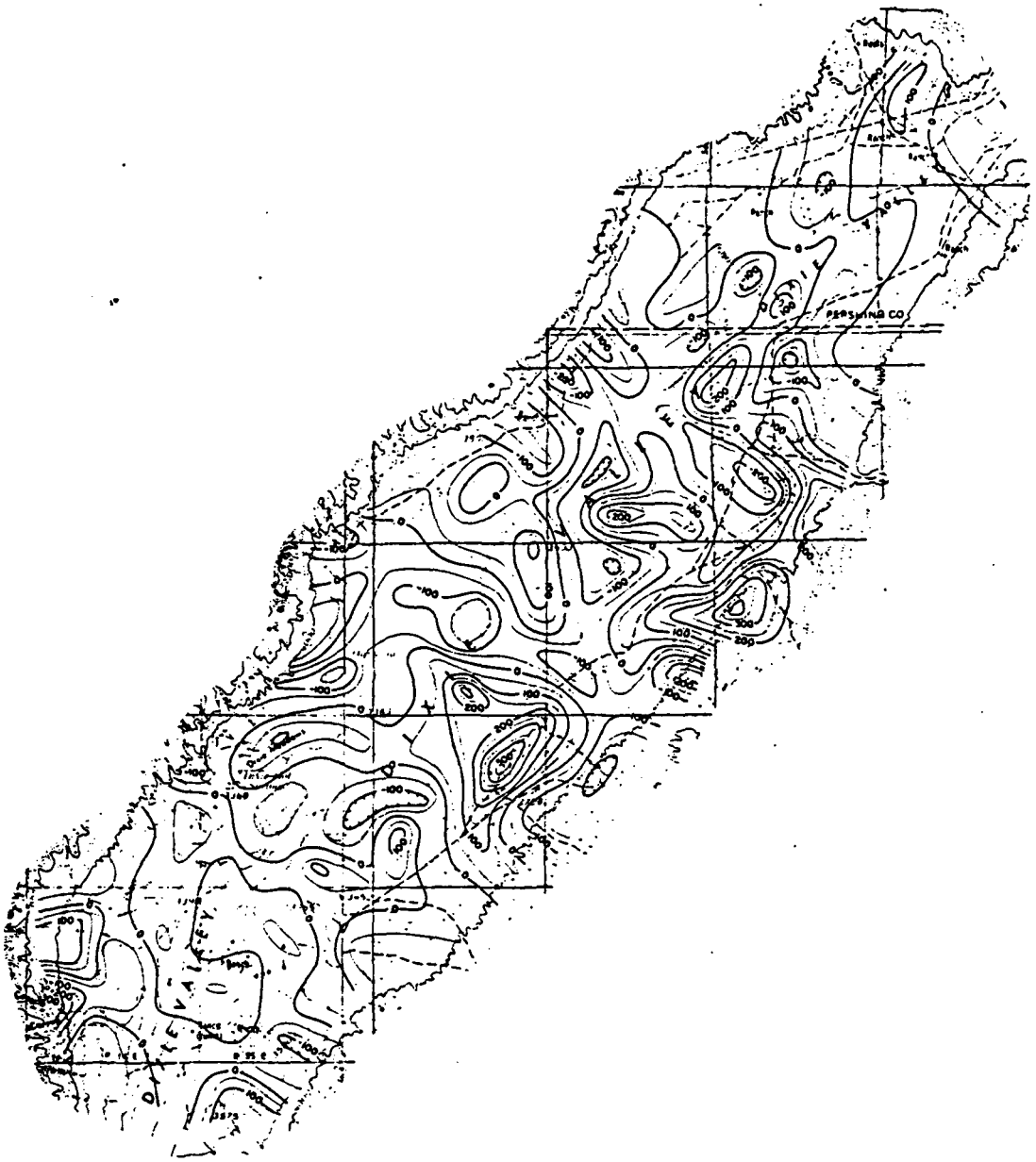

Figure 3-4. Second vertical derivative of aeromagnetic data for Dixie Valley. (from Smith, 1971)

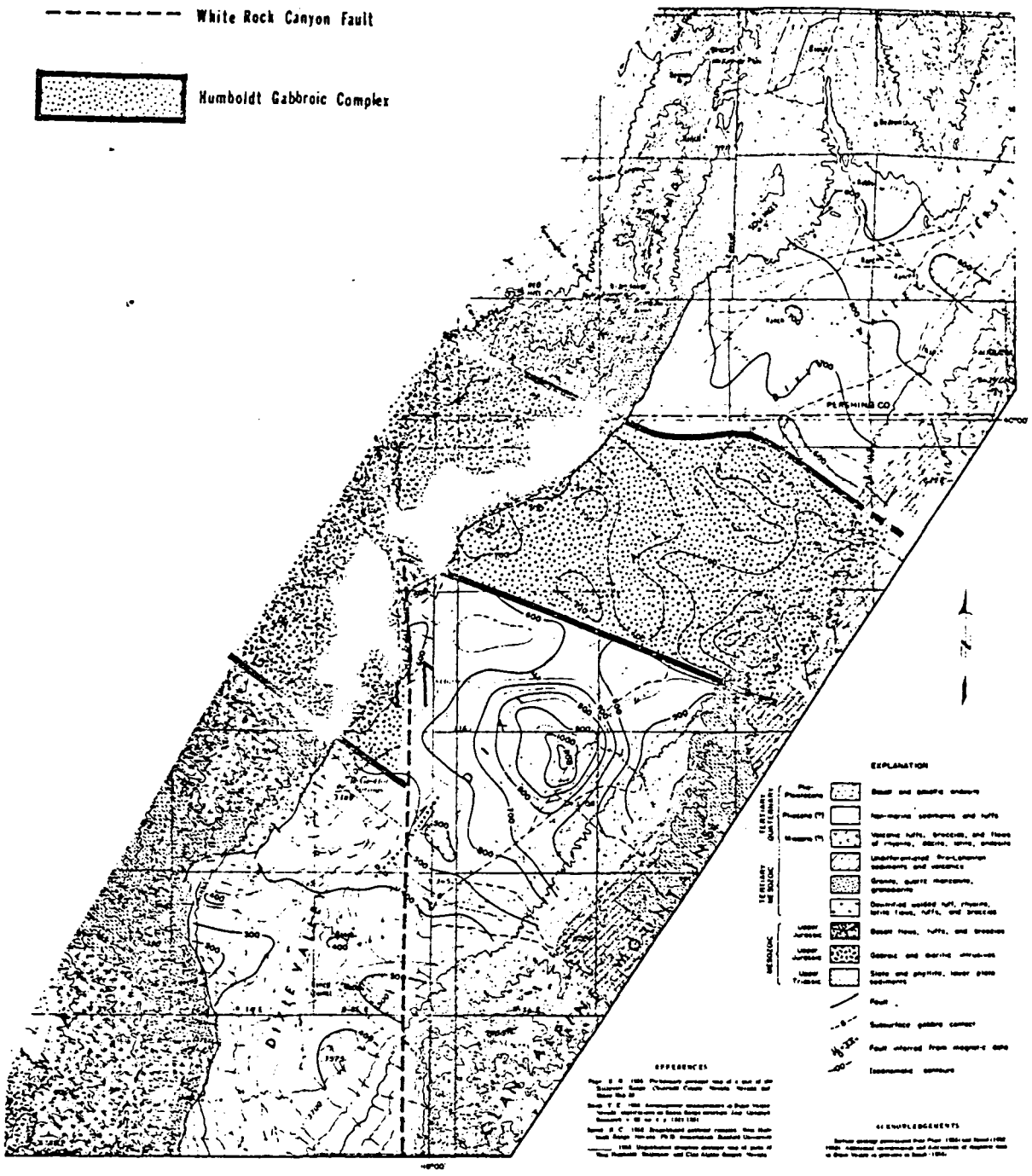

Figure 3-5. Re-interpretation of aeromagnetic map of Dixie Valley showing the left-lateral White Rock Canyon fault and the proposed boundaries of the Humboldt gabbroic complex. (aeromagnetic data from Smith, 1971)

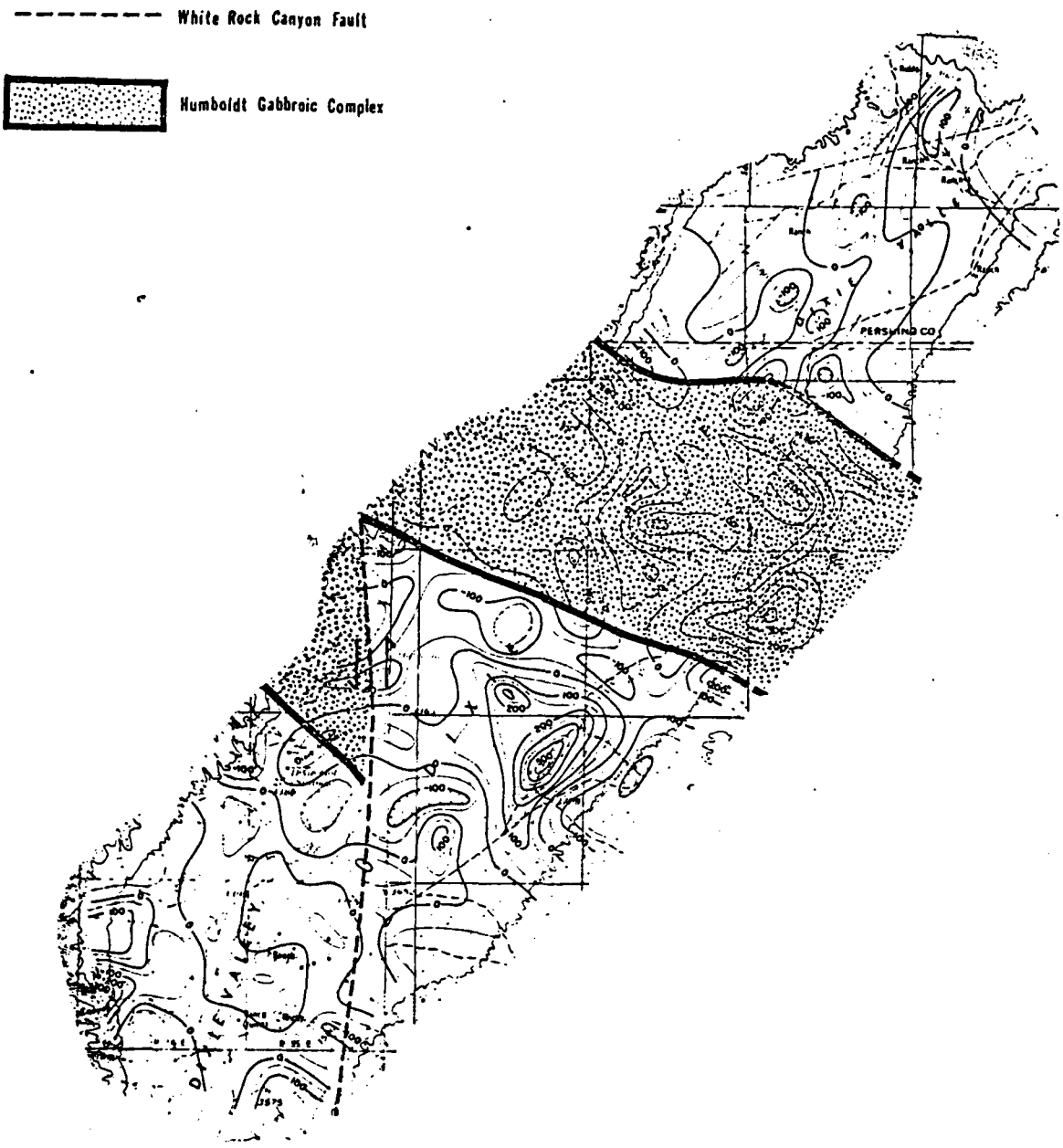

Figure 3-6. Interpretation of the second vertical derivative of the aeromagnetic data of Smith (1971) showing the left-lateral White Rock Canyon fault and the proposed boundaries of the Humboldt gabbroic complex.

Rock Canyon (Plate IV). The profiles show only one movement has occurred in this scarp with offset averaging 10.7 feet. This offset does not include a 15.5 foot offset on one traverse (#4) as this data may be invalid; the scarp profile at #4 may have been altered by lateral erosion at the scarp base or affected by liquefaction.

A scarp profile was measured on the Tobin fault (#6) to attempt to determine if this fault differs from the scarp observed near White Rock Canyon. The profile reveals three distinct movements of this fault, with displacement ranging from 3.5 to 10.9 feet.

This suggests that the Tobin and Stillwater faults represent different tectonic regimes with the Tobin fault more active in Quaternary and Recent time. The steeper faceted spurs on the Stillwater fault scarp indicate greater activity in the late Cenozoic however.

3.2.4 Bedrock Geology

The following discussion of the major geologic units and structure within the study area is synthesized from Page (1965), Willden and Speed (1974), Speed (1976) and Johnson (1977).

3.2.4.1 Triassic Rocks

The most important rock unit consists of upper Triassic metasediments, mostly phyllite and slate with about 10% metaquartzite and limestone. This complexly deformed unit is estimated to be 5000 to 10,000 feet thick, with the base unexposed. Locally this unit is overthrust by an upper Triassic massive limestone.

3.2.4.2 Jurassic Rocks

The Jurassic sequence of altered and locally schistic metavolcanics consist chiefly of fine-grained slaty andesite tuffs, breccias, andesite flows with minor quartzites and calcareous sandstone. This sequence is in excess of 5000 feet thick. The base is in thrust contact with the Triassic limestone.

The Humboldt gabbroic complex (Speed, 1976) outcrops in large areas of the Stillwater Range and Clan Alpine Mountains. The intrusive phase of this complex is gabbroic to dioritic in composition. Extrusive units include basalt flows, tuffs and breccias.

Jurassic and older rocks are metamorphosed to the greenschist fac-

ies.

The Boyer thrust (Fencemaker thrust of Speed, 1976) has transported quartzites of Jurassic age over lower Jurassic units with emplacement of the Humboldt complex as the propelling mechanism. Age dating of the gabbroic complex (Speed and Armstrong, 1971) at 151 to 156 my also dates the thrusting.

3.2.4.3 Jurassic to Miocene Rocks

Four sequences of volcanic units from 2000 to 10,000 feet thick include acidic tuffs and breccias and basaltic andesite flows. The lower units are intruded by granitic plutons of late Cretaceous age. The episode of acidic intrusion accentuated and coarsened the metamorphic fabric of the invaded units, inducing chiastolite growth and the formation of chloritoid porphyroblasts. Locally marble and skarn were produced. Most intrusions produced contact aureoles of black hornfels or chiastolite bearing phyllite.

3.2.4.4 Miocene Rocks

A widespread Miocene volcanic sequence, up to 4000 feet thick, includes tuffs, breccias and flows which vary in composition from latite through rhyolite. Riehle and others (1972) have located this Miocene volcanic center in the southern Clan Alpine Mountains.

3.2.4.5 Late Cenozoic Deposits

Plio-Pleistocene to Recent deposits include sediments of lacustrine and fluvial origin, locally interbedded with acidic ashes, tuffs, and flows. Pliocene basalt flows, aggregated up to 1600 feet thick, are present in the lower portions of the sequence. Thicknesses of greater than 5000 feet are postulated in Dixie Valley based on aeromagnetic data (Smith, 1968).

3.3 Interpretations and Conclusions

3.3.1 Geomorphic Surfaces

A distinct relationship is seen between the geographic position of geomorphic surfaces and the structural-tectonic features in Dixie Valley. In most obvious of these relationships, the active playa surface and the

Humboldt Salt Marsh are bounded on all four sides by structural features (Plate IV). On the northwest side of the playa the Marsh fault marks the boundary zone while to the southeast the boundary is marked by the Buckbrush fault. The two crosscutting features of Dixie Valley --the Bernice and Mississippi faults--lie close to the northeast and southeast boundaries of the Salt Marsh. The boundary of the active playa on the northeast extends over the Bernice fault and corresponds generally with a splay of the Buckbrush fault where it transects the valley. These studies place the active inner-graben to the northwest of the longitudinal axis of Dixie Valley and the salt marsh is displaced in the same manner with respect to the active playa surface.

The alluvial, lacustrine and aeolian deposits included in the undifferentiated valley fill are located northeast and southwest of the active playa surface. These sediments extend northward into both Pleasant and Jersey valleys, and southward beyond the study area. Like the playa deposits, these sediments are shifted northwest of the longitudinal valley axis.

Active alluvial fan surfaces extend from bedrock on both sides of the valley to the playa or valley fill deposits. These deposits are asymmetrically distributed as a narrow band (up to 4 miles wide) of steeply sloping fan surfaces extending southeast from the Stillwater Range, and a wide band (3 to 7 miles wide) of gently sloping surfaces extending northwest from the Clan Alpine and Augusta Mountains. A third narrow band encircles the southern end of the Tobin Range. The wider band of coalesced fan surfaces (bajada) on the east side of the valley are embayed deeply into the source mountain ranges but those on the west side extend only a short distance into canyons of the Stillwater Range.

The older alluvial deposits are nearly absent on the western, more active side of the valley but are more common to the north and east where they generally adjoin bedrock.

The lacustrine deposits, including deltas, strand lines, and longshore bars, are predominantly near the playa and some distance from bedrock on the eastern and northern portions of the valley where they overlie alluvium and valley fill deposits. The scattered small deltas on the west side of the valley overlie fan surfaces only and generally adjoin bedrock.

The valley fill, older alluvial fans, and lacustrine deposits are

all transected by active alluvial surfaces where major drainages have entrenched through these areas.

Boundaries between the geomorphic surface units are generally sharp with the exceptions of the facies changes between the valley fill and playa and the valley fill and active alluvial fans.

3.3.2 Structural-Tectonic Features

A three dimensional model of the northern portion of Dixie Valley depicts the structural relationships among the various tectonic elements, with the alluvium removed and bedrock surfaces restored (Figure 3-7). This modified interpretation incorporates all fault zones described in Section 3.2.2 with the exception of the postulated Stillwater thrust fault (Senturion Sciences, 1977, 1978). Although the relative movement on the Bernice and Mississippi faults is uncertain, a downthrown southwestern block is depicted in the model.

A mechanism for the formation of graben valleys similar to Dixie Valley is reviewed by Stewart (1971). Tchalenko (1970) and Cloos (1955, 1968) have assumed laboratory clay models of fault and/or deformation systems mimic geological systems. A model developed by Cloos (1968) for Basin and Range horst and graben formation (Figure 3-8) closely resembles the three dimensional model presented in Figure 3-7 for Dixie Valley.

The longitudinal assymetry of Dixie Valley also fits well with laboratory models developed by Cloos (1968). The downdropping of one side of the graben in the models corresponds with structural interpretation along the Stillwater margin of the Valley. Slump block faulting of the model closely resembles interpretation along the Clan Alpine and Augusta Mountains. A distinct arcuate crosscutting feature developed in the model may correlate with the arcuate crosscutting splays of the Buckbrush and Dyer faults.

The graben model postulated above would suggest more active (i.e., greater amounts of) subsidence in a zone along the western side of the valley. Alluvial fans (and other deposits) in this zone would tend to be covered more rapidly by playa deposition on this downdropping block. Conversely, older alluvial fans, older delta deposits, and a much wider zone of active alluvial deposition would be expected on the surface of the more brecciated side of the graben where the total displacement is distributed across a series of step faults. This is consistent with the

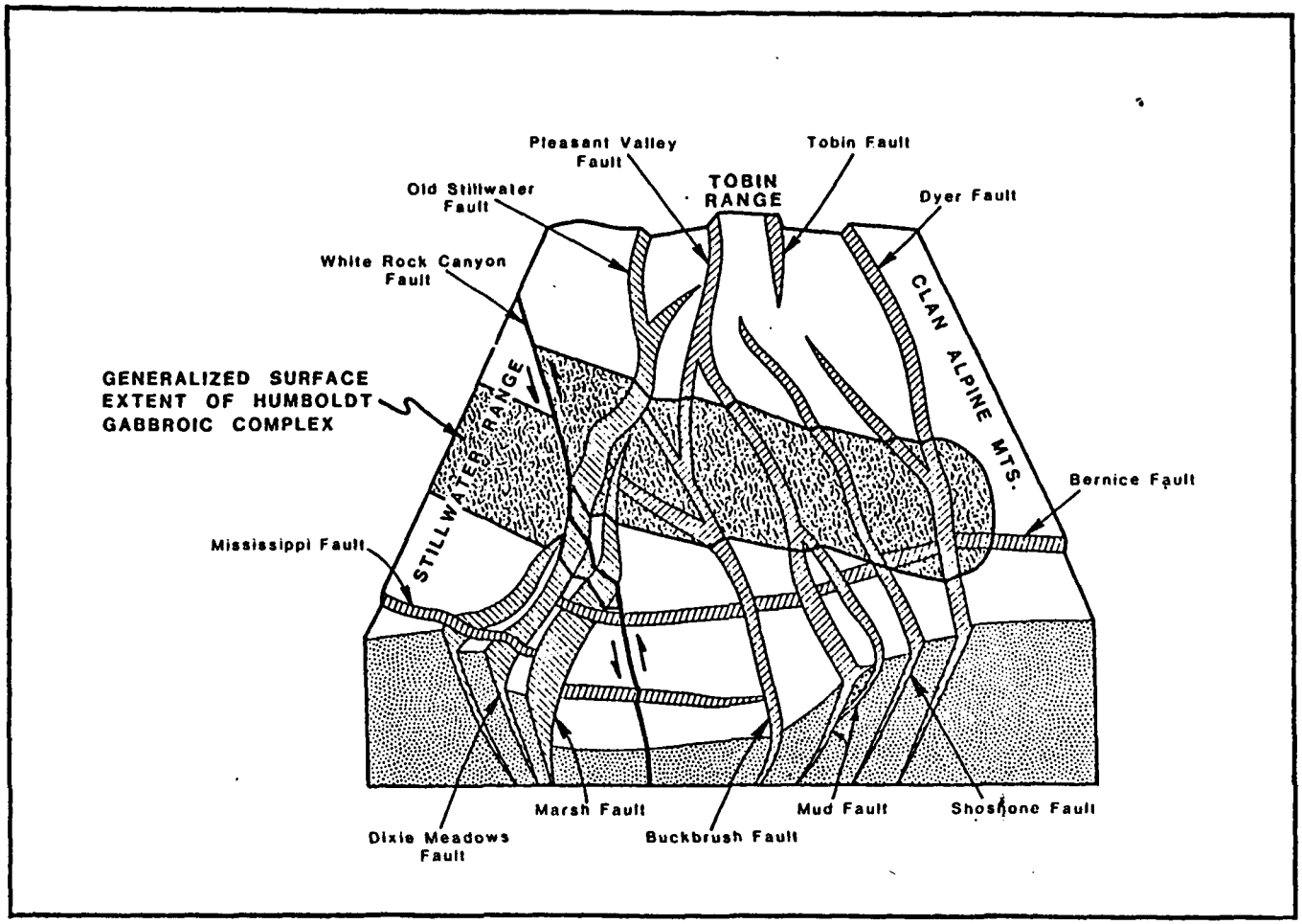

Figure 3-7. Three dimensional model of the northern portion of Dixie Valley. The structural relationships among the various tectonic elements are depicted, with alluvium removed and bedrock surfaces restored.

distribution of the various geomorphic surfaces within northern Dixie Valley (Plates III and IV).

The above model does not explain crosscutting features which extend into bedrock such as the Mississippi, Bernice, and White Rock Canyon faults. These are inferred to be older faults which predate the inception of Basin and Range faulting (15 to 17 m.y. ago; Stewart, 1971) but are still active. Geomorphic features along these fault zones include subtle scarps, spring alignments and vegetation contrasts indicating late Quaternary, possibly Recent, movement.

Gravity data (Stewart, 1971; Erwin and Bittleston, 1977; Erwin and Berg, 1977) are consistent with the model of a complex asymmetric graben. Structural relationships defined by aeromagnetic surveys (Smith, 1971; Nevada Bureau of Mines and Geology, 1977; Senturion Sciences, 1977, 1978) are in close agreement with clay model experimental data (Cloos, 1955, 1968) and the structural-tectonic features delineated by surficial expression in Dixie Valley (Plate II).

3.4 References

Burke, D.B., 1967, Aerial photography survey of Dixie Valley, Nevada, in U.S. Air Force Cambridge Research Labs. Spec. Rept. 66-848, 36 p.

Burke, D.B., 1973, Reinterpretation of the Tobin Thrust-Pre-Tertiary geology of the southern Tobin Range, Pershing County, Nevada: PH. D. thesis, Stanford Univ., Stanford, Calif.

Cloos, E., 1955, Experimental analysis of fracture patterns: Geol. Soc. America Bull., v. 66, p. 241-256.

Cloos, E., 1968, Experimental analysis of Gulf Coast fracture patterns: Am. Assoc. Pet. Geol. Bull., v. 52, no. 3, p. 420-444.

Erwin, J.W., and Berg, J.C., 1977, Bouguer gravity map of Nevada: Reno sheet: Nevada Bur. Mines and Geol., Map 58.

Erwin, J.W., and Bittleston, E.W., 1977, Bouguer gravity map of Nevada: Millett sheet: Nevada Bur. Mines and Geol., Map 53.

Exploration Data Consultants, Inc., 1976, Gravity and magnetic survey over the Humboldt Salt Marsh, Dixie Valley, Nevada; Report for Dow Chemical Company, 8 p.

Glass, C.E., and Slemmons, D.B., 1978, State-of-the-art for assessing earthquake hazards in the United States, Report 11 Imagery in Earthquake Analysis: U.S. Army Engineer Waterways Experiment Station, Misc. Paper S-73-1, 221 p.

Hooke, R., 1967, Processes on arid-region alluvial fans: Jour. Geol., v. 75, p. 438-460.

Hooke, R., 1968, Steady-state relationships on arid-region alluvial fans in closed basins: Am. Jour. Sci., v. 266, p. 609-629.

Johnson, M.G., 1977, Geology and mineral deposits of Pershing County, Nevada: Nevada Bur. Mines and Geol., Bull. 89, 115 p.

Keplinger and Associates, Inc., 1978, Interim evaluation of exploration and development status, geothermal potential and associated economics of Dixie Valley, Nevada: Rept. prepared for Millican Oil Company, Sept. 1978, 60 p.

Larson, E.R., 1957, Minor features of the Fairview fault, Nevada: Bull. Seis. Soc. America, v. 47, no. 4, p. 377-385.

Meister, L.J., 1967, Seismic refraction study of Dixie Valley, Nevada in U.S. Air Force Cambridge Research Labs. Spec. Rept. 66-848, 72 p.

Nevada Bureau of Mines and Geology, 1977, Aeromagnetic map of Nevada: Reno sheet: Nevada Bur. Mines and Geol., Map 54.

Page, B.M., 1965, Preliminary geologic map of a part of the Stillwater Range, Churchill County, Nevada: Nevada Bur. Mines, Map 28.

Riehle, J.R., McKee, E.H., and Speed, R.C., 1972, Tertiary volcanic centers, west-central Nevada: Geol. Soc. America Bull., v.83, p. 1383-1396.

Ritter, D.F., 1979, Alluvial fans and stream morphology in Geomorphic application in Engineering Geology, short course at California State University-Los Angeles, November 1979, Chapter 3, p. 21-45.

Ryall, A., and Malone, S.D., 1971, Earthquake distribution and mechanism of faulting in the Rainbow Mountain-Dixie Valley-Fairview Peak area, central Nevada: Jour. Geophys. Res., v. 76, p. 7241-7248.

Senturion Sciences, 1977, High-precision multi-level aeromagnetic survey over Dixie Valley, Nevada: Rept. prepared for Southland Royalty Company, Part I, Oct. 1977.

Senturion Sciences, 1978, High-precision multi-level aeromagnetic survey over Dixie Valley, Nevada: Rept. prepared for Southland Royalty Company, Part II, June 1978.

Slemmons, D.B., 1957a, Map of Dixie Valley-Fairview Peak earthquakes of December 16, 1954: Publ. by Pacific Fire Rating Bureau.

Slemmons, D.B., 1957b, Geological effects of the Dixie Valley-Fairview Peak, Nevada, earthquakes of December 16, 1954: Seis. Soc. America Bull. 47, no. 4, p. 353-375.

Slemmons, D.B., 1966, Guidebook for Nevada earthquake areas: Prepared for 2nd U.S.-Japan Conf. on Research related to Earthquake Prediction, and the National Science Found. Conf. on Earthquakes and Earthquake Engineering, June, 1966, 79 p.

Slemmons, D.B., 1969, New methods for studying regional seismicity and surface faulting: Geoscience, v. 10, Art, 1, p. 91-103.

Smith, T.E., 1967, Aeromagnetic measurements in Dixie Valley, Nevada: Implication regarding Basin-Range structure, in U.S. Air Force Cambridge Research Labs. Spec, Rept. 66-848, 23 p.

Smith, T.E., 1968, Aeromagnetic measurements in Dixie Valley, Nevada; Implications on Basin-Range structure: Jour. Geophysical Res., v. 73, no. 4, p. 1321-1331.

Speed, R.C., 1976, Geologic map of the Humboldt Lopolith and surrounding terrane, Nevada: Geol. Soc. America Map MC-14, 4 p.

Speed, R.C., and Armstrong, R.L., 1971, Potassium-argon ages of some minerals from igneous rocks of western Nevada: Isochron/West, no. 1, p. 1-8.

Stewart, J.H., 1971, Basin and Range structure: a system of horsts and grabens produced by deep-seated extension: Geol. Soc. America Bull. 82, p. 1019-1044.

Tchalenko, J.S., 1970, Similarities between shear zones of different magnitudes: Geol. Soc. America Bull., v. 81, p. 1625-1640.

Thompson, G.A., and Burke, D.B., 1973, Rate and direction of spreading in Dixie Valley, Basin and Range Province, Nevada: Geol. Soc. America Bull., v. 84, p. 627-632.

Thompson, G.A., and Burke, D.B., 1974, Regional geophysics of the Basin and Range Province: Ann. Rev. Earth and Planetary Sci., v. 2, p. 213-238.

Thompson, G.A., Meister, L.J., Herring, A.T., Smith, T.E., Burke, D.B., Kovach, R.L., Burford, R.O., Salehi, A., and Wood, M.D., 1967, Geophysical study of the Basin-Range structure, Dixie Valley region Nevada: U. S. Air Force Cambridge Research Labs. Spec. Rept. 66-848.

Trexler, D.T., Bell, E.J., and Roquemore, G.R., 1978, Evaluation of lineament analysis as an exploration technique for geothermal energy, western and central Nevada: Rept. for U. S. Dept. of Energy, NVO-0671-2, 78 p.

Wallace, R.E., 1977, Profiles and ages of young fault scarps, north-central Nevada: Geol. Soc. America Bull., v. 88, p. 1267-1281.

Wallace, R.E., 1979, Nomograms for estimating components of fault displacement from measured height of fault scarp: (pre-print---in press).

Willden, R., and Speed, R.C., 1974, Geology and mineral deposits of Churchill County, Nevada: Nevada Bur. Mines and Geol. Bull. 83.

Wright, L., 1976, Late Cenozoic fault patterns and stress fields in the Great Basin and westward displacement of the Sierra Nevada block: Geology, v. 4, p. 489-494.

Chapter 4. PETROLOGIC ALTERATION STUDIES

By: Thomas R. Bard

Section 4.2.6 WATER CHEMISTRY

By: Russell W. Juncal and Thomas R. Bard

4.0 PETROLOGIC ALTERATION STUDIES

4.1 Introduction

4.1.1 Purpose and Scope

The overall purpose and scope of the petrologic alteration studies, as part of a case study of a geothermal system in Dixie Valley, is to assist in the evaluation and definition of the reservoir characteristics. The intention here is to develop a working model of the geothermal system through the analysis and interpretation of the alteration mineralogy.

The usefulness of petrologic and geochemical investigation in evaluating geothermal reservoirs and evaluating their characteristics has been illustrated by many workers (Steiner, 1968; Browne and Ellis, 1970; Hoagland, 1976; Sumi and Maeda, 1968; Sigvaldason and White, 1962; Tomasson and Kristmannsdottir, 1972; Ballantyne, 1978).

The present study includes the mineralogical analysis of drill cuttings from six shallow thermal gradient holes (500 to 1500 feet) and two deep exploratory wells (DF 45-14, 9020 feet and DF 66-21, 9780 feet). Data on fluid chemistry and theoretical modeling of hot water-rock interaction are also used to interpret the distribution of specific mineral species in relation to temperature, depth, lithology, and their stability with regard to present conditions. Emphasis is placed on the identification and distribution of clay minerals as they are known to be sensitive to variations in temperature and pressure conditions. Integration of the petrologic alteration studies with the structural-tectonic analysis will be focused on determining the relative importance and character of the major faults as factors in influencing the distribution of the observed mineralogy.

4.1.2 Methods and Analytical Techniques

The analysis of the drill cuttings to determine their textural, structural, and mineralogic characteristics is basically a three-step process involving cursory binocular examination, petrographic analysis, and x-ray diffraction analysis of clay minerals.

4.1.2.1 Binocular Examination

The first step involves a rapid binocular examination of the drill cuttings to identify anomalous intervals. These intervals are charac-

terized by high clay content, fracturing, brecciation, veining, very fine drill cuttings, visibly altered minerals, or other anomalous features.

4.1.2.1 Petrographic Analysis

The second step consists of making epoxy impregnated grain-mount thin sections representing both specific ten-foot intervals in anomalous zones and intervals of one hundred feet to obtain overall distribution patterns. One-hundred foot composite samples are prepared by combining five original samples. Analyzing composite samples helps minimize potential random sampling biases of the original samples and reduces the number of samples which must be prepared and analyzed to a practical total while maintaining adequate spatial resolution for defining most types of mineralogical distribution patterns. While the examination of one-hundred foot composite samples defines the overall distribution of mineral species, the ten-foot interval thin sections are useful in evaluating specific anomalous intervals.

A factor which may affect the validity of any interpretation regarding the relative mineral abundances and their distribution is the ability to obtain a sample representative of a one-hundred foot interval in a small thin section. Additionally, obtaining a representative sample of a particular depth is hindered by sample contamination and mixing caused by variations in circulation rates, settling velocities, and by caving. A representative sample is also a function of the technique used by the well logger to provide a split of the bulk sample. Moreover, during thin section preparation, certain minerals or rock types may be preferentially "plucked out", thereby decreasing their relative abundance.

Each thin section is examined under a polarizing microscope to identify and visually estimate the relative abundance of individual mineral species and to determine their inter-relationships. Plates V and VI show the distribution of selected minerals as a function of various parameters, including depth, lithology, temperature, and percent plagioclase alteration for DF 45-14 and DF 66-21, respectively.

4.1.2.3 X-ray Diffraction Analysis

The third step is the x-ray diffraction analysis identification

and interpretation of clay minerals present in the drill cuttings. This is the most useful method in identifying the distribution of alteration effects. Studies of the occurrence of various types of clay minerals are widely applied in the evaluation of hydrothermal alteration associated with geothermal systems (Steiner, 1968; Hoagland, 1976).

One-hundred foot composite samples are examined to provide an overall distribution of the clay minerals while specific ten-foot samples are taken every fifty feet to delineate and characterize specific anomalous intervals. Moreover, the data from the thin section analysis are more meaningful when interpreted in light of the x-ray diffraction data. Plates V and VI also show the relative abundance and distribution of the clay minerals for DF 45-14 and DF 66-21, respectively.

The samples selected for x-ray diffraction analysis were pulverized, slurried in distilled water and then allowed to settle for two hours. This process isolated the clay fraction of 8 phi (Ø) and smaller size (Folk, 1974). This suspended fine fraction is then pipeted onto glass slides and allowed to dry. This procedure tends to preferentially orient the platy phyllosilicate minerals which enhances their basal reflections and facilitates their identification. The samples are placed in a dessicator for at least 24 hours before analysis. Data was obtained on a Philips x-ray diffractometer using CuKa radiation at an operating voltage of 20 KV, a current of 15 MA, and a scanning speed of 2^{o} two-theta per minute. Each sample was analyzed from 2^{o} to 30^{o}. Selected samples are heated to 550°C for one-half hour and/or placed in an ethylene glycol saturated atmosphere at 75°C for 24 hours and rerun for confirmation of certain clay minerals.

Clay minerals are identified from an examination of the basal x-ray reflections. Table 4-1 summarizes the parameters used for identification of the various clay minerals. Discrete illite was identified by its asymmetric d(001) peak at 10.0A°to 10.16A° which is unaffected by glycolation or heat treatment. Discrete montmorillonite was identified by d(100) = 12.25A° to 12.5A° or 14.2A° to 14.3A° in unglycolated samples, shifting to near 17A° upon glycolation. Na-montmorillonite is assumed at a d(001) of 12.25A° to 12.5A° and Ca or Mg-montmorillonite at a d(001) of 14.25A° (K. Papke, pers. commun., 1979). Randomly interstratified mixed-layer illite-montmorillonite was identified by the following properties:

Table 4-1. X-Ray Diffraction Data

Mineral	d(001) A^o	Glycolated d(001) A^o	Heated for ½ Hour d(001) A^o
Illite	9.9 - 10.16	No Change	No Change
Na-Montmorillonite	12.25 - 12.4	16.8 - 17.2	9.8 - 10.1
Ca/Mg Montmorillonite	14.5 - 15.0	16.7 - 17.2	9.8 - 10.1
Randomly Interstratified Illite/Montmorillonite	10.16 - 14.5	Varies Depending on % of Expandable Layers	Collapses to 9.8 - 10.0
Regular Mixed-Layer Chlorite/Vermiculite	27.7 - 29.0	No Change	Collapses to Lower Value
Kaolinite	7.1 - 7.2	No Change	Peaks Disappear
Chlorite	13.9 - 14.2	No Change	Increase in Intensity

(1) The appearance of an asymmetrical, sometimes broad peak intermediate between 10.16A° and 12.5A° on diffraction patterns of unglycolated samples. This peak represents an average reflection from the (001) reflections of both illite and montmorillonite, and will be referred to as Ill (001)/Mo (001) (Brown and MacEwan, 1950; Weaver, 1956). The precise position of this peak will depend upon the relative amounts of the two layers.

(2) In glycolated samples the Ill (001)/Mo (001) reflection between 10.16A° and 12.5A° is shifted to a higher d-spacing value up to 17A°.

The approximated percentage of expandable layers in the randomly interstratified illite-montmorillonite was estimated from the position of the glycolated Ill (001)/Mo (001) reflection, using the curve of Weaver (1956) (Figure 4-1) and the work of Steiner (1968) (Table 4-2).

Regular mixed-layer clays differ from random mixed-layer clays in that the (001) series is an integral sequence. That is, the (001) value of a regular mixed-layer clay is equal to the total thickness of the two or more types of layers which are present; for example, the d(001) value of a regular mixed-layer chlorite (14.1A°) and vermiculite (14.2A°) would be 28.3A° . Thus the observed appearance of a reflection in the vicinity of 28A° in some samples must be due to two 14A° clay minerals. As there is no observable shift in this 28A° peak upon glycolation it is assumed to be a chlorite-vermiculite. Some of the diffraction patterns of these regular mixed-layer clays also indicate the presence of a randomly interstratified mixed-layer mineral (K. Papke, pers. commun., 1979).

Chlorite is identified by the presence of (001), (002), (003), and (004) reflections of 14.1A°, 7.07A°, 4.72A° and 3.54A°, respectively; all unaffected by glycolation. Kaolinite is distinguished by the appearance of (001) and (002) reflections at 7.16A and 3.57A°, respectively. Heating kaolinite to 550°C for one-half hour destroys the internal structure and the reflections disappear. Difficulty was encountered in distinguishing chlorite from kaolinite due to an uncertain response of chlorite to heating that is mainly a function of grain size and crystallinity. The (001) reflection at 14.1A° for chlorite will increase slightly after heat treatment, indicating an Fe-rich variety (Steiner, 1968). In addition, chlorite with strong (002) and

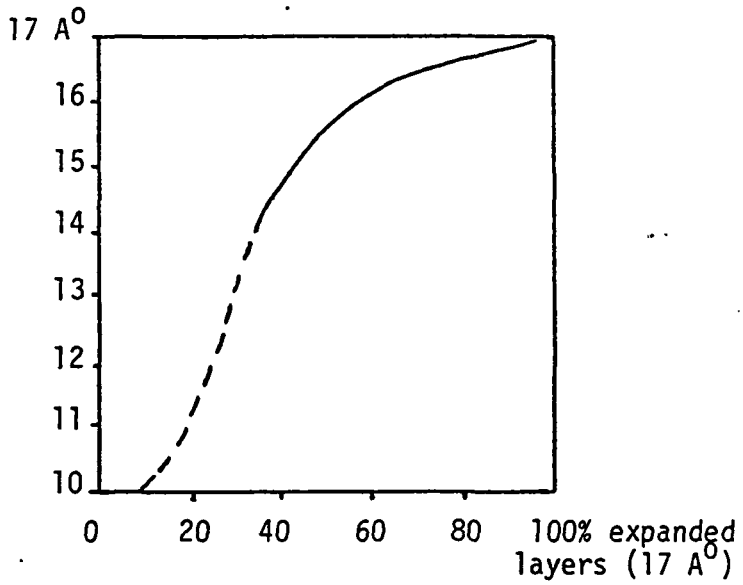

Figure 4-1. Curve showing migration of (001)/(001) peak of randomly interstratified 10 A° and 17 A° layers (Weaver, 1956).

Table 4-2. Montmorillonite Content of Micaceous Clay Minerals

(001)	(A^o)	Amount of Interstratified Montmorillonite Layers
Air-dried	Glycolated	(%)
12.45	14.97	> 40
11.78	13.60	< 35
11.63	13.39	> 30
11.33	13.19	> 30
11.05	12.98	30
11.19	12.77	< 30
10.91	11.94	25
10.78	11.33	> 20
10.52	11.19	20
10.40	10.91	< 20
10.40	10.65	> 15
10.28	10.16	< 10
10.16	10.16	0 or < 10
10.16	10.04	0 or < 10
10.16	9.93	0
10.04	10.04	0
9.93	9.93	0

Estimated proportions of interstratified montmorillonite in commonly observed micaceous clay minerals ranging from pure illite to randomly interstratified illite-montmorillonite with d(001) = 12.45 A^o (Steiner, 1968).

(004) reflections and relatively weak (001) and (003) reflections are assumed to be Fe-rich chlorites. The disappearance of certain reflections then is not conclusive evidence that only kaolinite is present. The appearance of the (002) kaolinite (004) chlorite double maxima at 3.57A^{o}, respectively, indicated the presence of both kaolinite and chlorite.

The above discussion shows that the identification of clay minerals is a difficult task. Certain factors inherent in x-ray analysis tend to bias results, including the structural characteristics of the mineral being analyzed, its degree of crystallinity, preferred orientation, and the ability to produce an internally consistent sample. All these factors will influence the observed peak intensity which is the parameter used to estimate relative abundances. Hence, the validity of the interpretations derived from these results must be viewed with discretion.

4.1.3 Previous Work

No previous petrologic and/or geochemical studies of the Dixie Valley Geothermal System are known to exist. It is believed that this study is the first of its kind to be conducted in this area. However, similar studies performed in other geothermal areas have provided useful guidelines and insights into the study of hydrothermal alteration in Dixie Valley. In particular, much use has been made of work done by Steiner (1968) in Wairakei, New Zealand, by Browne and Ellis (1970) at Ohaki-Broadlands, New Zealand, and by Hoagland (1976) in the Imperial Valley, California.

4.1.4 Acknowledgements

Special thanks are extended to Keith Papke, Industrial Minerals Geologist for the Nevada Bureau of Mines and Geology, for his time and assistance in interpreting x-ray diffraction patterns and to Russell Juncal for his assistance throughout this project. Numerous discussions with Burkhard Bohm, Roger Jacobson, Michael Campana, Burt Slemmons, Bob Whitney, Dennis McMurdie, Li Hsu, Scott Butler, Don Hudson, Larry Larson and Elaine Bell contributed to the development of the petrologic investigations. Appreciation is extended to Sue and Dick Nosker for their efforts in sample preparation. Technical

and editorial review by MMRI and SRC personnel, in particular, Dennis McMurdie, Bob Whitney, Elaine Bell, Larry Larson and Burt Slemmons, provided improvements in the the following report. The typing skills and patience of Mollie Stewart are also greatly appreciated.

4.2 Analytical Results

4.2.1 Shallow Thermal Gradient Holes

The results of the analysis of the six shallow thermal gradient holes (SR2, SR2A, S-8, DD-9, H-1, H-2) are presented in the November 1, 1979, report submitted to Southland Royalty Company and the U.S. DOE. The significant conclusions derived from the study are as follows:

(1) The propylitic mineral assemblage consisting of albite, calcite, quartz and clay is dominant in each of the drill holes.

(2) With the exception of S-8 and possibly H-1, none of the holes encountered bedrock material.

(3) The unconsolidated heterogeneous alluvial material is derived from a source area that was subjected to at least one episode of hydrothermal alteration prior to deposition.

(4) Zones of lost circulation encountered during drilling in some of the holes correlate with both more intense alteration and with the calculated depth of intersection with the range front fault.

(5) The distribution of clay minerals is the most useful indicator of alteration intensity.

(6) Alteration effects derived from the present hydrothermal system are only weakly developed and difficult to distinguish from previous regional alteration effects.

4.2.2 General Stratigraphy

Willden and Speed (1974) mapped and described seven rock groups within the Dixie Valley region. These include: Upper Triassic metasediments; Middle Jurassic quartz arenite, mafic volcanic rocks, and gabbroic rocks; Miocene rhyolites; and Pliocene and younger sedimentary rocks, basalt, and andesite. A few of the lithologies encountered, such as granodiorite and aplite, are distinctly atypical of the local Stillwater Range source area.

The dominant rock types encountered in the wells drilled in Dixie Valley are, in order of decreasing abundance: Upper Triassic metasedi-

ments, gabbroic to granodioritic intrusive rocks and silicic to intermediate volcanic rocks. The volcanic rocks are the dominant constituents of the alluvial sediments because these rocks are well exposed along the front of the Stillwater Range in the immediate catchment areas where the wells have been drilled. Although outcrops of the metasediments are present in the Stillwater Range, they are conspicuously rare or absent in the alluvial sediments.

The rock types encountered in the two wells are similar, however, the relative amounts and stratigraphic position of the units are quite different. The complex structural-tectonic and depositional history of Dixie Valley, as well as the effects of the hydrothermal system underlying the region, make stratigraphic correlations between the two deep exploratory wells tentative. A more thorough discussion of the correlation between DF 45-14 and DF 66-21 is presented in Section 4.2.7. Plate IV shows the location of the six shallow thermal gradient holes and the two deep exploratory wells in relation to the Stillwater Range front and the structural-tectonic features in Dixie Valley.

4.2.3 Lithology of Deep Exploratory Wells

4.2.3.1 Well DF 45-14

Rocks penetrated in the deep exploratory well DF 45-14, drilled to a total depth of 9020 feet, include 1100 feet of unconsolidated heterogeneous alluvial sediments, 1500 feet of silicic to intermediate volcanic rocks, 6500 feet of Upper Triassic metasediments and minor intrusions of diorite/gabbro. The different rock types exhibit varying degrees of hydrothermal alteration locally controlled by fracture permeability; however, the type of alteration is fairly consistent in the drill hole.

DF 45-14 penetrated approximately 6500 feet of a possible 10,000 feet (Page, 1965) of Upper Triassic metasediments. The unit as a whole is quite homogeneous; however, local facies variations are present, and their differential response to hydrothermal alteration is striking (compare Figures 4-2 and 4-3). The metasedimentary sequence consists chiefly of metasiltstone/metashale, quartz arenite/metaquartz arenite, and metalithic wacke.

The metasediments are here divided into two facies based mainly on grain size, as the mineralogy is quite consistent for the entire

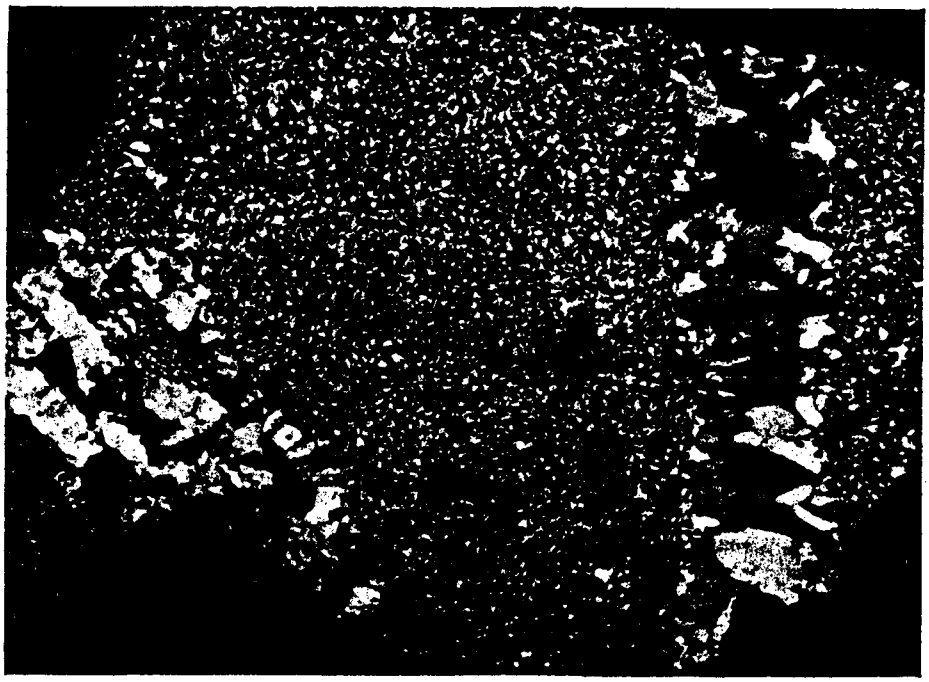

Figure 4-2. (a) Photomicrograph of metasiltstone/metashale facies under polarized light. Note the quartz vein. (scale 13 mm : 0.22 mm)

Figure 4-2. (b) Photomicrograph of metasiltstone/metashale facies. Note 'dirty' altered appearance (scale 13 mm : 0.22 mm)

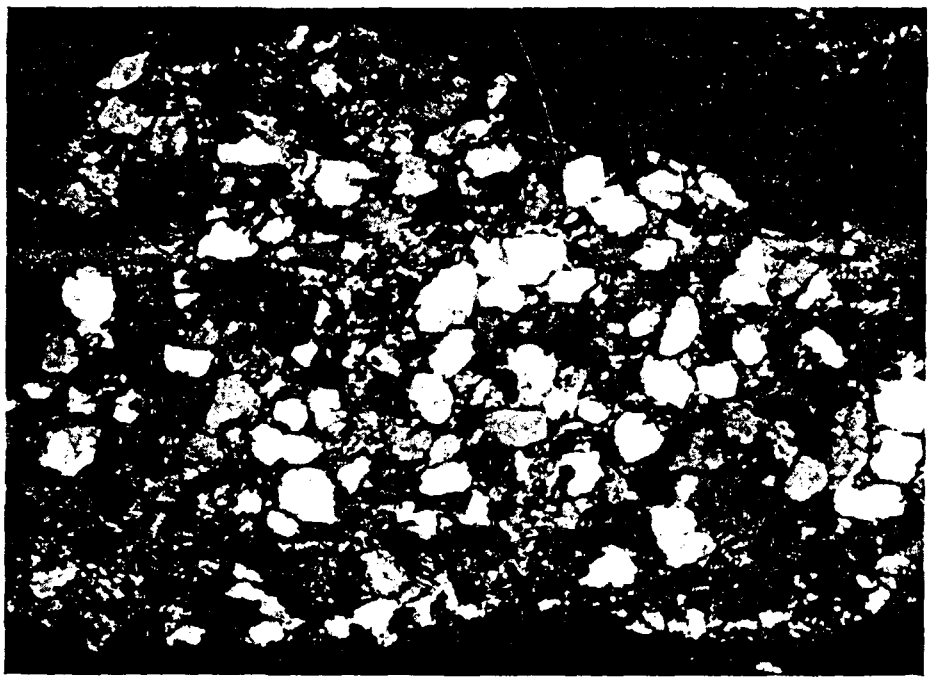

Figure 4-3. (a) Photomicrograph of metarenite facies under polarized light. (scale 13 mm : 0.22 mm)

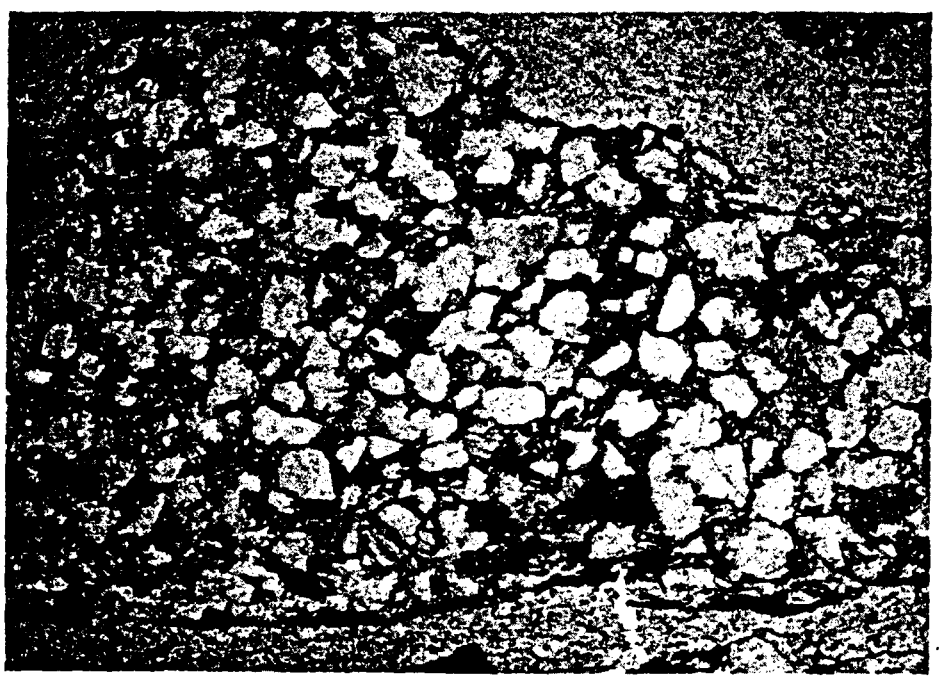

Figure 4-3. (b) Photomicrograph of metarenite facies. Note the lack of visible alteration. (scale 13 mm : 0.22 mm)

sequence. The majority of this metasedimentary sequence consists of a very fine-grained, black to medium-dark gray, well sorted, very hard, silicic, in places recrystallized and well foliated metasiltstone/metashale, often containing abundant carbonaceous matter and varying amounts of disseminated and crystalline pyrite. The foliation is a result of regional low grade metamorphism during the late Jurassic (Willden and Speed, 1974). The unit is quite dense, possesses limited porosity and shows only local signs of fracturing. Where it is intruded by diorite/gabbro dikes (sills?) contact metamorphism has resulted in the formation of andalusite/chiastolite porphyroblasts (Figure 4-4) and incipient spherulitic cordierite (?) (Figure 4-5).

The overall effects of the regional low grade metamorphic event on the metasediments include recrystallization, chemical reconstitution and textural changes. Figure 4-5a shows the well developed foliation observed in the organic-rich fine-grained metasiltstone/metashale (compare with Figure 4-3). The present mineral assemblage observed in the metasedimentary sequence (quartz, K-micas, chlorite, clay minerals $\pm$ calcite $\pm$ laumontite) is the result of the composite effects of the regional and contact metamorphic events and the hydrothermal activity. Figure 4-5b is an example of the chiastolite/cordierite bearing metasiltstone from an area approximately 45 miles south in the Stillwater Range showing a relatively unaltered appearance when compared with Figure 4-5a. The difference in appearance may be largely a function of the hydrothermal activity in the northern portion of Dixie Valley.

The andalusite/chiastolite crystals and the incipient spherulitic crystals of cordierite (?) were observed to occur only in the fine-grained facies of the metasedimentary sequence. Here, the foliation exhibited by orientation of the phyllosilicate minerals and carbonaceous matter, invariably wraps around the 'spots' (Figure 4-5a). The andalusite/chiastolite crystals, however, generally grow across the foliation. Spry (1976) used the term 'maculose' structure to describe porphyroblasts of andalusite/chiastolite in a fine-grained matrix. The organic 'cross' or inclusion characteristic of chiastolite (Figure 4-4) is believed due to preferred adsorption of carbonaceous particles against the prism faces, particularly at the prism edges (Spry, 1976). Chiastolite and its organic inclusion in particular are highly susceptible to sericitic alteration. This feature has

Figure 4-4. (a) Photomicrograph of andalusite/chiastolite porphyroblasts in organic-rich metasiltstone/ metashale from DF 45-14. (scale 13 mm : 0.34 mm)

Figure 4-4. (b) Photomicrograph of andalusite/chiastolite crystals in very organic-rich metasiltstone/ metashale. (scale 13 mm : 0.34 mm)

Figure 4-5. (a) Photomicrograph of andalusite/chiastolite and incipient spherulitic cordierite porphyroblasts. Note foliation wrapping around the spherules. (scale 13 mm : 0.34 mm)

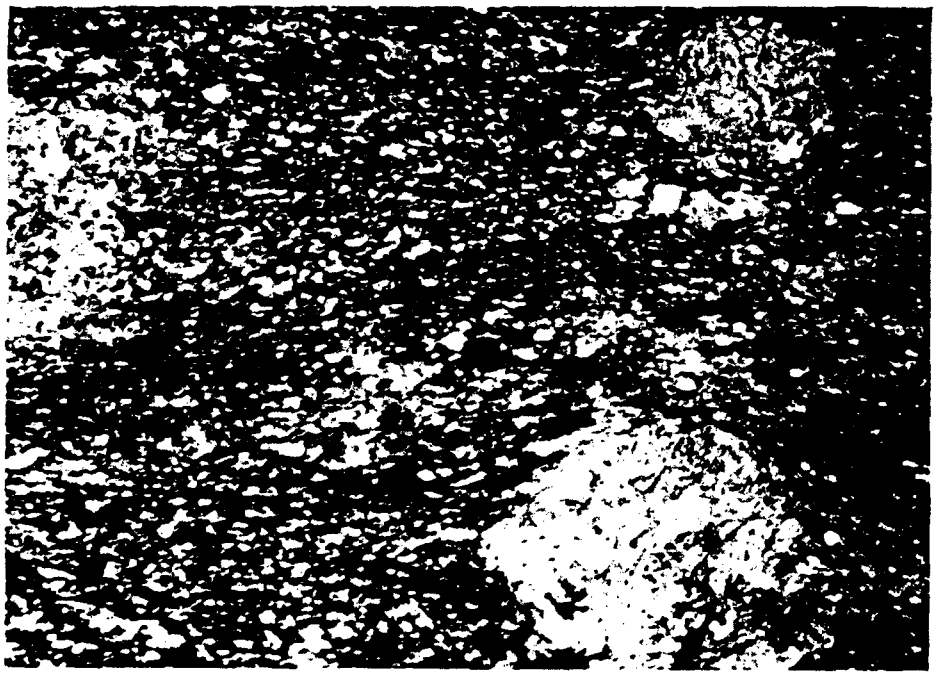

Figure 4-5. (b) Photomicrograph of relatively fresh andalusite/chiastolite and cordierite-bearing metasiltstone from the southern portion of the Stillwater Range. (scale 13 mm : 0.34 mm)

been widely observed in thin section as seen in Figure 4-6.

The second facies of the Triassic metasediments is a coarser-grained, light to dark gray to brown, very hard, silicic, recrystallized quartz arenite or meta-quartz arenite (Figure 4-3). It consists predominantly of round to subround optically clear and partially recrystallized quartz grains with varying amounts of micaceous minerals (chlorite, biotite, K-mica), calcite and clay occurring as intergranular phases. Trace amounts of magnetite, pyrite, garnet, epidote, tourmaline and carbonaceous matter are also present. Recrystallization of quartz in this unit is evidenced by grain boundary triple points and by overgrowths. This recrystallization may be responsible for the conspicuous lack of a well defined foliation as seen in the metasiltstone/metashale facies. This unit appears to have been largely unaffected by the metamorphism. The mineralogy of the finer-grained facies is essentially the same as that described above except for the occurrence of andalusite/chiastolite and cordierite porphyroblasts and the abundance of carbonaceous matter and pyrite.

Several intervals of the metasedimentary sequence in DF 45-14 (3700-3800, 4100-4200, 4600-4700, 7600- 7700, 8000-8100 feet) (Plate V) have been intruded by Middle Jurassic (?) diorite/gabbro dikes. The average thickness of these intrusions is about 30 feet as described in driller's logs. They consist predominantly of a medium to coarse-grained crystalline network of plagioclase and clinopyroxene with little or no potassium feldspar or quartz. Secondary minerals include hornblende, chlorite, magnetite, epidote, albite, calcite, and pyrite. An x-ray fluorescence analysis of the diorite/gabbro indicated the presence of significant quantities of titanium suggesting the presence of ilmenite. Similarly the presence of leucoxene also indicates the existence of ilmenite. Figure 4-7 shows the mineralogy and texture of diorite/gabbro although it commonly takes on a more altered, 'dirty' appearance.

A total of 1500 feet of volcanic rocks were encountered in DF 45-14 in the intervals 700 to 800 feet and 1100 to 2500 feet. These consist primarily of andesite and basalt and lesser amounts of silicic tuff. The tuffs are gray to green and brown and consist of fine-grained interlocking plagioclase lathes in a very fine-grained, glassy, often devitrified matrix that is altering to clay. These vitric and

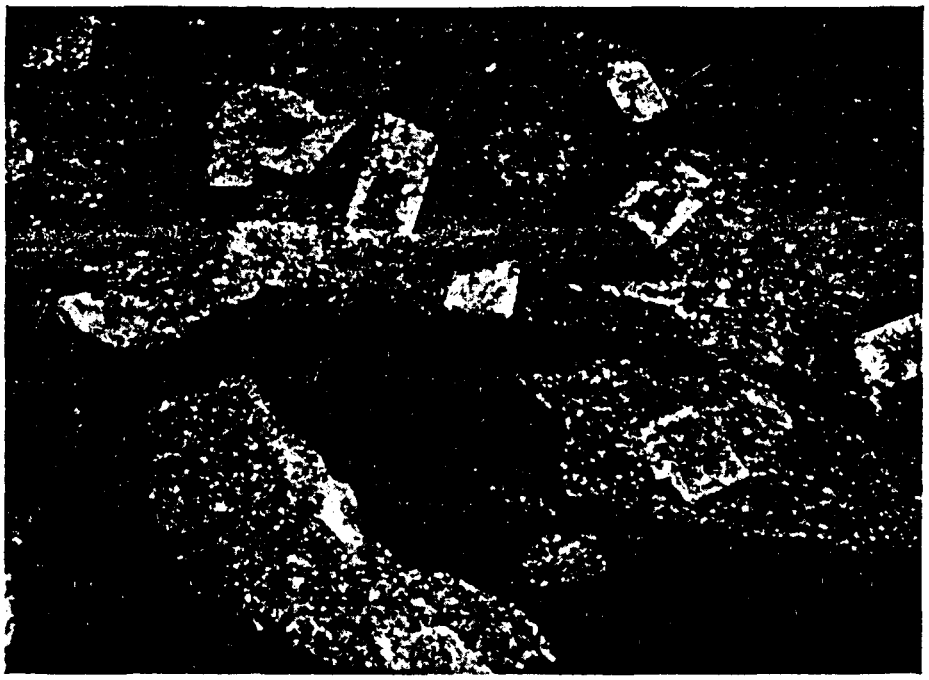

Figure 4-6. Photomicrograph of highly sericitized andalusite/cordierite porphyroblasts in metasiltstone/metashale from DF 45-14 under polarized light. (scale 13 mm : 0.34 mm)

Figure 4-7. Photomicrograph illustrating the texture and mineralogy of diorite/gabbro under polarized light. (scale 13 mm : 0.34 mm)

lithic tuffs contain varying amounts of disseminated and crystalline pyrite. The andesites and basalts are predominantly medium to dark brown, dark gray to green, medium to fine-grained rocks consisting of interlocking plagioclase lathes in a groundmass of very fine-grained plagioclase and minor quartz. Pyrite, hornblende, epidote, and traces of original pyroxene are also observed. The age of this sequence of volcanic rocks is unknown, however they are believed to be of Tertiary age.

The approximately 1100 feet of alluvial sediments penetrated in DF 45-14 are an unconsolidated heterogeneous mixture of all the rock types described above except for the conspicuous rarity of the metasediments. The majority of the alluvium consists of volcanic fragments with lesser amounts of diorite/gabbro fragments. The volcanic material is intensely altered (Figure 4-8) as it has largely been derived from the erosion of the nearby highly altered, vari-colored volcanic rocks in the Stillwater Range (Figure 4-9). This alteration zone represents a previous period of more intense and possibly more acidic hydrothermal alteration. This zone of altered volcanics is probably indicative of the alteration of the volcanic sequence at depth. Delineating the weak overprint produced by the present hydrothermal activity from the effects of the previous alteration is difficult in the alluvial material.

4.2.3.2 Well DF 66-21

The rock types encountered in DF 66-21 are essentially the same as those observed in DF 45-14 although the proportions of each are rather different as indicated by a comparision of the lithologic logs (Plates V and VI). The thicker sequence of alluvial sediments in DF 66-21 is in part a function of increased distance from the range front and at least one additional increment of downdropping along normal faults (Plate IV). DF 66-21 also contains a much greater amount of intrusive material (granodiorite and diorite/gabbro). The mineralogy of these intrusive rocks are quite similar and it is uncertain if they originated from the same magma body. The relative ages of these two types of intrusives are unknown. The most obvious difference between the two wells is the much smaller amount and type of metasediments encountered in DF 66-21. The detailed description of the rock types in DF 45-14

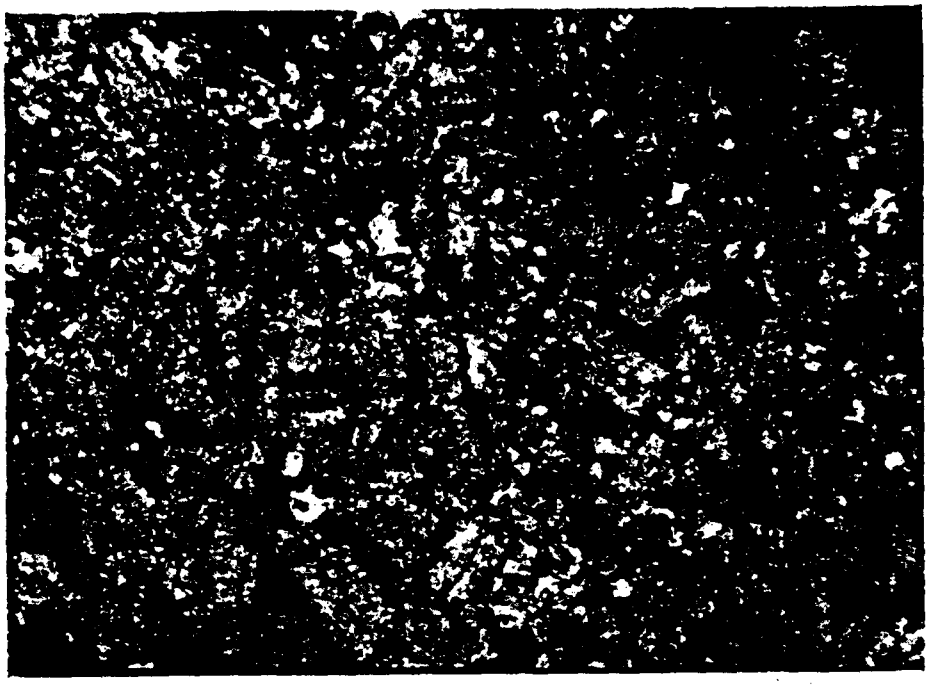

Figure 4-8. Photomicrograph of altered volcanic rock from alluvial material under polarized light. Note relict sericitized plagioclase lathes. (scale 13 mm : 0.27 mm)

Figure 4-9. Photograph of vari-colored zone of alteration of volcanic rocks in the Stillwater Range.

given above can also apply to the rock types in DF 66-21. Only obvious departures from these descriptions will be noted below.

The sequence of alluvial sediments encountered in DF 66-21 consists of essentially the same rock types as found in the alluvium in DF 45-14. In many intervals, however, the proportion of volcanic fragments is much greater in DF 66-21. Additionally, the presence of abundant reddish-brown clay in the alluvium in the lower 2000 feet and extending into the upper portions of the volcanic sequence, is unique to DF 66-21. This clay is essentially a montmorillonite which is fairly uniform in composition throughout the interval. This clay constituted up to 75 percent of the sample taken by the well logger. The origin of this layer and its significance as a possible cap rock will be discussed later.

The lithology and thickness of the sequence of volcanic rocks in DF 66-21 (1300 feet) is nearly the same as in DF 45-14 (1500 feet). One difference was the relative abundance of pyroxene blebs and greater amounts of disseminated magnetite in the andesitic rocks of DF 66-21. The significance of this observation, however, is uncertain. Drilling into these volcanic rocks encountered hot water and steam under high pressure. Presumably, all or part of this volcanic sequence has been highly fractured and brecciated, evidenced by increased porosity on logs and by calcite deposition.

A relatively homogeneous granodiorite/diorite (?) unit was encountered from 5300 to 6600 feet in DF 66-21. The mineralogy of this unit is not significantly different from the intrusive rocks encountered in DF 45-14, although the proportions of the various minerals are different. The 'granodiorite' intrusive in DF 66-21 does not contain as much magnetite; biotite and hornblende, rather than pyroxene and hornblende, are the dominant ferromagnesian minerals. This observation may be a secondary effect. Additionally, the 'granodiorite' in DF 66-21 contains more plagioclase and minor amounts of K-spar. The question is whether these two rock types represent parts of the same major intrusive body or not. The structural-stratigraphic relationships of this intrusive unit(s) is complex, and the lack of any granodiorite in DF 45-14, however, does suggest that it is of limited areal extent. It is possible that the granodiorite intrusion pinches out to the south toward DF 45-14, or that its absence is fault-controlled. This intrusive body

is considered to be part of the Humboldt gabbroic complex (Speed, 1976).

The metasediments in DF 66-21 are poorly represented, as only about 1100 feet of them were encountered. They consist primarily of quartz arenite, meta-quartz arenite (?) and metasiltstone/metashale. The mineralogy and structures are similar to those for similar rocks in DF 45-14. The difference is in the greater amount of coarse-grained quartz arenite (meta-quartz arenite) relative to the metasiltstone/metashale in DF 66-21. As in DF 45-14 the fine-grained facies is more intensely altered, whereas the coarse-grained facies is relatively unaltered in appearance. Another difference is the lack of andalusite/chiastolite porphyroblasts in the metasiltstone/metashale facies in DF 66-21.

Several intervals within the drill hole were reported to contain mineralized zones. Petrographic examination and a rapid binocular scan of the cuttings, however, could not verify the presence of any significant quantities of metal sulfides or oxides with the exception of pyrite, magnetite, and possible traces of chalcopyrite/bornite.

4.2.4 Alteration Effects in Deep Exploratory Wells

The varied rock types in DF 45-14 and DF 66-21 with their differential responses to the processes of alteration have given rise to a complicated assemblage of alteration minerals. The alteration in the two wells, however, is quite similar, the difference being one chiefly of degree rather than type.

4.2.4.1 Well DF 45-14

The alteration described below is not solely due to the effect of the hydrothermal activity that exists in Dixie Valley, as many of the rocks encountered have experienced regional low-grade metamorphism and/or contact metamorphism. Delineating the effects of these metamorphic events from those derived from the hydrothermal activity is at times difficult, as only a very fine line separates the two processes.

The sequence of volcanic rocks and the alluvial materials, which consist primarily of altered volcanic fragments, exhibit a very similar alteration mineral assemblage. This assemblage consists of albite, chlorite, sericite (illite), epidote, calcite, and clay minerals. A similar alteration assemblage for altered volcanic rocks of the Comstock Lode is described by Coats (1940) and is termed propylitic alteration.

Coats attributes the origin of propylitic alteration to hydrothermal alteration at relatively high temperatures. The same mineral assemblage has been documented as being indicative of low grade regional metamorphism (Winkler, 1976) or the equivalent greenschist facies of Eskola (1915).

The basic mineral assemblage described above has been noted in other geothermal areas. Work by Brown and Ellis (1970) at Ohaki-Broadlands, New Zealand, found hornblende and biotite replaced by chlorite, illite, calcite, quartz, or pyrite, with plagioclase replaced by albite, epidote, illite, calcite, adularia, wairakite, and quartz in rhyolitic and tuffaceous volcanic rocks. Steiner (1968) at Wairakei, New Zealand, described ferromagnesian minerals altering to chlorite, micaceous clay minerals (illite, illite/montmorillonite), epidote, calcite, quartz, and pyrite with plagioclase altering to montmorillonite, micaceous clays, epidote, calcite, quartz, and K-feldspar in tuff, andesite, and ignimbrite. Work by Schoen and White (1965) at Steamboat Springs, Nevada, identifies hornblende altering to epidote, calcite, mixed-layer illite/montmorillonite clays, and K-feldspar in acidic to intermediate volcanic rocks.

Propylitic alteration in DF 45-14 is best developed in the acid to intermediate volcanic rocks where it imparts a greenish-gray color to the rocks. It renders the albite phenocrysts less translucent and the twinning becomes diffuse or is totally destroyed. Widespread albitization of the plagioclase in both the volcanic rocks and the intrusive rocks is supported by x-ray diffraction data of random whole rock samples of the alluvial material which revealed an abundance of albite. Albitization is the process whereby the more reactive Ca-rich plagioclase is converted to the Na-rich end member of the plagioclase series, albite (An_0 - An_{10}). Presumably, Na-rich solutions attack the Ca-plagioclase through a cation exchange process, thereby releasing Ca-ions which are probably incorporated into the formation of epidote, calcite, Ca-montmorillonite and/or possibly laumontite. This process is most likely a function of the low-grade metamorphism although albitization due to hydrothermal activity cannot be completely ruled out.

Sericitization of plagioclase, or its replacement by illite, is pervasive and in some instances complete as it consumes entire crystals, leaving only a relict form of the crystal (see Figure 4-10a). This

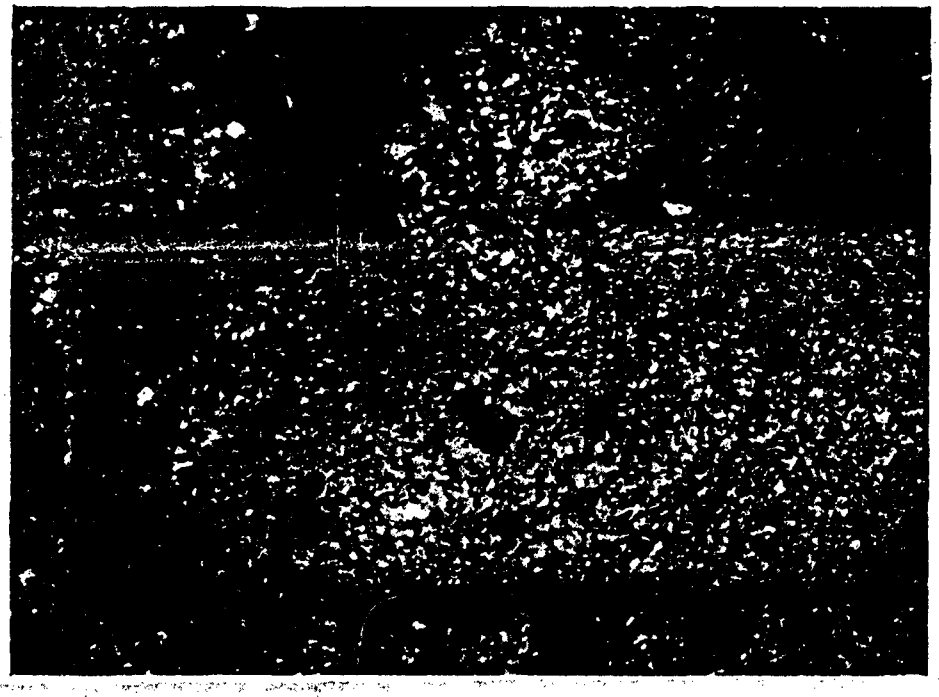

Figure 4-10. (a) Photomicrograph of a plagioclase crystal completely consumed by sericite. View under polarized light; note retention of crystal form. (scale 13 mm : 0.27 mm)

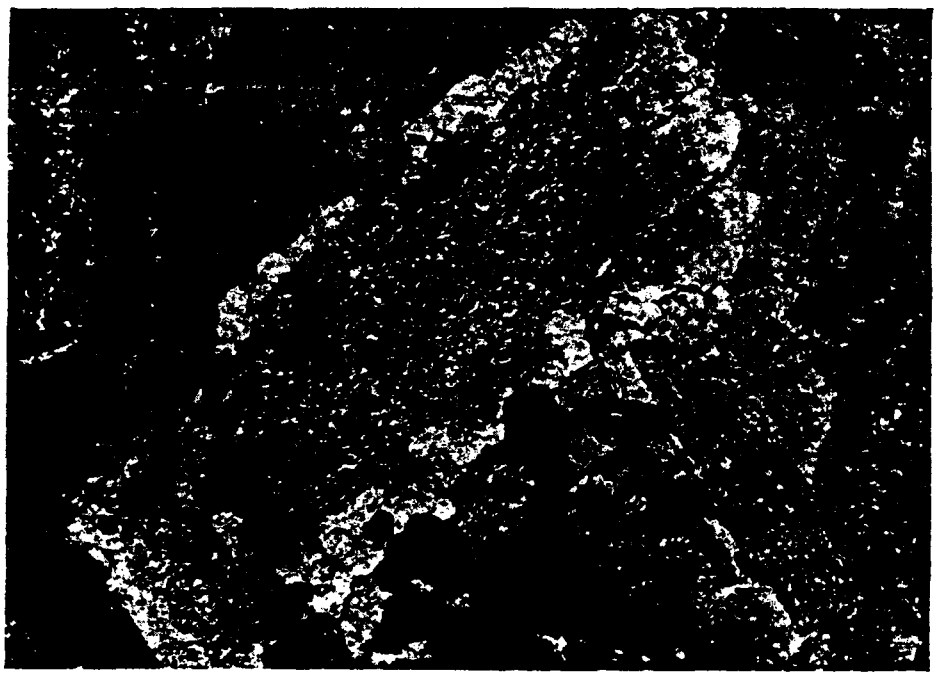

Figure 4-10. (b) Photomicrograph of sericitization confined to the core of a zoned plagioclase crystal. View under polarized light. (scale 13 mm : 0.27 mm)

process is most commonly developed in the cores of plagioclase crystals (Figure 4-10b) as the calcic cores of zoned plagioclase are more susceptible to alteration. Somewhat of a conflict exists in the literature regarding the physical and chemical conditions necessary for sericitic alteration. Turner and Verhoogen (1960) state that the process of sericitization is indicative of alteration by alkaline solutions of higher concentrations of potash. Lovering (1950), on the other hand, says that sericitic alteration takes place in mildly acidic solutions at higher termperatures. The preponderence of sericite (illite) in thin section and in the x-ray diffraction patterns support the ongoing process of sericitization.

The plagioclase is also altered to an epidote (clinozoisite (?)) mineral. This process is generally confined to the calcic cores of the plagioclase crystals (Figure 4-11) as the Ca ions necessary for the formation of epidote are available. Some of the intrusive rocks are saussuritized, although the epidote (clinozoisite (?)) is commonly coarsely crystalline. White and Sigvaldason (1962) suggested there are upper limits to the depth of formation of epidote in hydrothermal environments. In this regard, epidote may be useful in defining limits for depth of original cover in areas of altered volcanic rocks and epithermal ore deposits. If epidote occurs at the present land surface, for example, erosion of at least 400m (1300 feet) of cover is indicated (White and Sigvaldason, 1962). However, a hydrothermal origin for the epidote is very difficult to ascertain in many instances. When the epidote occurs in veins it may be assumed to be hydrothermal.

Replacement of plagioclase by clay and lesser amounts of calcite is commonly developed in the groundmass of the volcanic rocks and has largely masked much of the original texture. The presence of montmorillonite and mixed-layer illite/montmorillonite in the upper 2500 feet of DF 45-14 is evidence for this process as the volcanic rocks contain abundant plagioclase. Montmorillonite is characteristic of relatively low temperatures and its formation by alkaline solutions appears to be compatible with the near-surface water chemistry as will be discussed later.

The alteration of the primary and, in some instances, the secondary ferromagnesian minerals and ilmenite in the rocks of DF 45-14 is pervasive and commonly complete. The end product is generally either bio-

Figure 4-11. (a) Photomicrograph of epidote alteration in cores of plagioclase crystals. View under polarized light. (scale 13 mm : 0.34 mm)

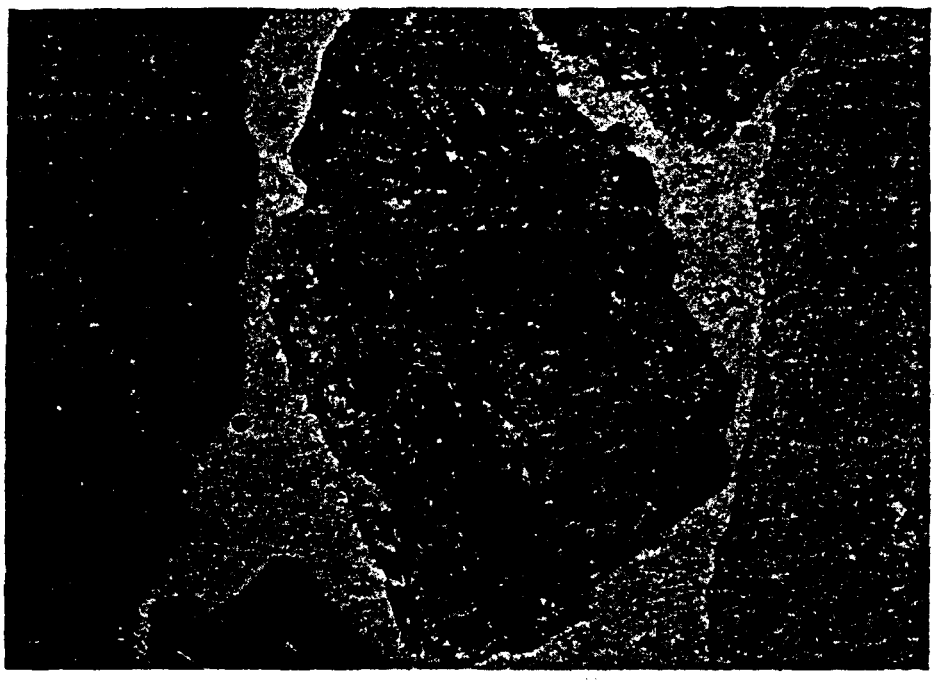

Figure 4-11. (b) Photomicrograph of epidote alteration in cores of plagioclase crystals. (scale 13 mm : 0.34 mm)

tite, chlorite, magnetite, clay minerals and/or epidote or combinations of these minerals. Leucoxene is believed to represent the alteration of ilmenite under hydrothermal conditions. Original clinopyroxenes of the intrusive and volcanic rocks are replaced by hornblende, biotite, chlorite, epidote and magnetite. Primary and secondary hornblende is replaced by biotite, chlorite, magnetite, epidote and calcite; biotite is replaced by chlorite, vermiculite and magnetite. The iron derived from the alteration of these minerals as well as pyrite is probably responsible for the pervasive limonite and hematite staining of the alluvial material and possibly the abundance of magnetite. The precipitation of magnetite from solution is evidenced by its deposition in some veins and in intergranular positions as seen in Figure 4-12. X-ray diffraction patterns for the chlorites show that the second and fourth orders of the basal reflection are consistently stronger than the first, indicating an iron-rich type (Grim, 1968).

The propylitic alteration developed in the alluvium and the volcanic sequence in DF 45-14 is also recognized, to a lesser extent, in the intrusive rocks. For instance secondary hornblende is replaced by chlorite and magnetite with plagioclase altered to albite, sericite (illite), epidote, clay and calcite. Propylitic alteration of a diorite is described in the Tongonan Geothermal Field, Leyte, Philippines (Kingston, 1979). Despite these phase transitions, the diorite/gabbro maintains a relatively fresh unaltered appearance, except in localized areas where fracturing may be a factor.

The alteration products of primary minerals in the alluvial material, in the sequence of volcanic rocks, and in the intrusive rocks are all similar, differing only in the degree of alteration. This observation along with a similar mineralogy documented in other geothermal areas indicates a hydrothermal origin for much of the observed alteration assemblage in DF 45-14. The degree of alteration is mainly a function of rock texture. The texture will determine both the porosity and permeability and hence the fluid migration rates and ultimately the reaction times. Grain size is also an important consideration. The finer-grained material, as a rule, is more altered because of higher susceptibility to hydrothermal solutions and closer contact to flow channels as a result of a greater amount of surface area (compare Figures 4-2 and 4-3). The porosity-permeability relationships in DF 45-14 are very important as

Figure 4-12. (a) Photomicrograph of magnetite completely surrounding a vitric clast in a fragment of volcanic rock. View under polarized light. (scale 13 mm : 0.1 mm)

Figure 4-12. (b) Photomicrograph of magnetite completely surrounding a vitric clast in a fragment of volcanic rock. (scale 13 mm : 0.1 mm)

they are the dominant control in the distribution of the various hydrothermal alteration effects.

The hydrothermal alteration observed in the metasediments is rather limited except in localized regions associated with inferred zones of fracturing and/or faulting (Plate V). The post-metamorphic mineral assemblage of quartz, K-mica, biotite and chlorite has not been significantly changed. This is supported by x-ray diffraction data and thin section analysis.

Sericitization (illitization) has been an active process, particularly in the fine-grained metasiltstone/metashale, where it occurs predominantly as an intergranular phase alteration product of the primary K-micas. Quartz is essentially nonreactive, except for recrystallization which most probably was a result of the regional metamorphic events. Alteration of biotite is observed predominantly in the coarse-grained quartz-arenite and/or meta-quartz arenite facies where it is altered to chlorite and vermiculite (?). Petrographic evidence for biotite altering to vermiculite includes: (1) lack of the "bird's-eye" extinction characteristic of biotite, (2) a decrease in birefringence, (3) a decrease in pleochroism and a bleached appearance, and (4) pseudomorphs after biotite. One of the major occurrences of vermiculite is as an alteration product of biotite by weathering or by hydrothermal action (Deer and others, 1966). Vermiculite has also been documented in the Roosevelt Hot Springs Thermal Area, Utah (Ballantyne, 1978) where it has replaced biotite.

Andalusite/chiastolite porphyroblasts in the foliated, organic-rich metasiltstone/metashale are invariably partially or wholly sericitized, particularly the included organic material. The stability of chiastolite is such that even under normal atmospheric conditions its alteration to sericite is entirely possible (Spry, 1976). A large proportion of the 'spots' or incipient cordierite (?) porphyroblasts are altered to clay. Apart from the above observations, the metasediments are not highly altered; rather, they appear to be relatively impervious to the altering solutions. Only in localized zones, where the various well logging techniques (gamma-ray and neutron density logs) indicate anomalous porosity, is there any variation in the observed mineralogy, in particular the clay mineralogy. The clay mineralogy is discussed in Section 4.2.5.

Calcite and quartz are the dominant vein and fracture fill material along with the Ca-zeolite laumontite and lesser amounts of adularia and gypsum (?) in the metasediments of DF 45-14. The distribution and relative abundance of calcite and laumontite in relation to lithology and postulated fault and fracture zones are depicted on Plate V. These minerals exhibit a variety of structural and temporal relationships. Laumontite and adularia invariably occur in post-metamorphic veins whereas calcite and quartz are less predictable. Both laumontite and adularia have been described as minerals typically found in geothermal systems (Steiner, 1968; Browne and Ellis, 1970; Ellis and Mahon, 1977).

The presence of the Ca-zeolite laumontite ($CaAl_2Si_4O_{12}.4H_2O$) was confirmed by x-ray diffraction data as well as in thin section analysis (Figure 4-13). The main diffraction peaks at 9.1A^o to 9.3A^o and 6.7A^o to 6.9A^o disappear after heating to 550^{o}C for one-half hour. Laumontite reportedly dehydrates with increasing temperature to wairakite (Winkler, 1976); however, this was not observed to occur. Leonhardite is a slightly dehydrated form of laumontite. The stability range of laumontite ranges from about 200^{o}C to 300^{o}C at relatively low pressures of about 3.0 Kb (Winkler, 1976). The first appearance of laumontite is often cited as indicating the beginning of metamorphism.

In thin section, laumontite is coarsely crystalline with low birefringence, low relief and exhibits two directions of observable cleavage, one distinct and the other obscure. Laumontite occurs with quartz and calcite in veins and fracture fillings (Figure 4-13b). The assemblage quartz-laumontite is typical of the zeolite facies (Deer and others, 1966; Winkler, 1976). This same assemblage is described in Onikabe, Japan (Ellis and Mahon, 1977), where it was indicative of a temperature of 170^{o}C. The occurrence of laumontite has been reported elsewhere in other geothermal areas, including: Reykjavik and Jveragerdi, Iceland (Sigvaldason and White, 1962); Wairakei, New Zealand (Steiner, 1968); and in Matsukawa, Japan (Ellis and Mahon, 1977).

Lovering (1950) stresses the fact the zeolites have been synthesized only in alkaline aqueous solutions and that the temperature in some cases was as low as 60^{o}C. According to Lovering, the zeolites develop near the end of the reaction series of hydrothermal solutions.

The distribution and relative abundance of laumontite (Plate V)

Figure 4-13. (a) Photomicrograph of a fragment of laumontite vein material under polarized light. (scale 13 mm : 0.22 mm)

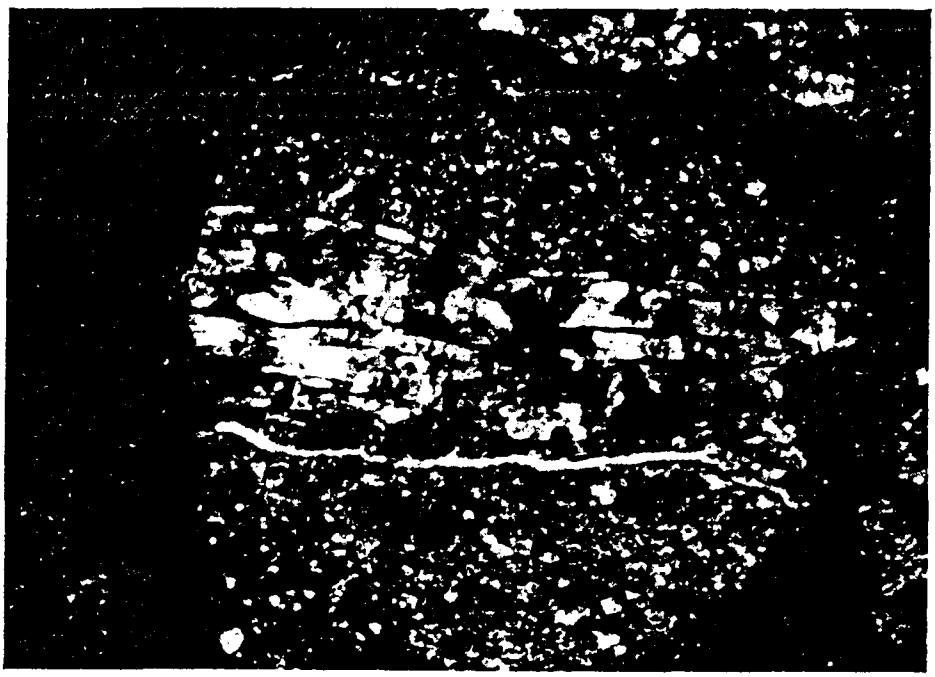

Figure 4-13. (b) Photomicrograph of laumontite vein in metasiltstone/metashale under polarized light. (scale 13 mm : 0.22 mm)

is spatially related to the known or inferred areas of increased porosity and permeability, i.e. fractures or faults. The laumontite occurrences in the intervals between 4000 and 6000 feet correlate not only with anomalous clay occurrences, but also with increases in porosity deduced from the various well logs. Temperatures in this interval range from 110°C to approximately 140°C . Large concentrations of illite (sericite) occur in this interval, which as noted earlier may be indicative of alteration by alkaline solution (Turner and Verhoogen, 1960). Randomly interstratified illite/montmorillonite is also concentrated in this interval (4000 to 6000 feet) further supporting the idea that slightly alkaline solutions may exist or have existed at depth. This idea will be discussed in more detail in Section 4.2.6 Water Chemistry.

4.2.4.2 Well DF 66-21

The propylitic alteration assemblage characteristic of the alluvial sediments, volcanic rocks and, to a lesser extent, the intrusive rocks in DF 45-14 is likewise well developed in their counterparts in DF 66-21. Detailed descriptions of the effects of propylitic alteration on the rocks are given above; only significant differences in the alteration mineralogy of DF 66-21 are discussed.

Examination of Plate VI shows that the distribution of various mineral species is quite localized, particularly for the clay minerals. This evidence, in conjunction with the interpretation of available electric logs, indicated the following intervals are anomalous: 3900 to 4700, 5000 to 5200, 5300 to 6100, 6300 to 6900, 7100 to 7400, 7600 to 8800, and 9100 to 9200 feet. The distribution of calcite, epidote and, to a lesser degree, chlorite and the percentage of plagioclase alteration as well as the various clay minerals is evidence that these zones represent regions of more intense hydrothermal alteration. Although lithology cannot be ruled out as a controlling factor, fracture porosity and permeability appear to be the dominating influences in the distribution of many of the various mineral species.

The intervals mentioned above are interpreted as representing zones of increased porosity, i.e. fault or fracture zones, which provide permeable avenues for migrating thermal fluids and hence the greater degree of alteration. The percent plagioclase alteration, although mainly a function of rock type, does show a weak correlation with structure

especially in the interval 4000 to 4500 feet. The distribution of chlorite is likewise somewhat indistinct, however certain correlations are discernible, i.e. 4000 to 5500 feet and 6300 to 6700 feet. Here again the distribution may be primarily controlled by lithology; however the structural correlations in the above instances are rather strong. Epidote is fairly localized as well, although in this instance the dominating control is the occurrence of the granodiorite intrusive rock. This relationship is clearly visible on Plate VI. In thin section, the intrusive rock was observed to be highly saussuritized although this is likely a function of the metamorphism.

The relative amount and distribution of calcite exhibit strong correlation with the position of known or inferred zones of fracturing and/or faulting. This is particularly evident in the intervals 4000 to 5500, 6400 to 6700 and 7600 to 9400 feet. It may be that these intervals represent zones of boiling where CO_2 is lost and calcite is precipitated according to the following equation:

$$2HCO_3^- + Ca^{++} = H_2O + CO_2 + CaCO_3$$

As CO_2 is lost, the equilibrium constraints cause the equation to move to the right resulting in calcite precipitation. Figure 4-14 shows the intense amount of fracturing in the zone around 6500 feet and the filling of these fractures with calcite. Calcite as vein material is much more abundant in DF 66-21 than in DF 45-14. Minor amounts of adularia, epidote and quartz were also observed in veins in DF 66-21. Most of the epidote veins were altered to calcite and clay.

Limonite and hematite are abundant in the upper 4000 feet of alluvium and then drop off dramatically below 5100 feet. Sporadic increases occur at 6200 to 6700 feet and 8800 to 9100 feet, corresponding closely to zones of inferred fracturing or faulting. These occurrences may indicate the presence of oxygenated waters at great depths suggesting possible communication with the surface via faults and fractures.

The alluvial sediments in DF 66-21 not only differ in amount from those in DF 45-14 but also in their preponderance of volcanic fragments. Many intervals in DF 66-21 are comprised almost solely of volcanic fragments or more appropriately, 'volcanic gravels'. This is probably a function of the location of the well in relation to the zone of altered volcanic rocks directly to the west in the Stillwater Range. This all-

Figure 4-14. (a) Photomicrograph of an intensely fractured zone at 6500 feet in DF 66-21 with abundant calcite deposition. View under polarized light. (scale 13 mm : 0.34 mm)

Figure 4-14. (b) Photomicrograph of an intensely fractured zone at 6500 feet in DF 66-21 with abundant calcite deposition. View under polarized light. (scale 13 mm : 0.34 mm)

uvial material also exhibits a greater degree of hydrothermal alteration, apart from the observed propylitic alteration, that is a result of the ongoing hydrothermal activity in the area.

4.2.5 Clay Mineralogy of Deep Exploratory Wells

4.2.5.1 Well DF 45-14

Plate V shows the relative abundances and distribution of the clay minerals identified by x-ray diffraction techniques and their relationships to fracture zones, lithology, temperature and other mineral species in DF 45-14. The clay minerals are the most useful indicators of the distribution of alteration effects. The clay minerals exhibit a consistent and highly localized pattern of distribution, particularly the mixed-layer and micaceous clays (illite). In Wairakei, the distribution of the montmorillonite zone and the micaceous clay mineral (illite, mixed-layer illite-montmorillonite) zones are related to temperature and fissures carrying geothermal fluid (Steiner, 1968). This seems to be the case in both DF 45-14 and DF 66-21.

The x-ray diffraction analysis of the fine fraction from selected intervals in DF 45-14 reveals the presence of the following clay minerals, in order of increasing temperature and depth: Ca/Mg-montmorillonite, Na-montmorillonite, mixed-layer illite-montmorillonite, and illite. This relationship very closely parallels the clay mineral distribution in Wairakei, New Zealand (Steiner, 1968). It is also documented in other geothermal areas, including Ohaki-Broadlands (Browne and Ellis, 1970), Reykjanes, Iceland (Tomasson and Kristmannsdottir, 1972), and in the Imperial Valley, (Hoagland, 1976).

The temperature/depth relationships of chlorite and kaolinite in DF 45-14 are less certain. Both chlorite and kaolinite have fairly wide stability fields. The difficulties associated with distinguishing kaolinite from chlorite using x-ray diffraction techniques make these minerals tenable indicators of varying conditions of hydrothermal alteration. However the presence of kaolinite is an important indicator of the pH conditions. It occurs in close proximity to fracture zones.

Montmorillonite is indicative of temperatures of 100° to 200°C in altered rhyolitic tuffs in Wairakei (Steiner, 1968). In the Salton Sea Geothermal Area, a temperature of about 100°C is observed for the termination of mixed-layer illite-montmorillonite, while the conversion to

illite is complete at water temperatures of about 210°C (Ellis and Mahon, 1977). At Wairakei, Steiner (1968) found that low temperatures between about 120°C and 230°C prevail at shallow depths (i.e. low lithostatic and water vapor pressures) where mixed-layer minerals are forming. He found that high pressures and temperatures above 230°C are required for the formation of illite and mixed-layer clays deficient in montmorillonite. In Reykjanes, Iceland, montmorillonite is the dominant sheet silicate up to temperatures of about 200°C; for temperatures of 200° to 300°C, the most common sheet silicates are random mixed-layer minerals of chlorite and montmorillonite. Chlorite in Reykjanes characterizes a higher temperature range of 230° to 280°C (Tomasson and Kristmannsdottir, 1972). Thus a fairly wide range of temperatures have been reported for clay minerals. In DF 45-14, montmorillonite is found in zones at water temperatures of 40° to 80°C. Random mixed-layer clays deficient in montmorillonite exist at water temperatures of 80° to 140°C. Illite occurs in a wide temperature range, but it generally indicates higher temperatures (100°C) and pressures. This is evidenced by its concentration in the interval 8000 to 9000 feet in DF 45-14. The available temperature logs were taken only down to a depth of about 5500 feet in DF 45-14. Chemical geothermometers however indicate a downhole temperature of about 215°C.

The zone of montmorillonite clays in the interval 300 to 1200 feet occurs directly above the sequence of volcanic rocks. The change from Ca/Mg-montmorillonite to Na-montmorillonite corresponds to the transition from alluvium into a tuff unit at 700 to 800 feet. Thus in this interval, the abundance and distribution of montmorillonite is related either to rock composition or to the lithologic contacts which may provide permeable avenues for migrating thermal fluids. Another possible interpretation of the occurrence of montmorillonite clays in this zone is that they may represent vestiges of playa lake sediments, formed when the playa covered a much larger area. A very similar occurrence was observed in DF 66-21 but to a much larger extent. This clay layer appears to be very important as it may serve as a 'cap rock' for the geothermal system. Below this impermeable clay layer in DF 66-21 (below 4700 feet) large quantities of hot water under high pressure were encountered during drilling. From 1100 to 2400 feet, in DF 45-14, the tuff/andesite sequence does not exhibit any appreciable degree of

clay mineral formation. The interval 2300 to 2400 feet, corresponding to the contact between the metasediments and the overlying volcanics, is characterized by a regular mixed-layer chlorite/vermiculite clay. The genetic significance of this type of clay occurrence is uncertain.

The interval 4500 to 5500 feet in DF 45-14 is also anomalous with respect to clay mineral distribution. Electric logs indicate that these intervals have anomalous porosity, suggesting these intervals may be fracture or fault zones. This interval is characterized by high concentrations of random mixed-layer illite-montmorillonite deficient in montmorillonite. Steiner (1968) found that with an increase in temperature the relative amount of expandable layers decreased. Steiner also noted that a temperature inversion occurred below a fracture, characterized by a slight increase in the amount of expandable layers. The presence of illite is indicative of higher temperatures as thermal fluids may be migrating along these postulated fractures.

The interval 5100 to 5500 feet corresponds to the intersection of the range front fault zone projected at depth at an angle of 55 to 60 degrees. This zone is marked by a reduction in the amount of cuttings and an abundance of 'trash' in the cuttings indicating a zone of lost circulation. Thus in this instance, the distribution and type of clay minerals is directly related to temperature and proximity to permeable structures. The random mixed-layer illite-montmorillonite clay minerals give way at greater depths to illite in the interval 8000 to 9000 feet. This is compatible with observations in other geothermal systems where illite is indicative of higher temperatures as noted above.

The limited and highly localized nature of the distribution of the various clay minerals is strong evidence in support of the interpretation that hydrothermal alteration in DF 45-14 is structurally controlled and that the majority of the rocks encountered have not been significantly affected by the hydrothermal activity.

4.2.5.2 Well DF 66-21

Referring to Plate VI, the first 4500 feet in DF 66-21 is characterized by a gradual increase in the amount of random mixed-layer clay. This clay is abundant in the interval 2000 to 4500 feet where it appears to act as an impermeable cap rock. Below 4500 feet the amount of this clay gradually decreases. This clay has been identified by x-ray diff-

raction as a randomly interstratified mixed-layer illite-montmorillonite with abundant montmorillonite. The d(001) of unglycolated samples ranges from 12.0A^{o} to 12.45A^{o} and shifts to a value of 13.8A^{o} to 14.7A^{o} suggesting the presence of 35 to 40 percent or more of expandable layers (refer to Figure 4-1 and Table 4-2). The composition of this clay is fairly uniform. It persists throughout the alluvium and into the sequence of volcanic rocks (?). At 5000 feet, corresponding to a change from intercalated tuff-andesite to a homogeneous tuff unit, the type of clay changes to a randomly interstratified mixed-layer illite-montmorillonite with illite dominating. The d(001) of unglycolated samples ranges from 11.8A^{o} to 12.1A^{o} and shifts to an average d(001) of 14.0A^{o} upon glycolation. This same relationship was observed in Wairakei (Steiner, 1968) where the d(001) of mixed layer illite-montmorillonite gradually decreased with an increase in depth and temperature. The random mixed-layer illite-montmorillonite (with illite dominating) in DF 66-21 persists to a depth of 6100 feet where it gives way to a small amount of randomly interstratified mixed-layer illite-montmorillonite with abundant montmorillonite (35 percent) possibly as a result of a temperature inversion below a fracture zone. This clay is found in small amounts in the 6100 to 6300 foot interval.

In the intervals 6400 to 6900 feet and 7100 to 7400 feet and in sporadic occurrences throughout the remainder of the well is a clay mineral which has been identified as a regular mixed-layer chlorite-vermiculite occasionally mixed with a randomly interstratified chlorite-vermiculite or illite-montmorillonite (K. Papke, pers. commun., 1979). The d(001) of this mineral averages about 28.25A^{o} in unglycolated samples. Successive orders of the basal reflection are an integral sequence of the d(001) reflection. To get a d(001) of 28.2A^{o}, two 14.1A^{o} clay minerals must be combined (i.e., chlorite d(001) = 14.1A^{o} and vermiculite d(001) = 14.1A^{o}). Glycolation resulted in a variable shift of only some of these samples indicating the presence of expandable layers probably in a mixed-layer relationship with illite or chlorite. The significance of the regular mixed-layer chlorite-vermiculite is uncertain, although it most likely represents conditions of higher temperature and pressure in the well. Its occurrence also coincides with fracture zones. The relative amount of illite increases dramatically at approximately 6500 feet and predominates from this depth

down to 8800 feet where it begins to gradually decrease. It increases again in the interval 9100 to 9200 feet and is fairly abundant to the total depth of the well at 9780 feet. Thus illite again appears to represent the alteration taking place at higher temperatures and pressures, in association with postulated fracture zones.

The general relationship of the illite and the mixed-layer clay minerals can be expressed as follows, in order of increasing temperature and depth: (1) randomly interstratified mixed-layer illite montmorillonite (with more than 30 percent montmorillonite), (2) randomly interstratified mixed-layer illite-montmorillonite (with less than 30 percent montmorillonite), (3) regular mixed-layer chlorite/vermiculite mixed with randomly interstratified illite-montmorillonite, and (4) discrete illite. Steiner (1968) states that mixed-layer clays with abundant interstratified montmorillonite (1 above) form at low lithostatic and water vapor pressures, whereas comparatively high pressures are required for the formation of illite and mixed-layer clays deficient in montmorillonite (2 and 4 above). This same overall temperature/depth relationship is well documented in other geothermal regions.

Weaver (1956) states that mixed-layer clays in most cases are derived from the degradation or aggradation of pre-existing clay minerals; for example, during weathering, K^+ can be removed from some biotite layers, Mg^{++} and H_2O deposited and a mixed-layer biotite-vermiculite formed; or in sea water the Ca^{++} and H_2O between some montmorillonite layers can be replaced by K^+ and a mixed-layer illite-montmorillonite formed.

The concentration of kaolinite in the interval 4200 to 5400 feet is directly correlated with a zone of increased porosity where abundant water and steam were encountered in the highly fractured and brecciated volcanic rocks (the identification of kaolinite in this interval is certain). It is also associated with the red mixed-layer clay in this interval. The formation of kaolinite at high temperatures (above 150°C) requires relatively acidic conditions whereas montmorillonite is formed under alkaline conditions (Krauskopf, 1967). Thus the occurrence of these two minerals in the interval 4200 to 5400 feet seems contradictory. Kaolinite and montmorillonite may coexist in a very narrow range of temperature-pressure conditions (refer to Figures 4-16, 4-24). This observation may represent the superposition of the alteration effects of the present system on the alteration derived from an earlier system char-

acterized by different chemical conditions. However it is uncertain which of the phases, kaolinite or montmorillonite, is indicative of the present hydrothermal activity.

Evidence from DF 45-14 in conjunction with the observations from DF 66-21 appears to favor the formation of montmorillonite as representing the present system. It is conceivable then that, at some time in the past, more acidic conditions attended by the formation of kaolinite in localized fault zones existed in DF 66-21. It is quite likely that these fracture or fault zones have had a communication with more acidic waters at depth. It is also possible that these acidic waters at depth still exist but that there is no communication with them at the present time. Rather, the avenues of communication have been closed off possibly by deposition of material and/or by tectonic adjustment within the rocks. One other likely alternative is that kaolinite is presently forming from acidic waters in the immediate vicinity of fracture zones but that further away from these zones these acidic waters mix with more alkaline waters thereby making kaolinite unstable.

The interpretation of the alteration mineralogy with regard to kaolinite and chlorite is a problem as a result of the difficulty in distinguishing the two in x-ray diffraction patterns. The distribution pattern of chlorite depicted on Plate V does not exhibit any strong correlations with known or inferred structure or zones of increased porosity as do the other clay minerals. Chlorite does appear though to represent higher temperatures and pressures as it is concentrated in the lower portions of the drill hole. Because of its fairly wide range of stability, chlorite would not seem to be a good indicator of changes in temperature or pressure or alteration conditions.

4.2.6 Water Chemistry

The relationship between the fluid chemistry and the alteration mineralogy in geothermal systems is typically complex and Dixie Valley is no exception. It is evident from an examination of the alteration mineralogy that the chemical flow rate conditions of the hydrothermal system in Dixie Valley have varied through time. The variation of these conditions has resulted in complex mineralogical relationships. The water samples collected from DF 45-14 are considered to be reliable as indicating the chemical conditions at depth. On the other hand, the

reliability of the samples from DF 66-21 must be viewed with discretion as there are holes in the near-surface portions of the casing and the samples were very 'dirty' (D. McMurdie and M. Campana, pers. commun., 1979). Thus the chemical conditions (i.e. pH) of the water samples collected from DF 66-21 are only rough approximations of the conditions at the sampling depth (4700 feet).

In studying the fluid compositions of the two deep wells, 4 samples will be considered; DV-90 and DV-30 from DF 45-14 and DV-80 and DV-93 from DF 66-21. DV-90 is assumed to be representative of deep water conditions in DF 45-14 while DV-30 represents shallow water conditions. Both samples from DF 66-21, DV-80 and DV-93 were collected from a depth of about 4700 feet however the analytical results of these samples are questionable (M. Campana, pers. commun., 1979). The water samples were collected and analyzed by Desert Research Institute personnel. Tables 4-3 through 4-6 list the chemical analyses for these samples. These samples have low to moderate total dissolved solids (TDS) (1900 to 5300 ppb) when compared to geothermal waters in other areas. This suggests that the waters are largely of meteoric origin or that they have been greatly diluted by meteoric water during their migration upward. The waters have apparently achieved their chemical nature largely through interaction with the host rock. The low TDS value may also indicate a relatively short residence time.

The presence of constituents such as lithium, boron, fluorine, arsenic, carbon dioxide and hydrogen sulfide have been suggested in the past as indicating at least a partial magmatic origin of the fluids. More recently though experimental work has shown that concentrations of these elements can occur through normal water-rock interaction at moderate temperatures (Ellis and Mahon, 1977). The high boron content in the Dixie Valley water is not particularly uncommon for geothermal waters, especially within high organic content rocks as those encountered in DF 45-14 and to a lesser extent DF 66-21.

White (1957) has pointed out that within very dense formations sufficient rock/water contact could not occur to maintain the chemical output of a system over its lifetime. For the Wairakei system, Grindley, (1956) showed that over its lifetime (500,000 years) its water would have to have been completely replaced 100 times. Fluid flow through formations of limited permeability (tight, fracture-porosity formations

Table 4-3. Chemical Analysis of Sample DV-90

I	SPECIES		PPM	MOLALITY	LOG MOL	ACTIVITY
1	CA	2	.48496E+01	.12120E-03	-3.9165	.53220E-04
2	MG	2	.84886E-02	.34973E-06	-6.4563	.15628E-06
3	NA	1	.35839+03	.15615E-01	-1.8065	.12621E-01
4	K	1	.39987E+02	.10243E-02	-2.9896	.82217E-03
64	H	1	.19079E-03	.18959E-06	-6.7222	.15849E-06
5	CL	-1	.49287E+03	.13925E-01	-1.8562	.11177E-01
6	SO4	-2	.40033E+00	.41743F-05	-5.3794	.18185E-05
7	HCO3	-1	.44848E+02	.73623E-03	-3.1330	.60024E-03
18	CO3	-2	.50945E-02	.85036E-07	-7.0704	.37571F-07
86	H2CO3	0	.64823E+03	.10468E-01	-1.9801	.10531E-01
27	OH	-1	.74611E+01	.43942E-03	-3.3571	.35248E-03
62	F	-1	.75984E+01	.40061E-03	-3.3973	.32135E-03
19	MGOH	1	.43867E-02	.10634E-06	-6.9733	.87426E-07
23	MGSO4 AQ	0	.15420E-04	.12831E-09	-9.8917	.12884E-09
22	MGHCO3	1	.21796E-02	.25586E-07	-7.5920	.20617E-07
21	MGCO3 AQ	0	.43908E-02	.52159E-07	-7.2827	.52372E-07
20	MGF	1	.36344E-02	.84055E-07	-7.0754	.68025E-07
29	CAOH	1	.70743E-01	.12413E-05	-5.9061	.10167E-05
32	CASO4 AQ	0	.68908E-02	.50699E-07	-7.2950	.50906E-07
30	CAHCO3	1	.11779E+02	.11671E-03	-3.9329	.95593E-04
31	CACO3 AQ	0	.36282E+02	.36310E-03	-3.4400	.36458E-03
44	NASO4	-1	.26616E+03	.22394F-02	-2.6499	.18257E-02
69	NA2SO4	0	.12514E-03	.88249E-09	-9.0543	.88609E-09
43	NAHCO3	0	.33201E+00	.39595E-05	-5.4024	.39757E-05
42	NACO3	-1	.15273E+00	.18432E-05	-5.7344	.15027E-05
49	NA2CO3	0	.29631E-05	.28003E-10	-10.5528	.28118E-10
94	NACL	0	.20495E+00	.35126E-05	-5.4544	.35270E-05
46	KSO4	-1	.12745E-01	.94451E-07	-7.0248	.77004E-07
95	KCL	0	.17712E-01	.23796E-06	-6.6235	.23893E-06
63	HSO4	-1	.15942E-02	.16450E-07	-7.7833	.13313E-07
96	H2SO4	0	.44544E-15	.45492E-20	-20.3421	.45678E-20
93	HCL	0	.86357E-05	.23724E-09	-9.6248	.23821E-09
24	H4SIO4AQ	0	.50928E+03	.53074E-02	-2.2751	.53291E-02
25	H2SIO4	-1	.10447E+02	.11002E-03	-3.9585	.88655E-04
26	H2SIO4	-2	.50997E-01	.54285E-06	-6.2653	.23984E-06
8	FE	2	.16100E+01	.28877E-04	-4.5395	.12997E-04
51	AL	3	.12522E-17	.46486E-22	-22.3327	.92667E-23
52	ALOH	2	.11694E-11	.26627E-16	-16.5747	.11765E-16
53	AL(OH)2	1	.14773E-06	.24260E-11	-11.6151	.19779E-11
54	AL(OH)4	-1	.35213E+00	.37124E-05	-5.4303	.30044E-05
55	ALF	2	.31660E-14	.68970E-19	-19.1613	.30472E-19
56	ALF2	1	.17570E-06	.27085E-11	-11.5673	.22082E-11
57	ALF3	0	.13526E-10	.16134E-15	-15.7923	.16200E-15
58	ALF4	-1	.65881E-12	.64083E-17	-17.1933	.51862E-17
59	ALSO4	1	.17806E-19	.14496E-24	-24.8388	.11731E-24
60	AL(SO4)2	-1	.75821E-23	.34663E-28	-28.4601	.28052E-28
36	H3BO3 AQ	0	.48620E+02	.78761E-03	-3.1037	.79083E-03
81	LI	1	.99965E+00	.14430E-03	-3.8407	.11819E-03
82	LIOH	0	.35696E-01	.14931E-05	-5.8259	.14992E-05
83	LISO4	-1	.11872E-03	.11545E-08	-8.9376	.93823E-09
88	SR	2	.10572E+01	.12086E-04	-4.9177	.52715E-05
89	SROH	1	.33177E-02	.31763E-07	-7.4981	.25813E-07

TDS=2493

Field pH=6.8 Temperature=210°C

Table 4-4. Chemical Analysis of Sample DV-30

I	SPECIES		PPM	MOLALITY	LOG MOL	ACTIVITY
1	CA	2	.12095E+03	.30238E-02	-2.5194	.15347E-02
2	MG	2	.22001E+02	.90666E-03	-3.0426	.46847E-03
3	NA	1	.36560E+03	.15933E-01	-1.7977	.13370E-01
4	K	1	.18356E+02	.47034E-03	-3.3276	.39125E-03
64	H	1	.14996E-03	.14906E-06	-6.8266	.12882E-06
5	CL	-1	.57484E+03	.16245E-01	-1.7893	.13514E-01
6	SO4	-2	.19579E+03	.20420E-02	-2.6899	.10216E-02
7	HCO3	-1	.19462E+03	.31957E-02	-2.4954	.26977E-02
18	CO3	-2	.18287E+00	.30532E-05	-5.5152	.15505E-05
86	H2CO3	0	.43660E+02	.70525E-03	-3.1517	.71001E-03
27	OH	-1	.22192E-01	.13073E-05	-5.8836	.10863E-05
62	F	-1	.40840E+01	.21538E-03	-3.6668	.17898E-03
19	MGOH	1	.14983E-01	.36330E-06	-6.4397	.30913E-06
23	MGSO4 AQ	0	.14637E+02	.12183E-03	-3.9143	.12270E-03
22	MGHCO3	1	.20723E+01	.24333E-04	-4.6138	.20309E-04
21	MGCO3 AQ	0	.13993E+00	.16626E-05	-5.7792	.16746E-05
20	MGF	1	.71891E+00	.16631E-04	-4.7791	.13940E-04
29	CAOH	1	.35595E-02	.62471E-07	-7.2043	.52970E-07
32	CASO4 AQ	0	.56750E+02	.41765E-03	-3.3792	.42065E-03
30	CAHCO3	1	.17118E+02	.16965E-03	-3.7705	.14385E-03
31	CACO3 AQ	0	.13494E+01	.13508E-04	-4.8694	.13605E-04
44	NASO4	-1	.20044E+03	.16868E-02	-2.7729	.14240E-02
69	NA2SO4	0	.40590E+00	.28631E-05	-5.5432	.28837E-05
43	NAHCO3	0	.15755E+01	.18794E-04	-4.7260	.18929E-04
42	NACO3	-1	.11817E+00	.14264E-05	-5.8457	.12041E-05
49	NA2CO3	0	.13678E-03	.12930E-08	-8.8884	.13023E-08
94	NACL	0	.26163E+00	.44853E-05	-5.3482	.45175E-05
46	KSO4	-1	.82496E+00	.61151E-05	-5.2136	.51621E-05
95	KCL	0	.10157E-01	.13650E-06	-6.8649	.13748E-06
63	HSO4	-1	.47326E-02	.48848E-07	-7.3112	.40943E-07
96	H2SO4	0	.15478E-12	.16833F-17	-17.7738	.16954E-17
93	HCL	0	.19774E-08	.54338E-13	-13.2649	.54729E-13
24	H4SIO4AQ	0	.15706E+03	.17414E-02	-2.7591	.17539E-02
25	H3SIO4	-1	.89482E+00	.94265E-05	-5.0257	.78678E-05
26	H2SIO4	-2	.82756E-03	.88114E-08	-8.0550	.44745E-08
8	FE	2	.40000E-01	.71761E-06	-6.1441	.37093E-06
51	AL	3	.16146E-09	.59957E-14	-14.2222	.16130E-14
52	ALOH	2	.22338E-06	.50877E-11	-11.2935	.25836E-11
53	AL(OH)2	1	.23584E-03	.38738E-08	-8.4119	.32701E-08
54	AL(OH)4	-1	.34991E+00	.36899E-05	-5.4330	.30928E-05
55	ALF	2	.26696E-06	.58172E-11	-11.2353	.29541E-11
56	ALF2	1	.11578E-02	.17853E-07	-7.7483	.15071E-07
57	ALF3	0	.13201E-03	.15749E-08	-8.8027	.15862E-08
58	ALF4	-1	.10650E-04	.10363E-09	-9.9845	.86856E-10
59	ALSO4	1	.60138E-09	.48969E-14	-14.3101	.41045E-14
60	AL(SO)2	-1	.10137E-09	.46353E-15	-15.3339	.38852E-15
36	H3BO3 AQ	0	.26723E+02	.43301E-03	-3.3635	.43612E-03
	H2BO3	-1	.15788E+00	.26006E-05	-5.5849	.21405E-05
81	LI	1	.97064E+00	.14015E-03	-3.8534	.11883E-03
82	LIOH	0	.12605E-04	.52738E-09	-9.2779	.53117E-09
83	LISO4	-1	.64736E-01	.62970E-06	-6.2009	.52993E-06
88	SR	2	.32000E+01	.36591E-04	-4.4366	.18353E-04
89	SROH	1	.20513E-04	.19643E-09	-9.7068	.16531E-09

Field pH=6.89 TDS=1903 Temperature=64.5°C

Table 4-5. Chemical Analysis of Sample DV-93

I	SPECIES		PPM	MOLALITY	LOG MOL	ACTIVITY
1	CA	2	.72161E+-0	.18192E-04	-4.7423	.55761E-05
2	MG	2	.74068E+00	.30632E-04	-4.5138	.98537E-05
3	NA	1	.15834E+04	.69249E-01	-1.1596	.50809E-01
4	K	1	.43966E+02	.11305E-02	-2.9467	.81199E-03
64	H	1	.12737E-04	.12705E-07	-7.8960	.10000E-07
5	CL	-1	.17184E+04	.48734E-01	-1.3122	.35004E-01
6	SO4	-2	.11898E+01	.12453E-04	-4.9047	.37114E-05
7	HCO3	-1	.69581E+03	.11465E-01	-1.9406	.8548E-02
18	CO3	-2	.46544E+01	.77982E-04	-4.1080	.24101E-04
86	H2CO3	0	.10141E+03	.16439E-02	-2.7841	.16764E-02
27	OH	-1	.31589E+02	.18675E-02	-2.7288	.13380E-02
62	F	-1	.78380E+01	.41480E-03	-3.3822	.19720E-03
19	MGOH	1	.90011E+00	.21903E-04	-4.6595	.16644E-04
23	MGSO4 AQ	0	.17047E-02	.14239E-07	-7.8465	.14474E-07
22	MGHCO3	1	.75992E+00	.89542E-05	-5.0480	.64898E-05
21	MGCO3 AQ	0	.84398E+01	.10064E-03	-3.9972	.10230E-03
20	MGF	1	.14148E+00	.32844E-05	-5.4835	.24061E-05
29	CAOH	1	.26825E-01	.47245E-06	-6.3256	.35604E-06
32	CASO4 AQ	0	.12351E-02	.91216E-08	-8.0399	.92720E-08
30	CAHCO3	1	.47974E+01	.47711E-04	-4.3214	.35955E-04
31	CACO2 AQ	0	.53334E+02	.53577E-03	-3.2710	.54460E-03
44	NASO4	-1	.48974E+03	.41361E-02	-2.3834	.30839E-02
69	NA2SO4	0	.60239E-02	.42640E-07	-7.3702	.43344E-07
43	NAHCO3	0	.18733E+02	.22425E-03	-3.6493	.22795E-03
42	NACO3	-1	.16564E+03	.20065E-02	-2.6976	.14961E-02
49	NA2CO3	0	.30318E-01	.28760E-06	-6.5412	.29235E-06
94	NACL	0	.25429E+01	.43748E-04	-4.3590	.44469E-04
46	KSO4	-1	.20125E-01	.14971E-06	-6.8248	.11162E-06
95	KCL	0	.53912E-01	.72705E-06	-6.1384	.73904E-06
63	HSO4	-1	.44368E-04	.45956E-09	-9.3577	.33667E-09
96	H2SO4	0	.35616E-17	.36512E-22	-22.4375	.37114E-22
93	HCL	0	.22891E-06	.63124E-11	-11.1098	.64165E-11
24	H4SIO4AQ	0	.20691E+03	.21644E-02	-2.6647	.22001E-02
25	H2SIO4	-1	.77758E+02	.82202E-03	-3.0651	.59578E-03
26	H2SIO4	-2	.16486E+02	.17625E-03	-3.7539	.54472E-04
51	AL	3	.34627-20	.12904E-24	-24.8893	.14965E-25
52	ALOH	2	.82517E-14	.18841E-18	-16.7233	.58290E-19
53	AL(OH)2	1	.37448E-08	.61728E-13	-13.2095	.46025E-13
54	AL(OH)4	-1	.35213E+00	.37264E-05	-5.4287	.27299E-05
55	ALF	2	.67344E-17	.14726E-21	-21.8319	.45512E-22
56	ALF2	1	.31126E-10	.48163E-15	-15.3173	.35911E-15
57	ALF3	0	.13015E-13	.15583E-16	-16.6074	.15840E-18
58	ALF4	-1	.85666E-15	.83643E-20	-20.0776	.61276E-20
59	ALSO4	1	.50555E-22	.41311E-27	-27.3639	.30264E-27
60	AL(SO4)2	-1	.40418E-25	.18547E-30	-30.7317	.13588E-30
36	H3BO3 AQ	0	.16682E+02	.27126E-03	-3.5666	.27573E-03
37	H2BO3	-1	.55050E+02	.90997E-03	-3.0410	.63549E-03

TDS=5310

Field pH=8.0 Temperature=165°C

Table 4-6. Chemical Analysis of Sample OV-80

I	SPECIES		PPM	MOLALITY	LOG MOL	ACTIVITY
1	CA	2	.58474E+00	.14653E-04	-4.8341	.44836E-05
2	MG	2	.44489E+00	.18379E-04	-4.7357	.64531E-05
3	NA	1	.12083E+04	.52785E-01	-1.2775	.39576E-01
4	K	1	.30984E+02	.79583E-03	-3.0992	.58651E-03
64	H	1	.12586E-04	.12541E-07	-7.9017	.10000E-07
5	CL	-1	.12071E+04	.34196E-01	-1.4660	.25202E-01
6	SO4	-2	.37303E+00	.39002E-05	-5.4039	.12671E-05
7	HCO3	-1	.82894E+03	.13644E-01	-1.8650	.10380E-01
18	CO3	-2	.46174E+01	.77279E-04	-4.1119	.25887E-04
86	H2CO3	0	.15291E+03	.24759E-02	-2.6063	.25145E-02
27	OH	-1	.37906E+02	.22385E-02	-2.6500	.16466E-02
19	MGOH	1	.72631E+00	.17654E-04	-4.7531	.13652E-04
23	MGSO4 AQ	0	.38458E-03	.32088E-08	-8.4937	.32494E-08
22	MGHCO3	1	.66015E+00	.77702E-05	-5.1096	.57710E-05
21	MGCO3 AQ	0	.86347E+01	.10255E-03	-3.9878	.10415E-03
29	CAOH	1	.28939E-01	.50912E-06	-6.2932	.39089E-06
32	CASO4 AQ	0	.37985E-03	.28023E-08	-8.5525	.28377E-08
30	CAHCO3	1	.60242E+01	.59848E-04	-4.2230	.45949E-04
31	CACO3 AQ	0	.81801E+02	.82083E-02	-3.0857	.83122E-03
44	NASO4	-1	.16074E+03	.13560E-02	-2.8677	.10316E-02
69	NA2SO4	0	.11848E-02	.83772E-08	-8.0769	.84832E-08
43	NAHCO3	0	.17804E+02	.21290E-03	-3.6718	.21560E-03
42	NACO3	-1	.15612E+03	.18892E-02	-2.7237	.14372E-02
49	NA2CO3	0	.19354E-01	.18814E-06	-6.7255	.19052E-06
94	NACL	0	.14330E+01	.24627E-04	-4.6086	.24938E-04
46	KSO4	-1	.51080E-02	.37955E-07	-7.4207	.28875E-07
95	KCL	0	.28173E-01	.37953E-06	-6.4208	.38433E-06
63	HSO4	-1	.18357E-04	.18994E-09	-9.7214	.14235E-09
96	H2SO4	0	.12219E-17	.12513E-22	-22.9026	.12671E-22
93	HCL	0	.22112E-06	.60910E-11	-11.2153	.61681E-11
24	H2SIO3AQ	0	.23207E+03	.24250E-02	-2.6153	.24557E-02
25	H3SIO4	-1	.86151E+02	.90977E-03	-3.0411	.67570E-03
26	H2SIO4	-2	.16441E+02	.17548E-03	-3.7558	.58784E-04
36	H3BO3 AQ	0	.62920E+02	.10220E-02	-2.9905	.10349E-02
81	LI	1	.12538E+01	.18147E-03	-3.7412	.13933E-03
82	LIOH	0	.12495E+00	.52408E-05	-5.2806	.53071E-05
83	LISO4	-1	.10456E-03	.10196E-08	-8.9918	.77-66E-09

TDS=4305

Field pH=8.0 Temperature=171°C

as encountered in DF 45-14 and DF 66-21) would be expected to rather rapidly (geologically) deplete the available constituents from the exposed rock. It might be postulated then that for the waters in Dixie Valley, some magmatic additions are responsible for the relatively high boron, fluorine, lithium and arsenic levels reported. However it must be considered that the water flow and composition have not been constant over time. Periods of appreciable inflow and outflow may occur over relatively short periods of time when tectonic activity creates new flow channels. Flow may be drastically reduced or cease altogether when these channels become sealed again by deposition of minerals or by deformations within the rocks.. Waxing and waning of the geothermal flow systems at Dixie Valley is supported by evidence of increased flows of quite different character at many of the springs, such as the tufa domes at Sou and Hyder Hot Springs. Evidence for the chemical variation of these geothermal fluids through time is also reflected in the hydrothermal alteration. Even though the origin of chemicals in the Dixie Valley water is not completely clear, local water-rock interactions appear to be the dominant control in determining well, spring, and fumarole fluid compositions.

The hydrothermal alteration in Dixie Valley involves a complex interaction of processes, including: devitrification, recrystallization, solution, and deposition. The end product of these processes is dependent upon a number of factors such as temperature, pressure, fluid compositions, original rock compositions, time of reaction, rates of fluid flow, permeability of the rocks and the type of permeability (fissure or interstitial porosity). The concentration of carbon dioxide and hydrogen sulfide in the waters also has an important control on the type of secondary mineralogy. However their concentrations in the water samples are uncertain. In Dixie Valley, the fluid compositions, flow rates and rock compositions and permeabilities exhibit considerable variation which contributes to the range of observed alteration. Because of these factors and the very limited extent of subsurface sampling (2 deep wells), the vertical zoning, characteristic of many geothermal fields, is somewhat obscure in Dixie Valley. Permeability is a very important factor since many mineralogical changes are not isochemical and any fluid present must be free to move, allowing an influx and outflux of chemical components. The water may impose a

new composition on the rock if a compositional or temperature gradient exists along the direction of water flow.

In New Zealand it was found that dense impermeable rocks such as fine-grained sediments and ignimbrites were little altered by near-neutral pH solutions, even at high temperatures. Breccias and pumice, however, were altered to an equilibrium assemblage (Ellis and Mahon, 1977). This type of effect is seen in the drill cuttings from both DF 45-14 and DF 66-21. Much of the metasiltstone/metashale, quartz arenite and basic intrusive rocks are only weakly altered, while the fractured and brecciated volcanics in the upper portions of both wells have been extensively altered. Significantly, fracture zones (zones of increased permeability indicated by lost circulation during drilling, by brecciation of the drill cuttings, and by the formation-density, neutron, and gamma-ray logs) within the various lithologies show extensive alteration, as would be expected for areas of high permeability.

In considering the alteration mineralogy and its relationship to fluid chemistry, the question of equilibrium is important. Given stable chemical conditions and temperature, it could be expected that the rock-water system would adjust to a new set of equilibrium conditions and minerals. From experimental silicate reaction rates, zones of slow water movement at temperatures above 200°C would probably produce an equilibrium mineral assemblage. However, in other cases equilibrium between rock and water may not be attained for reasons such as low rock permeability, rapid steam or water flow, boiling of water at particular depths, or condensation of steam into a water phase. The solubilities of the common rock-forming constituents (Si, Al, Na, K, Ca, Mg, Fe, Mn) are limited by particular mineral-water equilibria, which in all cases favor the retention of the elements in the mineral phases (Ellis and Mahon, 1977). In the two deep exploratory wells the flow rates are unknown and the downhole temperatures estimated from SiO_2 and Na/K geothermometry are approximately 190°C to 215°C for DF 45-14 and 165°C to 175°C for DF 66-21.

In correlating the alteration mineralogy to water chemistry, the computer program WATEQ (Truesdell and Jones, 1974) has been used to provide activities and saturation index data as determined from the laboratory water analyses. The following discussion is based upon the method of Helgeson (1969) for deriving phase diagrams expressing mineral stab-

ilities by ion concentration ratios in solution.

In the presence of quartz with aluminum assumed fixed, the formation of various silicates depends on the activity of metal oxides in solution. For example the activity of CaO may be expressed as follows:

$$CaO + 2H^+ = Ca^{++} + H_2O$$

$$K_a = aCa^{++} / (aH^+)^2 \cdot aCaO \quad ; \text{ with } aH_2O \text{ assumed} = 1$$

$$\text{Thus, } \log aCaO = \log (aCa^{++} / (aH^+)^2) - \log K_{Ca}$$

Since $\log K_{Ca}$ is a constant, the variation in CaO activity may be expressed in terms of the variation in the ratio $aCa^{++}/(aH^+)^2$ and similar expressions may be derived for other oxides.

Correlations can now be made between solution composition and mineral equilibrium using ion activities:

$$\underset{\text{(K-spar)}}{3KAlSi_3O_8} + 2H^+ = \underset{\text{(K-mica)}}{KAl_3Si_3O_{10}(OH)_2} + \underset{\text{(Qtz)}}{6SiO_2} + 2K^+$$

The equilibrium constant for the above reaction is directly related to the ratio of potassium ion activity to hydrogen activity.

The diagrams which follow (Figures 4-16 through 4-24) represent the thermodynamically stable phase for a given temperature and pressure, assuming quartz saturation but not amorphous silica saturation. The points plotted illustrate the migration of the fluid composition and stability fields with changing pH and temperature conditions. It should be noted that a fluid composition within a stabiltiy field for a given mineral phase does not imply its presence or indicate any quantity which may be present, merely that it should be a stable phase for the specified conditions. Other factors such as element availability, ability of a phase to nucleate, and the kinetics of grain growth must also be considered.

One of the major problems associated with the interpretation of these stability diagrams is the uncertainty of the pH at depth. Because of the combined effects of temperature, fluid mixing and degassing (especially CO_2) and/or boiling, the pH at the production depth may be considerably lower than the measured field pH. An increase in temperature with depth, such as that found in both wells, may lower the pH by one and as much as two pH units (R. Jacobson, pers. commun., 1979). As a generalization, the pH is controlled by the salinity of the waters and aluminosilicate equilibria involving hydrogen and alkali metal ions

(Ellis and Mahon, 1977). Figure 4-15 was used to provide an estimation of the pH in each of the wells using temperatures derived from chemical geothermometers and calculated salinities of the water samples. Temperatures of 170°C and 200°C for DF 66-21 and DF 45-14 yield pH values of 7.5-7.6 and 7.6-7.7, respectively (Figure 4-15). These values compare with measured field pH values of 8.0 for DV-93 (DF 66-21) and 6.8 for DV-90 (DF 45-14). The discrepancies between these pH values are likely an indication of fluid mixing wherein the salinities used in Figure 4-14 would not be truly representative. A water sample recently taken from DF 66-21, considered to be fairly reliable, yielded a pH of 5.8 (M.E. Campana, pers. commun., 1979).

Another mechanism which explains the apparent discordance between the measured pH and that determined from Figure 4-15 for DF 45-14 is the rise in pH associated with the release of CO_2 during boiling. Examination of the equation below illustrates this process.

$$H^+ + HCO_3^- = H_2O + CO_2$$

As CO_2 is driven off (vaporizes), the equilibrium constraints force the reaction to proceed to the right, thereby consuming H^+ (acid) in the process. CO_2 may also have been lost during sampling (R. Jacobson, pers. commun., 1979). Because of the uncertainty in the true down-hole pH in both wells, it is not totally clear which mineral phases represent an equilibrium assemblage. However it does appear that the downhole pH is slightly lower than the measured field pH in both wells.

At temperatures of 150°C and 200°C and the measured field pH, none of the samples are near equilibrium with kaolinite (Figures 4-16 through 4-24). This is particularly significant since kaolinite was prominent in localized intervals associated with postulated fracture zones in both wells (Plates V and IV). Considerably lower than field pH conditions (5.0 or less) or lower temperature conditions (100°C or less) would be required for kaolinite to exist as a stable phase. The presence of kaolinite together with montmorillonite is only possible in a very narrow range of physical and chemical conditions. It may be postulated that the presence of kaolinite represents a relict of a previous period of more acidic conditions and/or lower temperature conditions. The occurrence of kaolinite in the immediate vicinity of fault zones may indicate that the faults are in or have been in communication with

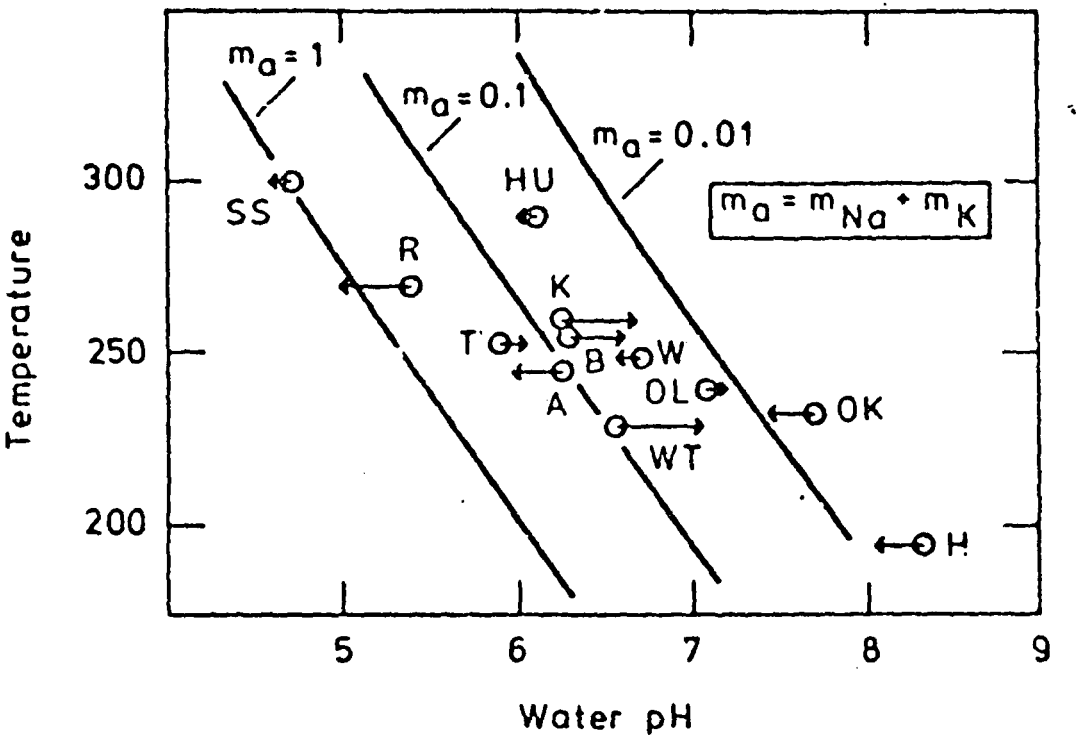

Figure 4-15. The calculated trends of pH with temperature for waters of three salinities. Open circles show pH of waters in geothermal systems; connected arrowheads indicate pH calculated for the salinity of the water. SS - Salton Sea; R - Reykjanes; H - Hveragerdi; HU - Hatchobaru; T - El Tatio; OL - Olkaria; A - Ahuachapan; W - Wairakei; K - Kawerau; B - Broadlands; WT - Waiotapu; OK - Orakeikorako. (from Ellis and Mahon, 1977)

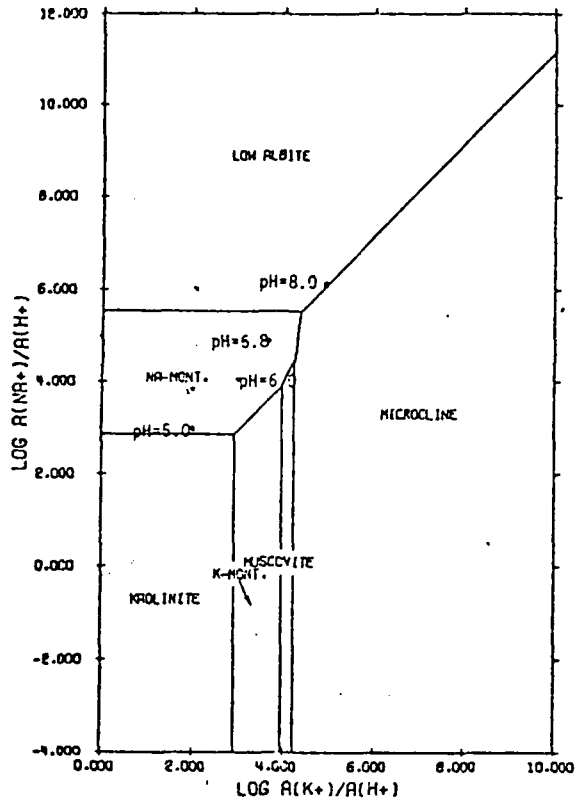

The System $HCl-H_2O-Al_2O_3-K_2O-Na_2O-SiO_2$ at 200°C; log $a_{H_4SiO_4}$ = −2.35 = quartz saturation.

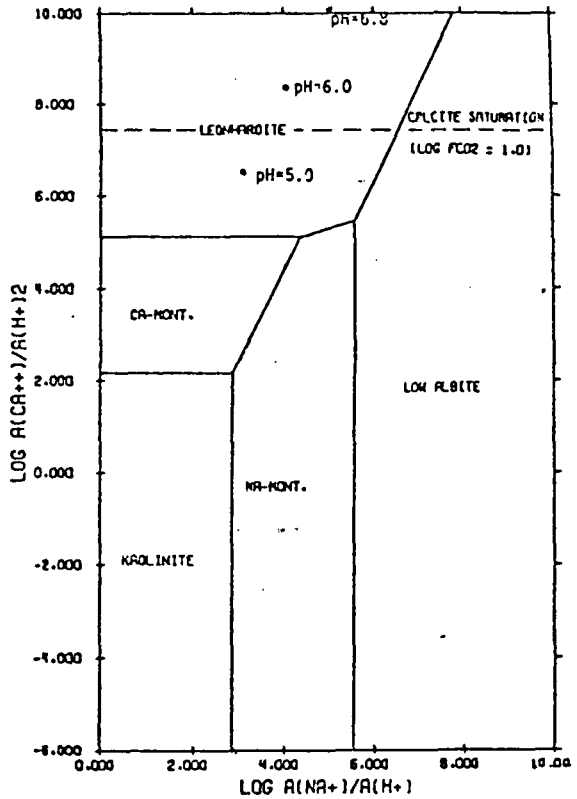

The System $HCl-H_2O-Al_2O_3-CaO-CO_2-Na_2O-SiO_2$ at 200°C; log $a_{H_4SiO_4}$ = −2.35 = quartz saturation.

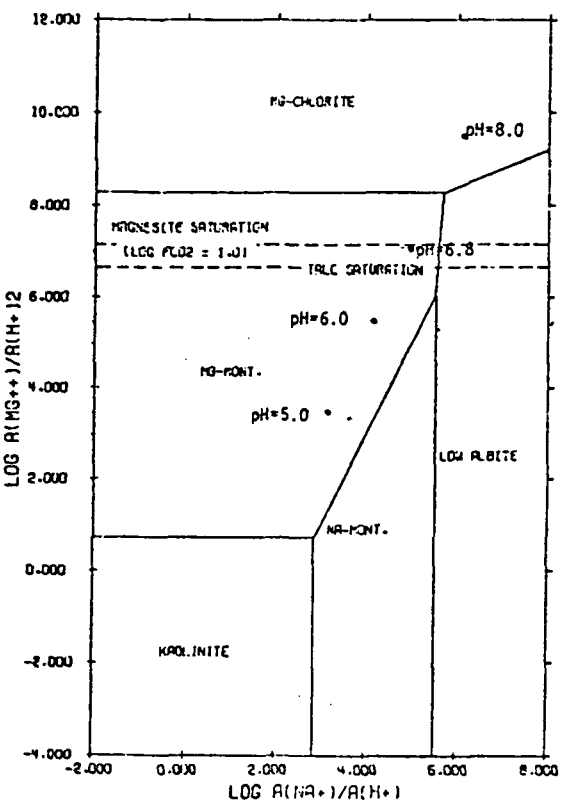

The System $HCl-H_2O-Al_2O_3-CO_2-MgO-Na_2O-SiO_2$ at 200°C; log $a_{H_4SiO_4}$ = −2.35 = quartz saturation.

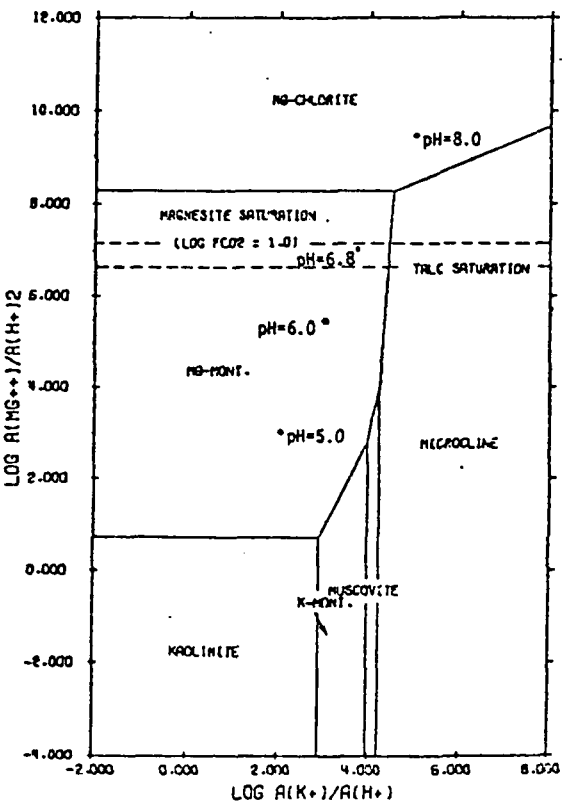

The System $HCl-H_2O-Al_2O_3-CO_2-K_2O-MgO-SiO_2$ at 200°C; log $a_{H_4SiO_4}$ = −2.35 = quartz saturation.

Figure 4-16. Phase stability diagrams for Sample DV-90 at 200°C.

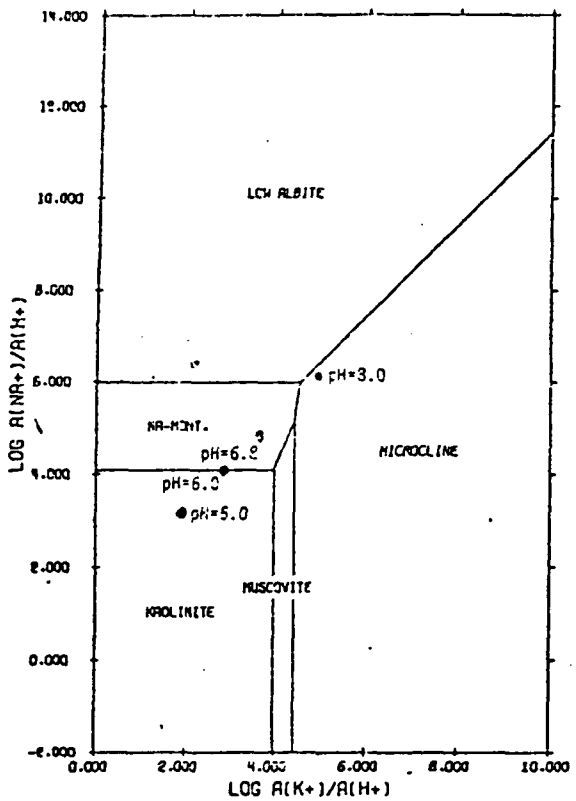

The System $HCl-H_2O-Al_2O_3-K_2O-Na_2O-SiO_2$ at 150°C; $\log a_{H_4SiO_4} = -2.67$ = quartz saturation.

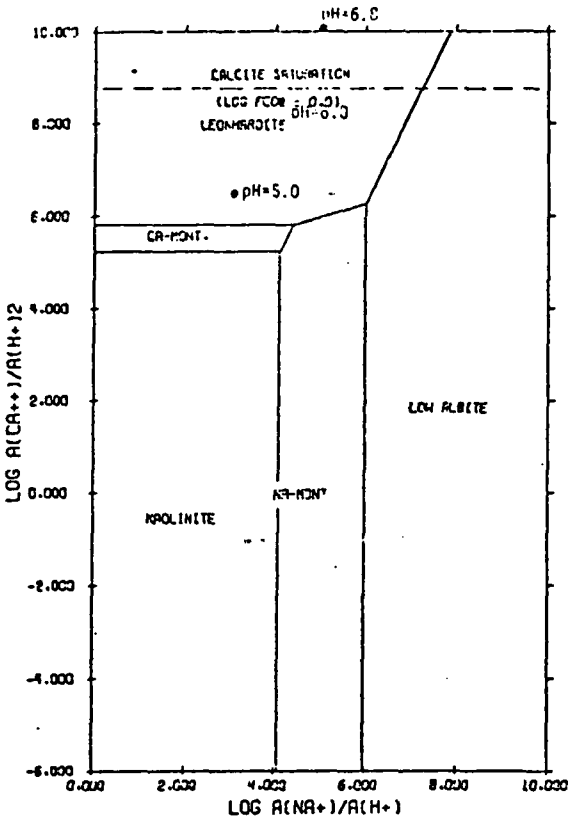

The System $HCl-H_2O-Al_2O_3-CaO-CO_2-Na_2O-SiO_2$ at 150°C; $\log a_{H_4SiO_4} = -2.67$ = quartz saturation.

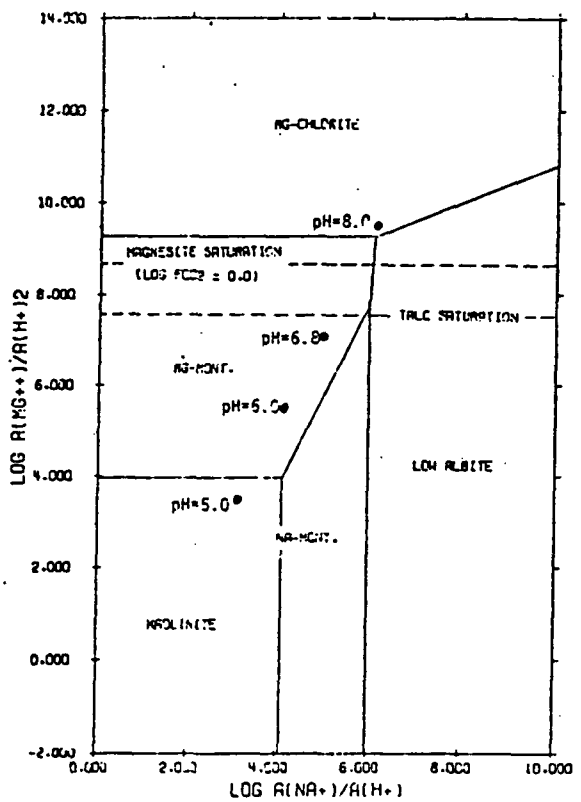

The System $HCl-H_2O-Al_2O_3-CO_2-MgO-Na_2O-SiO_2$ at 150°C; $\log a_{H_4SiO_4} = -2.67$ = quartz saturation.

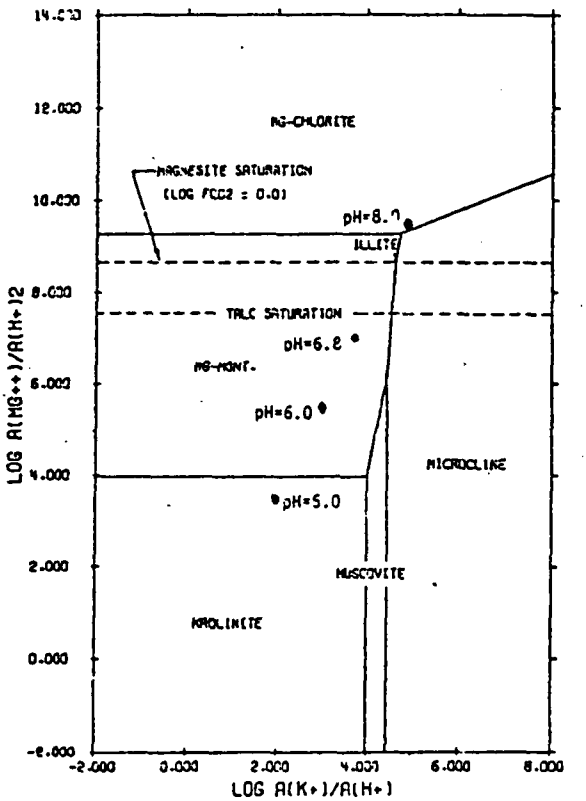

The System $HCl-H_2O-Al_2O_3-CO_2-K_2O-MgO-SiO_2$ at 150°C; $\log a_{H_4SiO_4} = -2.67$ = quartz saturation.

Figure 4-17. Phase stability diagrams for Sample DV-90 at 150°C.

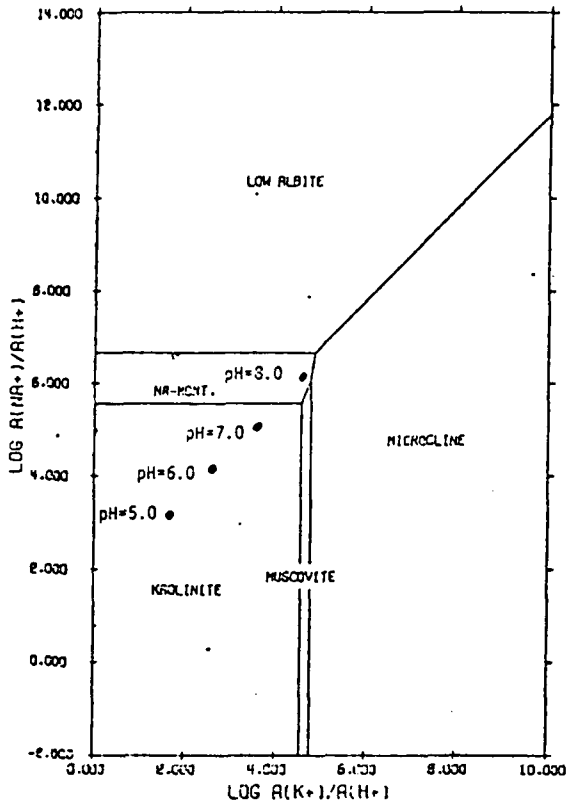

The System HCl–H_2O–Al_2O_3–K_2O–Na_2O–SiO_2 at 100°C; $\log a_{quartz} = -3.08$ = quartz saturation.

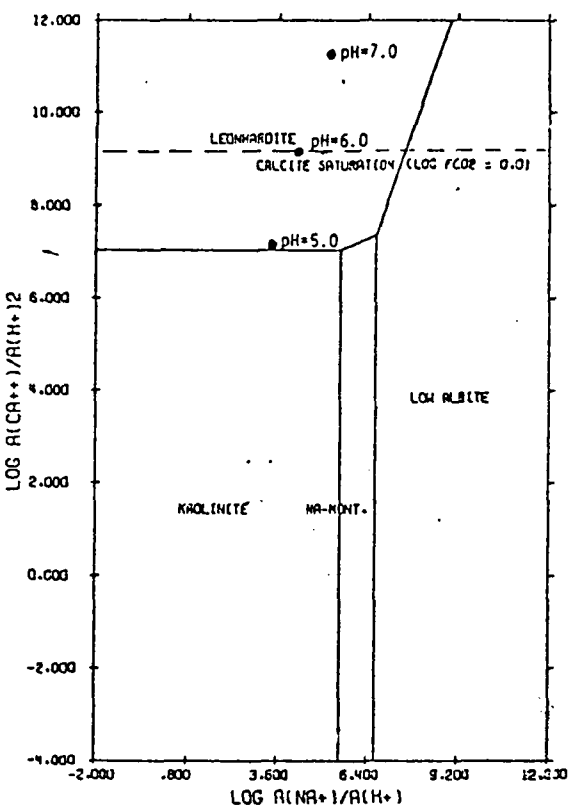

The System HCl–H_2O–Al_2O_3–CaO–CO_2–Na_2O–SiO_2 at 100°C; $\log a_{quartz} = -3.08$ = quartz saturation.

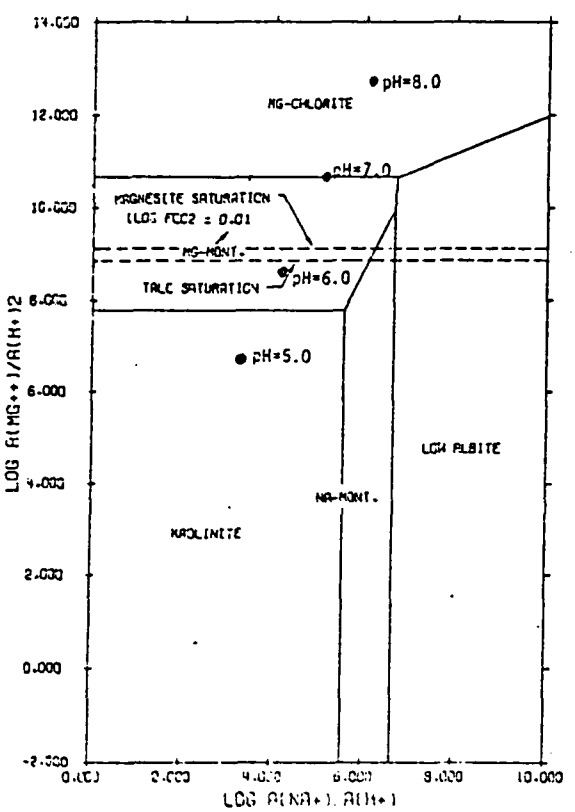

The System HCl–H_2O–Al_2O_3–CO_2–MgO–Na_2O–SiO_2 at 100°C; $\log a_{quartz} = -3.08$ = quartz saturation.

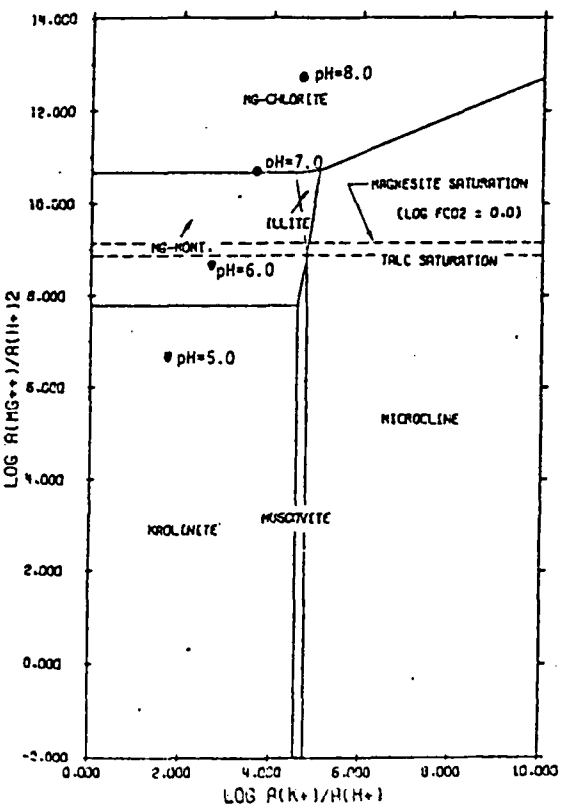

The System HCl–H_2O–Al_2O_3–CO_2–K_2O–MgO–SiO_2 at 100°C; $\log a_{quartz} = -3.08$ = quartz saturation.

Figure 4-18. Phase stability diagrams for Sample DV-30 at 100°C.

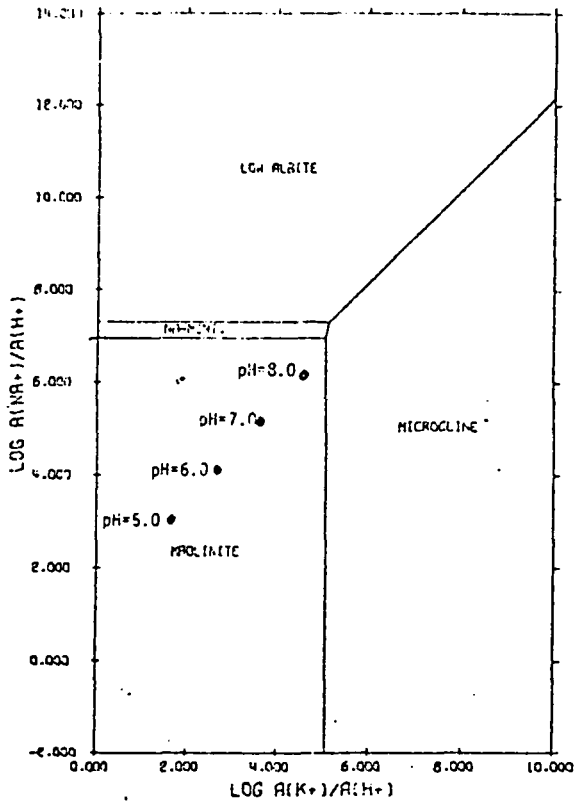

The System $HCl-H_2O-Al_2O_3-K_2O-Na_2O-SiO_2$ at 60°C; $\log a_{H_4SiO_4} = -3.52$ = quartz saturation.

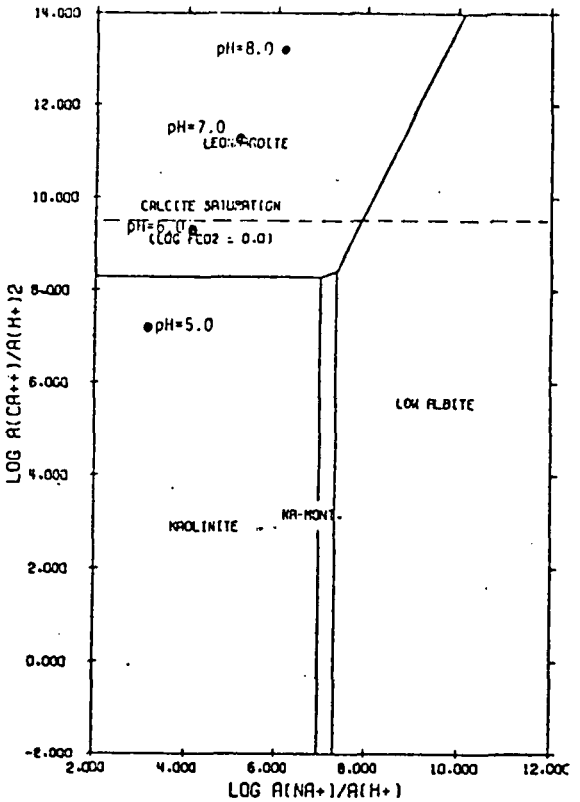

The System $HCl-H_2O-Al_2O_3-CaO-CO_2-Na_2O-SiO_2$ at 60°C; $\log a_{H_4SiO_4} = -3.52$ = quartz saturation.

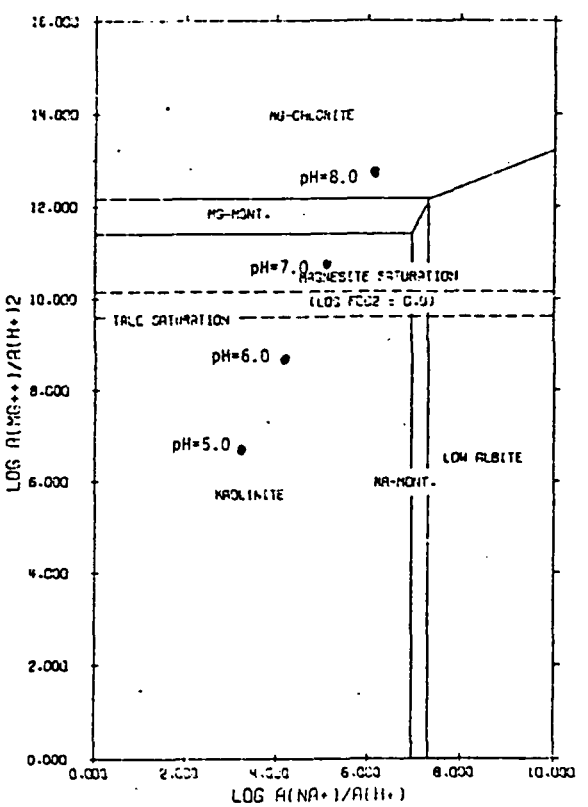

The System $HCl-H_2O-Al_2O_3-CO_2-MgO-Na_2O-SiO_2$ at 60°C; $\log a_{H_4SiO_4} = -3.52$ = quartz saturation.

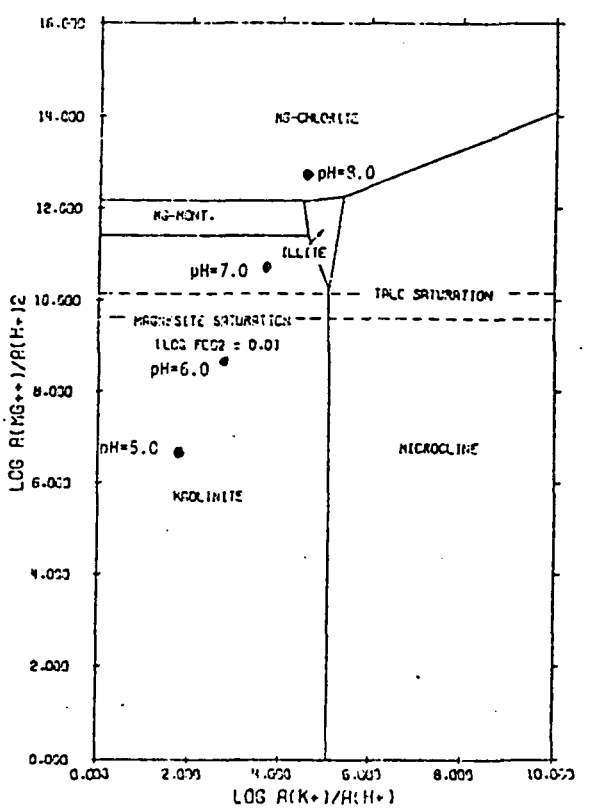

The System $HCl-H_2O-Al_2O_3-CO_2-K_2O-MgO-SiO_2$ at 60°C; $\log a_{H_4SiO_4} = -3.52$ = quartz saturation.

Figure 4-19. Phase stability diagrams for Sample DV-30 at 60°C.

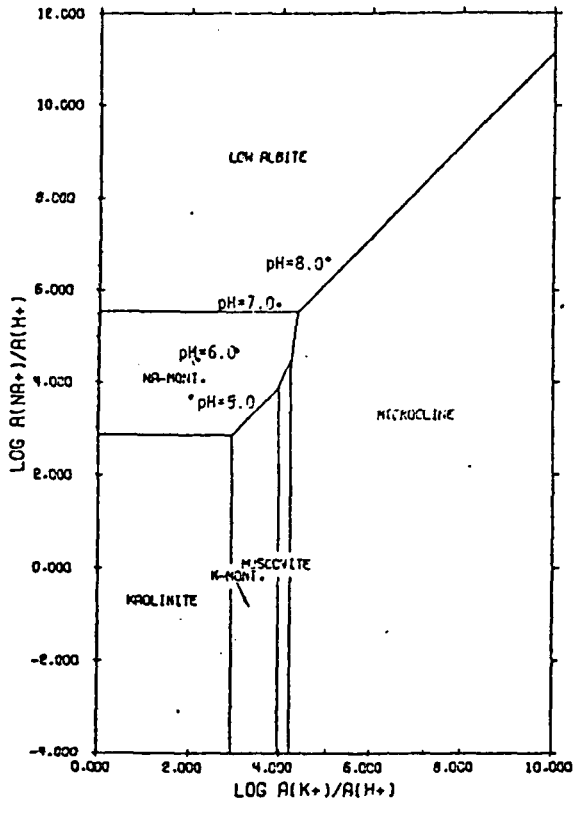

The System $HCl-H_2O-Al_2O_3-K_2O-Na_2O-SiO_2$ at 200°C; log a_{SiO_2} = −2.55 = quartz saturation.

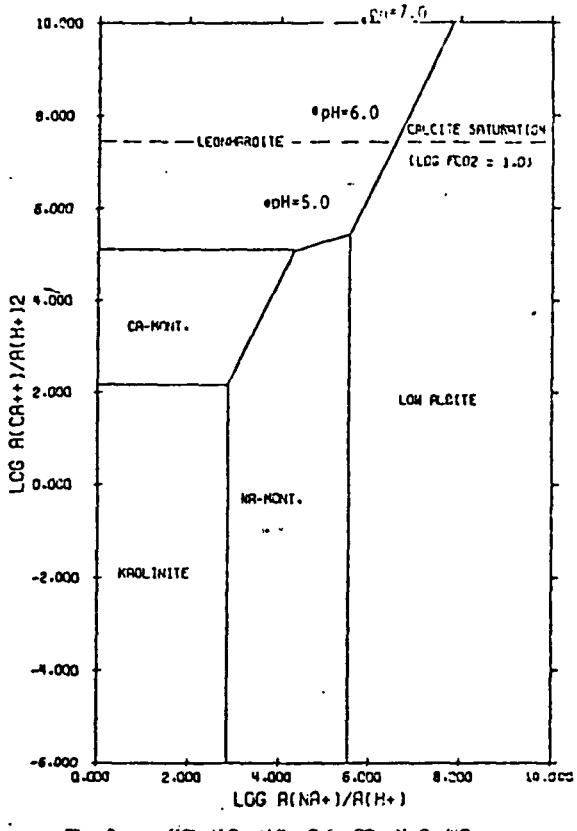

The System $HCl-H_2O-Al_2O_3-CaO-CO_2-Na_2O-SiO_2$ at 200°C; log a_{SiO_2} = −2.55 = quartz saturation.

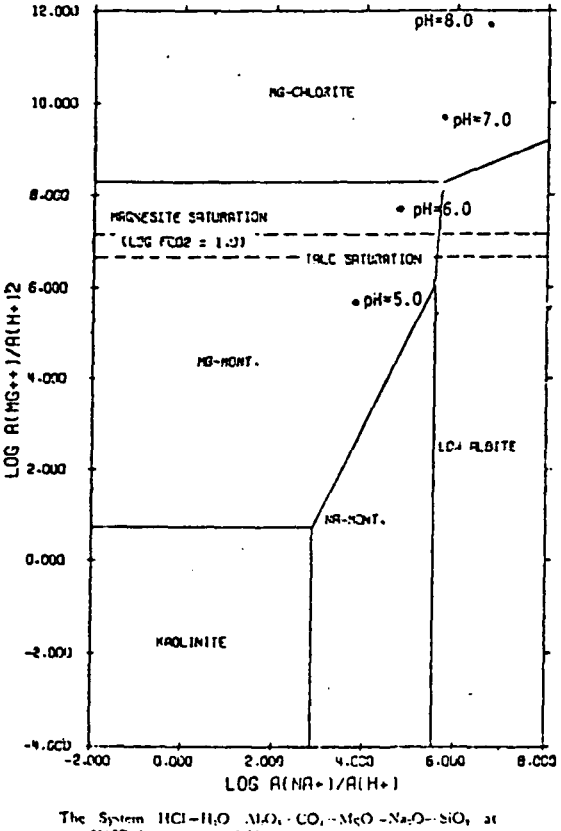

The System $HCl-H_2O-Al_2O_3-CO_2-MgO-Na_2O-SiO_2$ at 200°C; log a_{SiO_2} = −2.55 = quartz saturation.

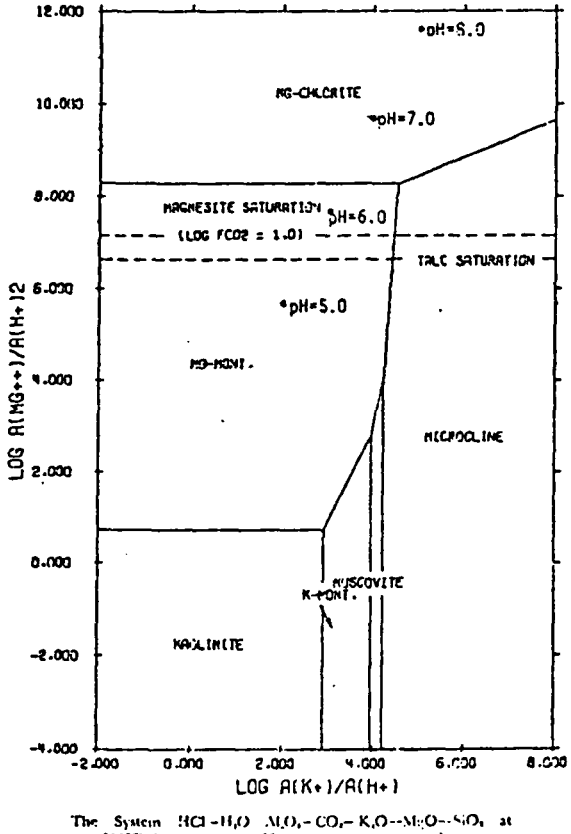

The System $HCl-H_2O-Al_2O_3-CO_2-K_2O-MgO-SiO_2$ at 200°C; log a_{SiO_2} = −2.55 = quartz saturation.

Figure 4-20. Phase stability diagrams for Sample DV-93 at 200°C.

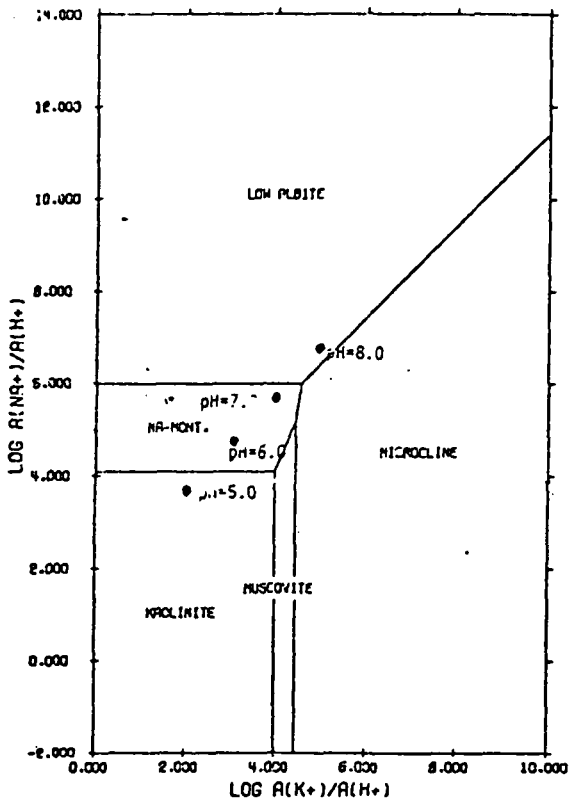

The System $HCl-H_2O-Al_2O_3-K_2O-Na_2O-SiO_2$ at 150°C; $\log a_{quartz} = -2.67$ = quartz saturation.

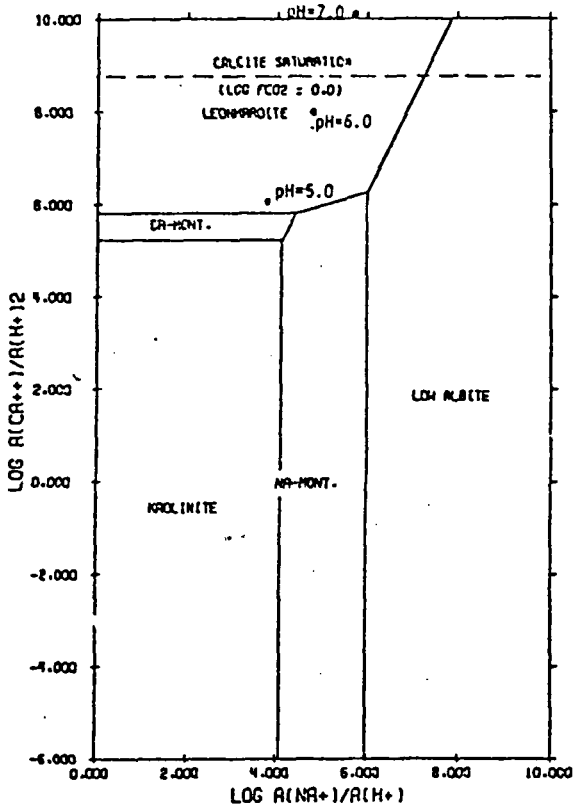

The System $HCl-H_2O-Al_2O_3-CaO-CO_2-Na_2O-SiO_2$ at 150°C; $\log a_{quartz} = -2.67$ = quartz saturation.

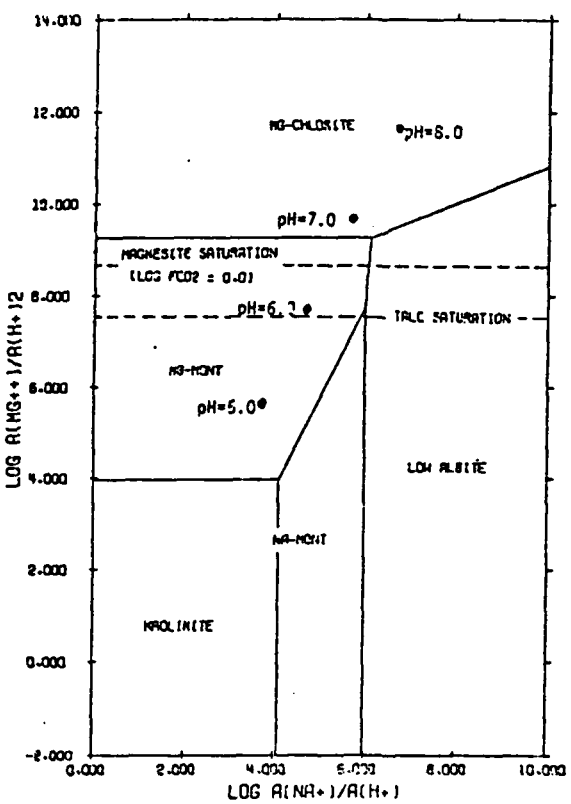

The System $HCl-H_2O-Al_2O_3-CO_2-MgO-Na_2O-SiO_2$ at 150°C; $\log a_{quartz} = -2.67$ = quartz saturation.

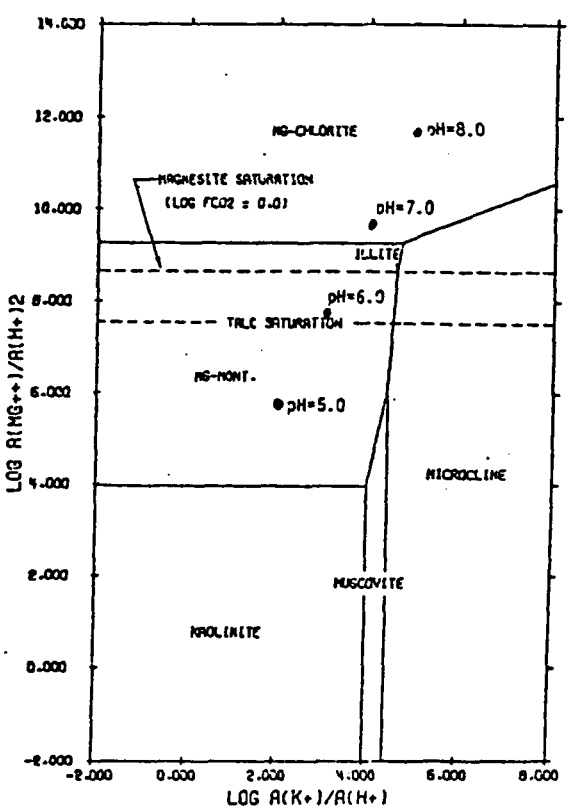

The System $HCl-H_2O-Al_2O_3-CO_2-K_2O-MgO-SiO_2$ at 150°C; $\log a_{quartz} = -2.67$ = quartz saturation.

Figure 4-21. Phase stability diagrams for Sample DV-93 at 150°C.

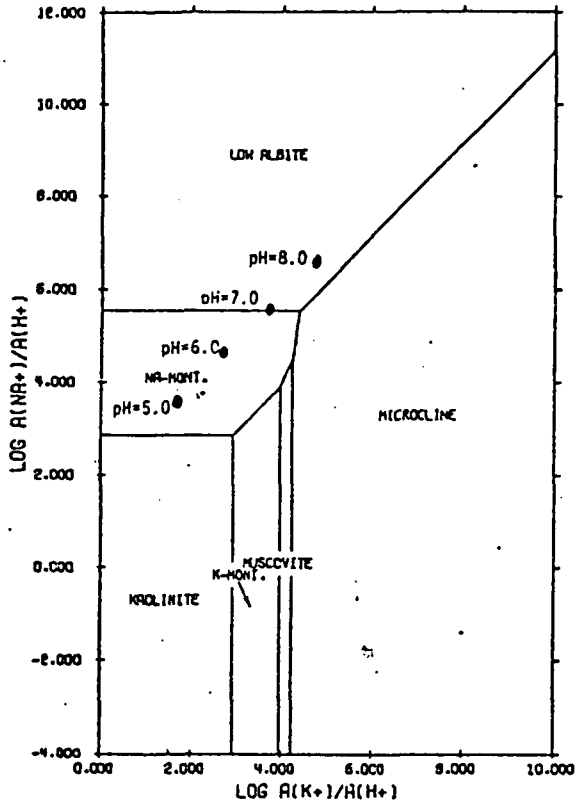

The System HCl—H_2O—Al_2O_3—K_2O—Na_2O—SiO_2 at 200°C; $\log a_{quartz} = -2.35$ = quartz saturation.

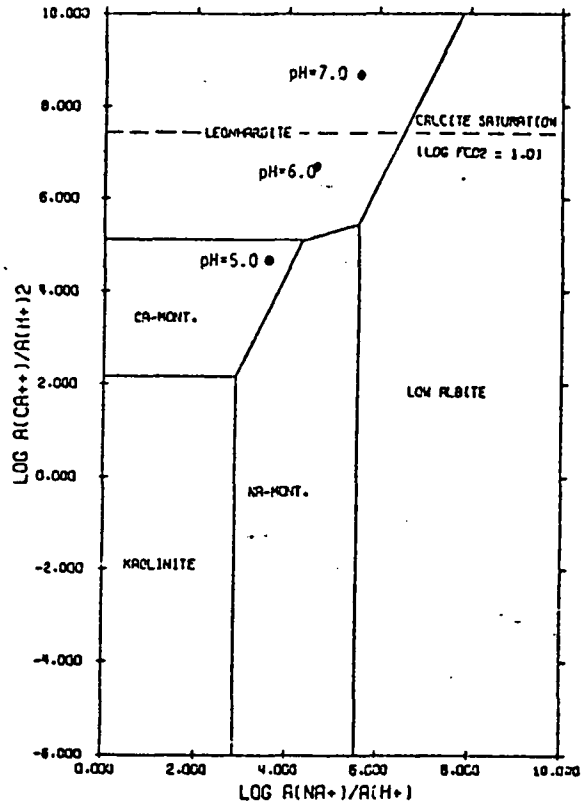

The System HCl—H_2O—Al_2O_3—CaO—CO_2—Na_2O—SiO_2 at 200°C; $\log a_{quartz} = -2.35$ = quartz saturation.

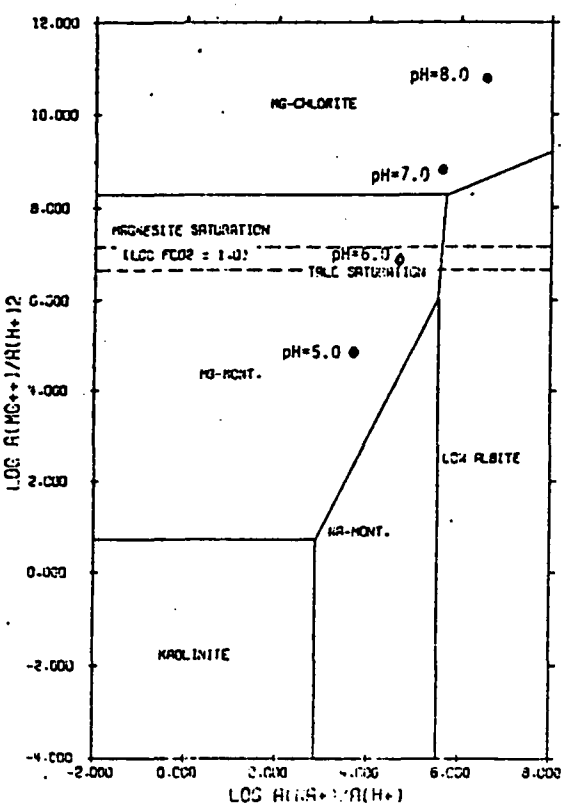

The System HCl—H_2O—Al_2O_3—CO_2—MgO—Na_2O—SiO_2 at 200°C; $\log a_{quartz} = -2.35$ = quartz saturation.

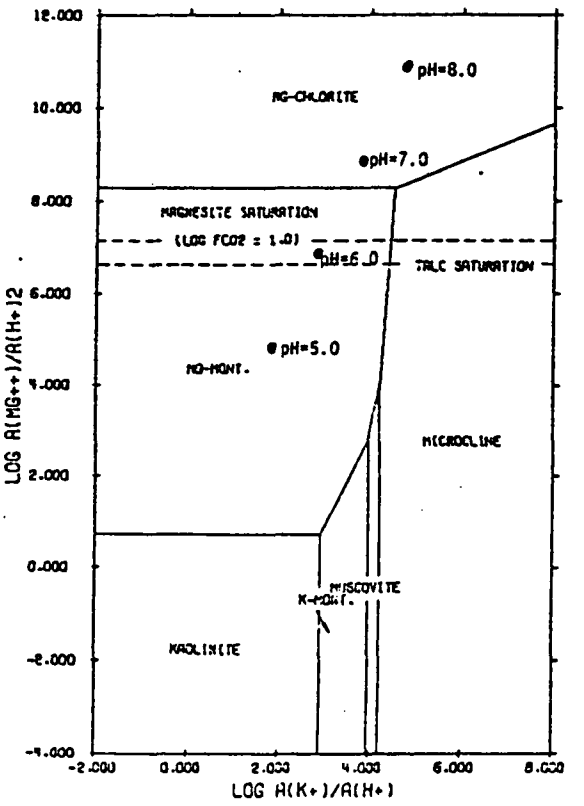

The System HCl—H_2O—Al_2O_3—CO_2—K_2O—MgO—SiO_2 at 200°C; $\log a_{quartz} = -2.35$ = quartz saturation.

Figure 4-22. Phase stability diagrams for Sample DV-80 at 200°C.

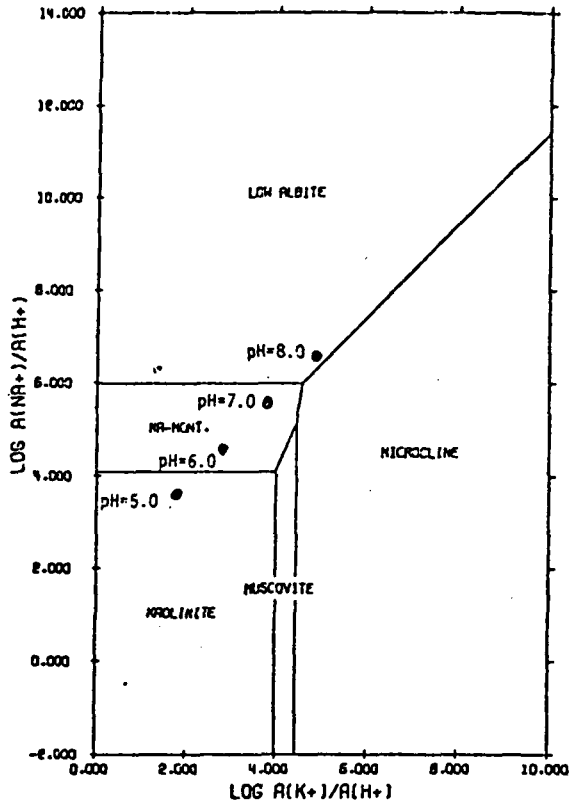

The System HCl—H_2O—Al_2O_3—K_2O—Na_2O—SiO_2 at 150°C: log a_{quartz} = −2.67 = quartz saturation.

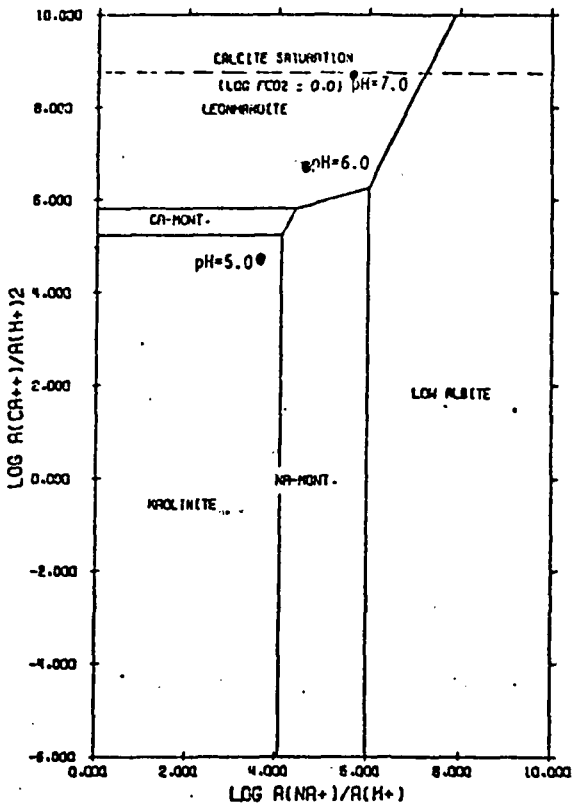

The System HCl—H_2O—Al_2O_3—CaO—CO_2—Na_2O—SiO_2 at 150°C; log a_{quartz} = −2.67 = quartz saturation.

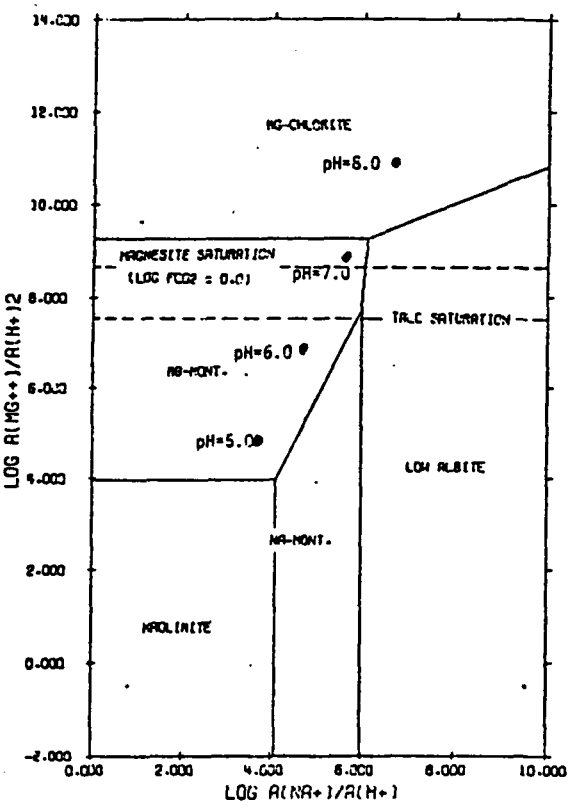

The System HCl—H_2O—Al_2O_3—CO_2—MgO—Na_2O—SiO_2 at 150°C; log a_{quartz} = −2.67 = quartz saturation.

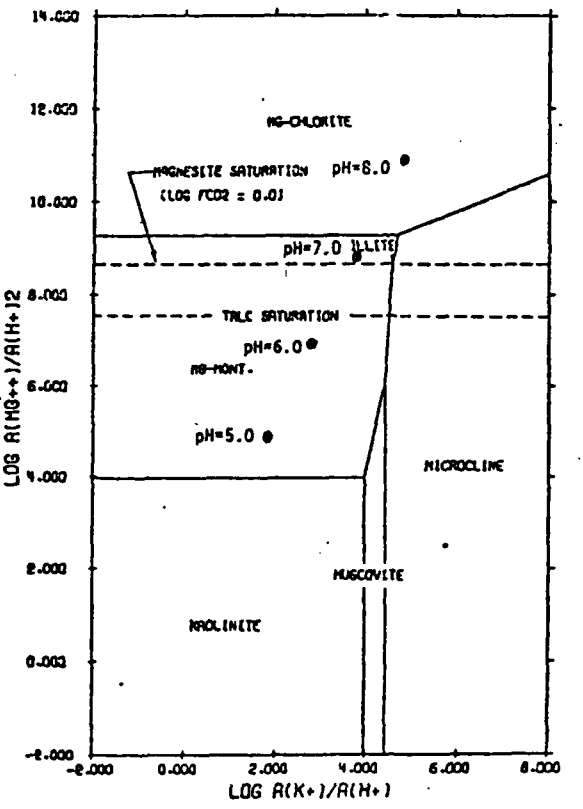

The System HCl—H_2O—Al_2O_3—CO_2—K_2O—MgO—SiO_2 at 150°C; log a_{quartz} = −2.67 = quartz saturation.

Figure 4-23. Phase stability diagrams for Sample DV-80 at 150°C.

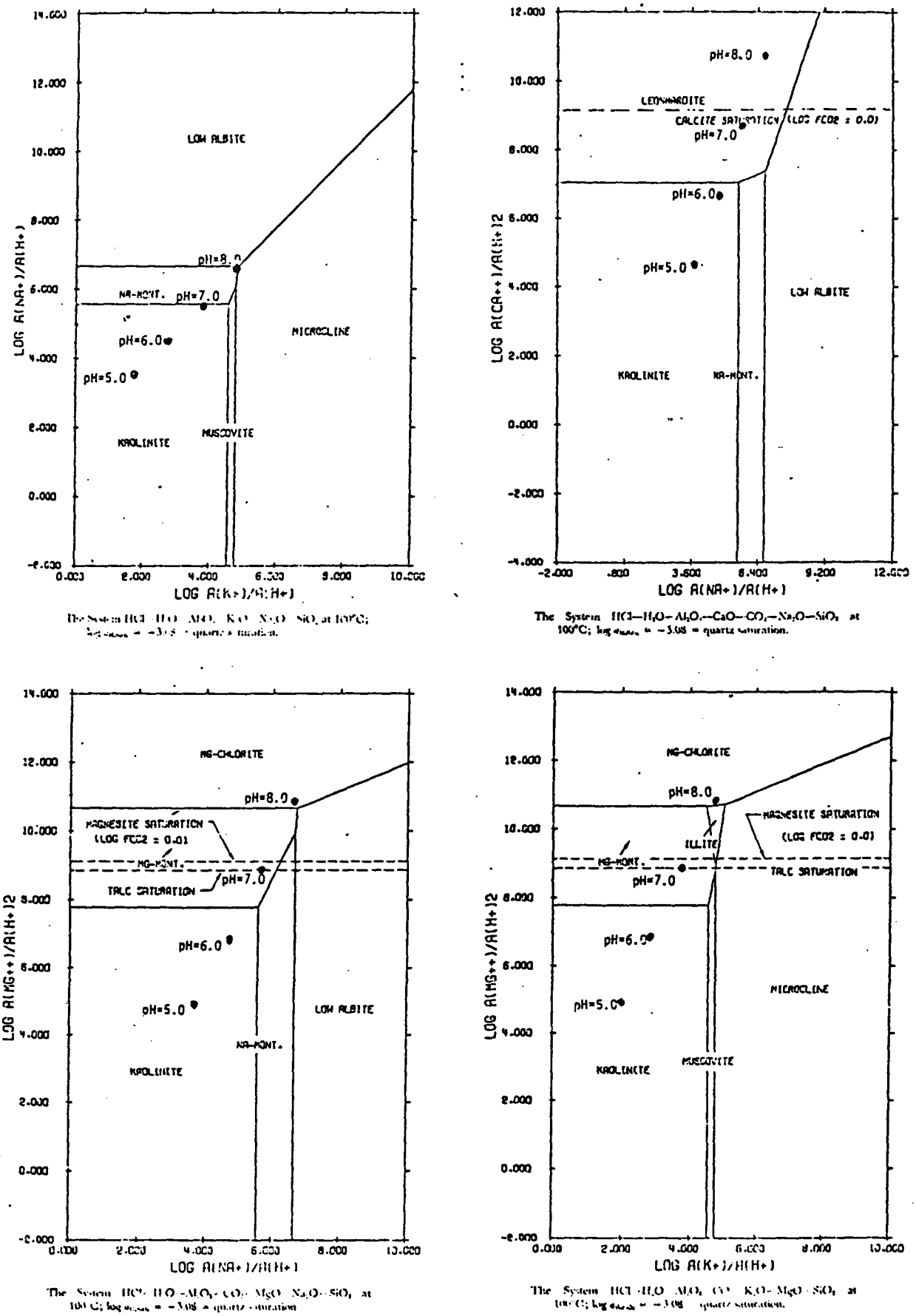

Figure 4-24. Phase stability diagrams for Sample DV-80 at 100°C.

more acidic waters at depth which affect the kaolinitic alteration as they migrate upward. On the other hand the occurrence of montmorillonite, which is favored under more alkaline conditions, may reflect the action of downward percolating alkaline surface waters. These same waters probably mix with the more acidic waters issuing from the fractures thereby confining kaolinite to the fracture zones.

The observed mineralogy in DF 45-14 below 6000 feet (approximate depth of casing) is chiefly K-mica, quartz, chlorite, calcite, andalusite/chiastolite, clay minerals $\pm$ laumontite. Potassium feldspar as adularia occurs in trace amounts as vein material, and albite and epidote are abundant within the basic intrusions. If sample DV-90 (pH = 6.8) truly represents the deep water conditions in DF 45-14 and assuming a temperature of 200°C, the assemblage quartz, Na/Mg-montmorillonite-leonhardite (partially dehydrated laumontite) and/or calcite, $\pm$ albite $\pm$ K-spar would represent an equilibrium assemblage (Figure 4-16).

Only when the temperature is lowered to 100°C or the pH is reduced to 5.0 or below will kaolinite become stable. Figure 4-17 shows the migration of the stability fields as the temperature is lowered to 150°C for DV-90 and as the pH changes. Another significant observation of the activity diagrams for DV-90 is the apparent disequilibrium of K-mica with the present physical and chemical conditions. This mineral occurred pervasively in the cuttings from DF 45-14. The activity diagrams indicate only a small stability field for K-mica. As in the case of kaolinite, lower pH values than the measured field pH of 6.8, as well as a higher potassium ion activity, are required to bring K-mica into equilibrium. Illite (K-mica) is also spatially related to fracture zones supporting the hypothesis that more acidic conditions exist in these intervals. The occurrence of laumontite, mentioned earlier, may reflect alkaline conditions and may also be due to the downward migration of near surface alkaline waters along fracture or fault zones. This may come about when deep communication with more acidic water is temporarily cut off due to mineral deposition or tectonic closures of the fractures at depth.

Two major zones of alteration appear in the lower 5000 feet of DF 45-14. Highly altered intervals (4700 to 5300 and 8300 to 8600 feet) are characterized by an assemblage of kaolinite, illite, and mixed-

layer illite-montmorillonite that is spatially associated with presumed fracture zones. Larger generally less altered zones are negatively correlated with fracture zones (Plate V). It is evident then that fracture porosity and permeability is the dominant control in influencing the intensity and distribution of the various alteration effects observed in DF 45-14.

The alteration mineralogy above 1500 feet in DF 45-14 is dominated by Na-montmorillonite, illite (K-mica) and lesser chlorite. In the deeper portions of the well mixed-layer illite-montmorillonite is the predominant clay mineral. Examination of the activity diagrams (Figures 4-18 and 4-19) for sample DV-30, believed to be representative of the conditions above 1500 feet, show this assemblage to be at or very near equilibrium. An important shift occurs in the water chemistry between the deep (DV-90) and shallow (DV-30) water samples from DF 45-14. Calcium and magnesium increase significantly while sodium and potassium decrease. This may indicate alteration of Mg and Ca-silicates to form K and Na clays in the upper portion of the well. At greater depths Ca and Mg are less abundant due in part to rock type and also because they may be held in chlorite and Ca-zeolites or calcite.

The apparent disequilibrium in the deeper portions of DF 45-14 may be due in part to mixing of downward moving meteoric water via faults and fractures with upward migrating thermal water that has been heated at depth. The amount and depth of fluid mixing is unknown but the process may be very important in influencing the physical and chemical conditions at depth. The deposition of quartz veins must occur from solutions moving upward from presumably hotter areas where silica is dissolving. This does not appear to be taking place in the SiO_2-saturated DV-90 water nor in the waters from DF 66-21. Also, more acidic, CO_2-charged waters may be rising from deeper in the system along fractures and faults affecting kaolinite alteration and depositing calcite as CO_2 is lost.

In considering the alteration effects by equilibrium activity plots it should be clear that this is not the whole picture. It is important to realize that only selected components have been considered, hence only selected phases. We have considered in part the 7-component system MgO-CaO-K_2O-Na_2O-Al_2O_3-SiO_2-CO_2-H_2O. This implies that for a given temperature and pressure seven stable phases should exist.

Muffler and White (1969) report for the Salton Sea Geothermal field the above components produce seven phases: quartz, albite, potassium feldspar, chlorite, K-mica, epidote and calcite. This approach, however, ignores other important components such as iron and sulfur. Iron is particularly important in Dixie Valley where biotite and/or vermiculite is encountered in much of the altered metasediments. The x-ray diffraction data indicate that the majority of the chlorites are iron-rich varieties. Additionally, the presence of abundant ilmenite ($FeTiO_3$) and its alteration product leucoxene have been established by x-ray fluorescence and optical data, respectively.

The relationship between the alteration mineralogy and water chemistry in DF 66-21 is likewise complex and, in some cases, obscure. The diversity and structural complexity of the rock units, in conjunction with the physical and chemical variations of the geothermal fluids, are the dominating factors contributing to this complexity. Two water samples, DV-93 and DV-80, are used to represent the chemical conditions at a depth of about 4700 feet in DF 66-21. The casing in DF 66-21 extends to a depth of 7300 feet. Tables 4-5 and 4-6 list the chemical analyses for DV-93 and DV-80, respectively. The analytical data for samples DV-93 and DV-80 were calculated at a pH of 8.0 rather than the recently acquired pH of 5.8.

For samples DV-93 and DV-80 the activity diagrams (Figures 4-20 through 4-24) depicting mineral equilibria at 150°C and to a lesser extent 200°C are believed to be most nearly representative of the conditions existing in DF 66-21 (170°C, pH = 5.8) The diagrams indicate an equilibrium assemblage of quartz, calcite, montmorillonite, illite, kaolinite, and albite. This essentially is what is observed in DF 66-21 in the upper 5000 feet where the water samples are applicable. Thus, excluding the abundance of kaolinite in localized zones, the above mineral assemblage appears to be in approximate equilibrium with the present physical and chemical conditions in DF 66-21. As described above for DF 45-14, it is possible that the pH in DF 66-21 is lower than the measured field pH (5.8) due to temperature effects, CO_2 loss upon boiling and fluid mixing. The decrease in pH results in a progressively more clay dominated mineral assemblage (Figures 4-21 through 4-24). The diagrams also indicate that the acidity required for kaolinite stability becomes less at lowere temperatures.

Abundant kaolinite in the interval 4300 to 5300 feet corresponds to a zone of highly fractured volcanic rocks where large quantities of hot water (100°C to 150°C) under high pressure (320 psi) were encountered during drilling. This phenomenon may indicate communication at depth with more acidic waters. This interval from 4300 to 5300 feet, as well as 6300 to 6700 feet, and a broad zone, from 7500 to 9500 feet are also marked by increased calcite abundance (Plate VI). These intervals are interpreted as representing fault zones where boiling is occurring. Water which was originally close to saturation with calcite rapidly becomes supersaturated following boiling, loss of carbon dioxide and rising pH. The changes in chemistry which occur when steam boils from high-temperature water can be summarized in the following equations (Ellis and Mahon, 1977):

$$CO_2(aq) = CO_2\ (vap)$$
$$HCO_3^- + H^+ = CO_2\ (aq) + H_2O$$
$$Ca^{2+} + 2HCO_3^- = CaCO_3 + CO_2\ (aq)$$

Samples DV-93 and DV-80 also reveal relatively high concentrations of boric and silicic acid (Tables 4-5 and 4-6). During the later stages of CO_2 loss, the following reactions may be occurring:

$$HCO_3^- + H_3BO_3 = H_2BO_3^- + CO_2(aq) + H_2O$$
$$HCO_3^- + H_4SiO_4 = H_3SiO_4^- + Co_2(aq) + H_2O$$

Bicarbonate ions are destroyed and the degree of supersaturation with calcite may be reduced possibly to the extent that the water becomes undersaturated again. The end effect of boiling and gas evolution is for the water to cool and for its pH to rise. The water is then no longer in equilibrium with the mineral assemblage with which it was in contact. This process would explain the localization of kaolinite near fracture zones. The effects produced depend mainly on the fluid flow rates. Calcite veining and fracture filling was much more abundant in DF 66-21 than in DF 45-14.

The distribution of chemical constituents between the reactant minerals and the product minerals listed in Table 4-7 suggests a relative chemical mass balance. This chemical balance is observed in both DF 66-21 and DF 45-14. One exception though is the addition of $CO_3^=$. The source of the carbon dioxide to bring about the $CO_3^=$ for calcite is

Table 4-7. Reactant and Product Minerals

Reactant Mineral	Chemical Formula
Biotite	$K_2(Mg,Fe)_2(AlSi_3O_{10})(OH)_2$
Hornblende	$Ca_2(Mg,Fe,Al)_5(Si,Al)_8O_{22}(OH)_2$
Epidote	$Ca_2(Al,Fe)_3(SiO_4)_3OH$
Muscovite	$KAl_2(AlSi_3O_{10})(OH)_2$
Augite	$Ca(Mg,Fe)(Si,Al)_2O_6$
Plagioclase	$NaAlSi_3O_8$ -- $CaAl_2Si_2O_8$
Pyrite	FeS_2
Magnetite	Fe_3O_4

Product Mineral	Chemical Formula
Biotite	$K_2(Mg,Fe)_2(AlSi_3O_{10})(OH)_2$
Hornblende	$Ca_2(Mg,Fe,Al)_5(Si,Al)_8O_{22}(OH)_2$
Epidote	$Ca_2(Al,Fe)_3(SiO_4)(OH)$
K-Mica	$KAl_2(AlSi_3(O,OH)_{10})(OH)_2$
Chlorite	$(Fe,Al)_6(Si,Al)_4O_{10}(OH)_8$
Magnetite	Fe_3O_4
Vermiculite	$(Ca,Mg)(Mg,Fe,Al)_6(Al,Si)_8O_{22}(OH)_4 \cdot 8H_2O$
Kaolinite	$Al_4(Si_4O_{10})(OH)_8$
Limonite/Hematite	$FeO(OH)/Fe_2O_3$
Montmorillonite	$(Na,Ca,Mg)O \cdot Al_2O_3 \cdot 5SiO_2 \cdot nH_2O$

uncertain; however, four possibilities can be considered. The first is that the carbon dioxide is derived from the organic matter identified in thin sections of the Triassic metasiltstone/metashale. The second possibility is that the CO_2 is derived from magmatic additions. A third possibility is that the CO_2 is derived from carbonate rocks at depth although much more evidence is needed to substantiate their existence. The fourth and most likely source is the release of CO_2 upon boiling and/or degassing. This rough chemical mass balance can be interpreted as representing relatively stagnant flow conditions at depth, meaning that a significant influx of chemical constituents is not necessary to account for the observed alteration mineralogy. It also emphasizes the idea that significant flow of fluids is confined to fracture zones. Thus the mechanics of alteration in the two drillholes consists mainly of the reconstitution of the chemical elements in the original rocks through the processes of solution, deposition and recrystallization according to the various equilibrium constraints.

There is a great deal more to learn and understand about the relationship between the alteration mineralogy and the water chemisty in the Dixie Valley region. However, a more thorough and detailed sampling of the deep wells is needed before this can be accomplished.

4.2.7 Well Correlations

4.2.7.1 Lithologic Correlation

The various lithologic units encountered in each of the two deep exploratory wells are compositionally very similar, differing mainly in the proportion of each unit present. The alluvium in both wells consists predominantly of altered volcanic fragments with lesser amounts of granodioritic to gabbroic igneous rocks. Fragments of the metasediments and quartz arenite are rare in the alluvial materials of both wells. The sequence of silicic to intermediate volcanic rocks in each well is very similar compositionally, texturally and structurally, although the degree of alteration is more intense in DF 66-21. The lithologies and textures of the metasediments in each well are essentially identical, although the association of andalusite/chiastolite porphyroblasts with igneous intrusion in these rocks appears to be lacking in DF 66-21.

A slight compositional variation exists between the intrusive

rocks observed in each well. The intrusions in DF 45-14 consist solely of rocks ranging in composition from diorite to gabbro. The predominant ferromagnesian minerals of these rocks are clinopyroxenes and hornblende. Equivalent intrusive material is encountered in DF 66-21. However, in DF 66-21, the majority of the intrusions are granodioritic to dioritic in composition. These rocks are characterized by biotite, hornblende, and lesser pyroxene as the dominant ferromagnesian minerals. Both compositional varieties contain magnetite and/or ilmenite that may in part be derived from the alteration of the ferromagnesian minerals. The textures of the two types are also similar. These slightly different intrusive rocks may represent two phases in the differentiation of a magma with the more basic intrusions representing earlier phases and the granodiorite/diorite representing the bulk composition. Detailed field relationships and age dates are required to evaluate this hypothesis.

4.3 Conclusions

The various lithologic units encountered in each of the two deep exploratory wells and, to the extent known, the Sun Oil Company well (SW Lamb #1) are compositionally and texturally similar, differing mainly in the proportion of each unit present. Plate VII shows the stratigraphic correlation between DF 45-14, DF 66-21 and SW Lamb #1. Figure 4-25 shows a generalized stratigraphic section of the Dixie Valley region. It can be seen that there is a strong correlation between all three wells in the occurrence of the sequence of volcanic rocks. This volcanic sequence can serve as a common datum plane.

In both DF 66-21 and SW Lamb #1, this volcanic sequence is overlain by an impervious red clay layer. Beneath this clay, both wells produced hot water and steam under high pressures from fractured volcanic rock (and underlying intrusive rock?). The general absence of an impermeable layer of this clay in DF 45-14 may explain the lack of a similar 'production zone'. The absence of this production zone may also be a function of the location of the well beyond the limits of the Humboldt gabbroic complex.

The distribution of the clay layer is very significant as it provides a capping mechanism for the geothermal system. Regardless of the origin, the clay represents a favorable cap rock and its association

GENERALIZED STRATIGRAPHIC SECTION OF DIXIE VALLEY

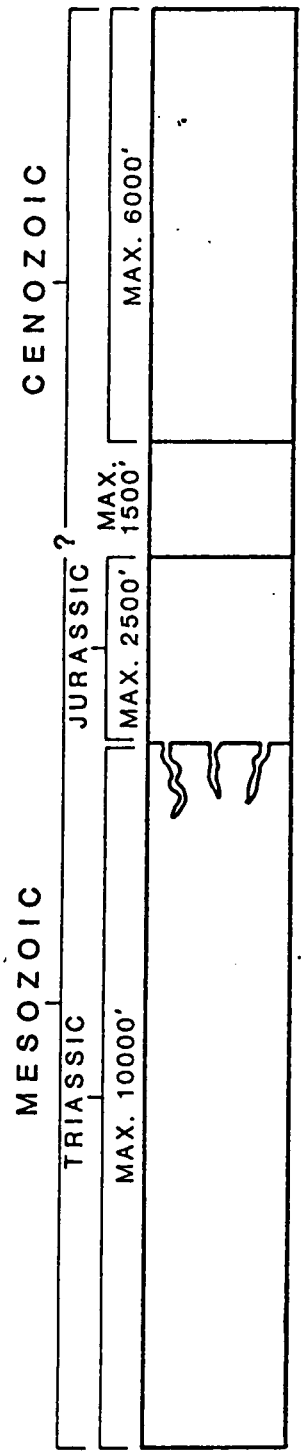

Tertiary & Quaternary Alluvial Deposits:

Consist of older gravels, older alluvium, pediment gravels, basalt and andesite flows and tuffs, younger alluvium, lacustrine and fluviatile deposits.

Tertiary(?) Volcanic Deposits: (may include Mesozoic volcanic rocks)

Include volcanic rocks of rhyolitic to basaltic composition as flows, tuffs and intercalated sediments and shallow intrusive rocks.

Jurassic Gabbroic Complex:

Consists mainly of a hornblende gabbro with highly differentiated facies near the periphery ranging to granodiorite. Intrudes comagmatic volcanic rocks, quartz arenite and Triassic metasediments.

Triassic Metasediments:

Predominantly hornfels, and schist (metasiltstone/metashale). Also includes metarenite and quartz arenite. Locally intruded by granodiorite to gabbroic rocks.

Figure 4-25

with the volcanic sequence overlying the Humboldt gabbroic complex may represent the key to exploiting the geothermal resource in Dixie Valley. The observations in the three wells support this hypothesis.

The absence of a sizeable intrusive body in DF 45-14 (Humboldt gabbroic complex) is significant for two reasons: first, if the boundary of the Humboldt gabbro represents the boundary of the 'producing' portion of the reservoir, this would indicate that DF 45-14 is located at the periphery of the unit. The distribution and stratigraphic relationships of the gabbroic complex in the three wells indicates that it pinches out toward the south. The gabbro however is too impermeable to act as a reservoir and so communication with the reservoir at depth is via fractures. Conductive heating in this body of rock may be an important factor. Another significant observation is that there are extensive exposures of the Humboldt gabbroic complex in the Stillwater Range in the immediate vicinity of DF 45-14 (Willden and Speed, 1974) yet very little was encountered in the well. Additionally, the nearest major outcrop of the Triassic metasediments is located about 10-12 miles to the south. This evidence suggests that post-Jurassic left-lateral displacement (up to 12 miles) has occurred in Dixie Valley along the White Rock Canyon fault (Bob Whitney, pers. commun., 1979).

Willden and Speed (1974) report that the only rocks intruded by the gabbro are quartz arenite and comagmatic basic volcanic rocks. However, minor gabbroic intrusions in the Triassic metasiltstone/metashale may be related to the complex. Willden and Speed (1974) also state that the quartz arenite forms a sort of ring surrounding the gabbro. This idea may be used in drilling to determine the relative position of the well in relation to the gabbroic complex.

The role of the Triassic metasedimentary sequence in the reservoir model is uncertain although it most likely functions as a cap rock as it is relatively impermeable. This unit is known to be fractured at depth but the extent of this fracturing is unknown. It is also known that these fractures are capable of conducting thermal fluids which may originate largely at depth. Willden and Speed (1974) postulated that Triassic carbonate rocks exist at depth below the Humboldt gabbroic complex. These carbonate rocks could conceivably serve as a reservoir for convecting thermal fluids. They could also supply the necessary CO_2 and CO_3 for the abundant calcite precipitation that was observed in DF 66-21.

The heat source for the geothermal system in Dixie Valley is elusive; although one surely exists. A couple of options are possible. The first is that heat is derived from the upper mantle which is relatively close to the surface in this region. The heat source may also be related to the gabbro which may conduct heat upwards from great depths. A shallow molten heat source is unlikely.

The vast discrepancy in the amount of alluvial material in DF 45-14 and DF 66-21 (1100 feet vs. 4100 feet) together with the distribution of alteration effects associated with areas of increased porosity and permeability provides evidence that DF 66-21 has been downdropped by at least one increment of normal faulting. Some of the difference may be due to its increased distance from the range front. Plate IV shows the location of the wells in relation to the structural-tectonic features. Surface expression of the faulting described above is to the west of DF 66-21. Assuming a 50 to 60 degree dip on these normal faults, they intersect the wells at depths of 4700 to 4800 feet and at about 6500 feet. These depths also correspond to zones of increased alteration indicating rocks with higher porosity and permeability. It is apparent that faulting has played a major role in influencing the distribution not only of rock types but also the hydrothermal alteration effects.

4.4 References

Ballantyne, G.H., 1978, Hydrothermal alteration at the Roosevelt Hot Springs thermal area, Utah: Chraacterization of rock types and alteration in Getty Oil Company well Utah State 52-21: Report prepared for U. S. Department of Energy, IDO/78-1701.a.1.1.4, 24 p.

Brown, G., and MacEwan, D.M.C., 1950, The interpretation of x-ray diagrams of soil clays: Jour. Soil Sci., v. 1, p. 239-253.

Browne, P.R.L., and Ellis, A.J., 1970, The Ohaki-Broadlands hydrothermal area, New Zealand: Mineralogy and related geochemistry: Am. Jour. Sci., v. 209, p. 97-131.

Coats, R., 1940, Propylitization and related types of alteration on the Comstock Lode: Econ. Geol., v. 35, no. 1, p. 1-16.

Deer, W.A., Howie, R.A., and Zussman, J., 1966, Introduction to the rock forming minerals: Longman Press, London, 528 p.

Ellis, A.J., and Mahon, W.A.H., 1977, Chemistry and geothermal systems: Academic Press, New York, 392 p.

Eskola, P., 1915, On the relation between chemical and mineralogical composition in the metamorphic rocks of the Orijarvi region: Bull. Comm. Geol., Finalande 44, p. 109-145.

Folk, R.L., 1974, Petrology of sedimentary rocks: Hemphill Pub. Co., Austin, 182 p.

Grim, R.E., 1968, Clay mineralogy: McGraw-Hill, 596 p.

Grindley, G.W., 1965, Geology, structure, and exploration of Wairakei Geothermal Field, Taupo, New Zealand: Bull. Geol. Survey, New Zealand, no. 75.

Hoagland, J.R., 1976, Petrology and geochemistry of hydrothermal alteration in borehole Mesa 6-2, East Mesa Geothermal Area, Imperial Valley, California: M.S. thesis, Univ. California-Riverside, 90 p.

Helgeson, H.C., Brown, T.H., and Leeper, R.H., 1969, Handbook of theoretical activity deagrams depicting chemical equilibrium in geologic systems involving an aqueous phase at one atmosphere and 0 to 300°C: Freeman, Cooper and Company, San Francisco, 253 p.

Johnson, M.G., 1977, Geology and mineral deposits of Pershing County, Nevada: Nevada Bur. Mines Geol. Bull. 89, 115 p.

Kingston, R., ed., 1979, The Tonogan Geothermal Field, Leyte, Philippines: Consultant report prepared by Kingston, Reynolds, Thom and Allondice Ltd.

Krauskopf, B., 1967, Introduction to geochemistry: McGraw-Hill, 721 p.

Lovering, T.S., 1950, The geochemistry of argillic and related types of rock alteration: Colorado School Mines Quart., v. 45, p. 231-260.

Muffler, L.P., and White, D.E., 1969, Active metamorphism of upper Cenozoic sediments in Salton Sea Geothermal Field and Salton Trough, southern California: Geol. Soc. America Bull., v. 80, p. 157.

Page, B.M., 1965, Preliminary geologic map of a part of the Stillwater Range, Churchill County, Nevada: Nevada Bur. Mines Map 28.

Schoen, R., and White, D.E., 1962, Hydrothermal alteration in GS-3 and GS-4 drill holes, Main Terrace, Steamboat Springs, Nevada: Econ. Geol., v. 60, p. 1411-1421.

Sigvaldason, G., and White, D.E., 1962, Hydrothermal alteration drill holes GS-5 and GS-7, Steamboat Springs, Nevada: U.S. Geol. Survey Prof. Paper 450-D, p. 113-117.

Speed, R.C., 1976, Geologic map of the Humboldt Lopolith and surrounding terrane, Nevada: Geol. Soc. America Map MC-14.

Spry, A., 1976, Metamorphic textures: Pergamon Press, 350 p.

Steiner, A., 1968, Clay minerals in hydrothermally altered rocks at Wairakei, New Zealand, in Clays and Clay Minerals, v. 16, p. 193-213.

Sumi, K., and Maeda, K., 1968, Hydrothermal alteration of main productive formulation of steam for power at Matsukawa, Japan, in Proc. of Symposium on Hydrogeochemistry and Biochemistry, v. I, p. 211-228.

Tomasson, J., and Kristmannsdottir, H., 1972, High temperature alteration and thermal brines, Reykjanes, Iceland, in Contri. Mineral. and Petrol., v. 36, p. 123-124.

Truesdell, A.H., and Jones, B.F., 1974, WATEQ, a computer program for calculation of chemical equilibrium in natural waters: U.S. Geol. Survey, Jour. 2, no. 2, p. 231.

Turner, F.J., and Verhoogen, J., 1960, Igneous and metamorphic petrology: McGraw-Hill, 694 p.

Weaver, C.E., 1956, The distribution identification of mixed-layer clays in the sedimentary rocks: Am. Min., v. 41, p. 202-221.

White, D.E., 1957, Thermal waters of volcanic origin: Geol. Soc. America Bull., v. 68, p. 1637-1658.

Willden, R., and Speed, R.C., 1974, Geology and mineral deposits of Churchill County, Nevada: Nevada Bur. Mines Geol., Bull. 83.

Winkler, H.G.F., 1974, Petrogenesis of metamorphic rocks: Springer-Verlag, New York, 334 p.

Chapter 5. HYDROLOGY AND HYDROGEOCHEMISTRY

By: Burkhard W. Bohm, Roger L. Jacobson, Michael E. Campana, and Neil L. Ingraham

5.0 HYDROLOGY AND HYDROGEOCHEMISTRY

5.1 Introduction

5.1.1 Purpose and Scope

The purpose of this portion of the study is to provide hydrologic and hydrogeochemical input to the construction of the Dixie Valley geothermal model. Since some of the most important aspects of hydrothermal reservoir assessment are the fluid characteristics and flow parameters, the hydrology and hydrogeochemistry of a particular reservoir must be considered in the formulation of any hydrothermal reservoir model, even a conceptual or qualitative one. Our primary efforts were devoted to extensive isotopic and hydrochemical sampling and interpretation of these data as direct and indirect indicators of the nature of the reservoir. Most of the work focused on the area of greatest interest to Southland Royalty Company, the northern half of Dixie Valley (between Dixie Meadows and Sou Hot Springs). The study also involved sampling outside this particular region.

The major tasks of the hydrologic-hydrogeochemical study are as follows:

(1) Review the available hydrologic and hydrogeochemical data.
(2) Obtain water samples from selected wells, hot springs and cold springs.
(3) Analyze water samples for major, minor and selected trace chemical constituents and environmental isotopes.
(4) Collect temperature and other data from selected wells and springs.
(5) Estimate recharge rates and source areas and groundwater flow rates.
(6) Estimate reservoir geometry.
(7) Provide estimates of reservoir water chemistry and, using geothermometry, reservoir temperatures.
(8) Provide hydrologic and hydrogeochemical input to the formulation of a conceptual model of the Dixie Valley hydrothermal system.

The interpretation of the environmental isotope data was intended to supplement the hydrogeochemical data and provide additional

hydrologic information, particularly with respect to recharge to the reservoir. However, the complete suite of isotope data has not yet been received. The interpretations and conclusions presented herein have been made without the benefit of any isotope data, and are based almost solely upon the hydrogeochemistry. This is not an ideal approach, but was dictated by circumstance. Therefore, this chapter is incomplete since it is devoted primarily to the hydrogeochemistry of the study area with little discussion of the hydrology. An addendum to this chapter will be written as soon as the isotope data have been received, interpreted and integrated with the rest of the information.

5.1.2 Methods and Analytical Techniques

Approximately 100 samples of the thermal and non-thermal waters were collected. The collection generally involved filtration through a 0.45 μm filter for a gross sample and an acidified sample. Nitric acid was added to lower the pH to approximately 2. Samples were collected for silica using a 1:10 field dilution of the thermal waters with distilled water. Isotope samples were collected by completely filling a 125 ml glass bottle and sealing the bottle with Parafilm and electrical tape.

Field measurements were made of temperature, electrical conductivity (EC), pH and dissolved oxygen (DO). Laboratory determinations were made for Ca, Mg, Na, K, HCO_3, Cl, SO_4, NO_3, SiO_2, F, B, Li, As, Cs, Al, Hg, Fe, Mn, Sr and Ba in the Water Resources Center Laboratories.

^3H analyses (both enriched and unenriched) were performed in Water Resources Center Laboratories. ^{18}O and ^2H samples were sent to the Laboratory of Isotope Geochemistry at the University of Arizona for analysis.

5.1.3 Previous Work

Very little previous work on the hydrology and hydrogeochemistry of Dixie Valley exists. A paper by Zones (1957) describes some of the hydrologic effects of the 1954 Dixie Valley earthquake. A reconnaissance study by Cohen and Everett (1963) gives an overview of the groundwater hydrology of Dixie and Fairview Valleys. This report also

includes a brief description of the groundwater chemistry of the Dixie-Fairview area. A total of 13 water chemistry samples were collected in an area of 2360 square miles, a very low sampling density. The data presented in this report were insufficient to draw any substantive conclusions concerning the groundwater system in Dixie Valley. Additional work of a limited nature in the valley was conducted by Keplinger and Associates (1977 and 1978) and by GeothermEx, Inc. (1976).

5.2 Analytical Results

5.2.1 Chemical Characteristics of Dixie Valley Waters

Table 5-1 shows the chemical analyses of all the samples collected during the study. Variations in gross chemical properties of Dixie Valley groundwater and surface water are evident on a trilinear diagram (Figure 5-1). Percentages of equivalents were plotted for major anions and cations (Cl, SO_4, HCO_3 and CO_3, Ca, Mg and Na + K). The three hot spring systems of the valley plot as separate groups. Dixie Hot Springs (D) show significant variation, but generally they are sulfate-chloride-potassium-sodium waters. Hyder Hot Springs (H) show little variation, and are bicarbonate-potassium-sodium type waters. Sou Hot Springs (S) is an intermediate type, having roughly similar equivalent percentages of the major ions. The hot springs of McCoy Ranch (M), Lower Ranch and southern Jersey Valley seem to be related to Hyder Hot Springs. Buckbrush Seeps (B) also seem to be closely related to Hyder, perhaps due to structural relationships. However, Buckbrush Seeps might be affected by evaporation. Surface runoff from the Stillwater Range, irrigation wells from the northern part of the valley and waters from the eastern ranges (Clan Alpine and Augusta Mountains) show wide variations. There is, however, a rough grouping of the water quality samples according to their areal distribution in the valley. For example, the samples from the deep wells (DF 45-14 and DF 66-21) and well SR2-A seem to be related to Dixie Hot Springs. It should be noted that samples from DF 45-14 and DF 66-21 may not be representative of the geothermal reservoir fluids because of contamination from drilling fluids and additives and/or shallow groundwater.

Table 5-1. Chemical Analyses of Dixie Valley Waters.

The letter or number in the first column identifies the group sample according to the following code:

A - Artesian wells in the vicinity of Dixie Settlement.
B - Buckbrush Seeps.
C - Carson Sink (western slopes of the Stillwater Range).
D - Dixie Hot Springs.
E - Spring or stream from the eastern mountain ranges (Clan Alpine and Augusta Mountains).
H - Hyder Hot Springs.
I - Irrigation wells in the northern part of Dixie Valley.
L - Wells in the vicinity of Dixie Settlement.
M - Intermediate temperature springs around McCoy Ranch.
S - Sou Hot Springs.
W - Spring or stream from the Stillwater Range.
1 - DF 45-14 (probably contaminated).
2 - DF 66-21 (probably contaminated).
3 - DF 45-14.
4 - DF 66-21 (probably contaminated).

Table 5-1. Chemical Analyses of Dixie Valley Waters.

		DATE	TEMP	PH	CA	MG	NA	K	CL	SO4	HCO3	SIO2	CO3	TDS
W	LL097	90878	15.00	8.00	105.600	43.300	133.000	.320	168.000	297.000	247.000	28.500	-0	1022.810
W	LL109	92878	16.00	6.90	270.400	31.300	211.000	4.000	203.000	682.000	308.000	33.400	-0	1743.190
W	DV21	32079	13.00	7.40	46.500	26.600	464.000	3.850	605.000	207.000	194.000	26.000	-0	1575.667
W	DV22	32079	11.00	8.50	56.000	32.000	116.500	3.000	12.600	92.400	302.000	19.800	-0	636.145
W	DV031	51579	17.00	8.35	82.500	33.500	108.000	2.600	126.000	218.000	225.000	20.000	-0	815.990
W	DV032	51579	26.00	8.77	54.500	52.500	176.000	10.700	258.000	178.000	251.000	31.800	-0	1012.820
W	DV045	51579	14.00	7.69	68.000	35.000	100.000	2.800	115.000	97.000	306.000	14.500	-0	738.600
W	DV046	51579	15.75	8.35	44.500	21.500	70.000	1.600	68.000	41.000	278.000	18.500	-0	543.390
W	DV047	51579	18.00	8.50	42.000	24.000	80.000	1.700	83.000	52.000	267.000	18.000	-0	567.700
W	DV048	51579	13.50	7.78	54.500	30.500	78.000	1.900	83.000	66.000	319.000	16.500	-0	649.400
W	DV049	51579	15.75	8.21	48.000	37.000	123.000	3.000	126.000	112.000	306.000	20.200	-0	775.200
W	DV050	51579	16.00	8.45	39.500	26.000	94.000	1.800	96.000	65.000	262.000	18.500	-0	603.110
W	DV051	51579	17.00	8.17	41.500	32.500	114.000	2.600	118.000	88.500	289.500	20.000	-0	706.940
W	DV052	51579	17.00	8.54	53.000	24.000	165.000	3.000	194.000	161.000	205.000	23.000	-0	828.490
W	DV053	62579	18.00	7.20	175.000	78.000	118.000	2.600	150.000	518.000	360.000	17.500	-0	1421.474
W	DV055	62579	15.00	7.86	66.000	34.500	120.000	3.800	140.000	105.000	346.000	19.500	-0	835.180
W	DV56	62579	15.00	7.66	65.000	37.800	117.000	3.500	130.000	114.000	379.000	20.000	-0	866.680
W	DV057	62579	15.00	8.45	44.000	40.000	138.000	3.300	149.000	122.000	316.000	20.000	-0	832.670
W	DV058	62579	15.00	8.60	41.500	27.800	105.000	2.100	109.000	86.000	279.000	18.000	-0	668.720
W	DV059	62579	28.00	8.70	38.000	31.300	123.000	2.600	127.000	104.000	215.000	19.500	20.000	681.090
W	DV067	62579	16.00	7.33	262.000	33.300	215.000	3.500	218.000	710.000	299.000	26.300	-0	1768.430
W	DV078	72379	22.00	7.40	95.700	16.900	187.000	2.700	227.000	171.000	327.000	26.000	-0	1056.785
W	DV092	091279	43.	8.48	32.000	65.000	197.000	7.500	255.000	168.000	282.000	32.500	17.100	1058.295
W	DV102	62579	14.00	7.71	104.000	36.000	138.000	1.600	226.000	126.000	348.000	46.500	-0	1026.430
W	DV103	62579	14.00	7.79	62.500	26.500	82.500	2.100	125.000	83.000	234.000	32.500	-0	648.320
W	DV104	62579	13.00	8.13	74.000	31.000	112.000	2.400	155.000	94.000	310.000	35.000	-0	813.710
W	DV105	62579	28.00	8.57	39.500	22.000	102.000	4.900	144.000	84.000	135.000	37.500	12.300	581.460
W	DV106	62579	26.80	8.32	42.000	26.500	118.000	3.300	148.000	88.000	207.000	35.000	3.900	672.000
W	DV107	62579	15.50	7.55	65.000	36.500	130.000	3.000	171.000	117.000	294.000	32.000	-0	848.860
W	DV108	62579	16.50	7.62	70.500	39.800	140.000	3.200	185.000	125.000	320.000	32.500	-0	916.400
W	DV109	62579	22.50	8.35	65.000	46.500	182.000	9.200	245.000	180.000	267.000	30.800	6.700	1032.820
W	DV110	62579	15.50	7.87	60.000	34.500	68.000	2.900	126.000	122.000	173.000	17.500	-0	604.430
W	DV111	62579	14.00	7.79	100.000	41.300	97.500	3.100	162.000	278.000	184.000	21.300	-0	888.570
C	CS01	72379	15.00	7.93	60.200	33.200	108.000	3.010	161.000	120.000	218.000	21.000	-0	724.410
C	CS02	72379	16.00	7.60	59.900	34.900	110.000	2.540	145.000	118.000	266.000	16.000	-0	752.340
C	CS04	72379	16.00	7.58	97.600	35.100	48.000	3.560	188.000	115.000	134.000	43.000	-0	664.460
C	CS06	72379	21.00	7.63	483.000	36.500	108.000	2.440	136.000	1134.000	278.000	32.000	-0	2218.485
C	CS07	72379	22.00	7.93	267.000	32.300	266.000	6.550	375.000	15.100	199.000	29.000	-0	1197.317
C	CS08	72379	24.00	8.73	135.000	31.800	266.000	1.880	318.000	342.000	318.000	29.000	-0	1445.505
B	DV041	51579	28.00	9.59	13.700	2.100	1150.000	16.900	360.000	450.000	1194.000	42.000	433.000	3661.700
B	DV042	51579	15.00	9.87	1.000	.600	352.000	3.200	120.000	112.000	321.000	61.000	132.000	1102.800
E	LL102	92878	10.00	7.60	14.200	2.300	18.000	1.000	10.500	12.000	69.700	25.600	-0	154.010
E	DV03	32079	11.00	7.70	37.500	4.500	154.000	8.600	134.000	98.800	194.000	35.000	-0	667.000
E	DV10	32079	15.00	7.33	165.000	66.000	55.500	2.200	64.000	472.000	277.000	15.300	-0	1121.805
E	DV12	32079	11.00	7.27	54.500	14.000	37.000	1.400	26.000	64.000	214.000	23.500	-0	435.755
E	DV060	62579	9.00	7.85	14.500	2.720	21.000	1.500	14.500	17.200	68.900	27.500	-0	168.180
E	DV061	62579	10.00	8.33	42.300	7.600	43.500	1.200	28.000	73.600	145.000	22.500	-0	363.990
E	DV062	62579	23.00	7.92	34.000	7.100	41.600	1.700	25.000	59.000	135.000	26.300	-0	330.000
E	DV063	62579	18.00	7.40	19.000	6.700	25.000	2.900	21.000	21.200	101.000	35.500	-0	232.905
E	DV091	091279	32.	8.58	3.700	.060	105.000	1.000	41.000	70.000	126.800	35.000	9.800	395.960
L	LL103	92878	19.00	7.70	20.900	2.070	62.800	3.900	25.800	78.800	99.000	64.000	-0	358.780
L	LL104	92878	16.00	7.90	28.300	2.200	56.000	4.300	25.000	78.000	111.000	64.800	-0	370.840

Table 5-1. Chemical Analyses of Dixie Valley Waters. (cont'd.)

		DATE	TEMP	PH	CA	MG	NA	K	CL	SO4	HCO3	SIO2	CO3	TDS
M	DV05	32079	39.00	7.10	39.000	13.700	144.000	12.000	27.000	65.600	454.000	39.000	-0	799.385
M	DV06	32079	29.00	6.95	68.000	19.100	164.000	12.300	28.000	124.000	554.000	44.000	-0	1019.315
M	DV11	32079	43.00	6.90	95.000	37.500	213.000	10.300	275.000	209.000	310.000	36.800	.100	1191.515
M	DV115	62579	50.00	7.31	94.000	36.500	218.000	10.000	286.000	216.000	312.000	32.500	-0	1206.370
M	DV116	62579	40.00	6.89	67.000	18.500	240.000	23.800	39.000	88.000	803.000	26.300	-0	1312.200
1	DV069	070979	68.5	9.5	20.500	.050	685.000	65.000	815.000	512.000	32.400	6.500	18.700	2163.205
1	DV70	070979	75.5	8.9	12.500	.010	605.000	53.000	740.000	352.000	5.100	31.000	52.200	1870.145
1	DV72	070979	76.5	9.1	22.500	.010	618.000	65.000	700.000	352.000	6.100	300.000	117.000	2201.726
2	DV080	81479	114.0	8.00	35.750	3.550	1288.000	31.000	1208.000	130.000	1410.000	-0	-0	4118.590
2	DV081	81479	51.00	-0	42.500	4.300	1238.000	27.000	-0	-0	-0	210.000	-0	1523.070
2	DV082	81479	86.00	7.90	27.000	3.900	1275.000	30.000	1150.000	127.500	1391.000	232.000	-0	4248.290
3	DV090	091279	94.	6.8	24.100	.015	410.000	40.000	493.000	215.000	130.500	325.000	-0	1657.545
4	DV093	091379	83.	8.	24.000	4.030	1730.000	44.000	1720.000	396.000	1283.000	189.000	-0	5410.600
4	DV094	091379	95.	8.5	23.600	9.900	2010.000	37.000	2315.000	280.000	1197.000	160.000	-0	6041.300
T	DV15	042679	71.	7.63	156.000	30.000	400.000	30.000	535.000	448.000	200.000	98.000	-0	1905.930
T	DV16		71.	7.42	145.000	28.800	398.000	18.000	550.000	445.000	203.000	100.000	-0	1898.660
T	DV030	51579	64.50	6.89	145.000	26.000	405.000	18.600	575.000	410.000	211.000	105.000	-0	1909.045

Table 5-1. Chemical Analyses of Dixie Valley Waters. (cont'd.)

		F	B	AL	FE	MN	LI	SR	NO3	AS	HG	CS
L	LL105	-0	-0	-0	-0	-0	-0	-0	1.200	-0	-0	-0
L	LL107	8.600	-0	-0	-0	-0	-0	-0	.310	-0	-0	-0
L	LL108	.750	-0	-0	-0	-0	-0	-0	4.380	-0	-0	-0
L	LL110	-0	-0	-0	-0	-0	-0	-0	2.260	-0	-0	-0
L	LL111	-0	-0	-0	-0	-0	-0	-0	.090	-0	-0	-0
A	LL106	-0	-0	-0	-0	-0	-0	-0	.220	-0	-0	-0
A	DV13	6.000	.310	.100	.010	.015	.050	.110	-0	-0	-0	-0
A	DV043	6.400	.320	.100	.010	.005	.052	.130	-0	-0	-0	-0
A	DV065	6.500	-0	-0	-0	-0	-0	-0	0	-0	-0	-0
A	DV066	5.800	-0	-0	-0	-0	-0	-0	0	-0	-0	-0
I	DV034	.490	1.000	.100	.020	.017	.260	1.730	-0	.010	-0	-0
I	DV037	.700	1.100	.100	.040	.021	.420	2.800	-0	.010	.006	.050
I	DV038	1.000	1.300	.100	.010	.008	.357	1.670	-0	-0	-0	-0
I	DV039	1.300	1.000	.100	.010	.005	.259	1.280	-0	-0	-0	-0
I	DV040	.800	.900	.100	.010	.016	.350	2.400	-0	.010	-0	.050
I	DV100	1.150	-0	-0	-0	-0	-0	-0	0	-0	-0	-0
I	DV101	.900	-0	-0	-0	-0	-0	-0	0	-0	-0	-0
I	DV113	.740	-0	-0	-0	-0	-0	-0	0	-0	-0	-0
I	DV114	.450	-0	-0	-0	-0	-0	-0	0	-0	-0	-0
P	DV20	.330	-0	-0	-0	-0	-0	-0	-0	-0	-0	.050
D	LL098	-0	-0	-0	-0	-0	-0	-0	1.150	-0	-0	-0
D	LL099	8.400	-0	-0	-0	-0	-0	-0	.090	-0	-0	-0
D	LL100	-0	-0	-0	-0	-0	-0	-0	.090	-0	-0	-0
D	LL101	-0	-0	-0	-0	-0	-0	-0	.400	-0	-0	-0
D	DV23	12.600	.860	.100	.030	.015	.380	.020	-0	.010	.000	.100
D	DV24	7.700	.900	.100	.010	.012	.550	4.350	-0	.010	.000	.170
D	DV054	13.000	.980	.100	.010	.005	.382	.020	0	.010	.000	-0
D	DH16	5.300	1.600	.100	.010	.005	.315	.380	0	.010	.000	-0
D	DH15	12.500	1.000	.100	.010	.005	.425	.030	0	.010	.000	-0
D	DH09	9.700	1.700	.100	.010	.008	.580	.950	0	.010	.000	-0
D	DH06	11.200	1.800	.100	.010	.005	.470	.050	0	.010	.000	-0
D	DH08	-0	-0	-0	-0	-0	-0	-0	0	-0	-0	-0
D	DH10	-0	-0	-0	-0	-0	-0	-0	0	-0	-0	-0
H	DV04	7.600	4.000	.100	.020	.022	1.600	1.200	-0	.030	.000	.280
H	DV033	7.500	4.200	.100	.040	.007	1.680	1.260	-0	.030	.000	.260
H	HHS01	8.100	4.900	.100	.020	.028	1.590	1.070	0	.020	.005	-0
H	HHS03	8.200	6.100	.100	.070	.033	1.610	1.150	0	.010	.003	-0
H	HHS05	8.100	5.000	.100	.010	.040	1.590	1.090	0	.010	.004	-0
H	HHS06	-0	-0	-0	-0	-0	-0	-0	0	-0	-0	-0
H	HHS12	8.200	4.900	.100	.010	.026	1.560	1.100	0	.010	.000	-0
H	HHS09	8.200	5.100	.100	.010	.021	1.630	1.060	0	.020	.000	-0
S	DV01	5.100	1.360	.100	.010	.054	.650	10.800	-0	.010	.000	.120
S	DV02	5.000	1.370	.100	.050	.045	.650	11.100	-0	-0	-0	-0
S	DV035	5.100	1.200	.100	.040	.009	.710	6.200	-0	.010	.000	.110
S	DV036	4.900	1.300	.100	.410	.006	.680	10.500	-0	-0	-0	-0
S	DV075	5.300	2.000	.100	.380	.063	.670	11.400	0	.010	.000	-0
S	DV076	-0	-0	-0	-0	-0	-0	-0	0	-0	-0	-0
S	DV077	-0	-0	-0	-0	-0	-0	-0	0	-0	-0	-0
S	DV112	4.900	-0	-0	-0	-0	-0	-0	0	-0	-0	-0

Table 5-1. Chemical Analyses of Dixie Valley Waters (cont'd)

		DATE	TEMP	PH	CA	MG	NA	K	CL	SO4	HCO3	SIO2	CO3	TDS
L	LL105	92878	20.00	8.20	13.100	.300	65.000	2.900	19.500	60.000	106.000	73.900	-0	341.900
L	LL107	92878	17.00	8.40	7.000	.200	67.000	1.900	17.500	50.200	80.500	70.800	7.100	311.110
L	LL108	92878	16.00	7.60	37.800	3.720	43.000	4.300	29.500	55.000	124.000	62.400	-0	364.850
L	LL110	92878	24.00	7.20	18.300	2.060	69.000	3.200	26.000	88.000	93.000	58.900	-0	360.720
L	LL111	92878	14.00	7.20	45.800	7.300	38.800	1.300	32.800	38.700	180.000	28.600	-0	373.390
A	LL106	92878	19.00	8.10	22.500	1.130	65.700	4.800	23.500	80.000	111.000	74.300	-0	383.150
A	DV13	32079	19.00	8.30	18.800	.950	68.000	4.500	23.000	72.800	98.000	74.500	-0	367.145
A	DV063	51579	18.30	8.26	18.000	.900	67.000	3.900	27.000	72.400	103.000	69.000	-0	368.217
A	DV065	62579	20.00	8.35	17.500	.900	68.000	4.100	23.000	72.000	101.000	70.000	-0	363.000
A	DV066	62579	20.00	8.18	19.000	1.150	65.000	3.700	23.500	69.000	104.000	62.500	-0	353.650
I	DV034	51579	19.50	7.44	182.000	60.500	206.000	8.850	515.000	194.000	265.000	52.000	-0	1486.967
I	DV037	51579	16.00	7.13	359.000	112.000	252.000	16.100	905.000	366.000	321.000	47.000	-0	2383.281
I	DV038	51579	18.50	7.25	147.500	44.500	191.000	13.800	330.000	234.000	361.000	63.000	-0	1389.445
I	DV039	51579	22.50	7.83	64.000	25.500	159.000	19.300	125.000	134.000	399.000	77.000	-0	1006.754
I	DV040	51579	15.50	7.50	305.000	99.000	195.000	14.900	715.000	332.000	297.000	49.500	-0	2011.976
I	DV100	62579	19.00	7.55	55.000	24.800	158.000	16.000	166.000	138.000	291.000	65.000	-0	914.950
I	DV101	62579	20.00	7.60	57.000	22.000	108.000	14.000	122.000	128.000	242.000	70.800	-0	764.700
I	DV113	62579	24.50	7.52	95.000	34.000	120.000	17.900	196.000	166.000	255.000	85.000	-0	969.640
I	DV114	62579	22.50	7.52	112.000	41.300	128.000	14.600	262.000	161.000	262.000	80.000	-0	1061.350
P	DV20	32079	21.00	7.60	50.000	19.700	102.000	6.800	134.000	78.800	200.000	40.800	-0	632.430
D	LL098	92878	53.50	7.80	77.200	.800	446.000	10.500	675.000	164.000	64.900	74.000	-0	1513.550
D	LL099	92878	73.50	8.70	3.900	.200	180.000	5.600	125.000	116.000	54.600	122.000	28.300	644.090
D	LL100	92878	70.00	8.40	7.600	.200	195.000	5.200	156.000	129.000	87.400	117.000	9.470	706.960
D	LL101	92878	25.00	7.40	51.800	2.900	232.000	2.600	250.000	160.000	163.000	52.700	-0	915.400
D	DV23	32079	73.00	8.65	4.300	.200	181.000	6.000	133.000	108.000	56.000	123.000	28.000	653.505
D	DV24	32079	55.00	7.80	67.500	.800	430.000	10.200	650.000	161.000	62.000	75.000	-0	1470.122
D	DV054	62579	73.00	8.77	4.000	.200	175.000	5.500	130.000	112.000	46.500	118.800	31.100	637.597
D	DH16	72379	26.00	7.65	55.000	2.950	228.000	2.270	250.000	150.000	166.000	44.000	-0	905.930
D	DH15	72379	52.00	8.25	9.600	.050	210.000	4.330	208.000	102.000	76.600	112.000	7.200	743.850
D	DH09	72379	73.00	7.80	31.000	.210	311.000	8.720	362.000	220.000	75.100	85.000	-0	1106.078
D	DH06	72379	73.00	8.20	11.500	.120	216.000	5.420	160.000	202.000	76.600	109.000	9.600	803.875
D	DH08	72379	57.00	-0	-0	-0	-0	-0	-0	-0	-0	102.000	-0	102.000
D	DH10	72379	76.00	-0	-0	-0	-0	-0	-0	-0	-0	66.000	-0	66.000
H	DV04	32079	63.00	6.61	46.500	10.300	362.000	22.000	49.000	122.000	936.000	68.500	-0	1630.842
H	DV033	51579	65.50	6.45	49.000	10.800	342.000	21.200	47.000	116.000	919.000	67.000	-0	1586.787
H	HHS01	72379	75.00	7.30	44.000	10.100	324.000	20.600	50.000	108.000	880.000	66.000	-0	1518.508
H	HHS03	72379	67.00	6.50	47.000	10.000	335.000	21.300	47.000	112.000	911.000	69.000	-0	1569.563
H	HHS05	72379	72.00	7.22	43.000	10.000	334.000	20.200	47.500	111.000	869.000	69.000	-0	1519.630
H	HHS06	72379	39.00	-0	-0	-0	-0	-0	-0	-0	-0	83.000	-0	83.000
H	HHS12	72379	63.00	6.90	47.000	9.900	322.000	20.400	50.000	110.000	884.000	66.000	-0	1525.196
H	HHS09	72379	58.00	7.50	38.000	10.200	334.000	21.000	47.000	113.000	897.000	67.000	-0	1543.321
S	DV01	32079	55.00	7.30	110.000	20.400	160.000	28.000	77.000	370.000	303.000	66.800	-0	1153.274
S	DV02	32079	51.00	7.39	103.000	21.200	163.000	28.000	77.000	370.000	292.000	71.000	-0	1143.515
S	DV035	51579	53.50	7.80	112.000	22.000	162.000	26.200	88.000	374.000	301.000	63.800	-0	1162.359
S	DV036	51579	73.00	6.50	105.000	21.500	155.000	26.000	78.000	366.000	321.000	-0	-0	1090.396
S	DV075	72379	73.00	6.05	105.000	20.800	150.000	22.000	76.000	348.000	309.000	53.000	-0	1103.713
S	DV076	72379	55.00	-0	-0	-0	-0	-0	-0	-0	-0	58.000	-0	58.000
S	DV077	72379	30.00	-0	-0	-0	-0	-0	-0	-0	-0	54.000	-0	54.000
S	DV112	62579	73.50	6.80	105.000	20.500	162.000	28.000	78.000	352.000	313.000	60.000	-0	1123.400

Table 5-1. Chemical Analyses of Dixie Valley Waters. (cont'd.)

		F	B	AL	FE	MN	LI	SR	NO3	AS	HG	CS
W	LL097	-0	-0	-0	-0	-0	-0	-0	.090	-0	-0	-0
W	LL109	-0	-0	-0	-0	-0	-0	-0	.090	-0	-0	-0
W	DV21	.800	.810	.100	.080	.017	.050	.860	-0	-0	-0	-0
W	DV22	.370	.550	.100	.010	.015	.020	.780	-0	.010	.000	.050
W	DV031	.390	-0	-0	-0	-0	-0	-0	-0	-0	-0	-0
W	DV032	.320	-0	-0	-0	-0	-0	-0	-0	-0	-0	-0
W	DV045	.300	-0	-0	-0	-0	-0	-0	-0	-0	-0	.050
W	DV046	.290	-0	-0	-0	-0	-0	-0	-0	-0	-0	-0
W	DV047	-0	-0	-0	-0	-0	-0	-0	-0	-0	-0	-0
W	DV048	-0	-0	-0	-0	-0	-0	-0	-0	-0	-0	-0
W	DV049	-0	-0	-0	-0	-0	-0	-0	-0	-0	-0	-0
W	DV050	.310	-0	-0	-0	-0	-0	-0	-0	-0	-0	-0
W	DV051	.340	-0	-0	-0	-0	-0	-0	-0	-0	-0	-0
W	DV052	.490	-0	-0	-0	-0	-0	-0	-0	-0	-0	.050
W	DV053	.460	.550	.100	.010	.005	.039	1.210	0	.010	.000	-0
W	DV055	.380	-0	-0	-0	-0	-0	-0	0	-0	-0	-0
W	DV56	.380	-0	-0	-0	-0	-0	-0	0	-0	-0	-0
W	DV057	.370	-0	-0	-0	-0	-0	-0	0	-0	-0	-0
W	DV058	.320	-0	-0	-0	-0	-0	-0	0	-0	-0	-0
W	DV059	.340	-0	-0	-0	-0	-0	-0	0	-0	-0	-0
W	DV067	1.330	-0	-0	-0	-0	-0	.350	0	-0	-0	-0
W	DV078	.570	.950	.100	.010	.005	.090	1.760	0	.010	.000	-0
W	DV092	.300	1.100	.100	.010	.005	.030	.650	-0	.010	-0	.020
W	DV102	.330	-0	-0	-0	-0	-0	-0	0	-0	-0	-0
W	DV103	.220	-0	-0	-0	-0	-0	-0	0	-0	-0	-0
W	DV104	.310	-0	-0	-0	-0	-0	-0	0	-0	-0	-0
W	DV105	.260	-0	-0	-0	-0	-0	-0	0	-0	-0	-0
W	DV106	.300	-0	-0	-0	-0	-0	-0	0	-0	-0	-0
W	DV107	.360	-0	-0	-0	-0	-0	-0	0	-0	-0	-0
W	DV108	.400	-0	-0	-0	-0	-0	-0	0	-0	-0	-0
W	DV109	.620	-0	-0	-0	-0	-0	-0	0	-0	-0	-0
W	DV110	.530	-0	-0	-0	-0	-0	-0	0	-0	-0	-0
W	DV111	1.370	-0	-0	-0	-0	-0	-0	0	-0	-0	-0
C	CS01	-0	-0	-0	-0	-0	-0	-0	0	-0	-0	-0
C	CS02	-0	-0	-0	-0	-0	-0	-0	0	-0	-0	-0
C	CS04	-0	-0	-0	-0	-0	-0	-0	0	-0	-0	-0
C	CS06	2.500	1.000	.100	.010	.290	.045	4.600	0	.010	.000	-0
C	CS07	1.900	1.900	.100	.010	.032	.075	3.350	0	.010	.000	-0
C	CS08	.330	1.700	.100	.010	.005	.050	1.630	0	.010	.000	0
B	DV041	-0	-0	-0	-0	-0	-0	-0	-0	-0	-0	-0
B	DV042	-0	-0	-0	-0	-0	-0	-0	-0	-0	-0	-0
E	LL102	-0	-0	-0	-0	-0	-0	-0	.710	-0	-0	-0
E	DV03	.600	-0	-0	-0	-0	-0	-0	-0	-0	-0	-0
E	DV10	.160	.240	.100	.020	.015	.020	4.250	-0	-0	-0	-0
E	DV12	.300	.230	.100	.010	.015	.010	.690	-0	-0	-0	-0
E	DV060	.360	-0	-0	-0	-0	-0	-0	0	-0	-0	-0
E	DV061	.290	-0	-0	-0	-0	-0	-0	0	-0	-0	-0
E	DV062	.300	-0	-0	-0	-0	-0	-0	0	-0	-0	-0
E	DV063	.180	.220	.100	.010	.005	.010	.080	0	.010	.000	-0
E	DV091	.560	1.200	.100	1.610	.050	.050	.030	-0	.010	-0	.020
L	LL103	-0	-0	-0	-0	-0	-0	-0	1.510	-0	-0	-0
L	LL104	-0	-0	-0	-0	-0	-0	-0	1.240	-0	-0	-0

Table 5-1. Chemical Analyses of Dixie Valley Waters. (cont'd.)

		F	B	AL	FE	MN	LI	SR	NO3	AS	HG	CS
M	DV05	3.100	.900	.100	.010	.015	.270	.690	-0	-0	-0	-0
M	DV06	2.800	1.260	.100	.010	.015	.350	1.380	-0	-0	-0	-0
M	DV11	1.300	.800	.100	.010	.005	.150	2.450	-0	-0	-0	-0
M	DV115	1.370	-0	-0	-0	-0	-0	-0	0	-0	-0	-0
M	DV116	6.600	-0	-0	-0	-0	-0	-0	0	-0	-0	-0
1	DV069	1.550	5.200	-0	.030	.005	1.060	.160	-0	-0	-0	.130
1	DV70	8.500	9.200	-0	.100	.005	1.290	.190	-0	-0	-0	.290
1	DV72	9.500	9.600	-0	.100	.006	1.540	.320	-0	-0	-0	-0
2	DV080	-0	11.000	-0	-0	-0	1.290	-0	0	1.400	-0	.210
2	DV081	-0	-0	-0	-0	-0	1.270	-0	0	2.100	-0	.280
2	DV082	-0	10.600	-0	-0	-0	1.290	-0	0	1.800	-0	.200
3	DV090	7.600	8.500	.100	1.610	.050	1.010	1.060	-0	.590	-0	.325
4	DV093	7.900	12.700	-0	-0	-0	-0	-0	-0	.160	-0	-0
4	DV094	8.800	-0	-0	-0	-0	-0	-0	-0	.160	-0	-0
T	DV15	4.390	-0	-0	-0	-0	.970	3.440	-0	-0	-0	-0
T	DV16	4.400	5.500	-0	-0	-0	.960	-0	-0	-0	-0	-0
T	DV030	4.400	4.700	.100	.040	.030	.975	3.200	-0	.040	.000	.140

All concentrations are in parts per million (ppm) and temperatures are in ^{o}C.

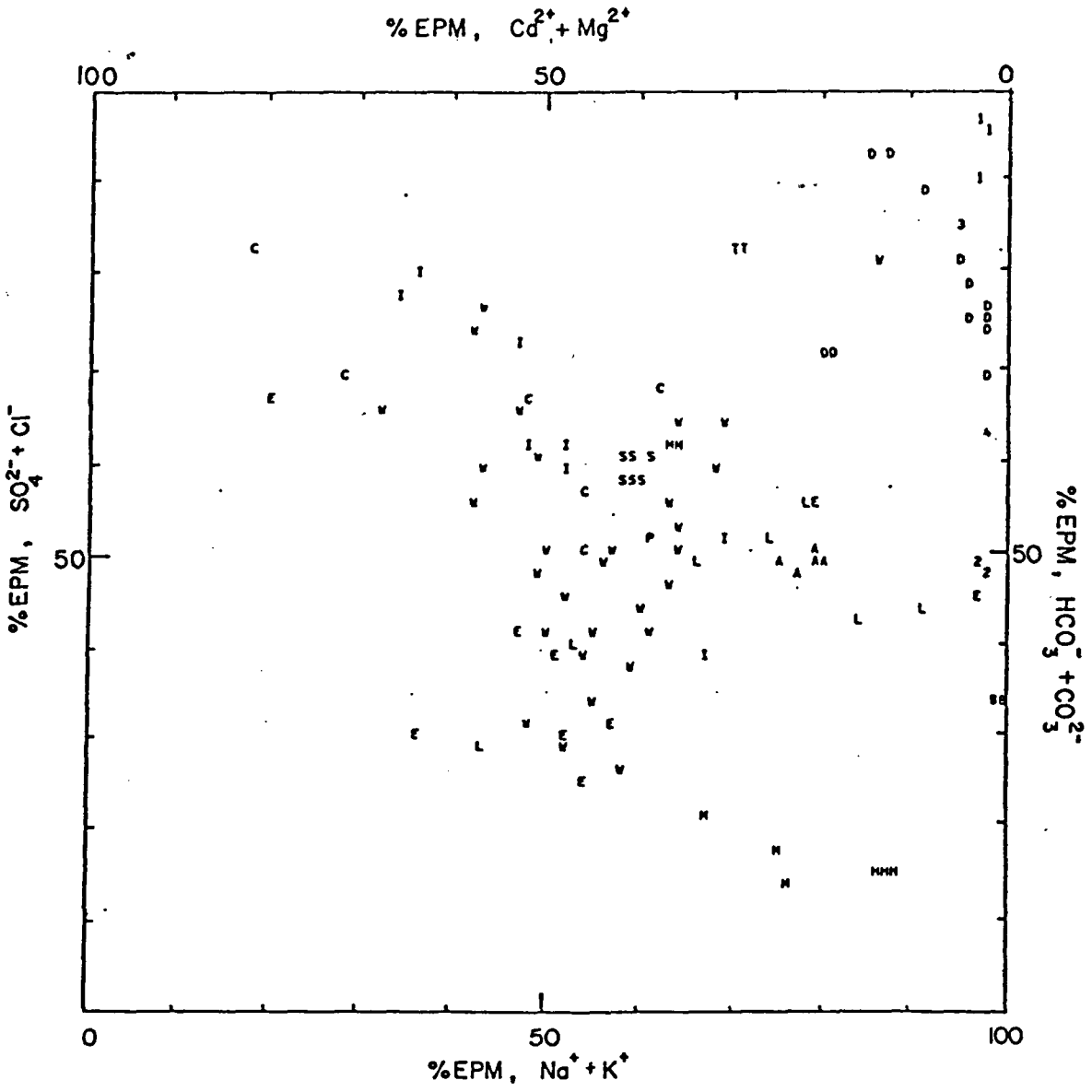

Figure 5-1. Trilinear Plot of Dixie Valley Waters. (See legend opposite Table 5-1 for letter and number code.)

All samples have comparatively low Ca and Mg levels. The hot spring systems, as well as the deep wells, seem to experience a substantial shift towards increased Na + K levels. The anions seem to indicate more clearly the differences among the three hot spring systems.

If one considers total dissolved solids (TDS), the variations in water chemistry become more apparent (Table 5-2).

Table 5-2 clearly illustrates the variations both within a given hot spring system and among the three hot spring systems. The Dixie Hot Springs system has the greatest TDS range, possessing both the lowest and highest levels. Sou and Hyder Hot Springs have very narrow TDS ranges, with Sou Hot Springs having the lower values of the two systems.

The artesian wells in the vicinity of Dixie Settlement have low values, similar to the surface water and spring water derived from the Clan Alpine Mountains. The hydrogeochemical evidence would tend to indicate that the Clan Alpine Mountains are a source of recharge for groundwater in the Dixie Settlement area. This situation is more likely than specifying the Stillwater Range waters as a source of groundwater recharge. These latter waters have high TDS levels for mountain spring water and surface runoff. These high TDS values definitely anomalous for "normal" mountain runoff will be discussed further in a later section.

5.2.2 Waters from the Clan Alpine Mountains

Most of the waters from the Clan Alpine Mountains are chemically similar to the waters from the wells at Dixie Settlement. Both groups of waters are low in TDS, but the Dixie Settlement waters exhibit relatively high temperatures for groundwater. Two Dixie Settlement samples, DV 13 and DV 66, have unusually high pH values (8.30 and 8.18) and fluoride levels (6.00 and 5.80 ppm). One anomaly in the Clan Alpine Mountains is Shoshone Spring (DV 91), which has a surprisingly low dissolved oxygen content for a mountain spring, a high pH (8.58) and temperature (32°C). The boron level in this spring, 1.2 ppm, is a significant amount.

Table 5-2. Total Dissolved Solids (TDS) Contents of Dixie Valley Waters.

Sample Location	TDS (ppm)
Dixie Hot Springs	640-3000
Sou Hot Springs	1100-1160
Hyder Hot Springs	1580-1630
McCoy and Lower Ranch Hot Springs	800-1190
Eastern Mountain Ranges (Clan Alpine and Augusta Mountains)	170-435
Stillwater Range	600-1770
Artesian Wells in Southern Dixie Valley (Dixie Settlement)	350-370
Irrigation Wells in Northern Dixie Valley	760-2380
DF 45-14	1657-2201
DF 66-21	4100-5410
SR2-A	1900

Another important aspect is that the calculated CO_2 pressures are oversaturated with respect to atmospheric CO_2 pressure in many Clan Alpine Mountain waters (Table 5-3). These elevated CO_2 pressures are caused by various dissolution reactions occurring in the subsurface, and the CO_2 pressures are indicators of the extents of these various reactions. At the present time the sources of CO_2 in geothermal systems are poorly understood.

5.2.3 Waters from the Stillwater Range

Even in the early stages of field work it was recognized that the waters from the eastern slopes of the Stillwater Range, which is considered one of the major recharge areas for the study area, are surprisingly high in TDS. One normally expects low TDS waters in a recharge area. Springs on the Carson Sink (west) side of the Stillwater Range also exhibited high TDS levels. Although some thermal springs are believed to exist in the mountains, none was found. All sampled springs have low discharges and most streams deposit travertine ($CaCO_3$). All computed CO_2 pressures are greater than atmospheric CO_2 (see Table 5-3). This tends to imply the existence of a source of CO_2 other than the atmosphere.

Samples from the eastern slopes have Cl levels as high as 260 ppm, SO_4 as high as 520 ppm, HCO_3 up to 380 ppm, SiO_2 up to 46 ppm, Mg up to 80 ppm, Na + K up to 190 ppm and Ca as high as 180 ppm. These waters apparently comprise most of the shallow groundwater north of Dixie Hot Springs. The ratios Cl/SO_4, $(Na+K)/SO_4$, Ca/SO_4 and Mg/SO_4 are relatively constant in these samples. The constancy of these ratios is apparently characteristic of volcanic rock weathering, since volcanic rocks are abundant in the Stillwater Range.

The question remains as to why the Stillwater Range waters have such high levels of TDS, a phenomenon which is usually not anticipated from waters derived from precipitation. One reason could be that these waters have a relatively long residence time in the subsurface, a hypothesis weakly supported by the few available tritium data. However, the waters from the Clan Alpine Mountains are from a similar rock environment, but have much lower TDS levels.

A second explanation might be the rapid dissolution of hydrothermal minerals, by either old or young waters. Another possibility that could also explain the high calculated CO_2 pressures (Table 5-3)

Table 5-3. Calculated log P_{CO_2} Values in Dixie Valley Waters.

Sample Locations	log P_{CO_2}
Stillwater Range	-3.4 to -1.5
Clan Alpine Mountains	-3.5 to -2.0
Artesian Wells (Dixie Settlement)	-3.5 to -3.7
Irrigation Wells	-2.5 to -1.8
Dixie Hot Springs	-4.0 to -2.6
Hyder Hot Springs	-1.4 to 0.0
Sou Hot Springs	-2.3 to 0.0
DF 45-14	-1.2
DF 66-21	-1.5
SR2-A	-2.2 to -2.0

is the ascension of thermal waters along deep reaching fault zones. These ascending thermal waters would then be slightly diluted by infiltrated precipitation, and the mixture would surface at springs.

Further work in the Stillwater Range itself will be required to verify the origin of the high TDS waters. It is possible that the isotope data will shed some light on this problem.

5.2.4 Thermal Waters in Dixie Valley

Thermal groundwaters commonly have chemical constituents that can serve as specific indicators of geothermal reservoirs. Elevated levels of F, Cl, B, SiO_2, H_2S, Na and TDS can indicate geothermal activity. SO_4 can be high if sufficient sulfide and free oxygen are available at depth. HCO_3 is commonly high in thermal waters if an appropriate source of CO_2 exists at depth. However, it should be emphasized that F, B and other trace elements are low if the reservoir rocks lack these constituents. Ca and Mg levels are usually low in thermal waters due to cation exchange with clay minerals and other similar reactions.

In the following discussion the aforementioned indicators are utilized to determine relative circulation depths of waters and reservoir temperatures.

5.2.4.1 Dixie Hot Springs

The Dixie Hot Springs system is comprised of about 35 springs and seeps. The springs show wide variations in temperature and electrical conductivity. All springs emerge from alluvium, which is about 1000 feet thick in this area. Springs and seeps discharge over an area of about four square miles.

The Dixie Hot Springs system is typical for its relatively low HCO_3 (60-90 ppm). The pH ranges between 7.4 and 8.77, which is considered rather high. Electrical conductivities change significantly between adjacent spring orifices. Temperatures are generally highest for the lowest TDS springs (Figure 5-2). Cl and Na are highest for the low temperature springs. SO_4 and Cl correlate very well, and reach their highest levels in the coldest springs. SiO_2 decreases with increasing Ca, which indicates an increasing influx of cold

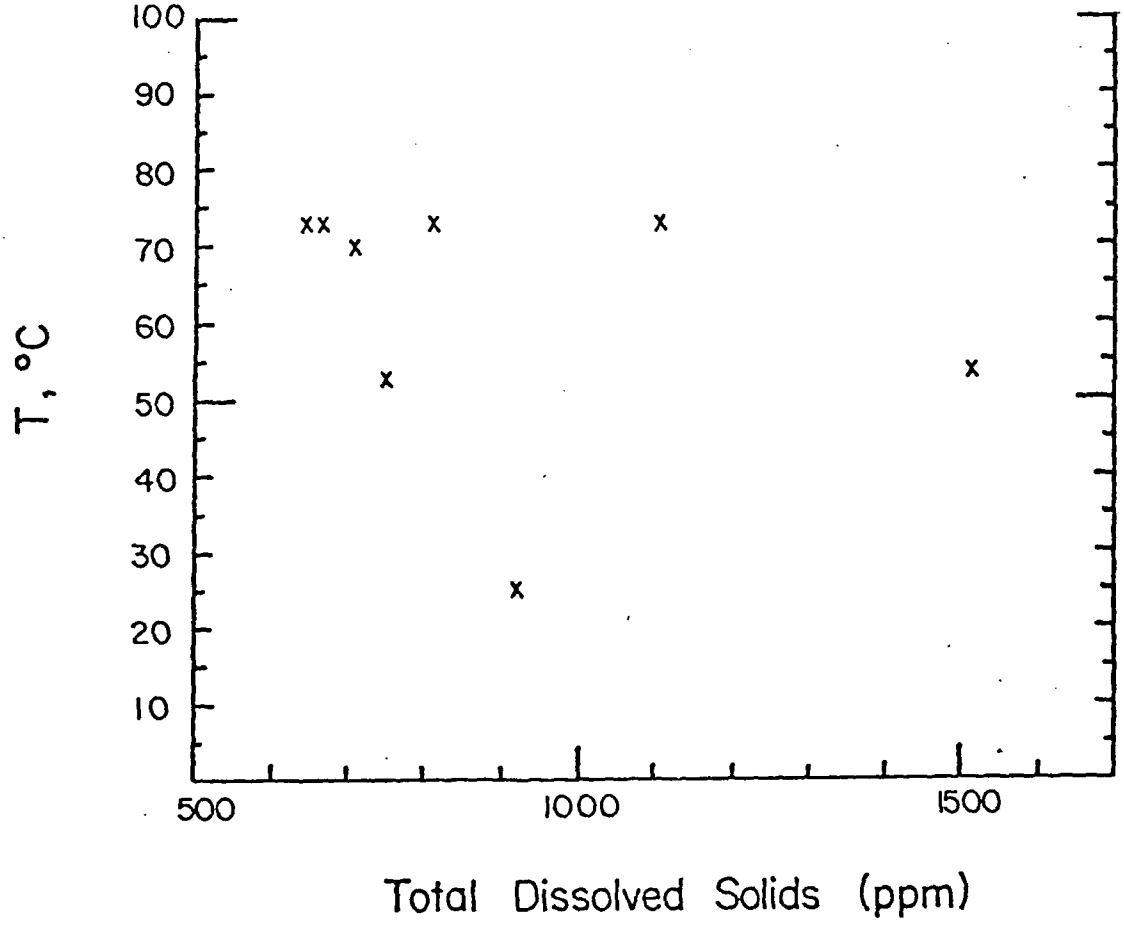

Figure 3-2. Temperature versus Total Dissolved Solids (TDS) for Dixie Hot Springs Waters.

water into the system. High Cl and Na levels indicate dissolution of shallow evaporites by cold water. F levels are the highest in the valley, whereas B, Li, As and Cs have comparatively low concentrations.

Table 5-4 shows estimated reservoir temperatures, calculated using chemical geothermometry. Conductive cooling was assumed for the silica method. Different temperatures between the two methods suggest that chemical equilibrium has not yet been attained.

The silica mixing model, based on a recharge water with 30 ppm SiO_2, yields completely different results. For DV 23 a temperature between 225 and 235^{o}C was computed. However, the mixing model is considered to be unreliable in this case, since the results are inconsistent.

In conclusion, the Dixie Hot Springs system probably shows various degrees of mixing between thermal and cold waters, which accounts for the varying temperatures and electrical conductivities. Based upon the structural analysis (Chapter 3), it is likely that the springs are fault-controlled. If fault control does exist then the colder waters with higher TDS could result from a less direct flow path that allows more cooling and more mixing within the alluvium which permits more dissolution of soluble salts. It is also possible that the low TDS waters are linked to the artesian wells of Dixie Settlement, since these are the only low TDS waters in the immediate vicinity. The increasing SO_4 with Cl (Figure 5-3) could also be attributed to cold waters from the Stillwater Range, since only there is the correlation between these ions good. Since the HCO_3 levels are low (less than 150 ppm), Dixie is probably not linked to any CO_2 source at depth. This accounts for the absence of any significant spring deposits. Low levels of most trace elements indicate that the Dixie Hot Springs system may be a relatively shallow system, whereas the high F could be due to the dissolution of ancient CaF_2 deposits. It is possible that the Dixie system is heated by a more extensive sealed geothermal reservoir at depth.

Table 5-4. Chemical Geothermometers Applied to Dixie Hot Springs Waters.

Sample No.	Quartz (°C)	Na-K-Ca (°C)	Field Temperature (°C)
DV23	149	139	73
DV54	147	137	73
DH6	142	97	73
DH15	143	95	52
DH9	128	100	73
DV24	122	88	55

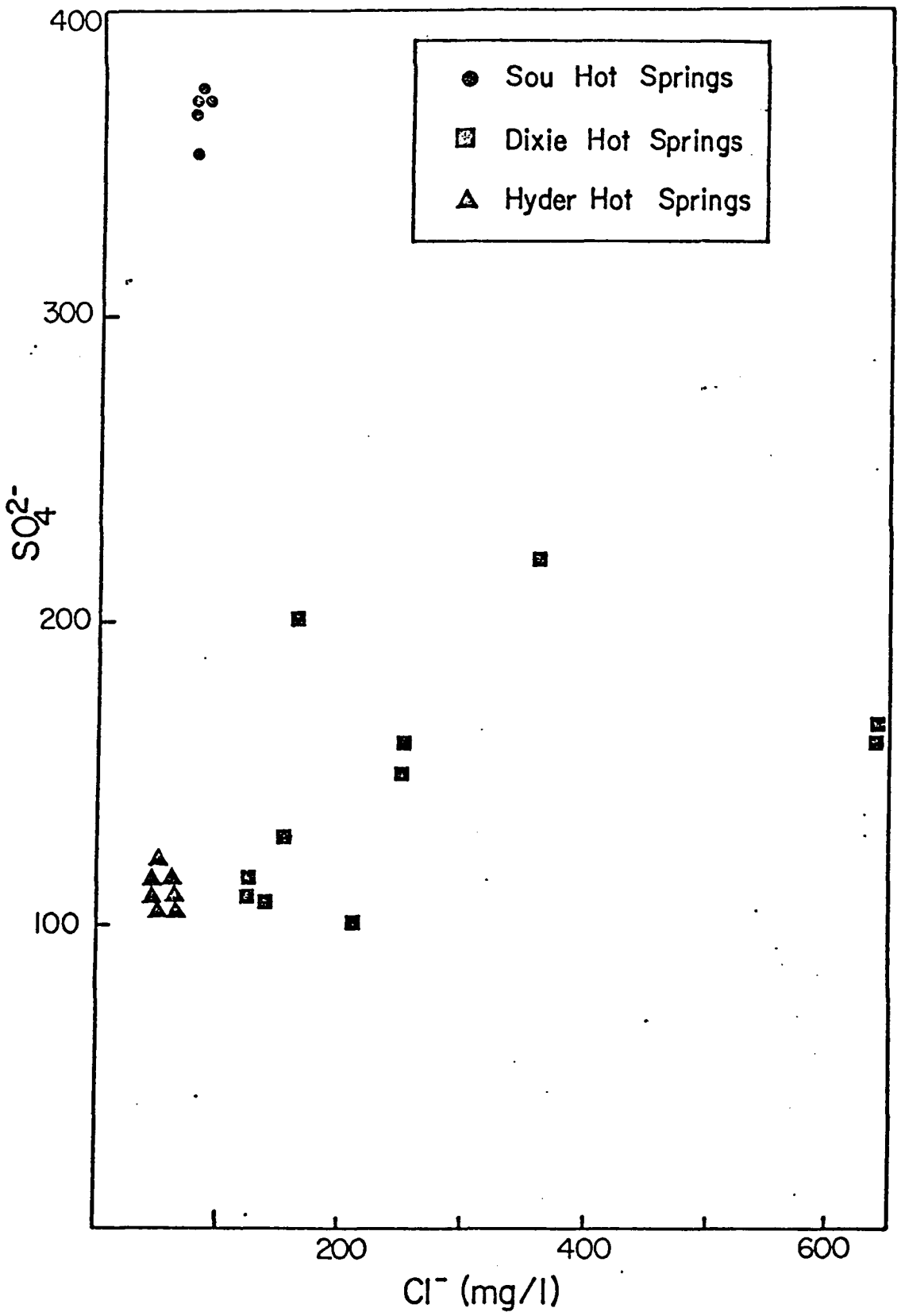

Figure 5-3. Sulfate versus Chloride for the Three Major Hot Spring Systems in Dixie Valley.

5.2.4.2 Hyder Hot Springs

The Hyder Hot Springs system emerges in the middle of the valley, where bedrock is apparently covered by a thick cover of alluvium. However, the chemical homogeneity of the springs seems to require a well-defined, fault-controlled flow system. The springs have deposited a vast amount of travertine up to 100 feet thick. Some of the springs are surrounded by delicate travertine structures.

A detailed survey of the system showed that all springs have electrical conductivities ranging from 1600 to 1850 micromhos (temperature compensated). Gross chemistry of the springs does not vary much, although temperatures differ considerably, ranging from 39°C to 75°C. Thus the system is probably relatively homogeneous, issuing from one reservoir.

Hyder waters are of the bicarbonate-sodium-potassium type. The bicarbonate levels range between 870 and 936 ppm and are the highest among all the hot springs. They are about six times as high as those from DF 45-14 but somewhat lower than those from DF 66-21. The high HCO_3 accounts for the extensive travertine deposits. The pH is as low as 6.5 in springs with high HCO_3 and as high as 7.5 in those with low HCO_3. Some evidence of degassing (probably CO_2) was found, which probably accounts for the inverse correlation of pH with HCO_3.

The SO_4 and Cl levels are among the lowest of the hot springs in the valley (108-116 ppm SO_4, and 47-50 ppm Cl). Sulfate is about as low as the first sample from DF 66-21. The relatively high bicarbonate concentrations indicate that Hyder is connected directly to a geothermal reservoir. In addition the low SO_4 indicates a relatively deep water with limited capability to oxidize sulfides (Figure 5-3). However, no evidence of H_2S was found in Hyder, and the dissolved oxygen content was as high as 2.9 ppm in some of the springs.

Since electrical conductivities and silica levels are relatively constant, the silica geothermometer, assuming conductive cooling and no mixing, was applied. Calculated temperatures range from 115°C to 127°C. The cation geothermometer yielded consistent temperatures between 159°C and 162°C. Slight calcite precipitation is possible for those springs with highest discharge temperature, but the increase in calculated temperature would be negligible in this case.

In conclusion, the Hyder Hot Springs system is of one water type and thus emerges from a well-defined flow system, with little mixing with shallow groundwater. The high HCO_3 values indicate connection to a CO_2 source at depth. However, the water chemistry is inconclusive; therefore the relationship of the spring water to the deep system is unknown.

5.2.4.3 Sou Hot Springs

Vast amounts of spring deposits are present at Sou Hot Springs. The chemistry of the hot springs do not vary considerably, and are of an intermediate type. The temperatures range between 30°C and 73°C. The pH is as low as 6.5; a pH of 6.05 was measured but it is believed to be too low due to a faulty meter. Among the three major hot spring systems, Sou has the highest Ca, Mg and SO_4 levels. Cl levels are comparatively low (less than 100 ppm) as are F and B (DV36 in Figure 5-4). Sr is the highest among all the hot springs. HCO_3 levels are lower (about 300 ppm) than they are at Hyder Hot Springs.

The silica geothermometer, assuming no mixing and conductive cooling, yields temperatures between 105°C and 118°C. The cation geothermometer yields temperatures between 93°C and 194°C. The drastic changes in the calculated reservoir temperatures are probably associated with seasonal fluctuations.

Evidence of extensive CO_2 degassing was found in a flowing well. This probably indicates that Sou Hot Springs is connected in some way to a CO_2-producing reservoir at depth.

In conclusion, Sou is probably a relatively shallow hot spring system. The low SiO_2 temperature, low F, B and Cl and high Ca and Mg are indicative of relatively shallow circulating meteoric water that is heated to low temperatures.

5.2.4.4 Well SR2-A

The measured temperature of the discharge water was 65°C (DV30).

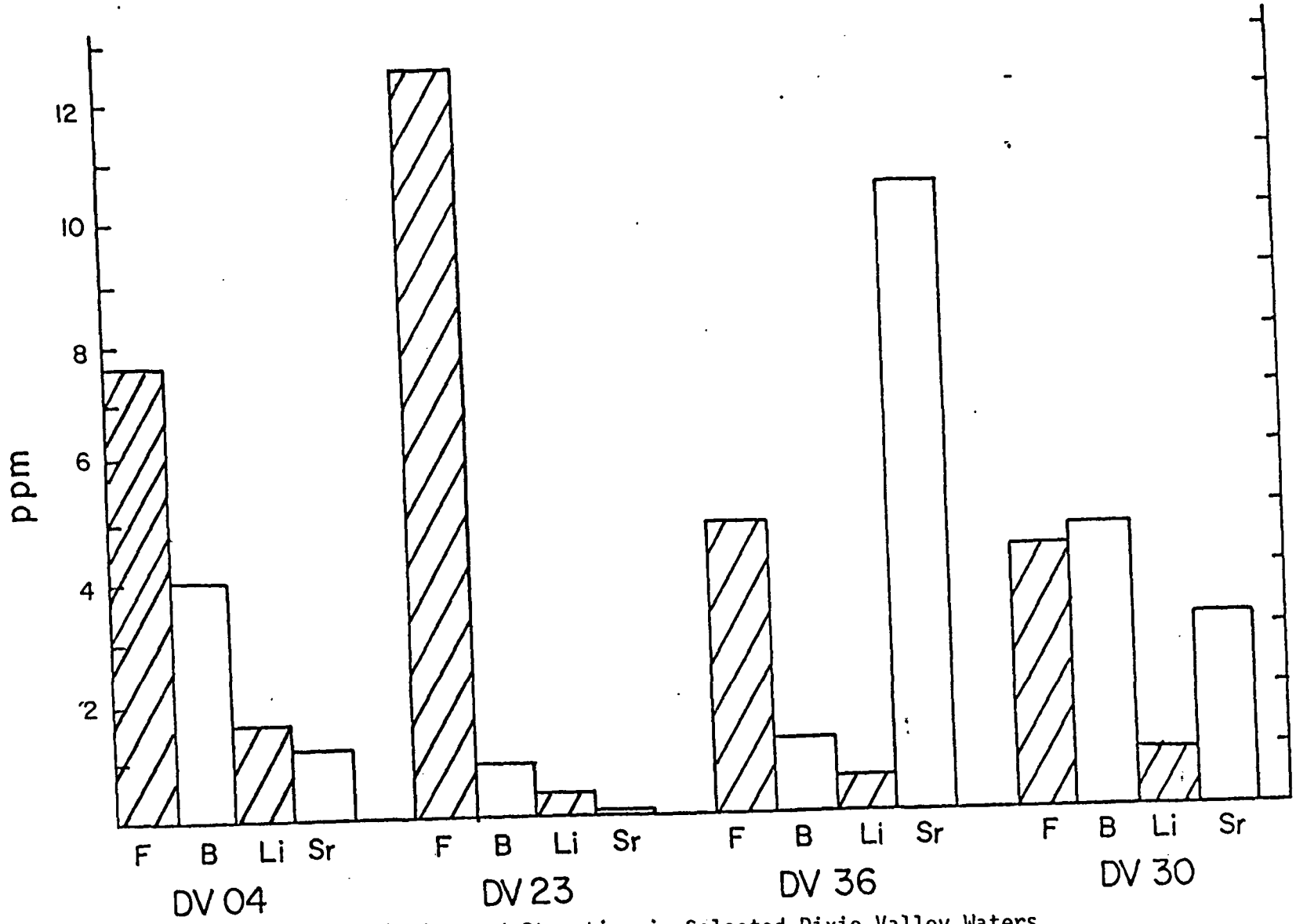

Figure 5-4. Fluoride, Boron, Lithium and Strontium in Selected Dixie Valley Waters.

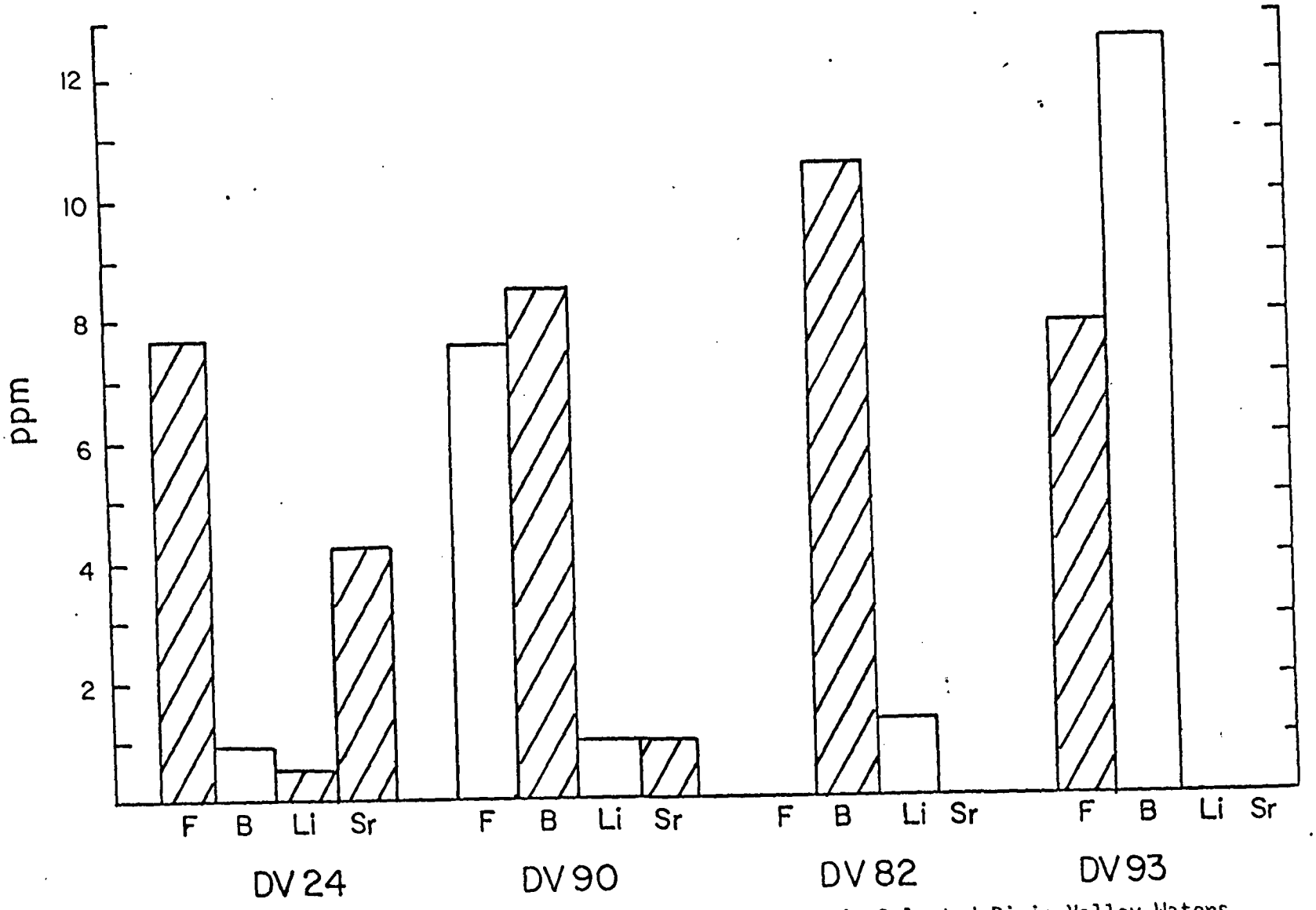

Figure 5-4 (con't.) Fluoride, Boron, Lithium and Strontium in Selected Dixie Valley Waters.

Ca and Mg levels are significant, indicating the influence of cold water. The Cl/SO_4 is very similar to that of the water from White Rock Canyon, indicating the influx of water from the Stillwater Range. F, B and Sr are also significant. Application of chemical geothermometers yields 91°C for the cation method and 139°C for the silica method. The different results indicate inadequate chemical equilibration of warm water at depth. However, the silica method seems to be more reliable. SR2-A is probably fed by a mixture of hot water from depth and cold recharge water from the Stillwater Range.

5.2.4.5 Deep Wells DF 45-14 and DF 66-21

A discussion of the water chemistry with special reference to the alteration mineralogy was given in Chapter 4. In this section the deep wells will be compared to the hot spring systems and the recharge waters. It must be indicated that more than 95% of our data is related to shallow groundwater systems and hot springs. The deep well samples are the only ones that represent deep thermal waters. However, the samples from DF 45-14 and DF 66-21 are not the most reliable because of suspected contamination from drilling operations and/or shallow groundwater. This is especially true of the samples from DF 66-21. Nevertheless, certain gross chemical features of the deep waters can be inferred from the existing samples.

DF 45-14 (DV90) has relatively low levels of Mg and Ca and high Cl and SO_4, which clearly indicate thermal waters. However, HCO_3 is low, much lower than in Sou Hot Springs. F is comparable to Hyder Hot Springs but much lower than in Dixie Hot Springs, whereas B is much higher than in any of the hot springs.

Application of the silica geothermometer (assuming no steam loss) indicates a reservoir temperature of 216°C for DF 45-14. Since the silica content at the sampling temperature is at the saturation level of amorphous silica, precipitation of amorphous silica might be expected in the ascending hot water. Thus, the silica temperature might be even higher. The cation geothermometer yields 193°C.

In DF 66-21 (DV82, DV93) the Cl and Na levels are about three times as high as in DF 45-14, although samples DV82 and DV93 are probably contaminated to a large extent. The SO_4 levels are comparable

to the hot spring systems. HCO_3 levels are extremely high. B and F are comparable to those of DF 45-14. Generally the fluids from DF 66-21 can be considered as Na-Cl waters, high in HCO_3.

The silica geothermometer yields a temperature of 190°C (assuming no steam loss) and the cation geothermometer gives 139°C for DV82. For DV93 176°C was calculated with the silica method and 148°C with the cation method. The silica method is considered to be more reliable. DV82 is from a depth of about 4700 feet and DV93 from about 9500 feet in DF 66-21.

5.3 Conclusions

The preceding discussion about the chemistry of the three hot spring systems indicates that it is unlikely all three systems are linked to a common source. The Dixie Hot Springs system seems to be isolated from a deep CO_2-supplying reservoir, and its waters probably originate from the Stillwater Range and/or other sources. The Sou and Hyder systems are different from each other as well as from the Dixie system as was seen in Figure 5-1. The comparatively low Cl levels in all three systems make a connection to a deep geothermal reservoir that supplies the deep wells unlikely. High HCO_3 levels could be produced by the upward diffusion of CO_2 from a source at depth. The fact that the maximum temperatures in all three systems are about the same (75°C) is conspicuous. F increases with SiO_2 if F is greater than 1 ppm, a relationship that applies to all the hot springs but not to the deep wells (Figure 5-5).

It is clear that the two deep wells tap waters that are different from all the other thermal waters in the valley. Additionally, DF 45-14 is apparently different from DF 66-21. The most significant differences are the higher HCO_3 in DF 66-21 and a TDS level almost double that of DF 45-14. However, since samples from DF 66-21 are undoubtedly contaminated to an unknown extent, these differences may be more apparent than real.

The origin of HCO_3 is unclear. One source could be the oxidation of organic materials at depth, evidence of which was found in some of the sedimentary rocks at depth (T. Bard, personal communication). Another source could be the dissolution of limestones under

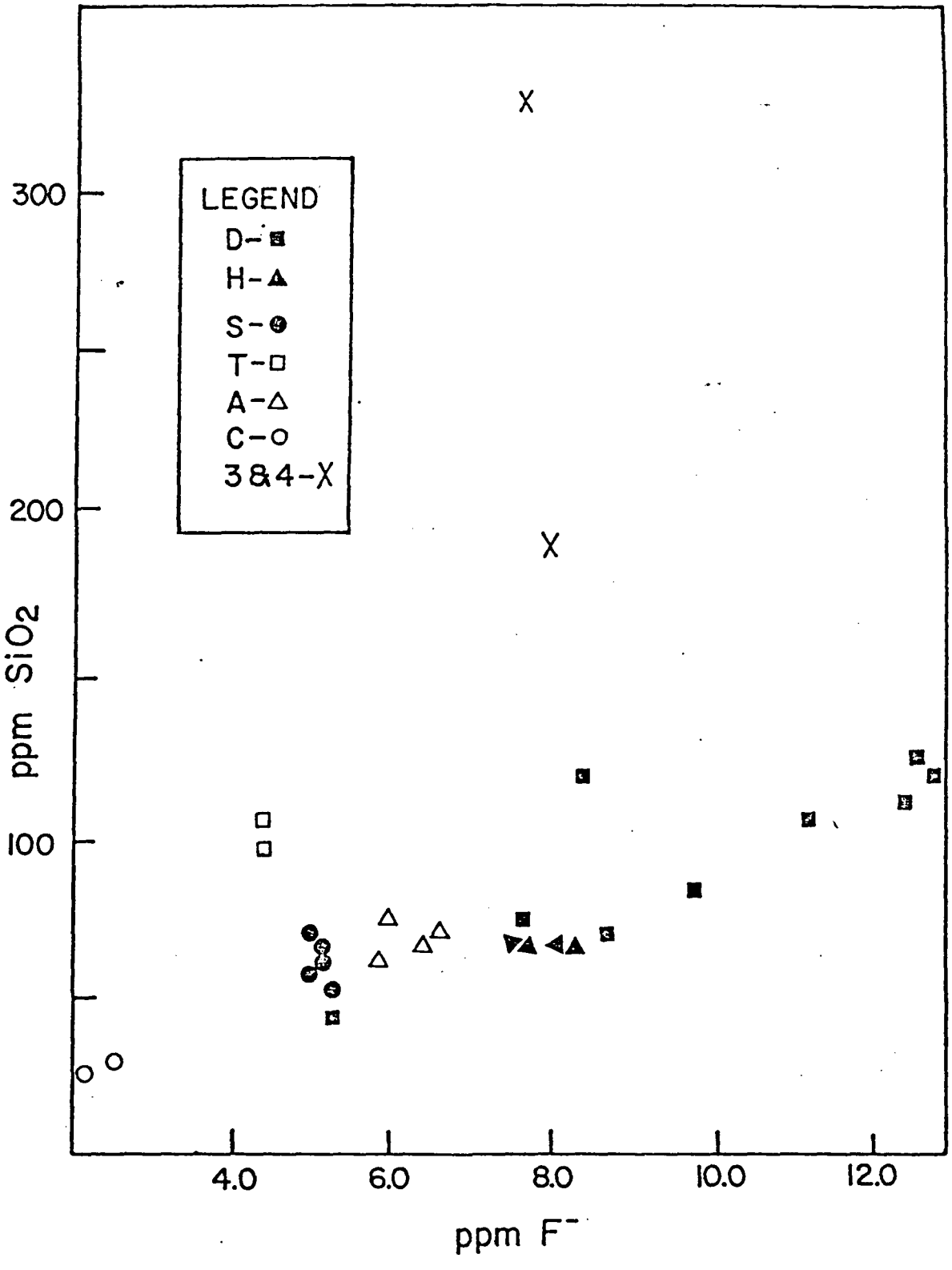

Figure 5-5. Silica versus Fluoride in Selected Dixie Valley Waters. (See legend opposite Table 5-1 for letter and number code.)

acidic conditions. Fracture zones could allow the CO_2 to escape to shallow aquifers, thus accounting for the high P_{CO_2} in most shallow groundwaters.

SO_4 probably originates from the oxidation of sulfides as well as the solution of SO_4 minerals. However, the level of SO_4 is probably limited at depth by the limited supply of free oxygen due to lack of deep-reaching circulation. This constraint might be active in both DF 45-14 and DF 66-21, thus accounting for the comparable levels of SO_4.

It is still not clear how the three hot springs are related to the deep reservoir(s) tapped by DF 45-14 and DF 66-21. The collection and analysis of valid samples from the deep wells might provide more information, as might the isotope data. Age determinations using ^{14}C would prove useful in determining circulation depths. Sulfur isotopes would be helpful in determining the sources of SO_4.

In summary, there appear to be different thermal systems in Dixie Valley. Their interrelationships are not clear, but it seems that there is little interaction among them other than occasional CO_2 transfer and conductive heat transfer.

5.4 References

Cohen, P., and Everett, D.E., 1963, A brief appraisal of the groundwater hydrology of the Dixie-Fairview Valley area, Nevada: Dept. of Conservation and Natural Resources, Ground-Water Resources Reconnaissance Series, Report 23, 40 p.

GeothermEx, Inc., 1976, Geothermal potential of the Quest Leasehold, Dixie Valley, Nevada: Rept. prepared for Dow Chemical Company, December, 1976.

Keplinger and Associates, Inc., 1977, Phase II preliminary evaluation of Dixie Valley, Nevada: geothermal potential and associated economics: Rept. prepared for Millican Oil Company, Sept. 1977.

Keplinger and Associates, Inc., 1978, Interim evaluation of exploration and development status, geothermal potential and associated econmics of Dixie Valley, Nevada: Rept. prepared for Millican Oil Oil Company, Sept. 1978, 60 p.

Zones, C.P., 1957, Changes in hydrologic conditions in the Dixie Valley and Fairview Valley areas, Nevada, after the earthquake of December 16, 1954: Seis. Soc. America Bull., v. 47, no. 4, p. 387-396.

Chapter 6. SHALLOW TEMPERATURE SURVEY

By: Michael E. Campana, Roger L. Jacobson, and Neil L. Ingraham

6.0 SHALLOW TEMPERATURE SURVEY

6.1 Introduction

6.1.1 Purpose and Scope

The purposes for utilizing a shallow (1 meter) temperature survey in the Dixie Valley geothermal area are to: 1) delineate the near-surface hydrothermal discharge system; 2) compare the temperatures obtained from the survey to the data from the thermal gradient holes; and 3) test the usefulness of the shallow temperature survey as a rapid and inexpensive geothermal exploration technique in Dixie Valley. The shallow temperature survey did not cover the entire valley, but focused on the area of greatest interest to Southland Royalty Company, the northern half of Dixie Valley between Dixie Hot Springs and Sou Hot Springs. Plate VIII shows the locations of both the 1 meter holes and the thermal gradient holes.

6.1.2 Methods and Analytical Techniques

The shallow temperature holes were installed by augering to a depth of approximately 1 meter in a predetermined location. A length of 1 inch (ID) PVC pipe, sealed at the bottom, was than emplaced in the hole, and the hole was then backfilled. A 25%-75% mixture of antifreeze and water was then poured into the pipe, and a removable cap placed on top of the pipe. Two hundred and forty-seven holes were installed in this manner. One hundred and seventy-five holes were emplaced by the end of March 1979; the remaining 72 were installed during May and June of 1979.

The network of holes was sampled once a month for six consecutive months (April through September). At each site, the ambient air temperature was recorded as was the temperature at the bottom of the fluid-filled hole. If necessary, fluid was added to the hole after measuring the temperature. During the early sampling runs, temperatures were recorded at the top, middle, and bottom of the hole. However, this practice was discontinued for two reasons: 1) it proved to be time-consuming; and 2) the bottom hole temperature was less affected by fluctuations in air temperature. At the end of each sampling run, the temperatures at a depth of 1 meter were plotted on a map similar to Plate VIII.

The analysis and interpretation of the data were performed by visual examination of the maps and by calculating and interpreting various statistical parameters (mean, standard deviation and range) for both the air temperatures and the 1 meter temperatures. The 1 meter temperatures were also compared to the data from the six thermal gradient holes.

6.1.3 Previous Work

No previous shallow temperature surveys have been conducted in Dixie Valley. Thermal gradient holes, some over 450 meters deep, have been drilled (see Plate VIII) in the valley. Data from these holes were provided to the authors by the Southland Royalty Company.

Shallow temperature surveys have been used in a variety of geological, geothermal and hydrogeological investigations. The first reported survey was by van den Bouwhijsen (1934), who used a thermocouple to measure temperatures at a depth of 1.5 meters to detect a buried fault zone in Holland. Poley and van Steveninck (1970) used temperatures at a depth of 2 meters in an attempt to delineate salt domes and faults near a natural gas field.

Shallow temperature surveys have shown to be very useful in groundwater investigations. The fact that subsurface temperature data can yield information on groundwater flow regimes has been known for some time. The first significant advance in applying subsurface heat measurements to groundwater flow problems was made by Stallman (1960) who derived a general partial differential equation relating conductive and convective heat flow through a saturated porous medium. He suggested that heat flow measurements could be useful in the study of groundwater flow systems. Stallman (1965) and Bredehoeft and Papadopulos (1965) developed solutions of Stallman's (1960) equation for vertical water flow under certain boundary conditions. Cartwright (1970) applied the solution of Bredehoeft and Papadopulos to groundwater discharge from the Illinois basin.

Groundwater flow in shallow aquifers has been shown to affect subsurface temperatures. Cartwright (1968) used soil temperatures at a depth of 50 centimeters to prospect for shallow glacial and alluvial aquifers. He based his method on the assumption that an aquifer acts as a heat sink. Birman (1969) studied shallow soil temperatures in

Johnson Valley, California, and developed an empirical relationship between shallow subsurface temperatures and the depth to the water table. Parsons (1970) studied the relationship between groundwater flow and subsurface temperatures in a glacial complex in Canada. He made comparisons between measured temperature profiles and those obtained by digital computer simulation. Cartwright (1971) developed a model to demonstrate the effect of a shallow confined aquifer on soil temperature. He concluded that the quantity of geothermal heat redistributed by moving groundwater in a shallow aquifer depends upon the velocity of the fluid and the thermal properties of the rock-fluid complex. Supkow (1971), using field data in conjunction with computer simulation developed a "valley mapping function" to delineate zones of maximum groundwater flow. His interpretations of subsurface temperature data in the Tucson basin were supported by independent studies of the subsurface properties of the Tucson basin groundwater reservoir. Cartwright (1974) measured soil temperatures in parts of Illinois and found that the greater the groundwater flow, the greater the temperature difference between recharge and discharge zones. He also discovered that the effect of fluid movement on soil temperature decreases with increasing horizontal distance between recharge and discharge zones. Smith (1974) used a shallow temperature survey to prospect for a buried glacial valley aquifer. He was unable to distinguish a summer low-temperature anomaly trend, which is indicative of a buried valley. He attributed his lack of success to the depth of the aquifer (90-150 feet), which was too deep to contact the summer portion of the annual temperature wave. Because of this, a near-surface low-temperature anomaly was not produced.

Geothermal investigations have also made use of shallow temperature surveys. Kintzinger (1956) conducted a 1 meter survey to outline the thermal effects in an area near Lordsburg, New Mexico where newly drilled wells discharged steam and boiling water. Kappelmeyer (1957) measured temperatures at a depth of 1.5 meters to locate natural steam occurrences in Italy. Banwell (1964) prospected the Wairakei hydrothermal region in New Zealand using a 1 meter temperature survey. He reported "some measure of correlation" between the spatial distribution of temperatures and the locations of some major faults. Combs (1975) stated that shallow temperature surveys have limited value for selecting deep drilling sites because of their ineffective depth of penetration

and the masking effects of shallow groundwater. Olmsted (1977) conducted 1 meter temperature surveys in Nevada and reported varying degrees of success in delineating temperature and heat flow anomalies at greater depths. Miller (1978), using a 1 meter survey in the Allen Springs - Lee Hot Springs area of Churchill County, Nevada, found evidence suggesting a structural control on the discharge portion of the hydrothermal system.

6.2 Analytical Results

6.2.1 Shallow Temperature Survey Data

Table 6-1 contains the entire assemblage of data collected during the survey. Table 6-2 shows the statistical data for the bottom hole temperatures, and Table 6-3 contains the statistical information for the air temperatures collected during the sampling runs.

6.2.2 Visual Delineation of Temperature Trends

A visual examination of the data reveals that, to no surprise, the strongest thermal activity lies in the vicinity of Dixie Hot Springs, where a maximum temperature of 42.1 ^{o}C was measured in August. This was the highest temperature measured during the entire survey.

The single line of holes running across the valley from Shoshone Creek to the west side of the valley also showed an interesting trend. The easternmost end of this line (hole 6) showed higher temperatures than the far western end (hole 5) of the line. This difference was not apparent during the first survey (April), but became evident during later surveys. Temperature differences between these two holes ranged from a low of less than 1^{o}C in April to a high of 6.9^{o}C in July. Between these two holes there was no clear trend.

Interesting temperature trends were also noted in the isolated grid of holes located in the Bernice Creek-Dyer Flat area. The April survey revealed a temperature difference of just 2.8^{o}C between the hottest (hole 98) and coldest (hole 91) locations. In May, June and July the temperature differences between these two holes were greater than 5.5^{o}C but by September the difference dropped down to about 3.3^{o}C. In fact, during April and September the temperatures in this area showed

Table 6-1. Monthly Shallow (1 meter) Temperatures in Dixie Valley, Nevada. (All temperatures in °C; I indicates no measurement taken.)

HOLE	APRIL	MAY	JUNE	JULY	AUGUST	SEPTEMBER
1	10.7	14.9	22.7	26.0	28.0	25.9
2	10.1	14.8	23.0	26.6	27.7	25.2
3	10.6	15.3	24.2	27.2	29.3	26.7
4	I	I	I	I	I	I
5	9.1	10.8	I	18.1	21.0	21.5
6	9.7	13.5	22.1	25.0	26.0	25.0
7	9.9	13.2	20.7	23.1	25.5	23.9
8	10.1	13.5	21.2	24.0	25.9	24.3
9	9.5	13.1	20.5	23.0	25.1	23.5
10	9.8	13.1	19.5	23.5	25.0	23.5
11	10.1	13.2	20.5	23.5	25.8	23.8
12	9.5	12.1	19.2	22.0	24.0	23.1
13	9.2	13.3	21.7	23.3	25.5	24.0
14	9.6	13.3	20.8	23.2	25.4	24.1
15	8.7	13.3	21.7	23.8	25.7	24.3
16	8.7	12.9	19.1	22.9	24.5	24.3
17	9.9	12.8	19.0	22.5	23.2	22.3
18	9.1	12.4	18.9	22.1	24.5	23.3
19	8.9	11.8	19.0	22.0	24.4	23.6
20	8.6	11.7	18.0	20.0	23.0	22.3
21	11.0	14.9	21.8	24.9	26.5	25.9
22	11.1	15.4	23.2	26.8	26.8	26.4
23	12.0	15.4	23.0	26.7	27.8	26.5
24	12.3	16.5	23.9	27.4	28.5	27.2
25	13.8	18.5	25.2	28.4	29.3	28.2
26	11.2	16.1	24.1	I	I	I
27	11.0	15.8	23.4	27.1	28.2	I
28	10.9	14.7	22.4	30.1	27.0	26.0
29	10.2	13.5	20.1	23.5	I	I
30	11.7	14.7	22.3	26.2	27.3	27.0
31	10.6	14.5	22.4	26.3	27.2	25.9
32	11.0	15.0	22.6	26.6	30.6	26.2
33	I	I	I	I	I	I
34	10.2	14.3	21.2	24.6	26.0	24.4
35	10.5	14.5	21.9	25.6	26.6	24.9
36	8.9	15.2	23.6	27.2	28.2	25.9
37	10.4	15.6	24.0	27.3	28.8	26.2
38	19.9	25.6	32.5	36.2	38.1	36.1
39	24.4	30.8	I	40.1	42.1	39.1
40	11.6	17.2	25.1	28.2	29.9	28.2
41	10.3	13.1	19.0	22.0	23.8	22.7
42	10.4	15.0	22.7	26.2	27.8	26.8
43	10.1	14.3	21.2	24.7	26.0	24.5

Table 6-1 (cont'd.)

Hole	April	May	June	July	August	Sept
44	10.5	16.0	21.9	25.5	27.6	26.7
45	8.7	13.7	21.4	25.6	26.9	24.0
46	9.3	14.5	21.5	25.4	26.9	24.8
47	10.5	15.3	22.8	26.6	27.8	25.8
48	10.5	15.7	23.2	26.4	27.8	25.7
49	I	-0	I	I	I	I
50	10.8	17.1	22.8	26.3	27.2	25.9
51	10.5	14.3	21.0	24.5	I	I
52	9.7	15.0	23.0	26.8	28.0	25.1
53	I	13.8	19.2	22.8	24.4	22.9
54	I	12.1	16.0	18.0	20.6	20.8
55	I	16.4	23.9	27.3	29.6	27.5
56	I	14.6	20.1	23.7	26.1	24.2
57	8.2	10.8	15.4	18.4	20.6	22.0
58	9.3	14.0	22.2	25.4	27.0	25.1
59	10.0	14.1	21.9	25.3	26.6	24.8
60	10.4	13.8	I	23.3	24.2	23.9
61	-0	21.5	30.1	33.8	34.3	31.5
62	9.9	14.9	23.2	25.3	28.1	26.1
63	9.4	12.2	17.6	19.0	22.7	21.3
64	9.1	12.1	20.3	22.9	24.5	22.7
65	9.4	I	17.5	21.0	22.0	21.8
66	9.8	13.6	I	24.9	I	I
67	7.8	9.9	17.0	18.0	21.8	21.2
68	8.4	10.6	16.4	18.7	21.9	21.2
69	9.7	14.7	22.4	26.0	I	25.9
70	9.4	14.1	21.8	25.3	I	24.7
71	10.9	13.9	21.1	24.9	I	25.0
72	10.6	14.9	22.5	25.9	27.2	26.6
73	11.2	13.3	21.0	23.8	25.9	25.2
74	11.3	14.0	24.4	24.8	27.0	26.2
75	10.9	14.9	23.4	26.8	28.4	27.0
76	10.4	12.8	27.2	23.9	25.7	24.8
77	8.9	11.1	17.6	21.2	22.0	21.9
78	8.8	11.5	18.2	20.3	22.2	21.2
79	9.2	11.2	18.8	22.0	23.5	22.9
80	8.5	11.1	17.4	19.8	21.9	20.9
81	8.4	12.5	20.4	22.8	24.6	23.5
82	9.9	11.8	I	23.1	25.3	23.9
83	9.7	12.4	20.5	23.7	25.0	24.0
84	-0	12.4	21.3	24.8	25.8	24.2
85	10.0	13.9	22.2	25.2	26.8	25.8
86	10.1	14.5	22.7	26.0	27.7	26.1
87	15.2	18.4	24.1	26.5	27.3	26.8

Table 6-1 (cont'd.)

Hole	April	May	June	July	August	Sept
88	I	13.3	21.7	25.3	27.0	25.5
89	10.1	15.2	24.4	26.8	29.3	26.0
90	9.6	14.0	22.3	I	27.7	24.7
91	8.3	11.0	17.8	19.5	23.5	22.9
92	9.2	13.0	21.3	22.5	25.4	23.3
93	10.3	16.0	24.6	27.1	29.4	26.5
94	9.8	14.1	21.3	23.8	27.1	24.3
95	9.7	18.2	24.5	26.5	29.4	24.9
96	11.0	17.8	23.6	26.1	I	25.8
97	10.2	15.4	21.1	22.8	I	23.6
98	11.2	17.5	23.9	25.5	I	26.1
99	9.3	15.1	26.1	23.1	I	23.5
100	9.4	15.8	21.0	24.0	I	23.7
101	9.2	12.6	18.5	22.0	23.2	22.8
102	9.4	11.7	19.8	22.2	26.1	24.3
103	10.7	14.3	23.1	25.0	28.8	26.5
104	10.7	13.2	20.5	23.0	26.4	23.7
105	11.0	13.1	20.5	23.6	26.3	24.7
106	9.9	11.7	16.8	18.3	21.8	20.7
107	9.2	I	16.0	17.8	21.6	20.4
108	10.4	14.2	22.6	25.7	28.0	25.2
109	9.2	11.6	19.0	22.5	25.6	23.4
110	10.1	I	18.9	22.4	25.1	23.0
111	9.2	I	16.9	18.8	23.3	22.5
112	8.9	11.4	19.3	23.0	25.5	22.8
113	9.1	10.6	17.9	21.0	24.2	21.8
114	10.8	14.1	I	25.8	I	I
115	9.9	14.4	21.2	23.9	26.8	24.9
116	10.7	13.4	19.9	24.0	25.8	24.3
117	9.1	11.9	18.4	20.0	22.6	20.8
118	10.1	13.6	21.2	23.7	26.2	23.8
119	10.7	13.4	21.6	23.8	26.1	24.1
120	9.9	12.7	17.0	19.0	22.8	22.8
121	11.7	14.7	22.8	25.7	26.7	25.8
122	10.6	13.7	21.2	23.8	27.1	24.8
123	10.7	I	23.2	25.9	28.3	26.4
124	9.6	15.8	22.1	25.4	26.9	25.0
125	I	14.2	I	I	I	25.8
126	I	16.1	22.5	26.2	29.0	21.5
127	I	15.4	22.8	26.0	28.7	26.2
128	I	13.3	I	20.7	22.1	I
129	I	10.0	14.3	16.8	20.6	I
130	I	14.2	21.1	24.8	I	I
131	I	14.6	21.1	23.5	25.7	23.8

Table 6-1 (cont'd.)

Hole	April	May	June	July	August	Sept
132	I	15.1	20.9	23.6	I	25.0
133	I	I	I	I	I	I
134	10.1	15.2	22.6	26.7	28.3	25.7
135	9.4	14.8	I	I	25.4	23.5
136	I	I	I	I	I	I
137	8.9	12.8	18.9	21.9	24.5	23.7
138	I	15.4	I	23.5	I	24.7
139	12.2	18.3	26.0	29.5	30.2	28.5
140	I	I	21.7	I	I	24.9
141	11.5	-0	I	I	I	I
142	10.5	15.8	21.9	25.3	26.1	24.7
143	10.2	16.2	24.4	28.3	29.4	27.1
144	9.8	17.9	25.9	29.8	30.3	26.9
145	10.0	16.7	I	26.5	27.7	26.2
146	10.3	14.9	24.8	28.4	28.8	26.3
147	10.5	14.9	22.8	25.6	27.5	25.2
148	13.3	18.9	27.5	31.2	32.9	29.3
149	16.7	21.5	29.2	33.2	34.8	32.0
150	8.7	14.4	21.5	25.1	26.0	24.0
151	10.4	14.6	22.3	26.1	27.7	26.0
152	9.7	14.2	22.8	25.6	27.8	25.1
153	10.6	14.3	21.4	25.2	26.1	24.9
154	10.0	16.7	23.1	26.7	28.5	26.5
155	10.1	16.8	23.4	26.7	28.2	26.2
156	9.2	16.1	I	27.0	28.7	26.5
157	9.5	14.8	21.9	25.5	26.8	I
158	9.2	14.4	22.4	26.1	28.1	I
159	11.0	14.7	I	24.9	I	I
160	I	15.4	I	27.0	I	I
161	10.0	15.1	I	I	I	I
162	12.1	17.9	I	I	I	I
163	10.5	I	26.7	30.4	I	29.4
164	I	I	I	I	I	I
165	10.7	16.1	23.8	27.1	I	I
166	11.6	17.8	25.7	29.3	30.6	28.8
167	10.4	-0	I	I	I	I
168	9.4	14.2	21.8	24.8	26.0	24.6
169	9.8	14.2	22.2	29.0	26.9	25.2
170	11.1	15.4	24.6	28.3	29.1	27.5
171	11.8	16.1	24.6	27.9	28.6	27.1
172	10.9	14.5	I	26.1	27.1	26.0
173	11.1	15.9	I	28.2	29.7	27.2
174	10.9	15.1	I	I	28.9	26.7
175	10.6	16.0	I	I	30.2	27.?

Table 6-1 (cont'd.)

Hole	April	May	June	July	August	Sept
176	10.0	13.5	I	25.3	I	26.8
177	9.6	13.7	21.4	I	26.6	23.6
178	9.1	13.9	21.3	I	26.1	23.8
179	I	I	I	I	I	I
180	I	I	21.8	25.5	27.2	25.0
181	I	I	I	28.8	29.6	I
182	I	I	I	I	I	I
183	I	I	I	I	I	I
184	I	I	21.0	25.1	26.7	25.5
185	I	I	22.3	24.6	26.2	24.0
186	I	I	24.2	27.8	29.5	27.9
187	I	I	24.5	27.9	29.8	28.2
188	I	I	22.4	27.1	28.0	26.4
189	I	I	23.0	26.3	28.0	26.5
190	I	I	22.9	26.6	28.0	25.9
191	I	I	22.8	26.3	27.9	25.9
192	I	I	22.4	I	28.1	26.2
193	I	I	22.2	I	27.5	24.7
194	I	I	23.5	I	29.0	26.1
195	I	I	22.0	I	I	I
196	I	I	23.1	26.3	I	I
197	I	I	I	I	I	I
198	I	I	I	I	I	I
199	I	I	I	I	I	I
200	I	I	21.2	22.7	25.2	23.9
201	I	I	18.0	21.0	23.2	23.4
202	I	I	16.7	I	I	I
203	I	I	19.8	23.0	24.4	23.4
204	I	I	19.8	23.0	24.0	23.1
205	I	I	17.2	I	I	I
206	I	I	15.3	18.2	I	I
207	I	I	19.9	23.6	24.8	23.8
208	I	I	23.9	26.7	27.6	25.3
209	I	I	22.7	25.5	27.1	23.8
210	I	I	22.8	25.8	27.3	24.9
211	I	I	22.9	25.8	I	I
212	I	I	23.1	27.2	28.1	26.0
213	I	I	I	I	I	I
214	I	I	22.3	24.4	25.5	24.0
215	I	I	22.2	25.4	26.5	24.4
216	I	I	23.7	26.1	27.5	24.8
217	I	I	I	I	I	I
218	I	I	23.1	I	28.6	I
219	I	I	22.7	26.0	28.5	27.2

Table 6-1 (cont'd.)

Hole	April	May	June	July	August	Sept
220	I	I	18.3	21.8	24.2	25.6
221	I	I	18.1	21.0	23.0	23.8
222	I	I	17.4	21.0	24.5	25.2
223	I	I	18.3	21.5	24.4	24.9
224	I	I	22.2	25.2	26.1	25.3
225	I	I	18.3	21.0	23.0	22.8
226	I	I	I	I	I	I
227	I	I	I	I	I	I
228	I	I	23.8	I	I	I
229	I	I	24.0	I	I	I
230	I	I	24.3	27.8	29.9	28.5
231	I	I	31.9	I	I	33.8
232	I	I	31.9	35.4	I	34.4
233	I	I	30.1	I	I	I
234	I	I	42.0	I	I	I
235	I	I	27.1	31.0	32.0	28.9
236	I	I	18.9	22.0	23.4	22.0
237	I	I	23.2	I	26.8	26.2
238	I	I	24.9	28.5	29.9	27.1
239	I	I	22.4	25.7	27.1	25.6
240	I	I	20.8	23.9	25.0	23.6
241	I	I	20.3	23.2	25.3	23.4
242	I	I	21.8	I	I	25.5
243	I	I	22.6	26.9	27.9	25.8
244	I	I	21.7	24.8	I	I
245	I	I	I	24.6	I	I
246	I	I	I	26.2	28.0	I
247	I	I	I	27.4	28.4	26.9
248	I	I	20.6	24.3	25.5	24.3
249	I	I	22.9	26.4	27.5	24.8
250	I	I	22.0	25.3	26.1	25.5
251	I	I	24.4	27.0	29.5	26.5
252	I	I	24.3	26.5	29.4	26.6
253	I	I	21.8	24.5	27.7	24.2

Table 6-2. Statistical Parameters for Dixie Valley Shallow Temperature Data.

Month	Number of Sites	Mean (°C)	Standard Deviation (°C)	Maximum Temperature	Hole Number	Minimum Temperature	Hole Number	Range (°C)
April	156	10.4	2.0	19.8	38	7.8	4	12.0
May	163	14.5	2.5	30.8	39	9.9	67	20.9
June	207	21.9	3.2	42	234	14.3	129	27.7
July	219	25.0	3.2	40.1	39	16.8	129	23.3
August	197	26.7	2.8	42.1	39	20.6	54,57,129	21.5
September	206	25.2	2.4	39.1	39	20.4	107	18.7

Table 6-3. Means and Standard Deviations of Monthly Air Temperatures at Dixie Valley Shallow Temperature Sites.

Month	Number of Sites	Mean (°C)	Standard Deviation (°C)
April	158	11.7	2.4
May	152	22.9	2.7
June	68	31.1	3.9
July	213	33.3	4.4
August	193	33.1	3.6
September	204	30.9	3.9

less variation than during May, June, July and August.

The grid encircling Hyder Hot Springs also produced some interesting results. The holes closest to the springs generally had lower temperatures than those farther away. These differences were pronounced in June and July (maximum differences greater than 8.8°C) than in August and September (maximum differences on the order of 3.9°C). It is possible that the lower temperatures are caused by evaporative cooling on the hot spring mound. Other than these variations in maximum temperature differences, the temperatures in the Hyder Hot Springs area were not particularly high. The same statement can be made for the Sou Hot Springs-Seven Devils Springs area.

A region of high temperature is hole 61, located in Section 16 about 2.5 miles west of the Boyer Ranch. A maximum temperature of 34.3°C was measured in August. A few holes to the east of hole 61 showed relatively high temperatures, but those to the south and west did not exhibit such high temperatures.

One trend that seems apparent even from a cursory visual examination is the change in the "uniformity" of the temperatures. The April temperatures are the most uniform. The sole exceptions are a few locations in the vicinity of Dixie Hot Springs. This apparent uniformity becomes less obvious as the surveys progress into the summer. However, the same general patterns occur each month.

It is apparent (and has been all along) that the shallow temperatures are strongly influenced by the local hydrologic system. We were somewhat surprised not to see the effects of the July 1979 flash floods on some of the temperatures. These floods occurred along portions of the western side of the valley. One would expect infiltrating flood waters to affect the temperatures in certain areas. This expectation is not strongly supported by visual examination of the August and September temperature data. It is possible that the effects of these floods had not manifested themselves by the last (September) survey or that the effects were not very substantial. Since no quantitative data exist for these floods, it is virtually impossible to quantify their effects on the shallow temperatures. However, temperatures are lower on the alluvial fans directly below the areas where the mountain canyons enter the valley. These lower temperatures could be manifestations of groundwater flow, possibly mountain-front recharge. The

lower temperatures could also be the result of previous, undocumented infiltration events.

Another observation is that the temperatures generally tend to increase as one approaches the Stillwater Range. This could possibly indicate stronger thermal activity around or beneath these mountains.

A study of Tables 6-2 and 6-3 shows a strong correlation between the mean monthly air temperatures and mean monthly 1 meter temperatures. The fact that the air temperature standard deviation for a given month is greater than that for the shallow temperatures indicates that the 1 meter temperatures are less susceptible to variations caused by topography, vegetation and other factors.

6.2.3 Relationship of Shallow Temperatures to Thermal Gradients

Table 6-4 gives the relevant data on the six thermal gradient holes; the locations of these holes are shown on Plate VIII. Table 6-5 shows temperatures in each gradient hole at various depths as well as the June temperatures of the 1 meter hole nearest each hole. The June temperatures were used because they showed the greatest variability (highest standard deviation). Table 6-5 also shows the correlation coefficients from a linear regression analysis which relates the 1 meter temperatures (dependent variable) to temperatures at various depths in the thermal gradient holes (independent variables).

There is a fair correlation between the 1 meter temperatures and the temperatures in the gradient holes. The correlation appears to be stronger at a depth of 1000 feet in the gradient hole, although the amount of data used is insufficient to make a definitive statement. Although not presented in Table 6-5, a correlation coefficient of 0.841 was obtained for a depth of 1500 feet. This number was obtained by assuming that the temperatures at the bottoms of both DD-9 and SR2-A (total depth = 1420 feet each) could be extrapolated to a total depth of 1500 feet. The poorer correlation at 250 and 500 feet (especially the latter) could be the result of quenching by groundwater flow. Groundwater quenching is probably the cause of the low thermal gradients in H-2 and S-8. The latter gradient hole is probably strongly affected by groundwater flow from White Rock Canyon Creek. DD-9 has a relatively cool 1 meter hole nearby but a high thermal gradient.

Table 6-4. Data from Dixie Valley Thermal Gradient Holes.

Hole No.	Depth (feet)	Maximum Temperature (°C)	Thermal Gradient (°C/100')
S-8	500	24	0.2
H-1	1500	97	4.7
H-2	1500	51	2.3
DD-9	1420	84	4.8
SR2	500	63	5.6
SR2-A	1420	91	3.6

Table 6-5. Correlations Between 1 Meter Temperatures and Temperatures at Various Depths in Thermal Gradient Holes.

Gradient Hole	Nearest 1-Meter Hole Number	June T (°C)	Gradient Hole Temperatures (°C) at Various Depths 250 feet	500 feet	1000 feet
S-8	155	24	19	24	--
H-1	61	26	61	68	82
H-2	34	21	25	30	41
DD-9	141	22	38	51	72
SR2	49	26	60	62	--
SR2-A	49	26	58	63	80
Correlation Coefficient			0.782	0.700	0.839

This could indicate a lack of groundwater quenching in DD-9. The other three gradient holes have both relatively high thermal gradients and warm 1 meter temperature holes nearby.

6.3 Conclusions

Shallow temperature surveys have been useful in geothermal investigations. In Dixie Valley, where there is abundant surface evidence of the hydrothermal discharge system, the survey was perhaps not as useful as it would have been in an area without such surface manifestations. With few exceptions, hot spots delineated by the survey corresponded to areas with surface evidence of thermal activity (hot springs and fumaroles). It was therefore difficult to delineate the near-surface hydrothermal discharge system solely on the basis of the shallow temperature survey.

The survey results did reveal that the 1 meter temperatures generally tend to increase toward the Stillwater Range. It would probably be worthwhile to extend the survey into these mountains, although this could be a difficult task. Similarly, it might prove useful to extend the single line of holes running approximately east-west across the valley farther into the Clan Alpine Mountains. Despite the generally warmer temperatures closer to the Stillwaters, temperatures on those portions of the alluvial fans closest to the canyon outlets generally had cooler temperatures. These depressed temperatures were the result of streamflow infiltration and/or groundwater flow. In addition, evidence for quenching at depth was found in thermal gradient holes H-2 and S-8 by comparing their gradients to the nearest 1 meter hole.

Some success was obtained correlating the shallow temperature distribution to faults in the valley. In a few isolated instances the location of faults could be confirmed, but success was not widespread.

Comparison of the six monthly surveys indicated that with the exception of the April survey, the same trends appeared each month. This implies that single monthly survey data are sufficient, and that six consecutive monthly surveys are unnecessary. A better approach than the one used herein would be to take one survey in the summer (perhaps July) and one in the winter (perhaps January) in order to

account for differing soil thermal conductivities (Olmsted, 1977). In fact, if only a single survey is to be done, it is probably best to conduct it during a winter month. A winter-month survey should show the maximum temperature contrast at a depth of 1 meter. The reason for this is the depletion of stored heat in the near surface which would otherwise equalize temperatures at a shallow depth (Miller, 1978).

Although no measurements were made of the soil thermal diffusivities at the 1 meter locations, Miller (1978) states that for most types of soil, temperatures at a depth of 1 meter scarcely react to diurnal temperature fluctuations. However, the soil temperature per se was not being measured, but the temperature of a water-antifreeze mixture at the bottom of a PVC pipe. The one meter depth should provide sufficient protection from the diurnal changes, although we did not substantiate this belief. Two meter or 1.5 meter holes would probably have been better. No corrections were made for the annual temperature wave, which penetrated to depths much greater than 1 meter.

In conclusion, the shallow temperature survey in Dixie Valley did yield useful information, although not as much as would have been obtained in an area without surface evidence of faulting and hydrothermal activity. The local hydrology, particularly the shallow groundwater flow system, undoubtedly affected the shallow temperatures to an unknown degree by masking and redistributing geothermal heat.

6.4 References

Banwell, C.J., 1964, Geothermal drillholes--physical investigations: UN Conference on New Sources of Energy, Rome, Proceedings E/Conf. 35/6/53, p. 61-71.

Birman, J.H., 1969, Geothermal exploration for ground water: Geol. Soc. America Bull., v. 80, n. 4, p. 617-630.

Bouwhijsen, Van Den, J.N.A., 1934, The thermocouple proves useful on a geophysical survey: Engineering and Mining Journal, v. 135, n. 8, p. 342-344.

Bredehoeft, J.D. and I.S. Papadopulos, 1965, Rates of vertical groundwater movement estimated from the earth's thermal profile: Water Resources Research, v. 1, n. 2, p. 325-328.

Cartwright, K., 1968, Temperature prospecting for shallow glacial and alluvial aquifers in Illinois: Illinois Geol. Survey Circular 433, p. 1-41.

Cartwright, K., 1970, Groundwater discharge in the Illinois basin as suggested by temperature anomalies: Water Resources Research, v. 6, n. 3, p. 912-918.

_____, 1971, Redistribution of geothermal heat by a shallow aquifer: Geol. Soc. Amer. Bulletin, v. 82, n. 11, p. 3197-3200.

_____, 1974, Tracing shallow groundwater systems by soil temperatures, Water Resources Research, v. 10, n. 4, p. 847-855.

Combs, J., 1975, Summary of section IV geophysical techniques in exploration: Second U.N. Symposium on the Development and Use of Geothermal Resources, San Francisco, Proceedings, p. xxxi-xxxvi.

Kappelmeyer, O., 1957, The use of near-surface temperature measurements for discovering anomalies due to causes at depths: Geophysical Prospecting, v. 5, n. 3, p. 239-258.

Kintzinger, P.R., 1956, Geothermal survey of hot ground near Lordsburg, New Mexico: Science, v. 124, p. 629-630.

Miller, D.W., 1978, Hydrogeologic analysis of shallow hole temperatures at Allen Springs and Lee Hot Springs, Churchill County, Nevada: unpublished M.S. thesis, Univ. of Nevada-Reno, 73 p.

Olmsted, F.H., 1977, Use of temperature surveys at a depth of 1 meter in geothermal exploration in Nevada: U.S. Geological Survey Professional Paper 1044-B, 25 p.

Parsons, M.L., 1970, Groundwater thermal regime in a glacial complex: Water Resources Research, v. 6, n. 6, p. 1701-1720.

Poley, J.P. and J. Van Steveninck, 1970, Delineation of shallow salt domes and surface faults by temperature measurements at a depth of approximately 2 meters: Geophysical Prospecting, v. 18, p. 666-700.

Smith, E.M., 1974, Exploration for a buried valley by resistivity and thermal probe surveys: Ground Water, v. 12, n. 2, p. 78-83.

Stallman, R.W., 1970, Notes on the use of temperature data for computing groundwater velocity: 6th Assembly on Hydraulics, Rep. 3, p. 1-7, Soc. Hydrotech. de France, Nancy, France.

_____, 1965, Steady one-dimensional fluid flow in a semi-infinite porous medium with sinusoidal surface temperature: J. Geophysical Research, v. 70, n. 12, p. 2821-2827.

Supkow, D.J., 1971, Subsurface heat flow as a means for determining aquifer characteristics in the Tucson basin, Pima County, Arizona: unpublished Ph.D. dissertation, Univ. of Arizona, 182 p.

Chapter 7. MODELS OF THE DIXIE VALLEY GEOTHERMAL SYSTEM

By: Elaine J. Bell, D. Burton Slemmons, Robert A. Whitney, Thomas R. Bard, Roger L. Jacobson, Michael E. Campana, Russell W. Juncal, Lawrence T. Larson, Burkhard W. Bohm, and Neil L. Ingraham

7.0 MODELS OF THE DIXIE VALLEY GEOTHERMAL SYSTEM

7.1 Introduction

The purpose of the MMRI program of investigation was to develop an integrated model of the Dixie Valley area for a geothermal system that is based on both available data and new data derived from the specific investigations in four general disciplines or fields of study (structure-tectonics, petrology, hydrology-hydrogeochemistry, and shallow temperature surveys). The results of these individual investigations are presented in the preceeding chapters of this report. While developing the program of study, an initial model based upon a knowledge of the general regional relationships and limited site-specific data was prepared; this initial model will be referred to as the "proposal model". During the MMRI program this proposal model was evaluated and modified as new data were generated. The second stage of developing a new model was to re-evaluate the data as a series of specific models for each of the disciplines. Finally, these models are now consolidated and integrated to form a new model, to be referred to as the "integrated model" of the Dixie Valley Geothermal System.

7.2 Proposal Model

The initial model for the proposal was based on an evaluation of limited site-specific data (Keplinger and Associates, 1978; Senturion Sciences, 1977, 1978a, b; Thompson and others, 1967; Micro Geophysics, 1976; Exploration Data Consultants, 1976). Figure 7-1 illustrates, in map view, the major elements of the model, including faults and areas of aeromagnetic and gravity anomalies. Figures 7-2 and 7-3 present generalized east-west cross-sections of the model indicating the inter-relationships among the various tectonic elements, inferred heat sources, and distribution of the Humboldt Lopolith as a capping mechanism for the reservoir.

There are three major problems with this initial proposal model. First, the Stillwater fault is shown as a high-angle reverse fault. This is inconsistent with the extensional tectonic regime of the Basin and Range Province and with both the field expression of the fault and the focal plane solutions of the 1954 Dixie Valley earthquake (Ryall and Malone, 1971). Second, a thrust fault, the Stillwater thrust, is shown in

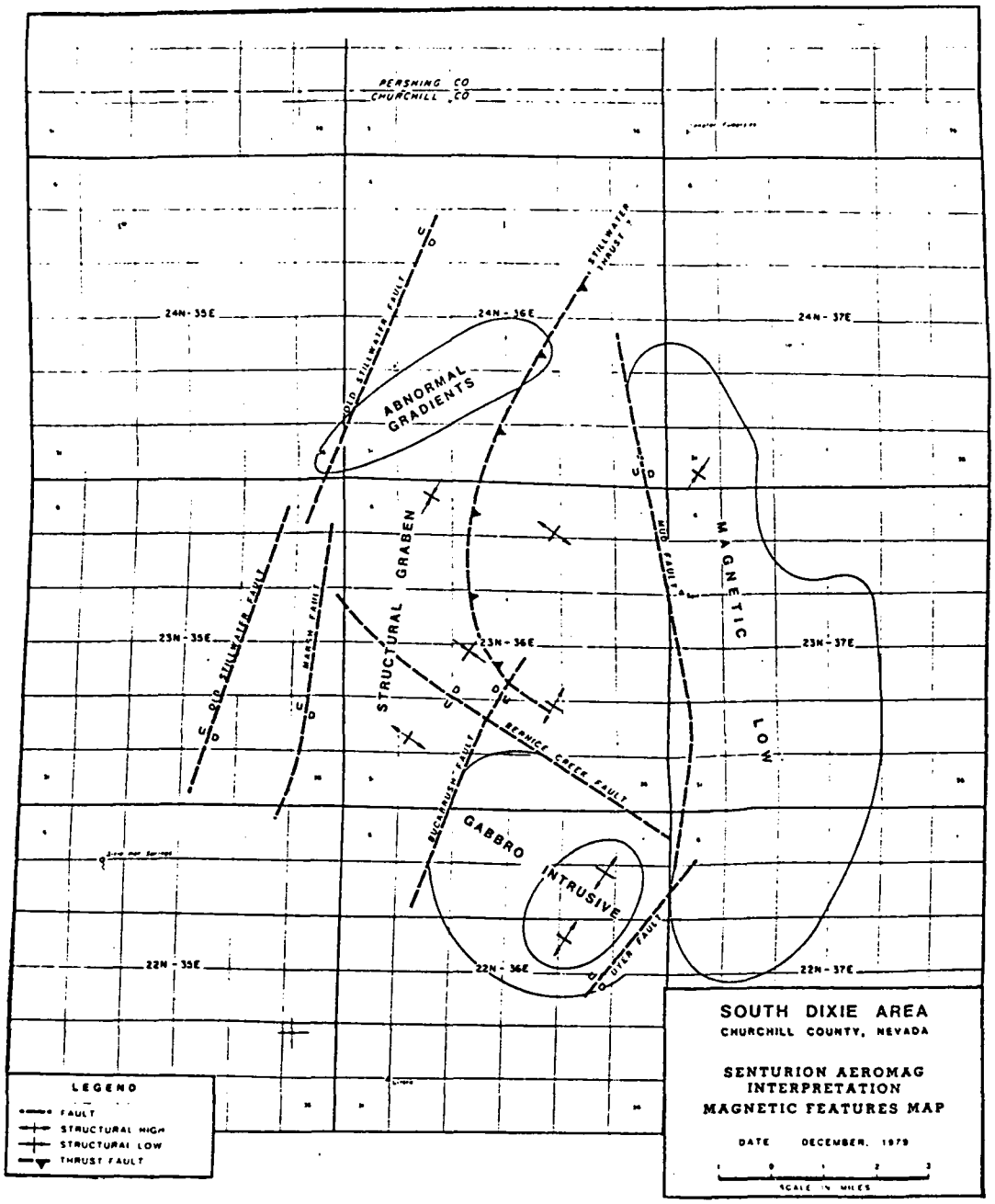

Figure 7-1. Map view of proposal model of the Dixie Valley Geothermal System. Faults and anomalous regions are based on an interpretation of aeromagnetic data by Senturion Sciences (1977, 1978).

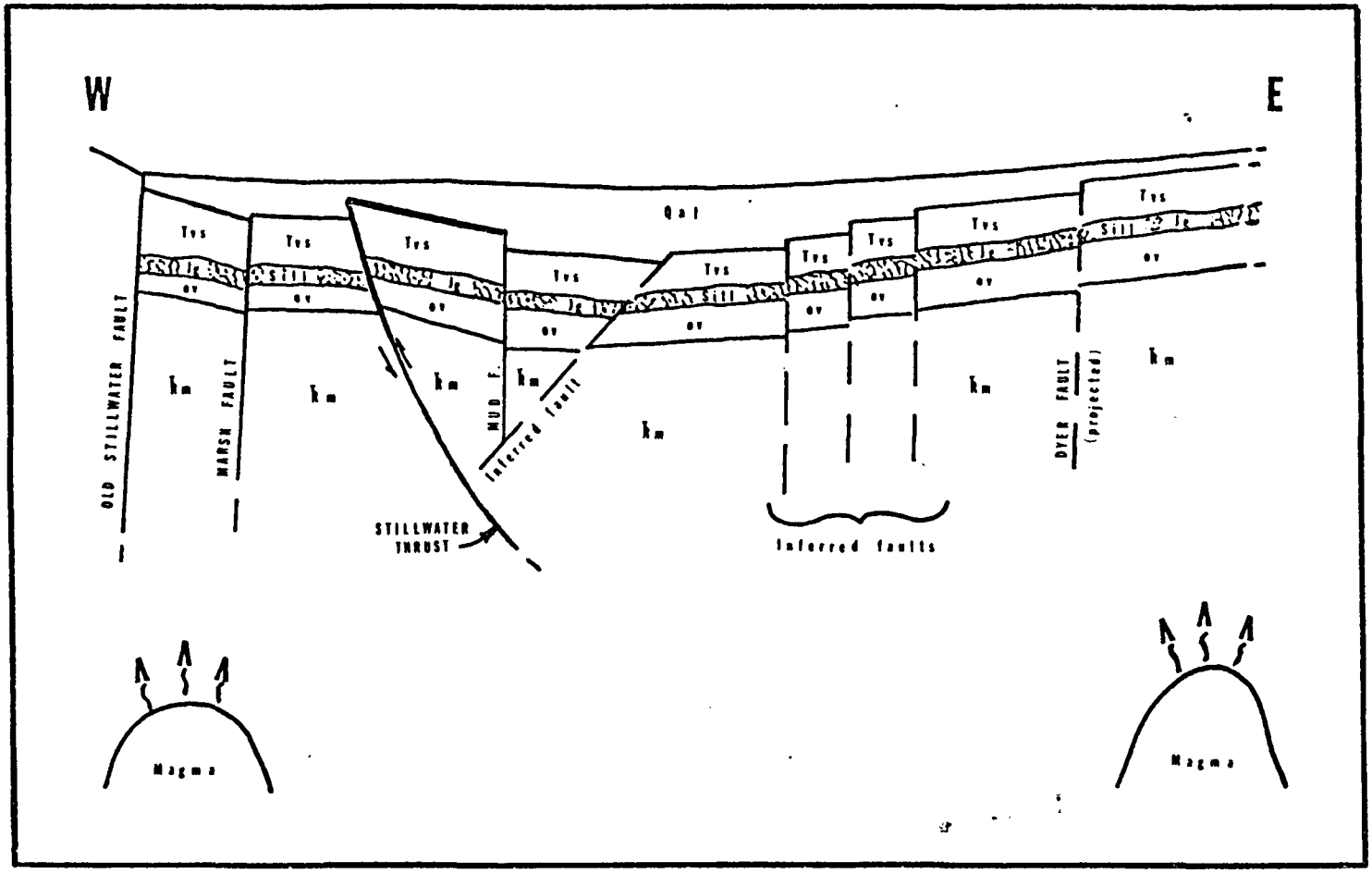

Figure 7-2. Generalized east-west cross-section of proposal model showing inter-relationships of the elements of the model. Qal - Quaternary alluvium; Tvs - Tertiary volcanics and sediments; Jg - Jurassic Humboldt Lopolith gabbro; ov - older volcanics; Trm - Triassic metasediments, highly fractured phyllite and slate; arrows indicate displacement vectors on faults.

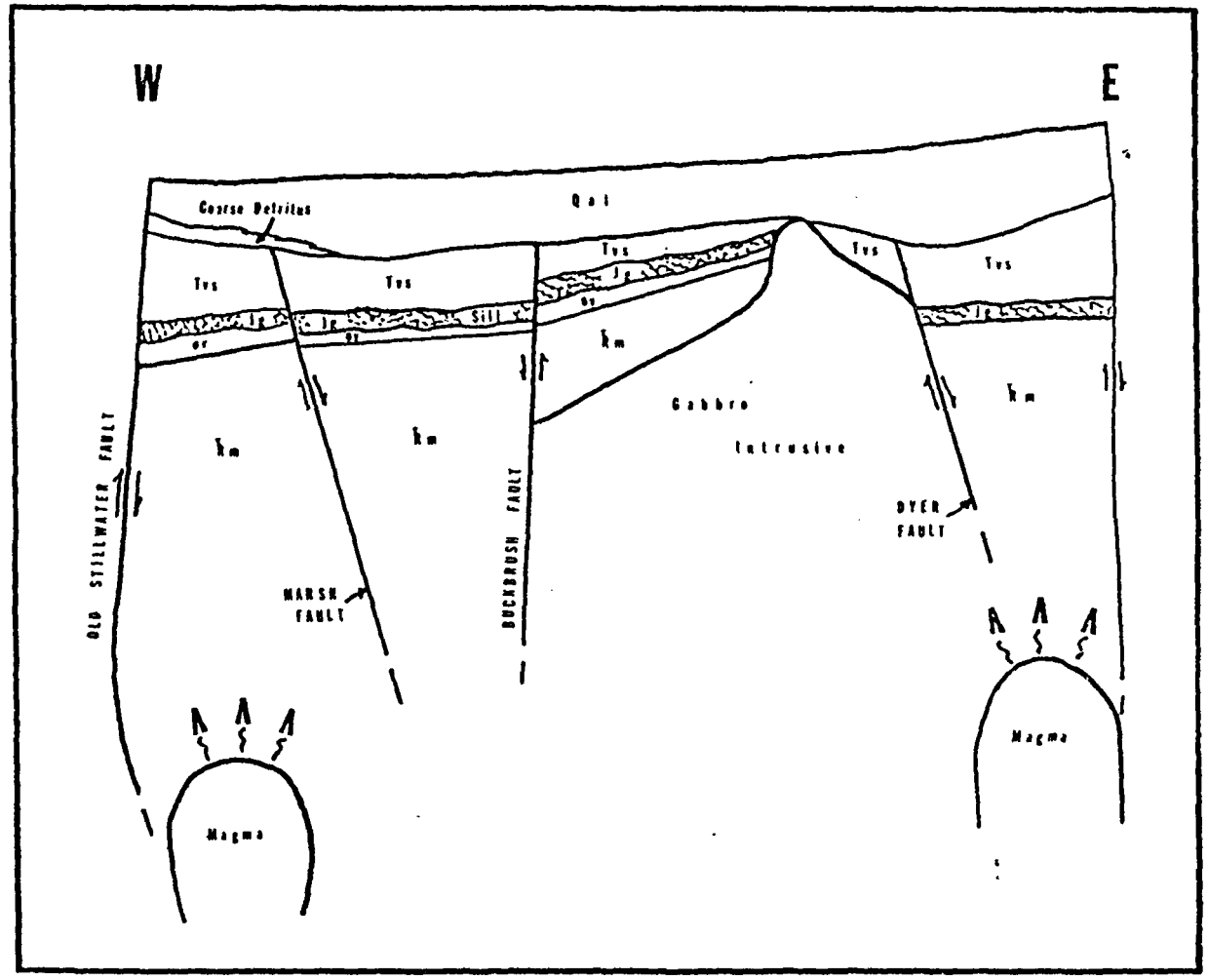

Figure 7-3. Generalized east-west cross-section of proposal model showing inter-relationships among the elements of the model. Qal - Quaternary alluvium; Tvs - Tertiary volcanics and sediments; Jg - Jurassic Humboldt Lopolith, gabbro sill; ov - older volcanics; km - Triassic metasediments, highly fractured slate and phyllite.

the central portion of the Valley; this too is inconsistent with the extensional tectonic regime. And third, the subsurface stratigraphy is projected as consistent throughout the Valley and corresponding to the range front stratigraphy, even though the subsurface data and comparison of the lithologies exposed in the Stillwater Range and Clan Alpine Mountains are not adequate to substantiate either the stratigraphic sequence and physical nature of the units, or the geographic distribution and continuity of the units as shown. A "cap" of Humboldt Lopolith gabbro overlying very highly fractured Tertiary metasediments was assumed to be an important characteristic of the model.

Thus, this initial model provided the basis for defining the MMRI program of investigation and served as a working model that required refinement and verification to allow development of an integrated model of the Dixie Valley Geothermal System.

7.3 Integrated Model

The integration of the single-discipline models based on structural-tectonic analysis, petrologic alteration studies, hydrology-hydrogeochemistry, and shallow temperature surveys resulted in a new model of the Dixie Valley Geothermal System as presented in Figures 7-4 and 7-5.

7.3.1 Structural Setting

The structural setting of the integrated model is presented in Figure 7-4. Key elements of this setting include: 1) Basin and Range extensional faults; 2) Humboldt gabbroic complex; and 3) White Rock Canyon fault.

7.3.1.1 Basin and Range Extensional Faults

The structure of the northern portion of Dixie Valley is a complex, asymmetric graben, with portions of the inner graben complex defined by splays of the bounding faults. These structural-tectonic features are delineated by various geophysical data, as well as by their surface expression. These faults, their geographic distribution within the Valley, inter-relationships, and observable displacements are all consistent with the regional extensional tectonics of Dixie Valley and the northern Basin and Range Province. Many of these faults serve as preferential conduits for fluid migration, as evidenced by the spatial correlation of surface

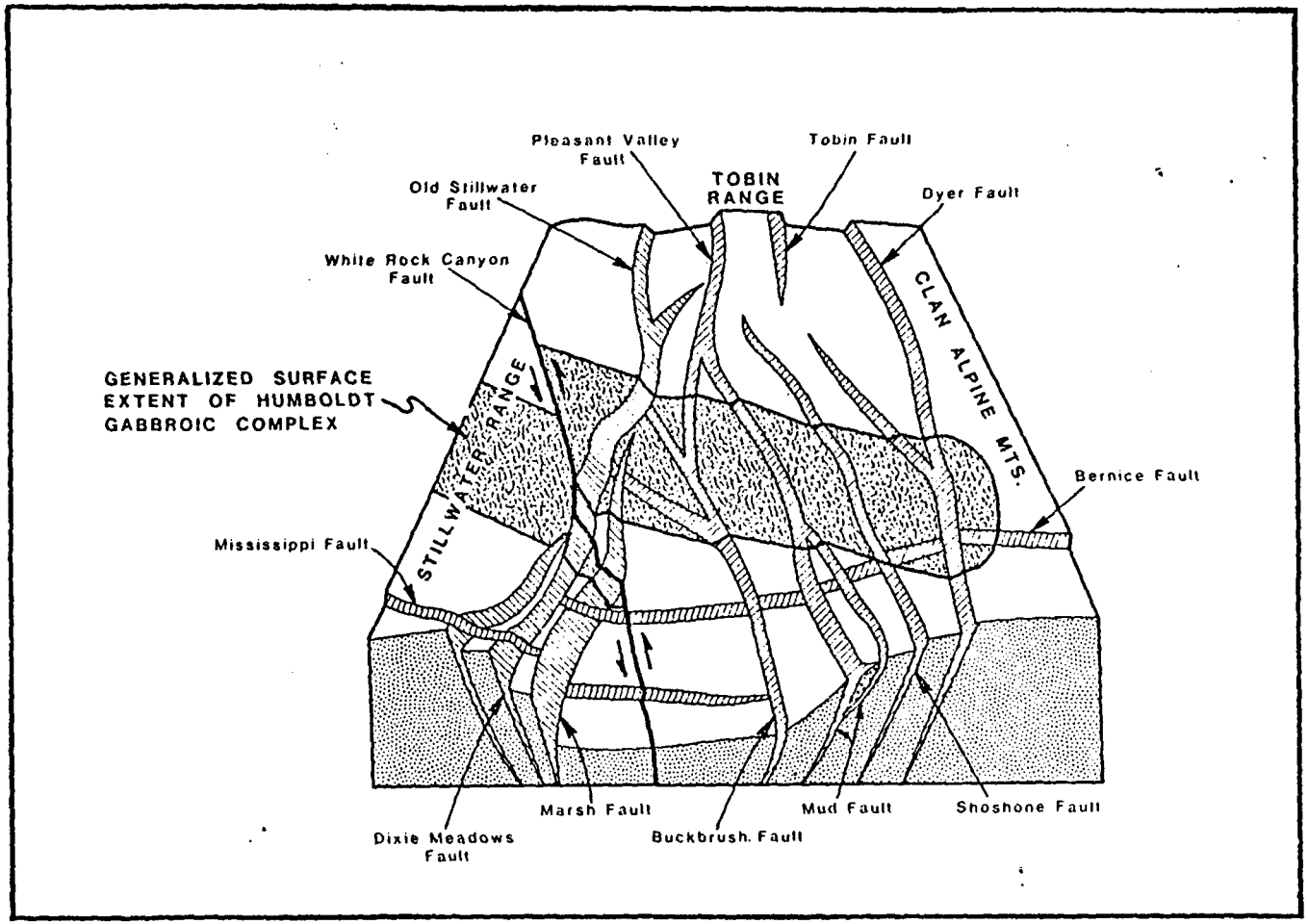

Figure 7-4. Three dimensional view of integrated model of the Dixie Valley Geothermal System. Note that the generalized surface extent of the Humboldt gabbroic complex merely defines an area within which the complex may be encountered, and in no way implies continuity of the unit within those boundaries.

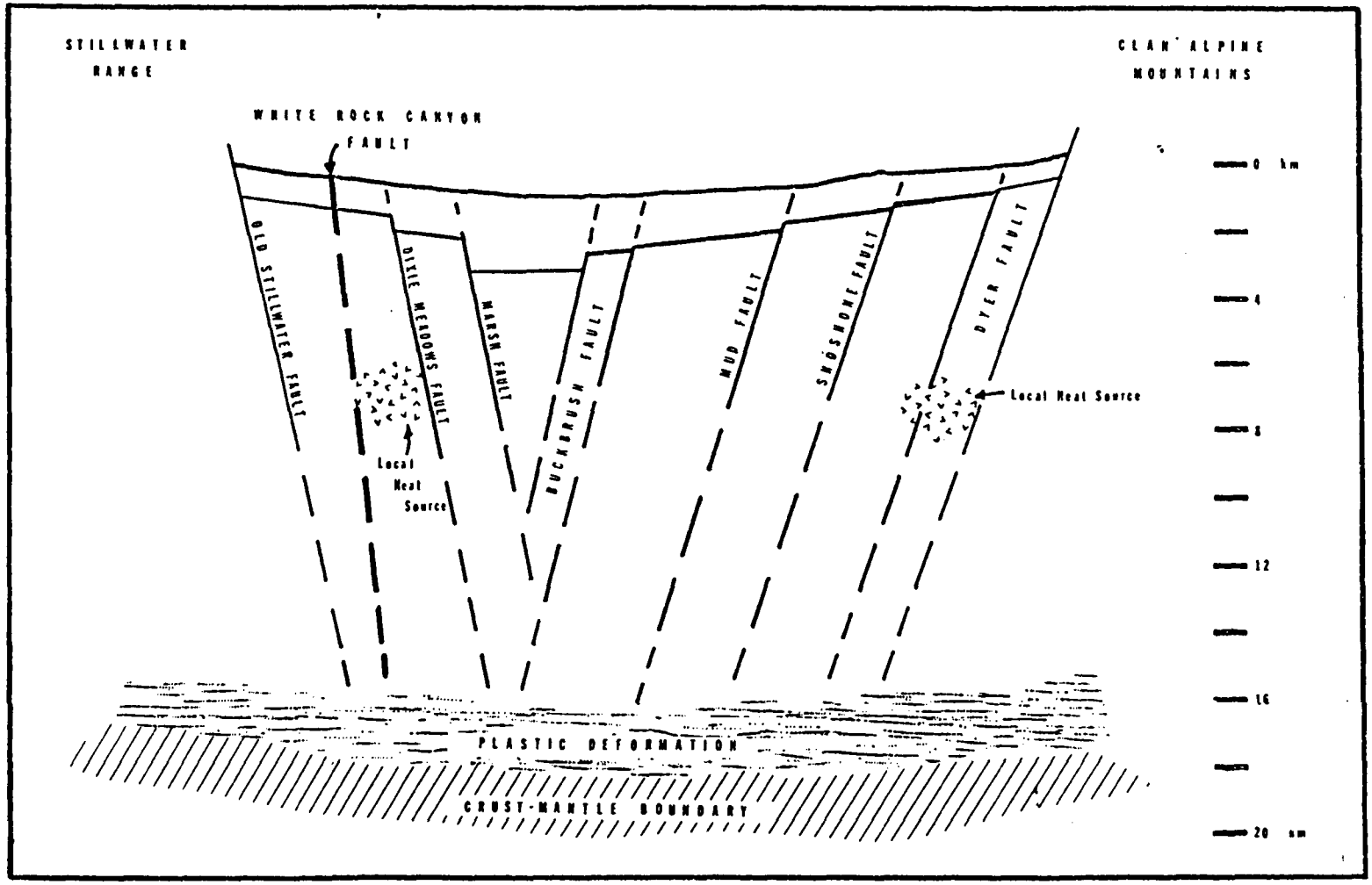

Figure 7-5. Generalized east-west cross-section of the integrated model of the Dixie Valley Geothermal System. Structural elements (faults) are propagated downward from the surface through the valley fill (alluvium with intercalated volcanics) and into the underlying undifferentiated bedrock and then projected through the zone of brittle failure.

springs, seeps and fumaroles, as well as the surface and subsurface concentration of intense hydrothermal alteration along these fracture zones, particularly along the major range front faults.

7.3.1.2 Humboldt Gabbroic Complex

The geographic distribution of surficial outcrops of the Humboldt gabbroic complex in the West Humboldt Range, Buena Vista Hills, Stillwater Range and Clan Alpine Mountains is accepted from Speed (1976). However, it appears that the Humboldt complex is not a continuous unit either on the surface or within the subsurface.

Two intrusive 'phases' of the complex were identified in the subsurface. The first, diorite/gabbro, is medium to coarse-grained primarily plagioclase and pyroxene, with secondary minerals including hornblende, chlorite, magnetite, epidote, albite, calcite, pyrite and titanium minerals (ilmenite and leucoxene). The second, granodiorite, has biotite and hornblende as the principal ferromagnesian minerals, with plagioclase and K-feldspar. These two phases have been reported in the Sun Oil Company wells SW Lamb #1 and #3, and SW Lamb #2, respectively, Only the diorite/gabbro phase was present in DF 45-14 as thin (average 30 foot thick) dikes intruding the Triassic metasediments; both phases were identified in DF 66-21 with the granodiorite phase much more dominant. The diorite/gabbro and the granodiorite phases of the Humboldt gabbroic complex exhibit evidence of deuteric alteration; however, obvious hydrothermal alteration is most intense and concentrated along fracture zones.

The intrusive phases of the Humboldt gabbroic complex are subjacent to an extrusive phase of a volcanic sequence and associated intercalated red clay ((?) hematitic mudstone of Speed, 1976). This relationship was identified in DF 66-21 and reported for the Sun Oil Company wells SW Lamb #1 and #3.

The subsurface stratigraphy encountered by the various deep exploratory wells, the surface outcrop pattern and a re-evaluation of the geophysical data (particularly the aeromagnetic data) suggest that the Humboldt gabbroic complex is not a continuous lopolithic unit, but rather is a discontinuous intrusive-extrusive complex of dikes, sills, plugs, and volcanics. Furthermore, distribution of the complex is controlled by faults associated with post-emplacement graben formation within the extensional Basin and Range tectonic regime and also with major basement

faults, including the White Rock Canyon fault.

The concentration of intense hydrothermal alteration along fracture or fault zones in the Humboldt gabbroic complex is also characteristic of other lithologic units encountered in the surface, such as the Triassic metasediments and younger volcanics and alluvium. Where units are not fractured, the alteration is much less intense and the water chemistry suggests that fluids within the non-fractured rock are essentially stagnant or have very long residence times.

7.3.1.3 White Rock Canyon Fault

The north-south trending White Rock Canyon fault exhibits left-lateral displacement suggested by geophysical data and by surficial expression of the fault. The 10 to 12 miles of apparent left-lateral offset of the Humboldt gabbroic complex is post-middle Jurassic. The location and orientation of the fault zone appears to have been determined by pre-middle Jurassic structural control. Major left-lateral displacement on this fault zone may be related either to development of the mid-Miocene Cortez Rift, or to a conjugate structure of the apparent post-mid-Miocene right-lateral displacement of the Cortez Rift across the high lava plains at the northern boundary of the Great Basin (Figure 2-15). These relationships may also be due to compressional tectonics as the Farallon Plate was being subducted along the west coast margin. Surficial expression as vegetation and tonal contrasts and lineations within the young alluvial sediments of Dixie Valley indicates Quaternary fault activity, including Holocene displacement along this zone.

Regardless of the time of initiation and major deformation on the White Rock Canyon fault, it appears to be a significant regional structural element critical to the model of the Dixie Valley Geothermal System. The White Rock Canyon fault, as a major basement fault, may act as a western boundary for a region of fluid (i.e., heat) migration from depth to the surface. The overall geochemical difference between Dixie Meadows hot springs to the south and Hyder and Sou Hot Springs to the north implies that a major structural barrier may exist northeast of Dixie Meadows -- i.e., the White Rock Canyon fault. Major tectonic activity, including the 1954 Dixie Valley earthquake, along the Old Stillwater fault south of the intersection with the White Rock Canyon fault may have effectively terminated direct communication of the Dixie Meadows hot springs

with a deep heat source. It should be noted that there are distinct geochemical differences between the Hyder-Buckbrush system (linked by the Buckbrush fault) and Sou Hot Springs, both east of the White Rock Canyon fault, implying a lack of general communication among fluids within the Dixie Valley Geothermal System.

7.3.2 Structural Relationships

The structural relationships of the integrated model are depicted in a generalized east-west cross-section in Figure 7-5. The structural-tectonic features (faults) delineated by surficial expression and by geophysical surveys are propagated downward from the surface through a zone of brittle failure to approximately 12 to 15 km depth. From 16 to 18 km depth, is a zone where plastic deformation dominates. The crust-mantle boundary in the Dixie Valley region is between 18 and 20 km depth with the underlying mantle acting as a regional heat source. The White Rock Canyon fault is shown as a major western boundary for a region of upward migration of thermal fluids.

Localized heat sources are depicted within the crust at depths of 6 to 8 km. Based upon magnetotelluric data (Keplinger and Associates, 1978), shallow heat sources were defined along the eastern edge of the Stillwater Range in the vicinity of the Dixie Comstock mine and northward. Similar shallow crustal heat sources are depicted on the diagram; these may represent localized intrusions of magma, with locations and extent that are structurally controlled. For the Dixie Comstock area, the Old Stillwater and Marsh faults, and possibly the Bernice Creek fault, are inferred to be the conduits. Based upon an interpretation of the distribution of the shallow temperature survey data in which anomalies on the west side of the Valley correlate with the locations of these shallow crustal heat sources, a localized heat source is also inferred to exist under the east side of Dixie Valley associated with the Dyer and Bernice Creek faults.

7.3.3 Summary

The Dixie Valley Geothermal System thus appears to be a result of regionally high mantle heat flow through a thin crust, with preferential conduits for fluid migration structurally controlled by the White Rock

Canyon and other major basement faults, and by Basin and Range extensional faults within the Valley. The geothermal system apparently does not have a specific cap rock. Rather, it appears that several lithologies within the Valley such as the Humboldt gabbroic complex, the 'red clay', or the Triassic metasediments are impervious to general fluid flow and production zones may be found in association with any of these units if there is communication by fracture or fault zones with the reservoir at depth and sufficient fluid to transport the heat.

7.4 References

Exploration Data Consultants, 1976, Gravity and magnetic survey over the Humboldt Salt Marsh, Dixie Valley, Nevada: Cons. Rept. for Dow Chemical, December 1976, 8 p.

Keplinger and Associates, 1978, Interim evaluation of exploration and development status, geothermal potential and associated economics of Dixie Valley, Nevada: Cons. Rept. prepared for Millican Oil Company, September 1978, 59 p.

Koenig, J.B., Greensfelder, R.W., and Klein, C.W., 1976, Geothermal potential of the Quest Leasehold, Dixie Valley, Nevada: Rept. for Dow Chemical, December 1976, 10 p.

Micro Geophysics, 1976, Seismicity report on the Dixie Valley Prospect, Churchill County, Nevada: Cons. Rept. for Southland Royalty Company, December 1976, 46 p.

Ryall, Alan, and Malone, S.D., 1971, Earthquake distribution and mechanism of faulting in the Rainbow Mountain-Dixie Valley-Fairview Peak area, central Nevada: Jour. Geophys. Res., v. 76, p. 7241-7248.

Senturion Sciences, 1977, High-precision multilevel aeromagnetic survey over Dixie Valley, Part I: Rept. for Southland Royalty Company, October 1977, 15 p.

Senturion Sciences, 1978a, High-precision multi-level aeromagnetic survey over Dixie Valley, Part II: Rept. for Southland Royalty Company, June 1978, 13 p.

Senturion Sciences, 1978b, South Dixie Valley, Nevada, scalar magnetotelluric survey report: Cons. Rept. for Southland Royalty Company, February 1978, 45 p.

Speed, R.C., 1976, Geologic map of the Humboldt Lopolith and surrounding terrane: Geol. Soc. America Map MC-14, 4 p.

Thompson, G.A., Meister, L.J., Herring, A.T., Smith, T.E., Burke, D.B., Kovach, R.L., Burford, R.O., Salehi, A., and Wood, M.D., 1967, Geophysical study of the Basin-Range structure, Dixie Valley region, Nevada: U.S. Air Force Cambridge Research Labs. Spec. Rept. 66-848.

Chapter 8. EVALUATION OF THE INTEGRATED MODEL OF THE DIXIE VALLEY GEOTHERMAL SYSTEM

By: Elaine J. Bell, Michael E. Campana, Roger L. Jacobson, Lawrence T. Larson, D. Burton Slemmons, Thomas R. Bard, Burkhard W. Bohm, Neil L. Ingraham, Russell W. Juncal, and Robert A. Whitney

8.0 EVALUATION OF THE INTEGRATED MODEL OF THE DIXIE VALLEY GEOTHERMAL SYSTEM

8.1 Introduction

The integrated model of the Dixie Valley Geothermal System should be considered as a second phase of model development for the Dixie Valley region. Therefore, the following recommendations are presented as the types of additional investigations considered necessary to refine and verify the integrated model. These recommendations are focussed on obtaining additional data from previous sources (e.g., the deep exploratory wells) and on developing new sources of data, particularly for the subsurface. These recommendations indicate where insufficient data are available to completely verify inter-relationships of elements of the model or to define the specific role that an element has in the model, or where additional data could define additional elements critical to understanding the Dixie Valley Geothermal System.

8.2 Recommendations

The following recommendations were generated by the present MMRI program of investigation:

1. Theoretical analysis of the thermal gradient data from existing shallow gradient holes, existing deep exploratory wells, and any additional wells that may be drilled in Dixie Valley. In theory, it is often possible to obtain transmissive, mixing and other properties of the porous medium from these data. It is sometimes possible to distinguish (separate) conductive and convective heat transfer. Analysis of this type is not routine, i.e., a fair amount of theoretical work would be required. However, the methods developed would be applicable to evaluating any hydrothermal system.

2. The hydrogeochemical and isotopic investigations should be expanded to include all of Dixie Valley as well as surrounding valleys. Extensive work of this nature should also be conducted in the Stillwater Range and Clan Alpine Mountains. Additional isotopes should be used; these might include ^{14}C, ^{13}C, ^{34}S and ^{3}He, among others. The purpose of this investigation would be to substantiate the regional nature of the Dixie Valley hydrologic system(s), to better delineate the heat

sources, and to understand the origin and circulation patterns of both thermal and non-thermal waters.

3. Fluid samples should be collected with time from both DF 45-14 and DF 66-21. Both chemical and isotopic analyses should be performed on these samples. Useful information would also be obtained by conducting drill-stem and/or other tests on these wells or on any future wells drilled in the Valley. Drill-stem testing would yield pressure and permeability data, as well as fluid samples from depth. Regardless of the method used, obtaining fluid samples at depth (in situ and uncontaminated) would provide important information. Time series samples should also be obtained from selected springs; vapor samples should also be collected. Stable isotope geothermometry should be utilized to provide additional information on reservoir temperatures.

4. The construction of a quantitative (numerical or mathematical) model should be investigated. Data obtained from the testing of DF 45-14 and DF 66-21 would be invaluable in formulating a model of this type -- it should be noted that the testing of these wells would provide a wealth of information even if the model were not constructed. The proposed model would be more interpretive than predictive; its prime purpose would be to guide exploration and exploitation by enhancing our comprehension of the physico-chemical processes occurring in the reservoir.

5. The shallow temperature survey should be expanded into selected areas, mainly into the Stillwater Range and the Clan Alpine Mountains to verify the presence of high heat flow. A logical place for this extension would be along the cross-valley profile line. Other locations in the mountains and the Valley itself should be surveyed. Two-meter holes should be installed.

6. Efforts should be made to obtain data from between the shallow groundwater zone (i.e., a few hundred feet deep) and the geothermal reservoir zone. Both pressure and fluid samples should be obtained from this intermediate zone, either by using the existing exploratory

wells or by drilling holes specifically for this purpose. In any case, efforts should be made during future drilling programs to obtain reliable hydrologic, isotopic and hydrogeochemical data from the wells. Collection of these data will add to the expense of drilling, but will provide invaluable data. It might be useful to conduct a drilling program especially for this purpose. These holes would be on the order of a few thousand feet deep, and would be located in areas designed to maximize the amount and types of information obtained, as well as the geographic distribution of such data.

7. Shallow gradient holes should be drilled both at selected hot spring areas and at selected intervals along the cross-valley line. The piezometric surface and water chemistry should be evaluated with respect to depth, and lateral variation in the piezometric surface should be noted. This data along with aquifer properties, such as permeability, will allow calculation of fluid flow rates under present conditions and will be important in understanding how the geothermal reservoir may react to development.

8. Petrographic geothermometers based on the concentrations of trace elements in single minerals or mineral species may indicate past history of the reservoir or present reservoir temperatures. This type of geothermometer has an established theoretical and practical base; however, it has not been utilized to any extent in geothermal investigations but could prove useful. As various minerals are heated, larger concentrations of trace elements are able to be incorporated into the crystal structure. With carefully selected sampling, it is possible to determine which areas have undergone the highest temperatures in the past. This information does not duplicate any presently collected data and could prove to be a very useful technique for exploration and reservoir analysis.

9. A detailed bedrock geology study of the Stillwater Range and the Clan Alpine Mountains should be conducted to determine specific stratigraphic and structural relationships. This would delineate the limits of exposed key stratigraphic units in the mountains and would provide additional frame of reference for evaluating the stratigraphy en-

countered in the existing deep exploratory wells and future wells drilled in the Valley. In addition, critical units should be age-dated for correlation with the subsurface stratigraphy.

10. Core samples should be taken from critical units encountered in any future wells drilled in the Valley and side-core samples should be obtained from the existing deep exploratory wells. These samples should be age-dated to provide a basis for correlations between wells and with the regional stratigraphic sequence. Thin-sections of these cores would provide uncontaminated whole rock samples for petrologic and petrographic analysis of the hydrothermal alteration effects, as well as allowing for identification of the total mineral assemblage present at a specific depth. This data when correlated with the water chemistry for that depth would allow an evaluation of the equilibrium status of the system. These core samples could also be used for the petrographic geothermometry.

11. A regional analysis of the White Rock Canyon fault zone should be conducted. If the White Rock Canyon fault is indeed a significant regional structure that may have communication with a deep heat source or control the migration of heat from that source, then a regional analysis of the White Rock Canyon fault, beyond Dixie Valley, is necessary and could provide an understanding of the geothermal resources of western Nevada. Regionally, the fault is defined by a strong topographic lineament, by contrasts in lithologies, by the distribution of known surface manifestations of geothermal systems, and by a close spatial correlation with the Ventura-Winnemucca seismic zone. Multi-level aeromagnetic and gravity profiling along the White Rock Canyon fault zone would aid in delineating subsurface evidence of associated geothermal activity. Structural-tectonic analysis of the zone based on low-sun-angle aerial photographic analysis would delineate the fault zone and would provide a basis for generalized surficial mapping and identification of specific surface manifestations of any underlying geothermal systems along the zone.

12. Detailed tectonic analysis of selected structural-tectonic features within Dixie Valley would provide a basis for understanding the mechanics of faulting within the Valley as it relates to the regional tectonic regime and provides a structural framework for the geothermal system. Such analysis might include fault scarp profiling, trenching, age-dating of appropriate materials, detailed surficial geologic mapping and a re-evaluation of available low-sun-angle aerial photography.

13. A minimum of three cross-valley reflection seismic profiles should be conducted. The interpretation of these profiles would be invaluable in verifying the subsurface structure of the Valley and the general geographic and stratigraphic relationships and distribution of the critical lithologies. One profile should transect the northern end of the Valley between Hyder Hot Springs and Sou Hills; a second profile should transect the Valley intersecting DF 66-21 and extend across the Shoshone Creek area; and a third profile should intersect DF 45-14 and extend across the Valley to the vicinity of Hoyt Canyon. These profiles should extend as far as possible into the mountains on both sides of Dixie Valley.

14. The multi-level aeromagnetic survey of Dixie Valley should be extended to include a larger area to the north and east. This could define anomalies of significant geothermal potential for exploration and development.

15. A detailed gravity survey should be conducted within Dixie Valley. This technique has proven useful in other regions where the local geologic and tectonic parameters control 'hot spots' that may be associated with either gravity highs or gravity lows depending on the specific setting. The anomalies could define areas of significant geothermal potential for exploration and development.

16. Additional deep exploratory wells should be drilled in Dixie Valley. A well should be drilled on the west side of the White Rock Canyon fault in the vicinity of Dixie Meadows to determine the extent to

which this structure acts as a barrier to migrating fluids or heat, and to identify the nature of the possible shallow crustal heat source and the conduits associated with Dixie Meadows. A well should be drilled in the center of the Valley, preferably along a cross-valley seismic reflection profile, to provide verification of the subsurface structural and stratigraphic configuration. A well should be drilled to the north of DF 66-21 and toward the center of the Valley to determine the subsurface configuration and extent of the reservoir encountered by DF 66-21 and by the Sun Oil Company wells. Ideally, during drilling of these and any other wells both uncontaminated water and core samples will be collected and the appropriate well testing will be conducted to obtain the maximum amount of data pertaining to the hydrologic system(s) encountered, such as flow rates, permeability, and porosity. This data base could then serve as the basis for model development and verification, as well as provide a baseline for evaluating the effects of development on the Dixie Valley Geothermal System.

A P P E N D I X A

Grain-Size Distribution Diagrams for

Selected Geomorphic Surface Samples

(Locations for samples sites are indicated on Plate III.)

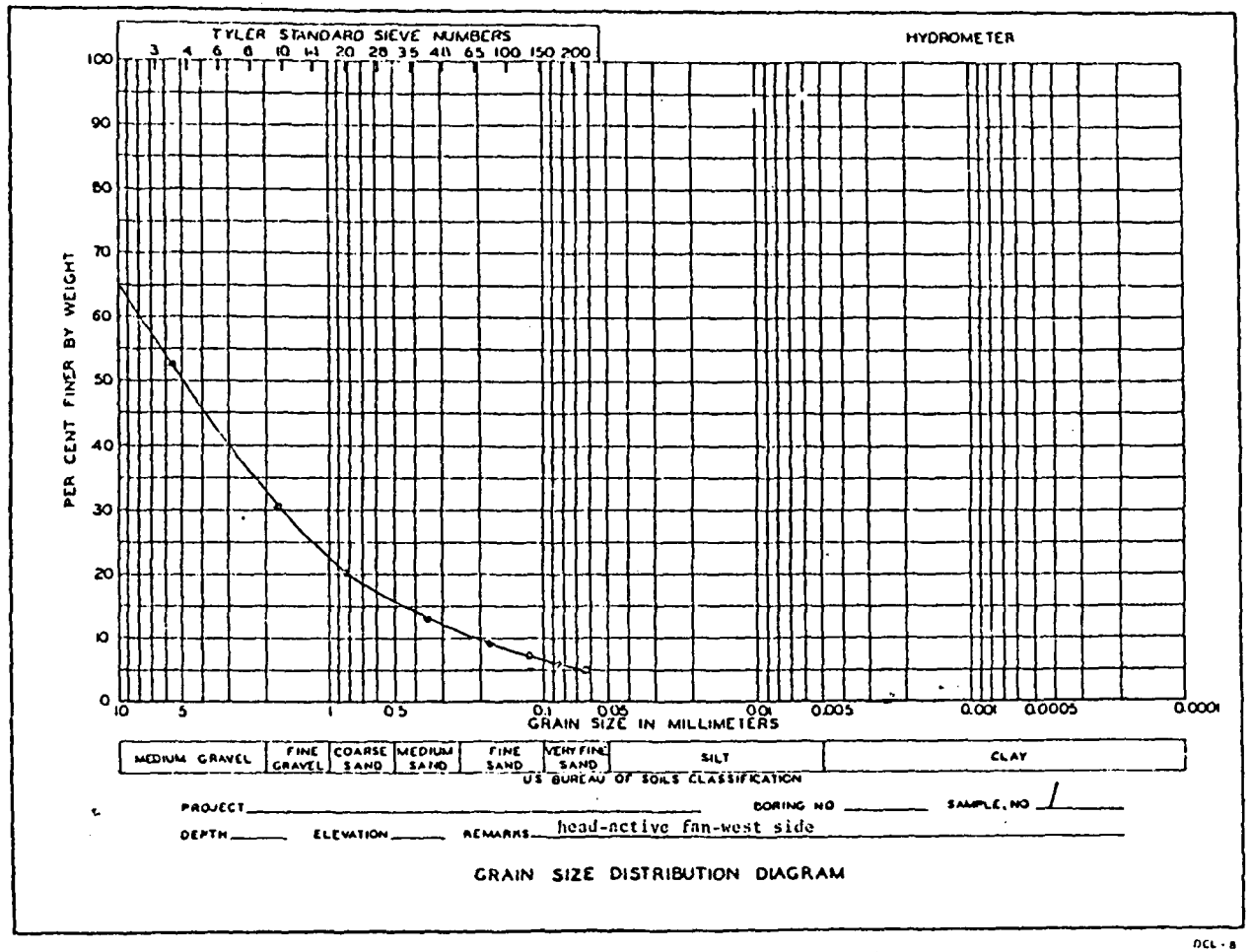

GRAIN SIZE DISTRIBUTION DIAGRAM

DCL - 8

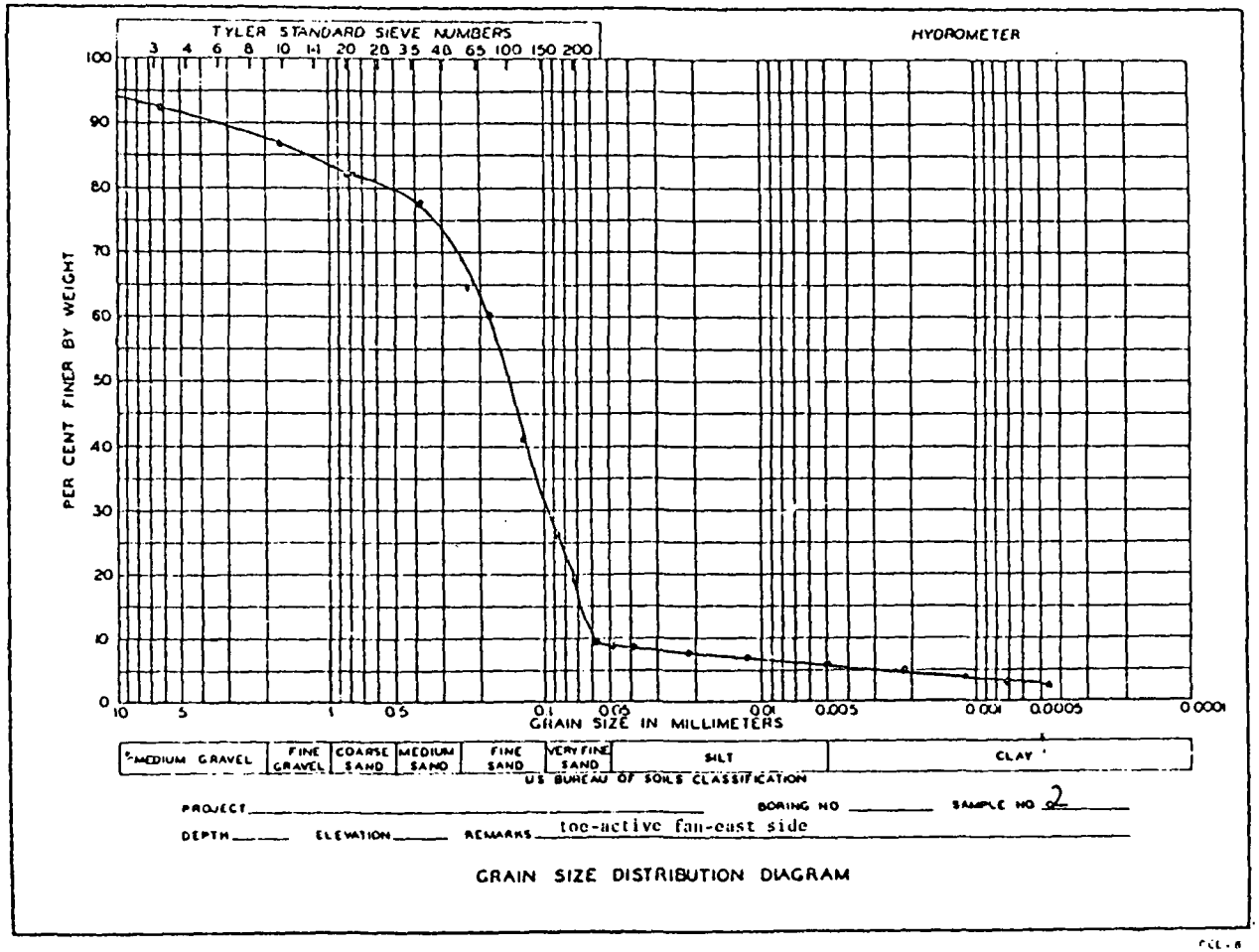

GRAIN SIZE DISTRIBUTION DIAGRAM

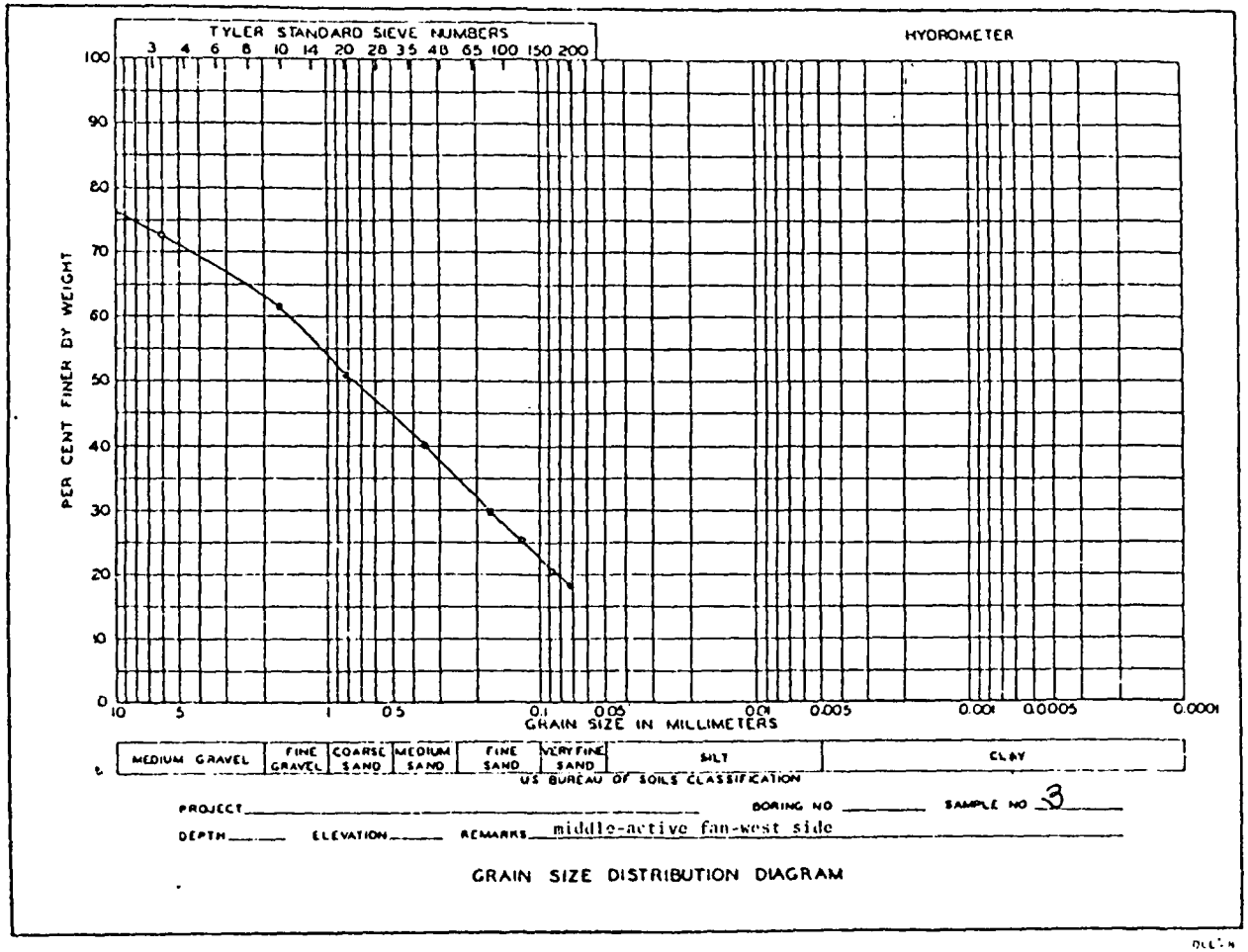

GRAIN SIZE DISTRIBUTION DIAGRAM

SOIL TEST INCORPORATED • 2205 LEE STREET • EVANSTON, ILLINOIS, U.S.A.

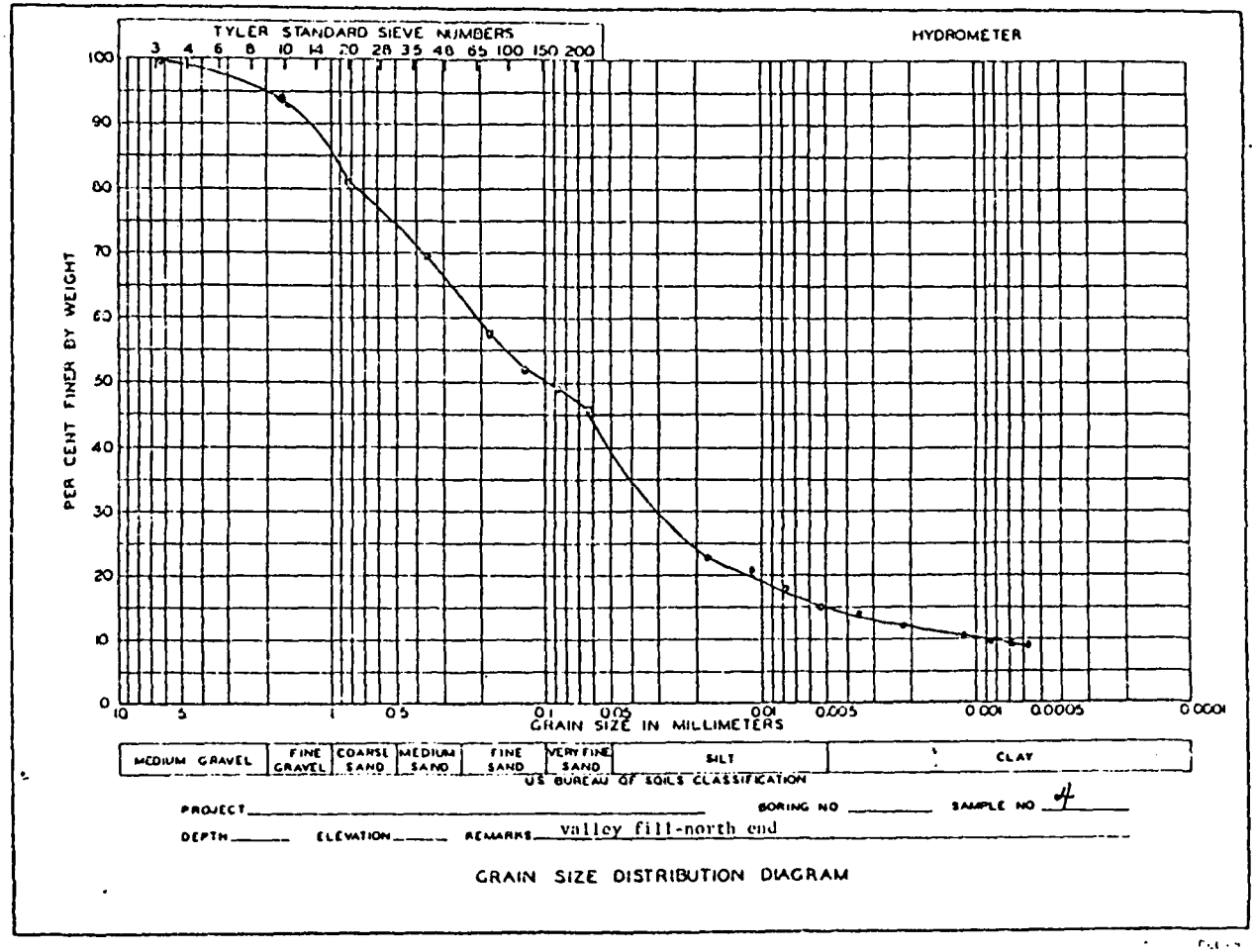

GRAIN SIZE DISTRIBUTION DIAGRAM

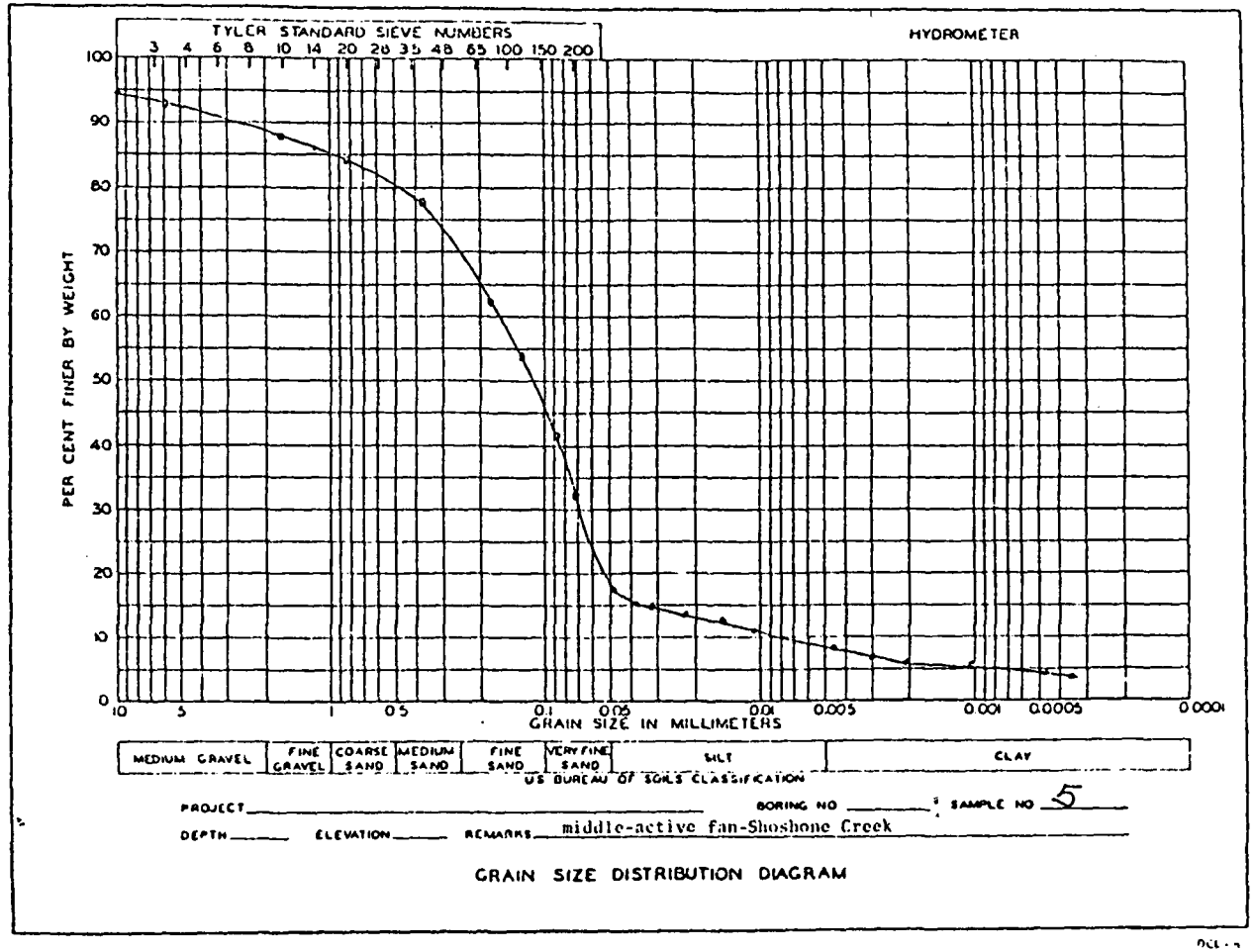

GRAIN SIZE DISTRIBUTION DIAGRAM

SOILTEST INCORPORATED • 2205 LEE STREET • EVANSTON, ILLINOIS, U.S.A.

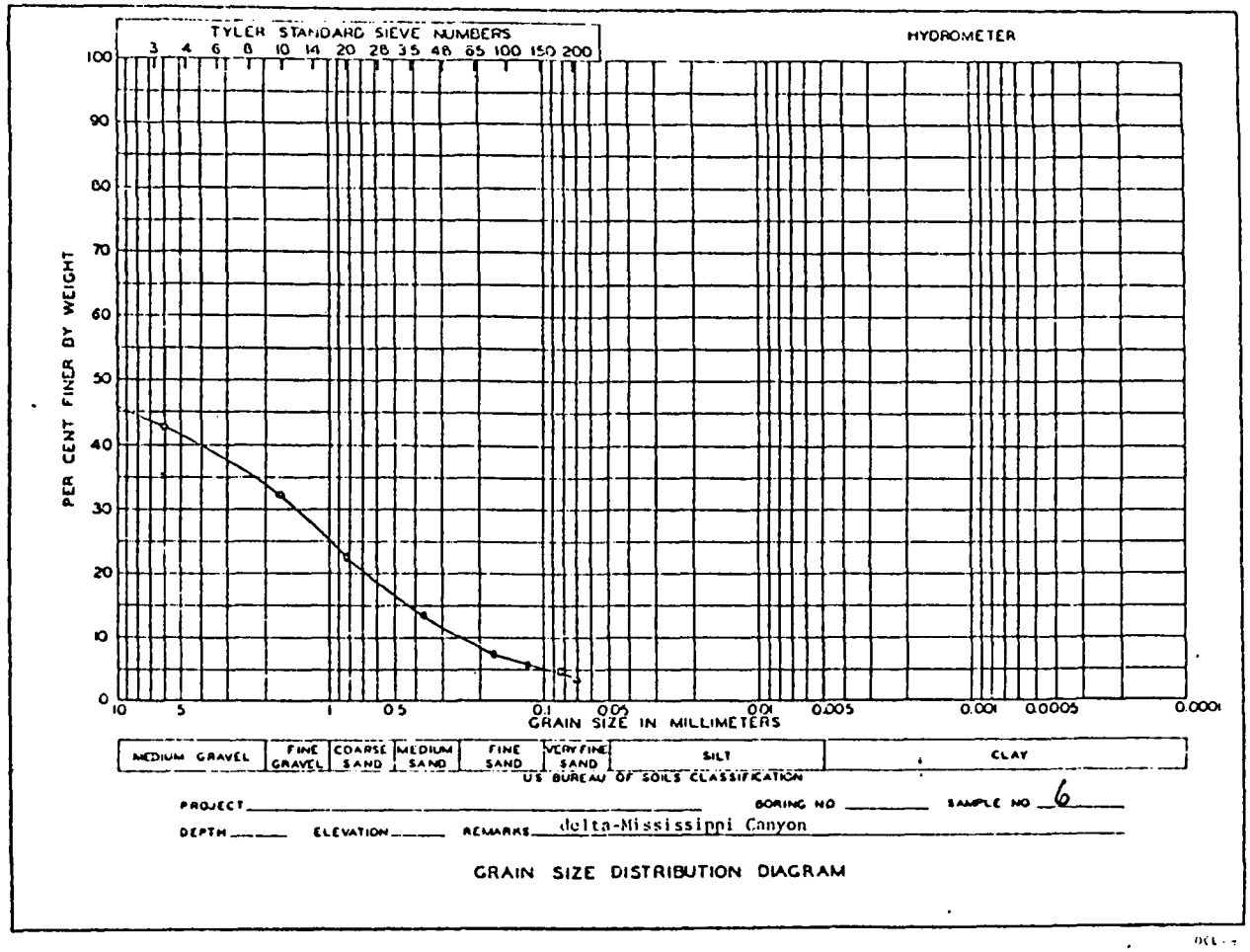

GRAIN SIZE DISTRIBUTION DIAGRAM

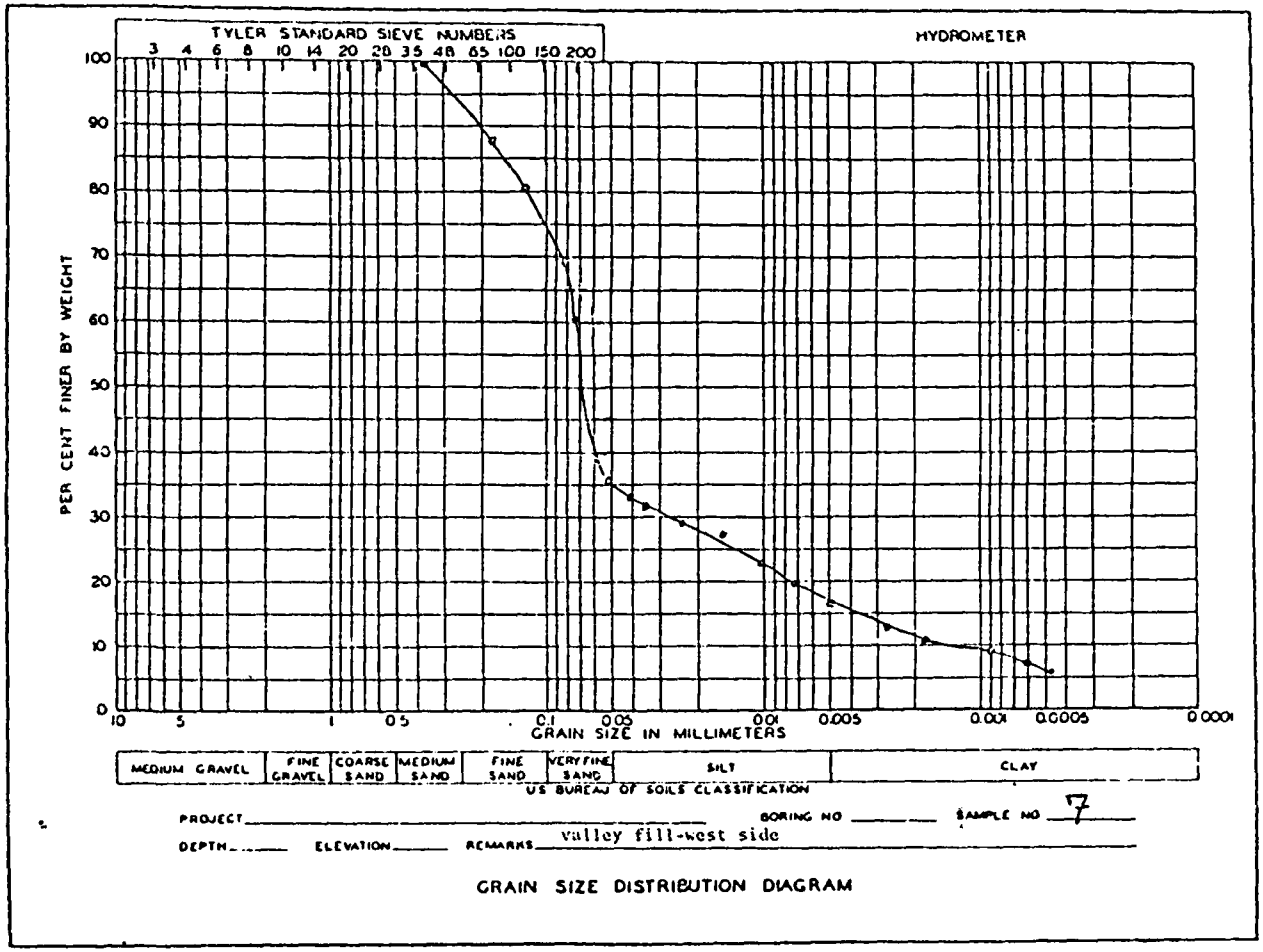

GRAIN SIZE DISTRIBUTION DIAGRAM

DCL-4

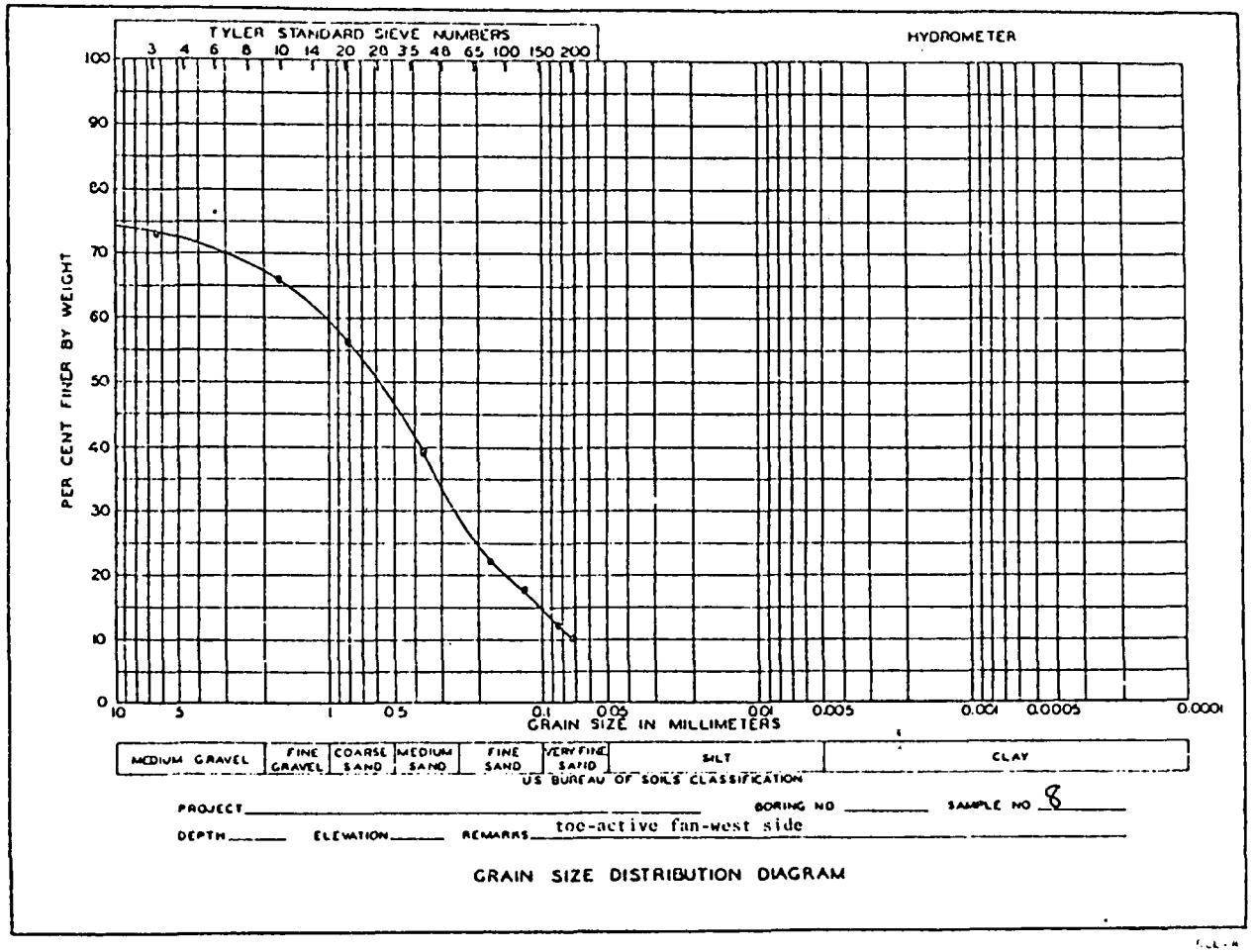

GRAIN SIZE DISTRIBUTION DIAGRAM

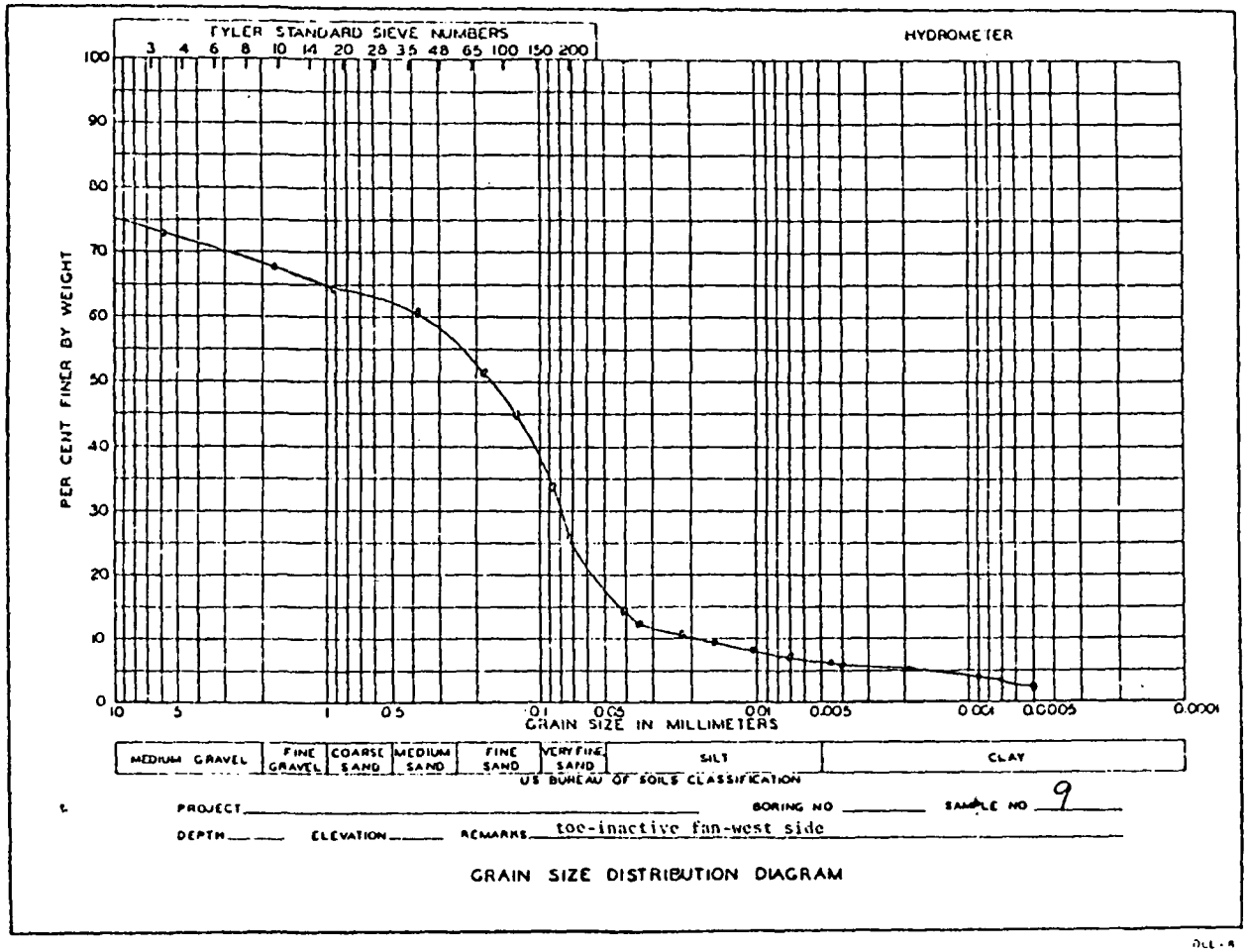

GRAIN SIZE DISTRIBUTION DIAGRAM

SOILTEST INCORPORATED • 2205 LEE STREET • EVANSTON, ILLINOIS, U.S.A.

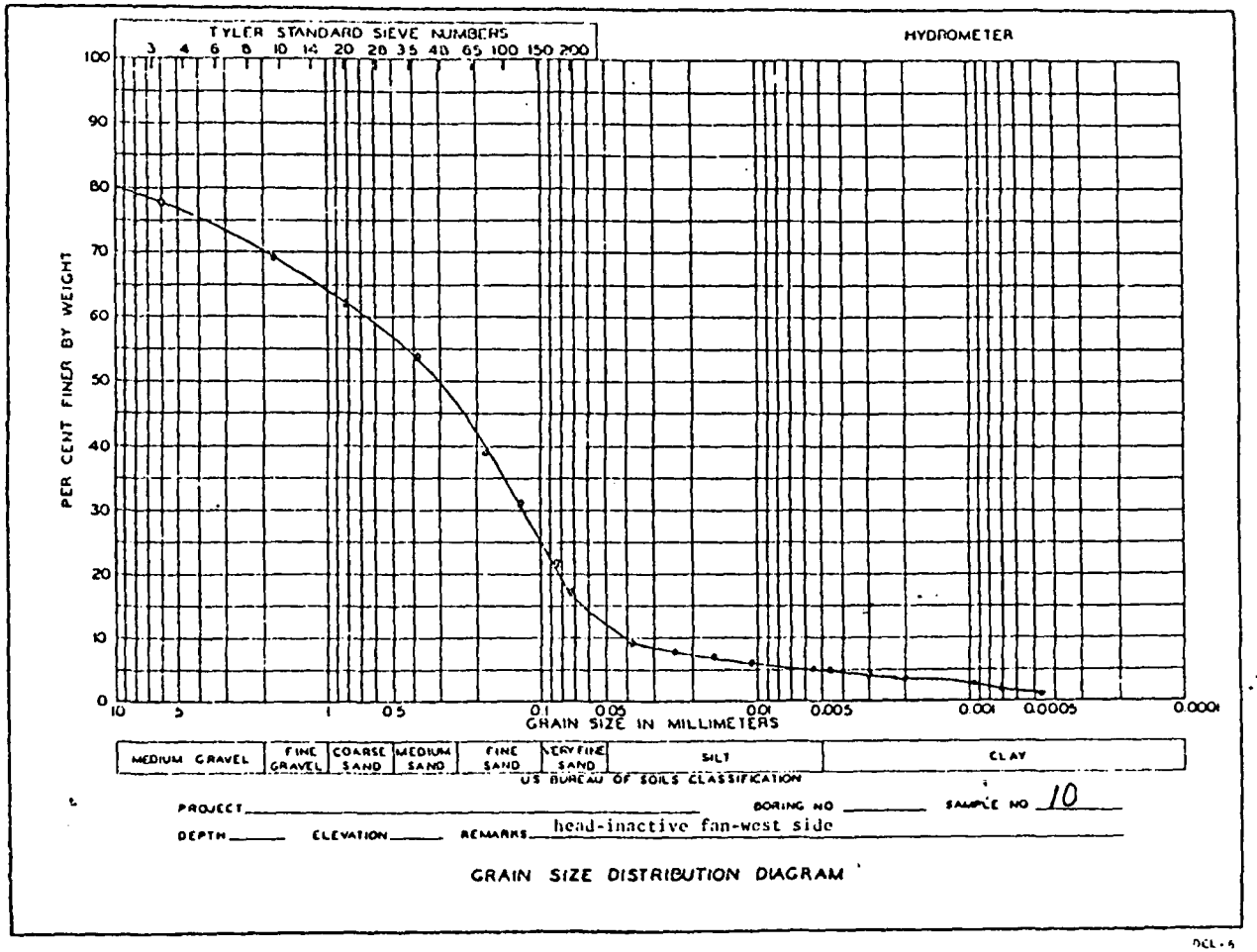

GRAIN SIZE DISTRIBUTION DIAGRAM

DCL-5

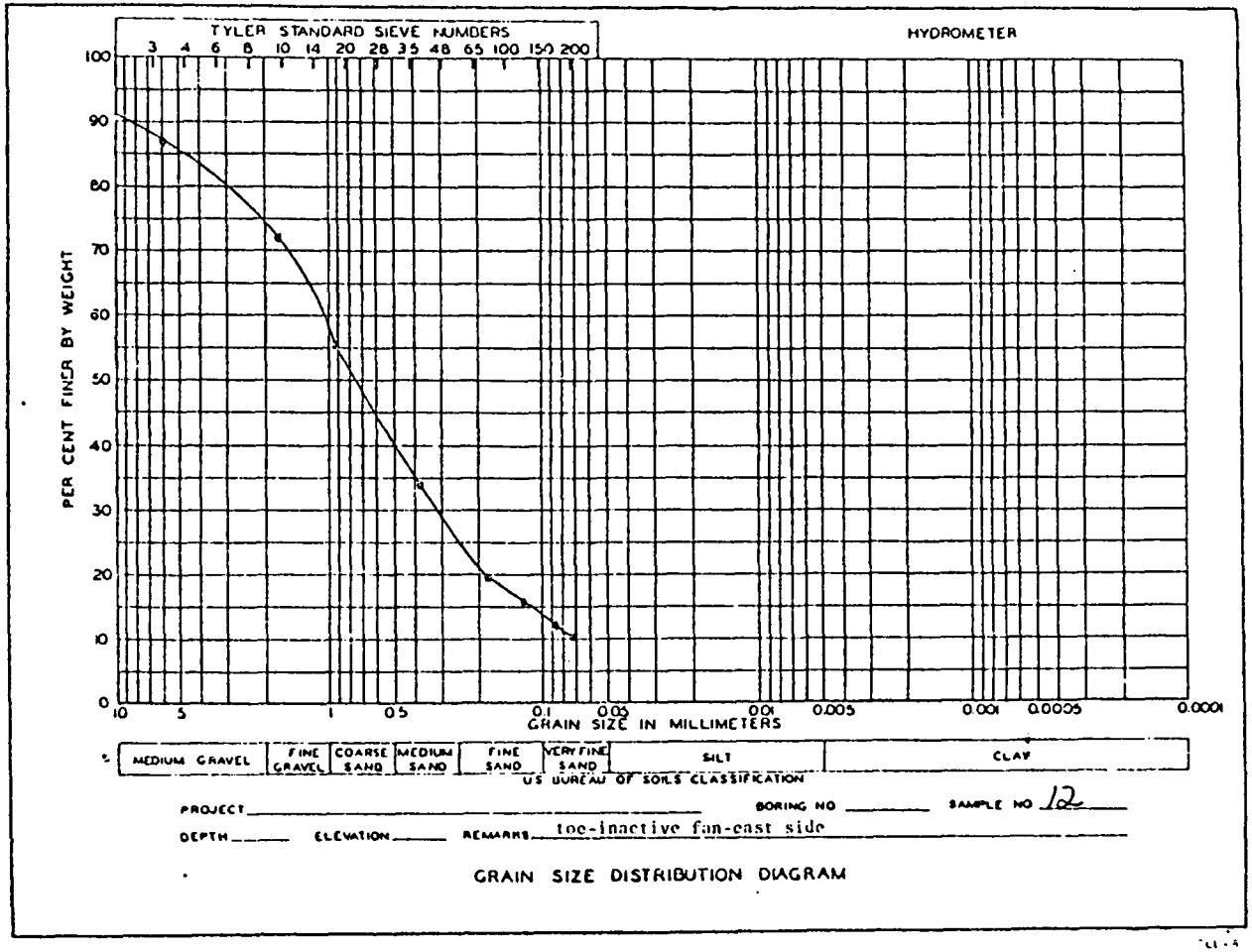

GRAIN SIZE DISTRIBUTION DIAGRAM

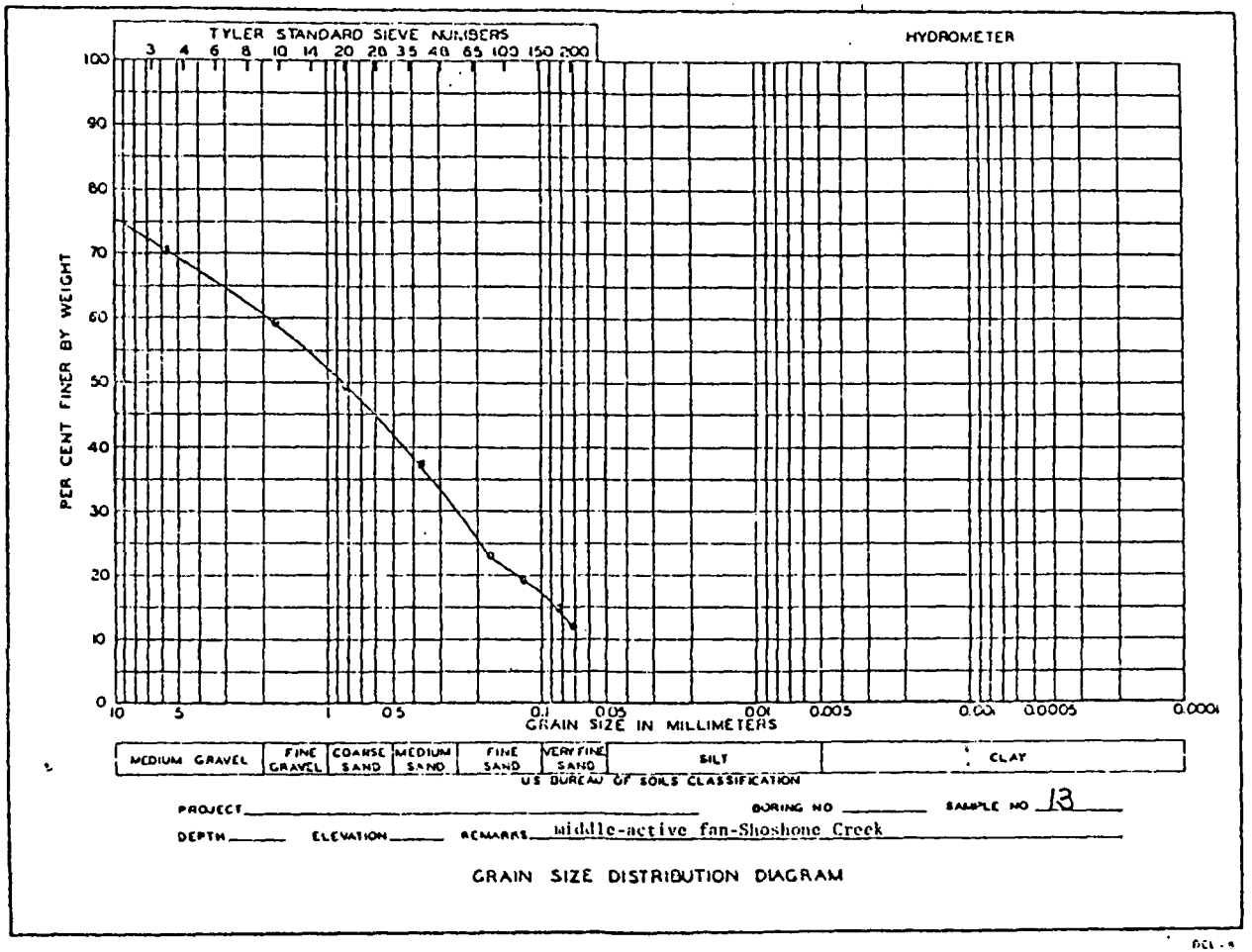

PROJECT _____ BORING NO _____ SAMPLE NO 13

DEPTH _____ ELEVATION _____ REMARKS middle-active fan-Shoshone Creek

GRAIN SIZE DISTRIBUTION DIAGRAM

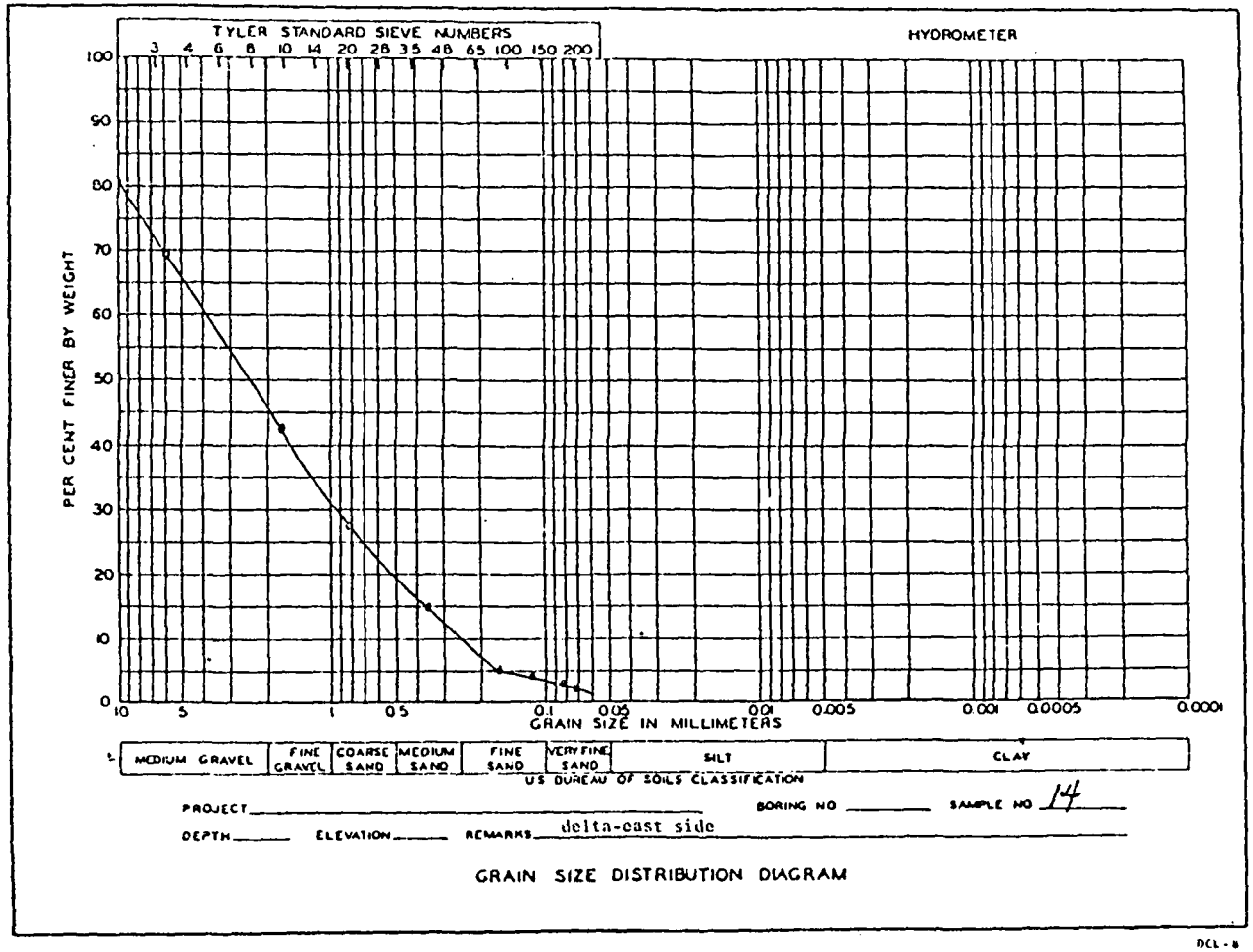

GRAIN SIZE DISTRIBUTION DIAGRAM

DCL-8

A P P E N D I X B

Profiles of Selected Fault Scarps

(Locations of profile sites are indicated on Plate IV.)

Fault Scarp Profile # 1

o = inflection point

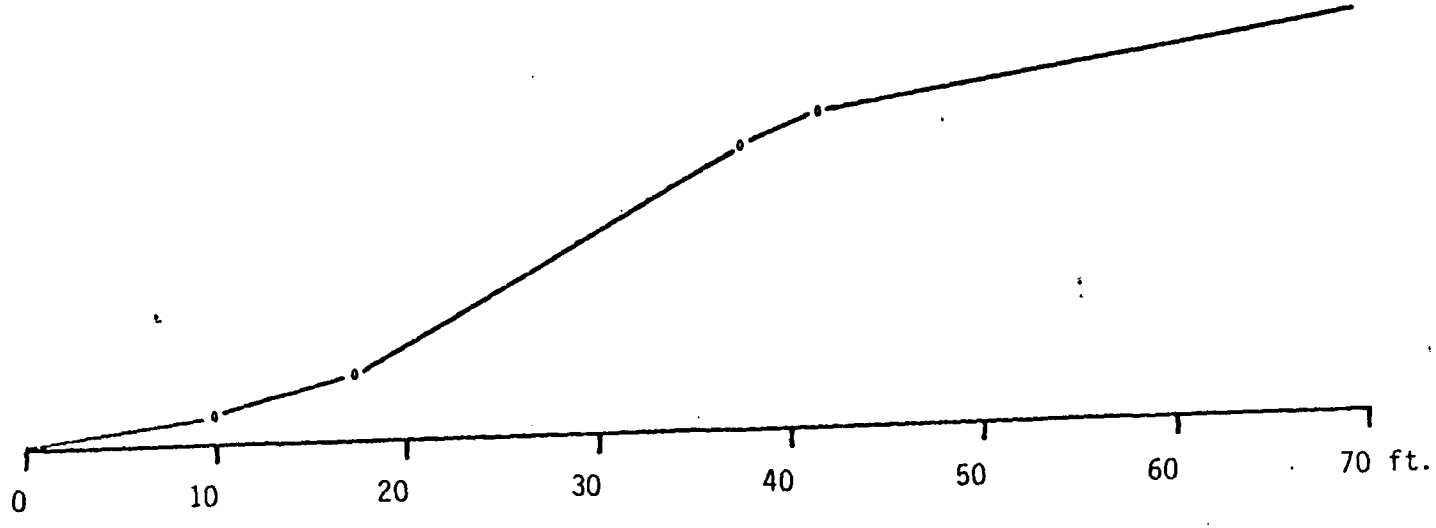

Fault Scarp Profile # 2

o = inflection point

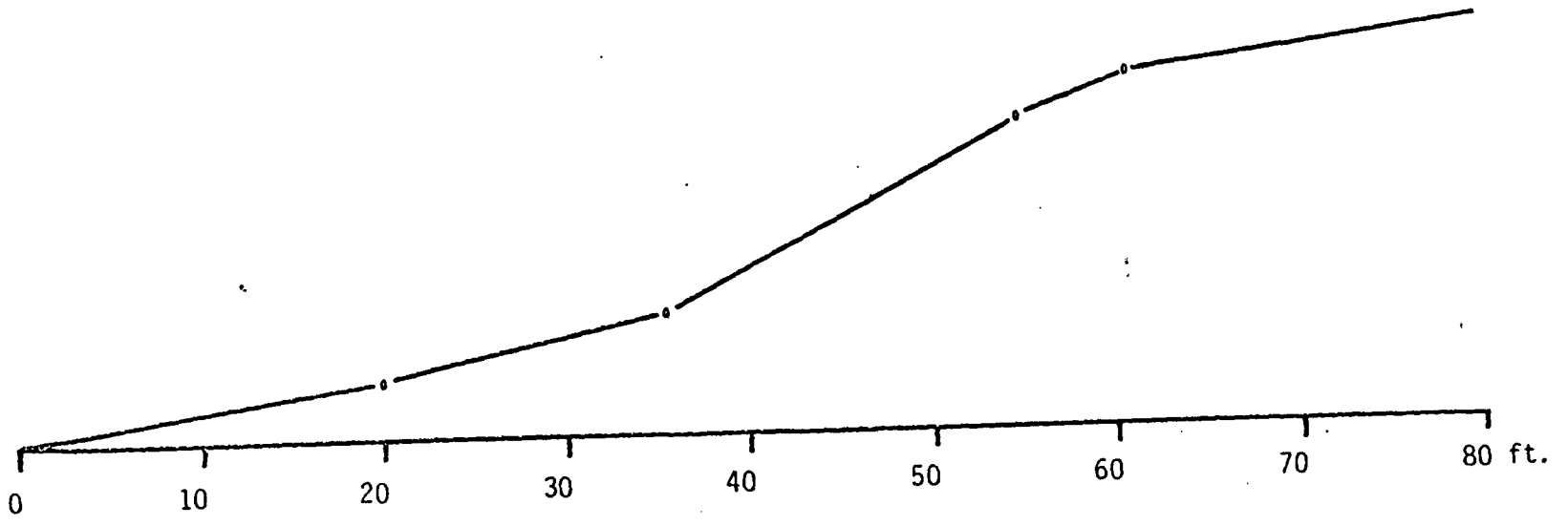

Fault Scarp Profile # 3

o = inflection point

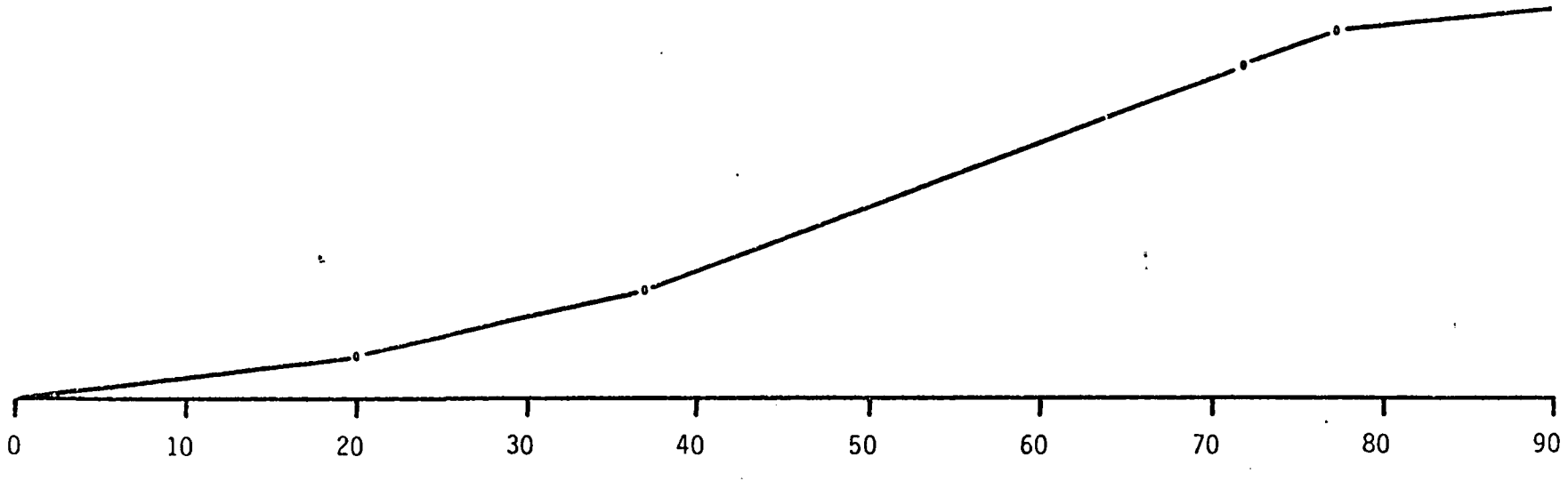

Fault Scarp Profile # 4

o = inflection point

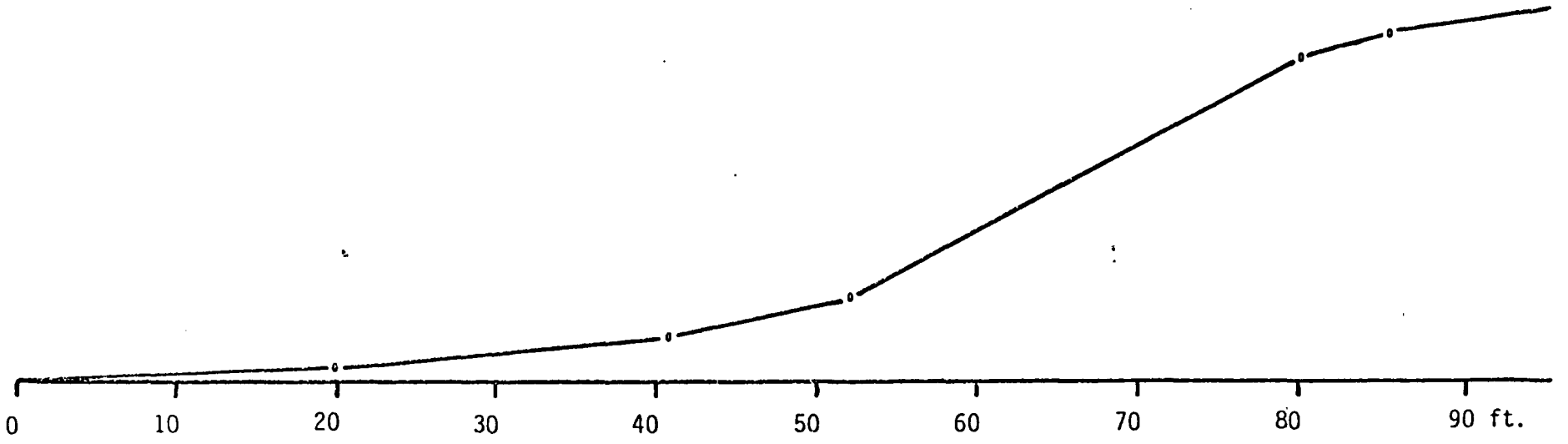

Fault Scarp Profile # 5

o = inflection point

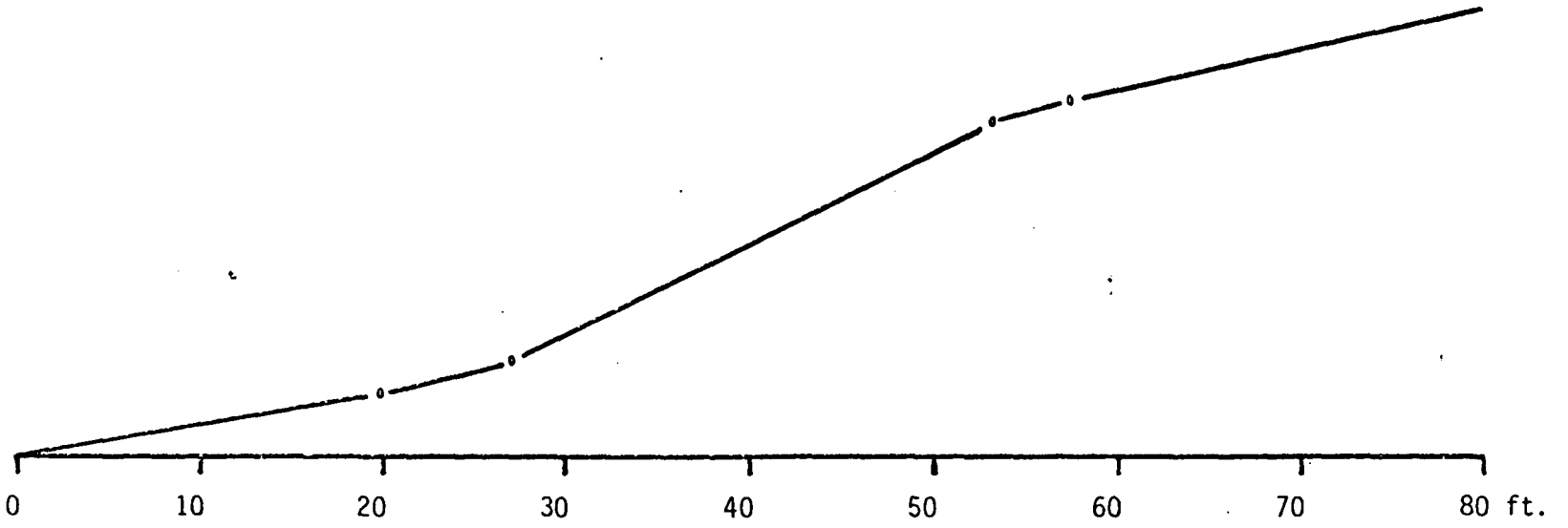

Fault Scarp Profile # 6

o = inflection point